ADDENDUM

Pg. 50: Start of Para 3: Delete, "Betaglycan heterozygous null (betaglycan+/-) mutants appear grossly phenotypically normal, but homozygous null (betaglycan-/-) mutants exhibit embryonic lethality between approximately e16.5 and birth, with defects in the developing heart, liver and gonads (Sarraj et al. ; Stenvers et al. 2003; Compton et al. 2007)." and change to "Betaglycan heterozygous null (betaglycan+/-) mutants express 50% of wildtype betaglycan expression levels, and appear grossly phenotypically normal. However, homozygous null (betaglycan$^{-/-}$) mutants exhibit embryonic lethality between approximately e16.5 and birth, with defects in the developing heart, liver and gonads (Sarraj et al. ; Stenvers et al. 2003; Compton et al. 2007)."

Pg. 55: Para 2, Line 6: Delete "Heterozygous null mutants for either *Ret* or *Pax2* exhibit severe renal dysplasia, coupled with a significant reduction in the number of nephrons developing within the kidney, a phenotype which is exacerbated in compound heterozygous mutants" and change to "Heterozygous null mutants for either *Ret* or *Pax2* exhibit a reduction in the number of nephrons developing within the kidney, a phenotype which is exacerbated in compound heterozygous mutants. Further, heterozygous and compound mutants deficient in *Pax2* expression exhibit renal dysplasia."

Comment: The use of the term 'dose-dependent' in describing the effects of Tgfb2 (Pg. 61) and betaglycan (see Pg. 192) mutations may be better represented by the use of 'expression-level dependent'. Such a term would not imply a linear relationship, and better represent the phenotypes which have been observed in betaglycan wildtype, heterozygous and null mutant metanephroi (see Pg. 191, Figure 6.1).

Pg. 114, Table 3.1: Delete figure legend and now read as "V_{kid} indicates 'volume of kidney', V_{ue} indicates 'volume of ureteric epithelium', $\%V_{ue}$ of V_{kid} indicates 'percentage of ureteric epithelial volume comprising overall kidney volume. Values are mean ± S.D. e13.5: (n) = +/+ (5), +/- (9), -/- (6); e15.5: (n) = 7 mice / genotype. Data were analysed via one-way ANOVA followed by a Tukey's post-hoc analysis. Those groups not sharing a common letter are significantly different ($p<0.01$)."

Pg. 117, Figure 3.4: Panels B and D Delete PN4 and change to PN5.

Comment: On Pg. 122, Figure 3.7, only phospho-SMAD activity was measured as interest was primarily in the level of activated SMAD signalling within the tissue, and not the total SMAD protein levels.

Pg. 128: Add to the end of Para 1: "In the current study, qPCR was adopted to investigate the expression of key genes involved in metanephric development. While this approach provides quantitative data of global metanephric gene expression across multiple time points, the approach is limited in its illustration and interpretation of spatial changes in gene expression. Accompanying *in situ* hybridisation would greatly strengthen the interpretation of quantitative gene expression changes observed via qPCR in this study. It is also important to note that generally, changes in gene expression observed in betaglycan heterozygous and null metanephroi, was less than two-fold. The biological significance of such moderate changes in

expression in the development of mutant phenotypes remains to be determined. However, it is likely that the cumulative effect of reduced gene expression in multiple signalling pathways was responsible for the phenotypes observed in heterozygous and null mutants."

Pg. 137, Table 4.1: Delete figure legend and replace with "Night and Day values represents 12 hour means. Values are mean ± SEM. Data analysed using one-way ANOVA."

Comment: On Pg. 138, creatinine clearance values reported in Table 4.2 are underpowered due to technical issues regarding sample analysis. The n values associated with this parameter are indicated in the table legend. The p value associated with creatinine clearance measurements should read 0.7.

Pg. 153, Figure 4.6: Incorrect labelling of panels. Panels should be labelled the following: **Normal Salt:** WT Renal Cortex (A), Outer Cortical Glomeruli (B), Juxta-Medullary Cortex LP (C), Juxta-Medullary Cortex HP (D); **Normal Salt:** *Tgfb2*$^{+/-}$ Renal Cortex (E), Outer Cortical Glomeruli (F), Juxta-Medullary Cortex LP (G), Juxta-Medullary Cortex HP (H). **Chronic High Salt:** WT Renal Cortex (I), Outer Cortical Glomeruli (J), Juxta-Medullary Cortex LP (K), Juxta-Medullary Cortex HP (L). **Chronic High Salt:** *Tgfb2*$^{+/-}$ Renal Cortex (M), Outer Cortical Glomeruli (N), Juxta-Medullary Cortex LP (O), Juxta-Medullary Cortex HP (P); **Acute High Salt:** WT Renal Cortex (Q), Outer Cortical Glomeruli (R), Juxta-Medullary Cortex LP (S), Juxta-Medullary Cortex HP (T); **Acute High Salt:** *Tgfb2*$^{+/-}$ Renal Cortex (U), Outer Cortical Glomeruli (V), Juxta-Medullary Cortex LP (W), Juxta-Medullary Cortex HP (X).

Pg. 154, Figure 4.7: Incorrect labelling of panels. Panels should be labelled the following: **Normal Salt:** WT Renal Cortex (A), Outer Cortical Glomeruli (B), Juxta-Medullary Cortex LP (C), Juxta-Medullary Cortex HP (D); **Normal Salt:** *Tgfb2*$^{+/-}$ Renal Cortex (E), Outer Cortical Glomeruli (F), Juxta-Medullary Cortex LP (G), Juxta-Medullary Cortex HP (H). **Chronic High Salt:** WT Renal Cortex (I), Outer Cortical Glomeruli (J), Juxta-Medullary Cortex LP (K), Juxta-Medullary Cortex HP (L). **Chronic High Salt:** *Tgfb2*$^{+/-}$ Renal Cortex (M), Outer Cortical Glomeruli (N), Juxta-Medullary Cortex LP (O), Juxta-Medullary Cortex HP (P); **Acute High Salt:** WT Renal Cortex (Q), Outer Cortical Glomeruli (R), Juxta-Medullary Cortex LP (S), Juxta-Medullary Cortex HP (T); **Acute High Salt:** *Tgfb2*$^{+/-}$ Renal Cortex (U), Outer Cortical Glomeruli (V), Juxta-Medullary Cortex LP (W), Juxta-Medullary Cortex HP (X).

Pg. 158: Add to end of Para 1: "Interestingly significant differences were observed in urine osmolality between WT and *Tgfb2*$^{+/-}$ fed a normal salt diet in this cohort of mice (n=6 per genotype), suggesting a greater urine concentrating ability in *Tgfb2*$^{+/-}$ mice. However, when the power of the analysis was increased (Table 4.1, WT: n = 23; *Tgfb2*$^{+/-}$: n = 22), there were no significant differences in osmolality between the genotypes."

Pg. 159: Add to end of Para 1: "It is widely acknowledged that the cardiovascular and renal physiological response to increased dietary salt intake differs considerably between male and females (Hilliard et al. 2011). It is for this reason that only male WT and *Tgfb2*$^{+/-}$ were utilised in this experimental chapter. Future studies should examine the impact of salt in female WT and *Tgfb2*$^{+/-}$ mice."

Pg. 184: Add to Para 2: Should read "Concentrations of 5 μg/g and 10 μg/g body weight of anti-TGFβ2 were used in the present study, in accordance with previous studies showing that 5 μg/g of anti-TGFβ2 was sufficient to neutralise 100% of biologically active TGFβ2 protein *in vitro* (Tsang et al. 1995). Similarly unpublished data from our laboratory has highlighted the ability of the selected anti-TGFβ2 neutralising antibody to inhibit the actions of exogenous TGFβ2 added to an *in vitro* metanephric culture system. As *in vitro* and *in vivo* systems are vastly different, and given the issue of route of administration discussed above, the present study also employed a concentration of 10 μg/g body weight of anti-TGFβ2. Similar concentrations of anti-TGFβ2 neutralising agents have previously been used to successfully neutralise TGFβ2 activity in the kidney *in vivo* (Hill et al. 2001; Juarez et al. 2007)."

Pg. 184: Add to Para 2, Line 18: Delete "Clearly, further optimisation of the *in vivo* protocol characterising antibody stability *in vivo*, neutralisation half-life, and antibody clearance are required to fully analyse the effects of partial TGFβ2 neutralisation on kidney development." And read "Clearly, further optimisation of the *in vivo* protocol utilising this antibody are required. Western blot and protein binding analysis illustrating the antibodies ability to bind TGFβ2 *in vivo* and prevent the protein associating with TGFβ signalling receptors is needed. Also characterisation of antibody stability *in vivo*, titration of antibody concentrations required for *in vivo* TGFβ2 neutralisation, as well as neutralisation half-life, and antibody clearance rate are all required to fully determine the ability of the antibody to neutralise the *in vivo* actions of TGFβ2. Following this, analysis of the effects of partial TGFβ2 neutralisation on kidney development can be undertaken."

Pg. 214: Add reference to reference list: "Hilliard LM, Nematbakhsh M, Kett MM, Teichman E, Sampson AK, Widdop RE, Evans RG, Denton KM. "Gender differences in pressure-natriuresis and renal autoregulation: role of the Angiotensin type 2 receptor." Hypertension **57**(2): 275-82."

Copyright Notices

Notice 1

Notice 2

The development and function of high nephron endowment

Kenneth Anthony Walker

Bachelor of Science (Honours)

Department of Anatomy and Developmental Biology
Monash University
Victoria, Australia

November 2010

Submitted in total fulfillment of the requirements for the degree of Doctor of Philosophy

TABLE OF CONTENTS

TABLE OF FIGURES

SUMMARY

An increasing amount of evidence suggests that low nephron number is a risk factor for development of chronic cardiovascular disease (particularly hypertension) and chronic kidney disease. In humans, nephron number varies as much as 13-fold, from approximately 210,000 to 2.7 million (mean approximately 875,000). While most human and animal studies have focused on the question of low nephron number, few studies have explored whether high nephron number provides protection against the development of hypertension or renal disease. This has largely been due to the absence of suitable experimental models of augmented nephron number. However, recent studies have demonstrated that perturbation to transforming growth factor-β2 (TGFβ2) or betaglycan (a TGFβ2 accessory receptor) gene expression is associated with augmented nephron number in heterozygous mice in adulthood. The experiments described in this thesis were designed to elucidate the developmental mechanisms responsible for augmented nephron endowment in betaglycan heterozygous (betaglycan$^{+/-}$) mice, to determine the functional consequences of a high nephron endowment, and to attempt to augment nephron number in the normal mouse kidney *in vivo* through manipulation of TGFβ2 signalling. The overall hypothesis of this thesis is that mild perturbation of TGFβ2 signalling during metanephric development augments nephron endowment and produces a renal phenotype which is functionally beneficial in the presence of physiological stressors.

To identify the mechanisms responsible for the augmented nephron number in betaglycan$^{+/-}$ mice, metanephroi from embryonic day (e) 11.5-15.5 wildtype, betaglycan$^{+/-}$, and betaglycan null (betaglycan$^{-/-}$) embryos were analysed using *in vivo* and *in vitro* approaches. Metanephroi of betaglycan$^{+/-}$ mice exhibited augmented ureteric branching morphogenesis that, in turn, correlated with a 32% increase in nephron endowment at e15.5. In contrast, betaglycan$^{-/-}$ metanephroi demonstrated impaired ureteric branching morphogenesis and reduced nephron endowment at e15.5 compared to wildtype metanephroi. Interestingly, the augmented and impaired ureteric branching phenotypes observed in betaglycan$^{+/-}$ and betaglycan$^{-/-}$ metanephroi respectively, appeared similar to that previously reported in *Tgfb2* heterozygous (*Tgfb2*$^{+/-}$) and null (*Tgfb2*$^{-/-}$) embryos. Finally, differing gene

expression profiles (determined using quantitative real-time PCR) in betaglycan$^{+/-}$ and betaglycan$^{-/-}$ metanephroi correlated strongly with their nephron number phenotype. Transient reduction in the expression of ureteric branching inhibitor *Bmp4* at e11.5, coupled with increased branching promoter *Gdnf* expression at e12.5 may underpin accelerated ureteric branching in betaglycan$^{+/-}$metanephroi. Interestingly, *Tgfb1* expression was significantly reduced to similar levels in betaglycan$^{+/-}$ and betaglycan$^{-/-}$ metanephroi from e13.5. However, *Tgfb2* expression was reduced in a dose-dependent manner, with betaglycan$^{-/-}$ metanephroi showing a greater reduction in *Tgfb2* expression than betaglycan$^{+/-}$ metanephroi. These findings suggest that manipulation of betaglycan signalling may provide a therapeutic avenue for augmenting nephron endowment. However, the contrasting mutant phenotypes (betaglycan$^{+/-}$ versus betaglycan$^{-/-}$) indicate that a greater understanding of the sensitivity of the developing metanephros to TGFβ superfamily signalling is required for these interventions to be successfully and safely developed.

The functional importance of high nephron endowment for the regulation of arterial pressure and renal function was studied using adult *Tgfb2*$^{+/-}$ mice, which have 60% more nephrons than wildtype mice. Arterial pressure, heart rate and renal function were determined under baseline, physiologically stimulated and pathological conditions. Renal function under basal conditions and in response to water deprivation was similar in wildtype and *Tgfb2*$^{+/-}$ mice. Acute and chronic high salt diets induced similar renal functional responses in both wildtype and *Tgfb2*$^{+/-}$ mice. Marked elevations in arterial pressure were observed in wildtype but not *Tgfb2*$^{+/-}$ mice when fed a chronic high salt diet. A 5% NaCl diet induced a mild elevation in mean arterial pressure (MAP; ~5 mmHg) in both genotypes, however when subsequently fed an 8% NaCl diet, wildtype mice displayed a further elevation in MAP (~16 mmHg) which was not observed in *Tgfb2*$^{+/-}$ mice. The chronic high salt diet also increased perivascular collagen deposition in wildtype kidneys, but not heterozygous kidneys. While data from this study have shown *Tgfb2*$^{+/-}$ mice to be protected from the pathological influences of a chronic high salt diet, it remains unclear whether this is due to augmented nephron endowment or systemic reduction in TGFβ2 expression.

In the final experiment, an anti-TGFβ2 neutralising antibody was administered to neonatal mouse pups in an attempt to augment nephron endowment in their

developing kidneys. In mice, nephrogenesis continues until 5 days after birth, thus providing a window of postnatal nephrogenesis for intervention. The anti-TGFβ2 neutralising antibody (at a dose of 5 μg/g body weight or 10 μg/g body weight) was administered to pups via single daily intraperitoneal injections between postnatal (PN) 0 – PN4. Pups were weighed and monitored until PN 14 at which time tissues were collected. Total nephron endowment was unchanged in mice that received the antibody. However, administration of the highest dose of antibody (10 μg/g) correlated with an increase in mean (15%) and total glomerular (12%) volume at PN14. While nephron endowment remained unchanged following antibody administration, this study provides a framework by which subsequent approaches for augmenting nephron endowment can be developed.

The findings presented in this thesis suggest that perturbations to TGFβ2/betaglycan signalling can result in altered nephron endowment. Furthermore, the findings demonstrate that the high nephron endowment in *Tgfb2*$^{+/-}$ mice does not impact upon baseline arterial pressure or renal function. Of great significance and consistent with the overall hypothesis, the high nephron endowment in *Tgfb2*$^{+/-}$ mice was associated with a beneficial protective phenotype in the presence of a chronic cardiovascular or renal stressor, namely a chronic high salt diet. Manipulation of TGFβ2 signalling in the developing metanephros may provide a pathway towards nephron rescue in offspring at risk of developing kidneys with low nephron endowment.

GENERAL DECLARATION

I hereby declare that to the best of my knowledge and belief, this thesis contains no material previously published or written by another person nor material which has been accepted for the award of any degree or diploma at Monash University or any other tertiary institution, except where due acknowledgement is made in the text of this thesis. I also declare this thesis to be less than 100,000 words in length, exclusive of figures, tables and references.

Kenneth Anthony Walker
Department of Anatomy and Developmental Biology
Monash University

ACKNOWLEDGMENTS

Firstly, I wish to give thanks to my team of supervisors – John, Gina, Kaye and Michelle. Each of you has given so much of your time and effort to support my quest to become a scientist, and I can never thank you each enough for this. I do not think I would be the person I am without having had the guidance and generosity of each of you. Again, thank you for every second you have given to help me reach my goals.

To my family, I thank you for your unwavering support through my studies. Ken, Robin, Stacey, Jemma and more recently Nan, while you may not understand exactly what I do, your understanding of why I do what I do, along with your support and respect has been an endless source of motivation and inspiration. Thank you. Also to my new family, Warren, Wendy and Adam, I am greatly appreciative of the respect and support I have received for each of you during the short time we have known each other.

To my fellow scientists: Sunny, Steve, Christina, Sheri, Lisa and Rebecca. Each of you has become much more than a colleague; you have become some of my closest friends. Sunny - your passion for life and science is contagious. Steve – my best friend throughout this journey, I am proud of our friendship. Christina – fish have feelings and midnight conversations of music and life make me happy to have met you. Sheri – writing would not be the same without our coffee-less coffee breaks, thank you. Lisa – I still stand by you being the nicest person in the world, even when I am being a pain you still can bring a smile to my face. And Rebecca – you kindness and generosity can not go unthanked. For opening your home and heart to Eb and I, we are eternally grateful.

My friends outside of the Monash and science bubble – Jess and Paul, Thommo, Carlee, Raeoni and Andrew, Ashlee, Dean and Chris. Thank you so much for understanding that at anytime my life can be put on hold. Thank you for the beer, the hot chocolates, the games of pool, the singstar and the rocking out that has kept me sane.

I must extend a special thank you to Kerry McInnes. You introduced me to science and have helped shape my love and respect for the discipline. I truly believe that without your support and kind words I would not be at the end of PhD. Thank you for everything.

To those that helped me with skills, techniques, and random questions in the middle of experiments; Mai, Ruth, Maree, Luise, James, Debbie, Jinhua, Mali, Sharon, Lucinda and Xiaochu, I thank you so much for your time and help. I could not have done this work without fantastic support.

Finally to my beautiful partner Ebony. I promise to repay you for every moment I have committed to this thesis. Your love has helped me more than you can ever imagine. I thank you for the midnight cartoons, the road trips to no where, moments of insanity involving stuffed toys, and the punk bands that make us both smile. You make me smile every time I see you, and for this I owe you. I love you girl.

INVITED SEMINARS & ABSTRACTS

Invited Seminars

International

1. **"Is a high nephron number beneficial?"** - Harvard University, Cambridge, Massachusetts, USA, September, 2009

2. **"Is a high nephron number beneficial?"** - Children's Hospital, Pittsburgh, Pennsylvania, USA, September, 2009

National

1. "**Nephron number: The more the merrier?**" – *Healthy Start to Life Annual Scientific Meeting*, Monash Institute of Medical Research, Clayton, Australia, November, 2010.

2. **"The role of betaglycan in kidney development"** - *Transforming Growth Factor β (TGFβ) Workshop*, Monash Institute of Medical Research, Clayton, Australia, June 2008.

Abstracts

International

1. Walker KA, Caruana G, Sims-Lucas S, Sarraj M, Bertram JF & Stenvers KL. (2009). *"HIGH NEPHRON NUMBER IN BETAGLYCAN HETEROZYGOUS MICE".* Mechanisms of Development, 126 : S124. (Poster Presentation).

2. Walker KA, Sarraj M, Sims-Lucas S, Caruana G, Stenvers KL & Bertram JF. (2008). *"AUGMENTED NEPHRON NUMBER AND DEVELOPMENT IN BETAGLYCAN HETEROZYGOUS MICE"*. 1st New Zealand Kidney Biology Satellite meeting of the 18th Queenstown Molecular Biology Conference, 1 K29 (Poster Presentation).

   Winner: Quantum 'Scientific Excellence' Award – Best conference presentation by a Prince Henry's Institute of Medical Research student

National

1. Walker KA, Caruana G, Sims-Lucas S, Sarraj M, Bertram JF & Stenvers KL. (2009). *"HIGH NEPHRON NUMBER IN BETAGLYCAN HETEROZYGOUS MICE".* Healthy Start To Life Conference, A25 (Poster Presentation).

2. Walker KA, Caruana G, Sims-Lucas S, Sarraj M, Bertram JF & Stenvers KL. (2009). *"HIGH NEPHRON NUMBER IN BETAGLYCAN HETEROZYGOUS MICE".* Proceedings of the 2nd National Heart Foundation Conference, P-113 (Poster Presentation).

3. Walker KA, Sims-Lucas S, Sarraj M, Caruana G, Stenvers KL & Bertram JF. (2008). *"AUGMENTED NEPHRON NUMBER AND METANEPHRIC DEVELOPMENT IN BETAGLYCAN HETEROZYGOUS MICE".* Melbourne Cell and Developmental Biology Meeting Handbook, O13 (Oral Presentation).

Winner: 'Best Student Presentation' - Melbourne Cell and Developmental Biology Meeting, Melbourne, Australia

4. Walker KA, Sims-Lucas S, Sarraj M, Caruana G, Stenvers KL & Bertram JF. (2008). *"AUGMENTED NEPHRON NUMBER AND DEVELOPMENT IN BETAGLYCAN HETEROZYGOUS MICE".* A Healthy Start to Life Conference. (Poster Presentation).

Winner: Monash Student Award – Best Monash Student Poster Presentation in the area of kidney development / nephron number studies.

5. Walker KA, Sims-Lucas S, Sarraj M, Caruana G, Stenvers KL & Bertram JF. (2008). *"AUGMENTED NEPHRON NUMBER AND METANEPHRIC DEVELOPMENT IN BETAGLYCAN HETEROZYGOUS MICE".* The Proceedings of the Australian Society for Biochemistry and Molecular Biology, 40: A29 (Oral Presentation).

6. Walker KA, Sarraj M, Sims-Lucas S, Caruana G, Stenvers KL & Bertram JF. (2008). *"AUGMENTED NEPHRON NUMBER AND DEVELOPMENT IN BETAGLYCAN HETEROZYGOUS MICE"*. Nephrology. 13 (supplement 3) A213 (Poster Presentation).

7. Walker KA, Sims-Lucas S, Sarraj M, Chua HK, Caruana G, Bertram JF & Stenvers KL. (2007). *"BETAGLYCAN (TβRIII) IS REQUIRED FOR NORMAL METANEPHRIC DEVELOPMENT"*. Developmental Origins of Health and Adult Diseases, Satellite Conference: 73 (Poster Presentation).

Winner: Monash Student Award – Best Monash Student Poster Presentation in the area of kidney development / nephron number studies.

8. Walker KA, Sims-Lucas S, Sarraj M, Chua HK, Caruana G, Bertram JF & Stenvers KL. (2007). *"BETAGLYCAN (TβRIII) IS REQUIRED FOR NORMAL METANEPHRIC DEVELOPMENT"*. The Proceedings of the Australian Society for Biochemistry and Molecular Biology, 36: A117 (Poster Presentation).

Winner: Keith Dixon Prize in Developmental Biology – Best Student Poster Presentation in Developmental Biology, by the Australian and New Zealand Society of Cell and Developmental Biology at ComBio 2007.

ABBREVIATIONS AND SYMBOLS

Abbreviations

ad libitum **–** at one's pleasure
ALK - activin like kinase
ACTR-II - activin receptor type II
AVP - arginine vasopressin
β-ME - β-mercaptoethanol
BMP – bone morphogenetic protein
BP – blood pressure
bp – base pairs
BPM – beats per minute
BSA – bovine serum albumin
CAKUT – congenital anomalies of the kidney and urinary tract
Ccre – creatinine clearance
CKD – chronic kidney disease
Cl – chloride
CVD – cardiovascular disease
DAB - diaminobenzidine
DBA - *dolichus biflorus* agglutinin
DNA – deoxyribonucleic acid
e – embryonic day
ECM – extra-cellular matrix
ELISA – enzyme linked immunosorbent assay
ESRD – end stage renal disease
EYA1 – eyes absent 1
fg – femtogram (s)
FGF – fibroblast growth factor
FSA – glomerular capillary filtration surface area
g – gram (s)
gBW^{-1} – per gram of body weight
GDF – growth and differentiation factor
GDNF – glial cell line derived neurotrophic factor
GFR – glomerular filtration rate
GFRA1 - glial cell line derived neurotrophic factor family receptor alpha1
GMA - glycolmethacrylate
GREM-1 - gremlin 1
h – hour (s)
HPLC – high performance liquid chromatography
HR – heart rate
HS – high salt
IGF – insulin-like growth factor
IGFBP1 - insulin-like growth factor binding protein 1
INHBA - inhibin beta-A
In Vitro – an experiment performed not in a living organism, but in a controlled environment
In Vivo – *a*n experiment performed using a whole, living organism
K – potassium
kg – kilogram (s)
$kg\ H_20^{-1}$ – per kilogram of water
ratio
L – litre
L:BW – lung to body weight ratio
LIF – leukaemia inhibitory factor
LK:BW – left kidney weight to body weight
LV:BW – left ventricle to body weight ratio
M – molar
MAP – mean arterial pressure
MET – mesenchyme to epithelial transition
Min – minute (s)
mg – milligram (s)
ml – millimetre (s)
MM – metanephric mesenchyme
mm – millimetre (s)
mmHg – millimetres of mercury
mmol – millimole (s)
mOsmol – milliosmoles
mRNA – mitochondrial ribonucleic acid
n – number
Na – sodium
NaCl – sodium chloride; salt
ng – nanogram (s)
NKCC1 - Na-K-2Cl co-transporter
NS – normal salt
O_2 – oxygen
p – probability
PAS – periodic acid schiff's
PAX2 – paired box transcription factor 2
PFA - paraformaldehyde

PN – postnatal day
PNA - peanut agglutinin
RA – retinoic acid
RAS – renin-angiotensin system
RET - ret proto-oncogene
RLT - guanidine thiocyanate
RT-PCR - reverse transcription polymerase chain reaction
RK:BW – right kidney weight to body weight
RV:KW – right ventricle to body weight ratio
SD – standard deviation
Sec – second (s)
SEM – standard error of the mean
sFRP – secreted frizzled-related protein
SIX - sine oculis-related homeobox
SMAD – intracellular signalling molecules associated with TGFβ superfamily signal transduction
TGFβ – transforming growth factor β
TK:BW – total kidney weight to body weight ratio
UB – ureteric bud
V2R - vasopressin 2 receptors
Wk (s) – week (s)
WNT - wingless-type MMTV integration site family member
wt – weight
WT – wildtype
WT1 – wilms tumor 1
w/w – weight per weight
µg – microgram (s)
µm – micrometre (s)
µmol – micromole (s)
µl – microlitre (s)

Symbols

+/+ - wildtype
+/- - heterozygous mutant
-/- - null mutant
Δ – delta, change in
± - plus or minus
~ - approximately
X – multiply by
% - percent
< - less than
> - greater than
° C – degrees Celsius
α - alpha
β – beta
Σ – sum of
↑ – increase
↓– decrease

CHAPTER 1

INTRODUCTION

1.1 INTRODUCTION

Cardiovascular disease (CVD), a term pertaining to any disease associated with the heart or blood vessels, is currently the most expensive disease group in Australia, accounting for 11% of total health care expenditure in 2004 – 2005 (AIHW, 2009). Associated with the economic burden of CVD is the impact on quality of life. CVD is the leading cause of both disability and premature death in Australia (AIHW, 2009). Individuals in industrialised countries have a 90% risk of developing hypertension (sustained blood pressure greater than 140/90 mmHg), the number one risk factor for the development of CVD, over their lifetime (Messerli et al. 2007). In 2000, it was estimated that 972 million adults worldwide (639 million in developed countries; 333 million in developing countries), were living with hypertension (Kearney et al. 2005). By 2025, it is estimated that this will increase to 1.56 billion adults (29.0% of men : 29.5% of women) worldwide (Kearney et al. 2005).

Hypertension also increases the risk of disease in other organs, such as the brain, lungs, and in particular, the kidneys (Messerli et al. 2007). Hypertension is a major risk factor for chronic kidney disease (CKD) and subsequent end-stage renal disease (ESRD) (Chen 2010). One in seven Australians over the age of 25 years have evidence of CKD, defined as kidney damage or impaired/reduced kidney function which persists for longer than 3 months. In Australia, the cost of treating CKD is approximately $670 million a year, which is estimated to increase to $800 million a year by 2011 (Cass et al. 2006).

Evidence suggests that hypertension and CVD are risk factors for the development of CKD, but CKD may in turn result in the development of CVD. Indeed the American Heart Association concluded that patients with CKD are members of the 'highest risk group' for subsequent CVD events (Sarnak et al. 2003; Coresh et al. 2004). Analysis of a cohort of 5,104 white men and women over the age of 65, over a 3-year period determined that those who exhibited an increase in serum creatinine concentration greater than 0.3 mg/dl, an indicator of kidney damage, displayed a 'worsening' cardiovascular risk profile than those for whom serum creatinine levels were maintained over the same period (Fried et al. 2009). Thus, these studies suggest a complex interaction between cardiovascular and kidney health.

Of great concern is that despite the high prevalence of hypertension and CKD within the greater community, the aetiology underlying their development is largely unknown. One factor which has been implicated in the development of hypertension and CKD is low 'nephron endowment' or a low nephron number at birth. This Introduction reviews current knowledge of the regulation of kidney development and establishment of nephron endowment, with focus given to factors that increase nephron endowment, in particular members of the transforming growth factor β (TGFβ) superfamily. Finally, the potential for high nephron endowment to provide protection against hypertension and the development of disease will be explored utilising *Tgfb2* heterozygous (*Tgfb2*$^{+/-}$) mice, a recently described model of high nephron endowment (Sims-Lucas et al. 2008).

1.2 STRUCTURE AND FUNCTION OF THE MAMMALIAN KIDNEY

1.2.1 Anatomy of the adult mammalian kidney

In general, adult mammals contain a pair of kidneys known as metanephroi, located external to the peritoneal cavity on the posterior abdominal wall on each side of the vertebral column (Vander 1995). On the medial aspect of the kidney is a large indentation, the hilum, a site at which the renal artery and afferent renal nerves enter the kidney; and efferent renal nerves and the renal vein exit the kidney. It is also at this site that the renal pelvis, a funnel-shaped continuation of the ureter, is located (Figure 1.1A). At its proximal end, the human renal pelvis gives rise to the major calyces, each of which is further subdivided into minor calyxes. Each minor calyx is associated with a projection of renal medullary tissue known as a renal pyramid. Whilst the apex of the renal pyramid, known as the papilla, extends into the minor calyxes, the base of the pyramid is located at the renal cortical-medullary boundary. In contrast to the multilobar kidney of humans, the mouse kidney, on which this thesis will focus, is a unilobar kidney with only one papilla and associated calyx.

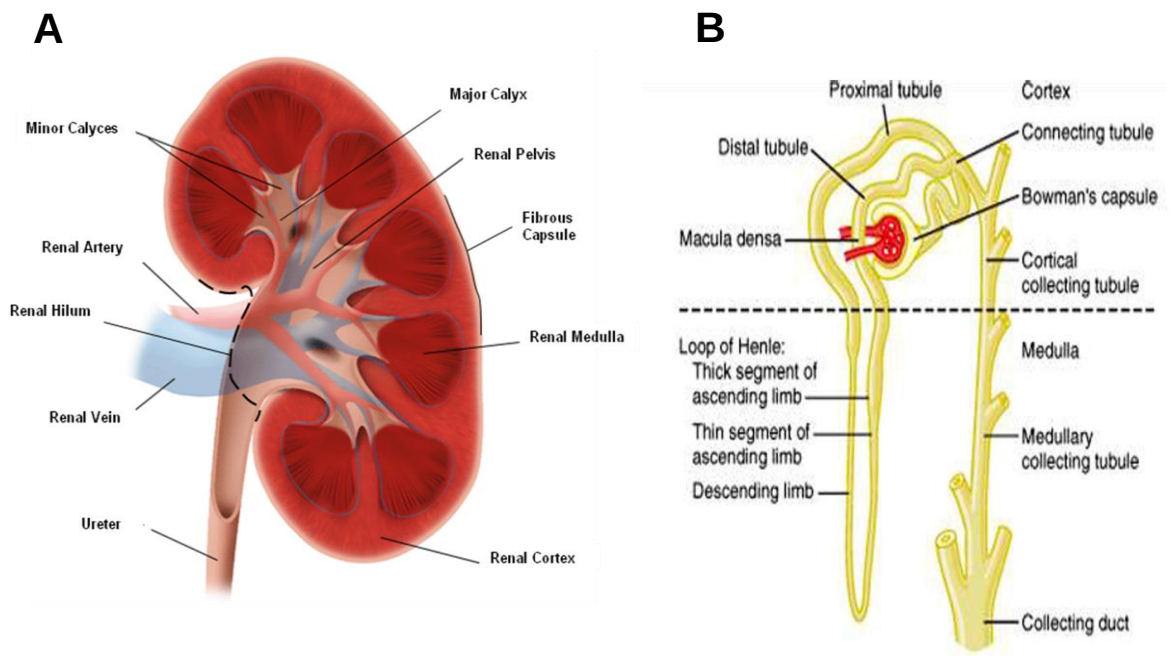

Figure 1.1: Anatomy of the mammalian kidney and nephron. (A) A fibrous capsule encompasses the kidney. On the medial aspect of the organ, the renal hilum allows passage of the renal vasculature and the ureter (the renal pelvis) into the inner portion of the organ. Further subdivision of the renal pelvis gives rise to the major and minor calyces. (B) Diagrammatic representation of the glomerulus and associated tubular network which form a nephron. The dotted line indicates the cortical-medullary boundary. As blood is filtered by the glomerulus, filtrate collects in the Bowman's capsule and passes through the proximal tubules, through the loop of Henle, into the distal tubule and finally into the collecting duct system. Image modified from (Guyton 2000).

The kidney is divided into an outer cortex and an inner medulla. The cortex contains the renal corpuscles, segments of the proximal and distal convoluted tubules, as well as portions of the collecting ducts. The medulla contains a specialised segment of the nephron, the Loops of Henle, associated vasculature (vasa recta and venulae recta) and the collecting ducts.

1.2.2 The nephron

Nephrons are the functional units of the kidney (Figure 1.1B). They filter wastes from the blood and reabsorb water, inorganic ions, glucose and amino acids to maintain homeostasis (Vander 1995). Blood enters the glomerulus, a tuft of

capillaries, via the afferent arteriole and is filtered through the glomerular filtration barrier, with the filtrate collected in the Bowman's space (urinary space) of the renal corpuscle. The remaining blood passes into the efferent arteriole and then to the peritubular capillaries, finally exiting the kidney via the renal venous system. The ability of filtrate to pass through the walls of the glomerular capillaries is dependent on the three structures which form the glomerular filtration barrier: the glomerular endothelial cells, the glomerular basement membrane, and the filtration slit diaphragms located between the interdigitating foot processes of glomerular podocytes (Pavenstadt et al. 2003). The glomerular filtration barrier is freely permeable to water and small solutes. However, larger molecules, such as proteins with a molecular weight greater than approximately 68,000 are unable to cross the barrier and are retained within the circulation (Pavenstadt et al. 2003).

Filtrate collected in the urinary space passes to the proximal convoluted tubule. It is here that approximately 65% of the filtered sodium and water are reabsorbed by the nephron. The specialised epithelial cells of the proximal tubule have an extensive apical brush border, are highly metabolic and contain a large number of mitochondria to support the energy requirements of the cell to participate in active transport. Filtrate then passes into the first of three segments (thin descending limb; thin ascending limb and thick ascending limb, respectively) of the Loop of Henle (Figure 1.1B). The passage of fluid through the Loop of Henle determines urinary concentration via a 'counter-current mechanism' (Guyton 1991). Under the 'counter-current mechanism', remaining sodium is removed from the filtrate by sodium pumps in the thick ascending limb of the loop and concentrated external to the nephron in the renal interstitium. The high concentration of sodium draws tubular fluid into the interstitium, decreasing tubular fluid osmolarity while conversely increasing renal interstitial osmolarity. Sodium and water are removed from the renal interstitium by the vasa recta. The remaining filtrate then passes from the thick ascending limb to the distal tubule where NH_3, H^+ and uric acid are secreted from the blood into the tubules.

The final process of urinary excretion involves the collecting duct system. While 90% of water reabsorption is carried out by the proximal and distal tubules, regulation of water reabsorption in collecting ducts is critical for the maintenance of

fluid homeostasis. The plasma membranes of collecting duct epithelial cells are permeable to water but impermeable to salt. Water therefore moves between renal tissue compartments according to the osmotic fluid gradient. This process is underpinned by hormonal regulation. Aldosterone, a hormone secreted by the adrenal gland, and arginine vasopressin (AVP) an antidiuretic hormone secreted by the hypothalamus in states of dehydration, are both critical regulators of sodium and water reabsorption by collecting ducts. Aldosterone and AVP activate basolaterally expressed sodium-potassium ATPase pumps and vasopressin 2 receptors (V2R) respectively. Activation of cell membrane targets by aldosterone increases luminal cell membrane permeability to sodium while AVP stimulation of V2R increases the permeability of collecting ducts to water (Guyton 2000).

1.2.3 Functions of the kidney

The kidney performs several important roles including removal and excretion of circulatory wastes and several endocrine functions; however, the major function of the kidney is to regulate fluid and electrolyte homeostasis. This is achieved through the excretion of water and electrolytes, in particular sodium (termed diuresis and natriuresis, respectively). Both processes occur under the influence of the renin-angiotensin-aldosterone system, renal nerves and the actions of AVP. As such, the kidney strongly regulates plasma volume and thus arterial pressure. Should sodium intake be increased, an accompanying increase in volume/water intake can result in an associated increase in arterial pressure (Vander 1995). Computer modelling approaches have demonstrated that to maintain arterial pressure in the presence of increased sodium or water intake, the kidneys will apply a negative feedback mechanism known as the 'pressure-natriuresis mechanism' (Figure 1.2) (Guyton et al. 1972; Guyton 1990). The pressure-natriuresis mechanism acts to counter any rise in arterial pressure and return to a point of equilibrium by increasing the excretion of sodium and water above the sodium and water intake. At the point of equilibrium, arterial pressure is maintained and the excretion of sodium and water by the kidneys is equal to the intake of both factors. Interestingly, the kidney will continue to excrete 'excess' sodium and water in an infinite capacity until arterial pressure has reached

equilibrium. It has therefore been described as having 'infinite gain' and is thus a powerful regulator of long-term blood pressure (Guyton et al. 1972; Guyton 1990).

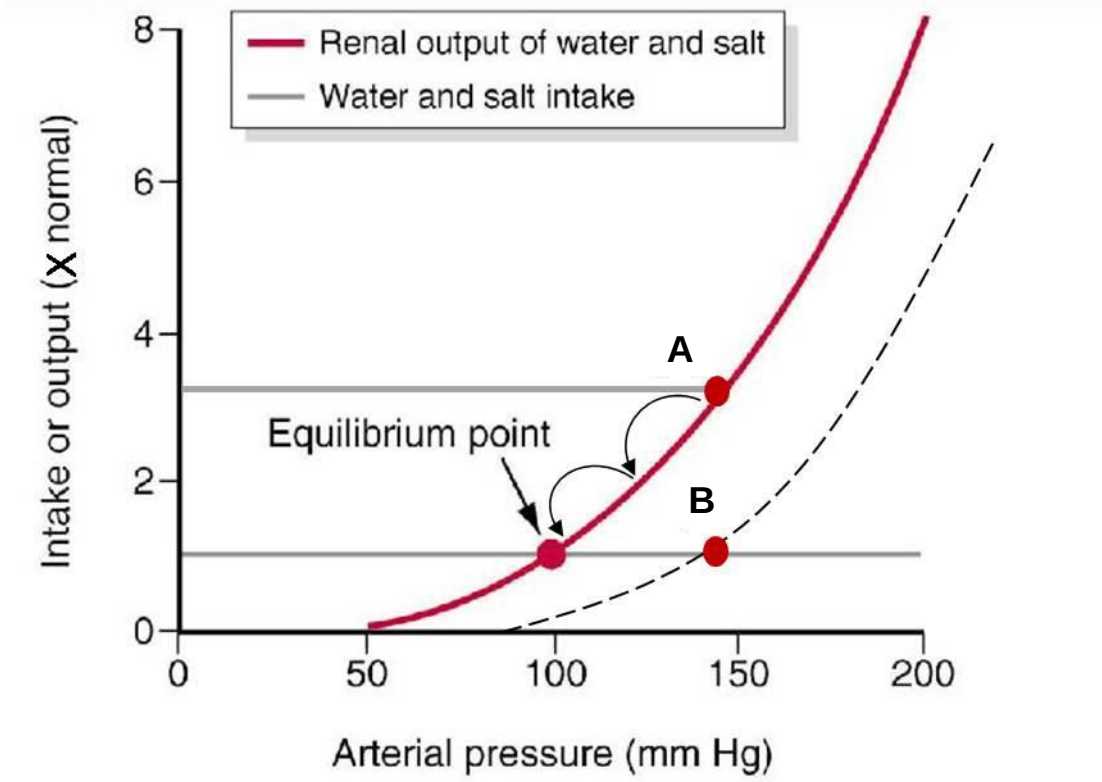

Figure 1.2: Pressure natriuresis curve. The curve represents arterial pressure in the presence of sodium (salt) intake. Arterial pressure homeostasis is established in the presence of normal sodium intake (red line). As intake increases, output must increase accordingly. Negative feedback, the 'pressure- natriuresis mechanism', returns arterial pressure to the equilibrium point (curved arrows). Elevation of arterial pressure is observed when either sodium intake is increased (A) or a rightward shift of the renal output curve occurs (B). Maintained shift of equilibrium point results in the development of hypertension. Image adapted from (Guyton 2000).

For chronic elevation of arterial pressure, or hypertension, to occur, it is considered that there must be a 'resetting' of the equilibrium set-point such that high arterial pressure is required to maintain sodium excretion. While chronic increases in sodium intake may play a role in the 'resetting' of this point, the development of hypertension remains largely idiopathic.

From this evidence it is quite clear that the kidney is critical in the regulation of homeostasis and for the sustainability of life. To fully understand the role of the

kidney in these processes, we must understand the origins and development of this organ.

1.3 DEVELOPMENT OF THE MAMMALIAN KIDNEY

In higher vertebrates, three pairs of excretory organs develop separately in a sequential manner; these are the pronephroi 'the primitive kidneys', the mesonephroi 'the middle kidneys' and ultimately the metanephroi 'the permanent kidneys' (Figure 1.3) (Kuure et al. 2000).

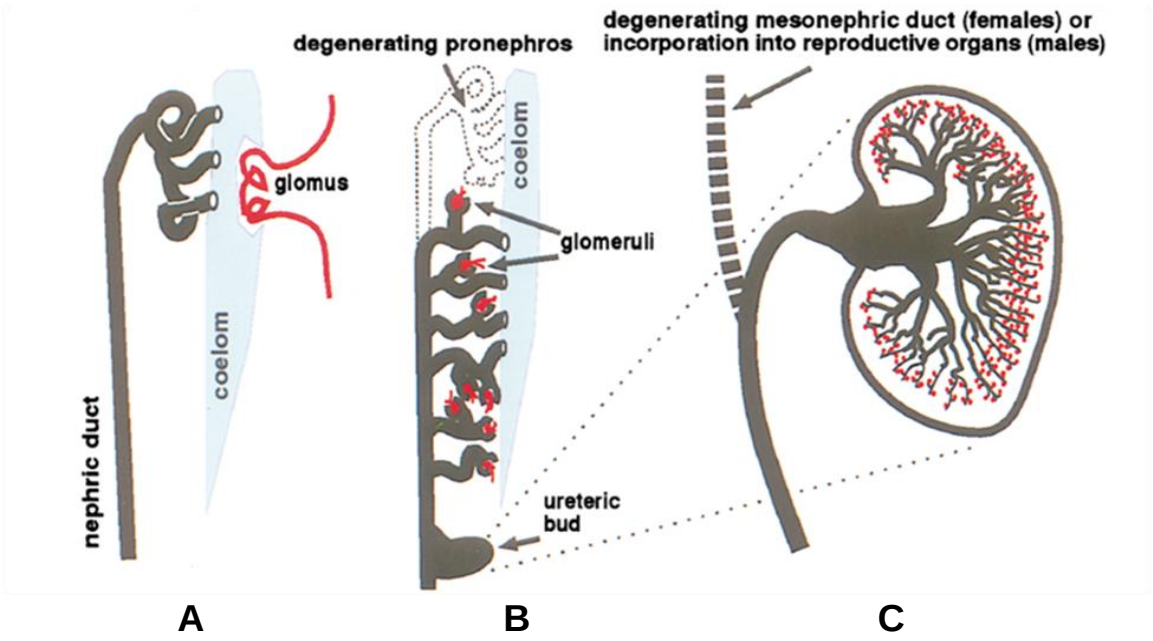

Figure 1.3: Three mammalian excretory organs: Pronephros, Mesonephros and Metanephros. (A) The pronephros comprises the glomus and associated nephric duct, projecting into the coelom. (B) Degeneration of the pronephros gives rises to structures which are incorporated caudally into the developing mesonephros. (C) Emergence of the ureteric bud from the Wolffian duct induces the formation of the permanent kidney, the metanephros. Image from (Vize et al. 1997).

1.3.1 Pronephros

During embryonic development, three primary tissue layers form: the ectoderm, mesoderm and endoderm. The mesoderm can be further subcategorised into the paraxial, intermediate and lateral plate mesoderm. The urogenital system arises from the intermediate mesoderm with the pronephros being the first tissue to form at approximately embryonic day (e) 8.0 in mice and in the third week of human gestation (Kuure et al. 2000). In mammals, the pronephros is a rudimentary structure containing a single non-integrated nephron consisting of multiple fused vascular structures forming a single structure called the glomus, and pronephric tubules attached to ciliated funnels called nephrostomes (Figure 1.3A) (Vize et al. 1997). Filtrate passes through the glomus into the coelom, where it is then propelled into the pronephric tubules via the action of the nephrostomes. Molecules are recovered from the filtrate in the pronephric tubules with waste passing to the pronephric duct. Whilst the filtration ability of the pronephros is poor in humans, the emergence of the pronephric duct, the early precursor structure for the Wolffian duct, is very important for subsequent kidney organogenesis (Solhaug et al. 2004).

1.3.2 Mesonephros

The mesonephroi develop caudally to the pronephroi between e10.0 – 10.5 in the mouse and in the third and fourth weeks of human gestation (Solhaug et al. 2004). The process begins with the pronephric duct inducing condensation of the mesonephric mesenchyme, leading to the development of mesonephric tubules along the Wolffian duct (Saxen and Sariola 1987; Kuure et al. 2000). These tubules give rise to primitive nephrons, which in mammals possess limited filtration and excretory functionality (Figure 1.3B). In females, the mesonephros regresses substantially and is replaced by the female gonad, whilst in males portions of the mesonephric tubules are incorporated into the developing male reproductive tissues (Smith and Mackay 1991; Solhaug et al. 2004). Formation of the mesonephros is not only a critical transitory stage in the development of the metanephric kidney but also contributes to the aorta-gonad-mesonephros region, a precursor region from which haemopoietic stem cells will migrate into the fetal liver (Kumaravelu et al. 2002).

1.3.3 Metanephros

The metanephros, the 'permanent kidney', is the functional kidney of mammals (Figure 1.3C) (Kuure et al. 2000). Development commences during the 5th week of human gestation and between e10.5 and e11.0 in mice. Metanephric development begins when an outgrowth from the Wolffian duct, known as the ureteric bud, grows towards and invades a specific mass of the intermediate mesoderm, the metanephric mesenchyme (MM), (Figure 1.4) (Saxen and Sariola 1987). Reciprocal molecular interactions between these two tissues induce arborisation of the ureteric bud into the ureteric tree and eventually into the collecting ducts, calyces and renal pelvis of the permanent kidney (Figure 1.4) (Vize et al. 1997). The process of invasion also induces condensation of MM cells forming the cap mesenchyme. Following condensation, a small number of cells, approximately 4 to 6 cells, located at the lateral edge of the cap mesenchyme proliferate rapidly and give rise to pre-tubular aggregates which subsequently undergo mesenchymal-to-epithelial transition, a process deemed one of the first stages of nephrogenesis (the formation of nephrons) (Sariola 2002). MM cells condensing at the tips of the ureteric tree are induced to form renal vesicles, which transition to comma-shaped and S-shaped bodies, the lower limb of which forms the renal corpuscle. Following nephrogenesis, developing nephrons undergo maturation to give rise to a functional nephron capable of filtration, the maintenance of fluid homeostasis and the regulation of the concentration of ions and inorganic solutes within the circulatory system (Vize et al. 1997).

Importantly, nephrogenesis is complete at 36 weeks gestation in humans (that is before term birth) with no new nephrons forming beyond this point. In contrast, nephrogenesis in rodents, including mice, is incomplete at birth. Cessation of nephron development occurs by approximately postnatal day (PN) 5 in mice (Solhaug et al. 2004; Sims-Lucas et al. 2008).

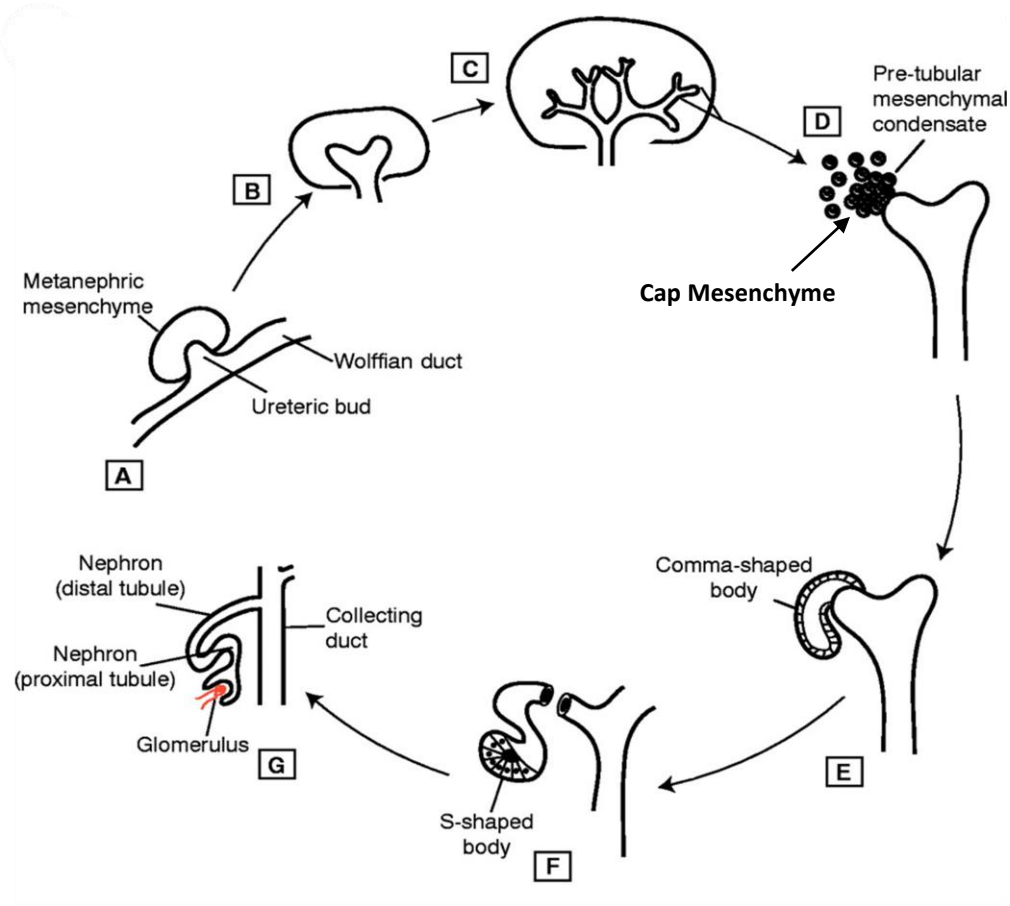

Figure 1.4: Overview of Metanephric Development. The ureteric bud emerges from the Wolffian duct and invades the MM (A) before undergoing initial branching morphogenesis (B) and giving rise to the ureteric tree, the presumptive collecting duct system of the mature kidney (C). Mesenchymal cells condense at the tip of ureteric branches to form cap mesenchyme and pre-tubular aggregates (D). Aggregates differentiate and transition to comma-shaped (E) and S-shaped bodies (F) eventually giving rise to components of the nephron, including the glomerulus and the renal tubules (G). Image adapted from (Shah et al. 2004).

1.4 MOLECULAR REGULATION OF METANEPHRIC DEVELOPMENT

Much of our understanding of the molecular regulation of metanephric development has come about through the advent of transgenic and knockout animal models, the ability to directly manipulate the expression of candidate genes and the ability to analyse tissue formation external to the developing embryo (Reidy and Rosenblum 2009). Such knowledge has led to greater understanding of both normal and abnormal development of the metanephros. In this section, our current

understandings of the molecular networks governing key stages of metanephric development are discussed. Metanephric induction, the regulation of GDNF expression, ureteric branch patterning and inhibition, and nephrogenesis will be described in turn.

As the number of molecular candidates and hypotheses regarding their possible roles is ever expanding, it is beyond the scope of this Introduction to discuss all regulatory factors. Rather, I have focused on key factors regulating important developmental stages as well as members of the TGFβ superfamily which are relevant to the animal models considered in this thesis. For recent overviews of the molecular regulation of metanephric development see (Michos 2009; Reidy and Rosenblum 2009; Shah et al. 2009).

1.4.1 Metanephric induction

1.4.1.1 GDNF, RET and GFRA1

Induction of the metanephric kidney is a simple process, but it is regulated by a complex molecular dialogue. Glial cell line-derived neurotrophic factor (GDNF), a distant member of the TGFβ superfamily, was the first defined inducer of metanephric development (Hellmich et al. 1996; Sainio et al. 1997; Shakya et al. 2005; Costantini and Shakya 2006). In *in vitro* experiments in which mouse Wolffian ducts were isolated and cultured in the presence of GDNF-soaked beads, GDNF alone induced ectopic budding of the ureteric epithelium proximal to the soaked bead (Sainio et al. 1997). In the developing mouse metanephros, the earliest detectable transcripts for *Gdnf* via reverse transcription polymerase chain reaction (RT-PCR) are observed in the MM at e10.0 (Hellmich et al. 1996; Towers et al. 1998). GDNF secreted from the MM, acts in a paracrine fashion on the developing ureteric epithelium through a receptor complex consisting of the RET receptor, a receptor tyrosine kinase and GDNF receptor alpha 1 (GFRA1), a GPI-linked protein which binds GDNF allowing activation of the RET receptor (Figure 1.5) (Cacalano et al. 1998; Tomac et al. 2000). Both receptors are expressed at the same developmental stage as *Gdnf* transcripts. However, whilst transcripts of *Gfra1* are detected in both

the MM and developing ureteric bud, transcripts for *Ret* are restricted to the ureteric bud (Towers et al. 1998).

Prior to invasion of the MM by the ureteric bud, a peak in *Ret* and *Gfra1* expression is observed on the caudal surface of the out-growing ureteric bud. However, as the bud invades the MM the expression of both receptors becomes localised to the tips of each branch of the ureteric tree. This consequently restricts GDNF signalling capacity and, in turn, ureteric branching morphogenesis, to these specific regions of the developing metanephros (Lechner and Dressler 1997; Tomac et al. 2000). Interestingly, *Ret* expression in the early ureteric bud has been shown to be required for ureteric epithelial cell arrangement prior to the subsequent initiation of ureteric budding and branching morphogenesis (Chi et al. 2009). The necessity for all three of these signalling components in the normal development of the metanephros is exemplified by the overlapping renal phenotypes exhibited by mice carrying null mutations for *Gdnf*, *Ret* or *Gfra1*: all three mice lines exhibit either complete renal agenesis due to a failure in the formation of the ureteric bud from the Wolffian duct or severe renal dysplasia due to severe deficiency in the branching of the ureteric tree (Moore et al. 1996; Sanchez et al. 1996; Schuchardt et al. 1996; Cacalano et al. 1998).

1.4.1.2 BMP4 and WNT11

The site at which GDNF induces ureteric budding is determined by the absence of BMP4, another member of the TGFβ superfamily of signalling molecules. In metanephric development, BMP4 is expressed from e10.5 by a specific subpopulation of mesenchymal cells located on the caudal surface of the MM adjacent to the Wolffian duct (Miyazaki et al. 2000).

The major function of BMP4 during the initial stage of metanephric development is to antagonise the actions of GDNF, orchestrating the site at which the ureteric bud will emerge from the Wolffian duct (Raatikainen-Ahokas et al. 2000). *In vitro* studies of the direct actions of BMP4 have highlighted that both ureteric budding and subsequent branching in e10.0 mouse urogenital ridges are arrested in the presence of increasing concentrations of rh-BMP4. Such concentrations also decreased *Gdnf* mRNA expression demonstrating a direct antagonistic relationship

between these signalling pathways (Raatikainen-Ahokas et al. 2000). Further analysis has suggested that the antagonistic relationship between GDNF and BMP4 may involve disruption to the functions of an epithelially-expressed secreted glycoprotein, wingless-related MMTV integration site 11 (WNT11) (Majumdar et al. 2003; Michos et al. 2007).

Wnt11 is expressed from e10.5 in the epithelium of the ureteric bud, and is a downstream regulator of ureteric budding and branching morphogenesis (Kispert et al. 1996). WNT11 functions in a positive feedback loop with GDNF to propagate GDNF secretion by the MM (Kispert et al. 1996; Majumdar et al. 2003). *Wnt11* null mutant mice exhibit ureteric budding and initiation of metanephric development. However, subsequent *Gdnf* expression is significantly decreased and ureteric branching is severely impacted resulting in a hypoplastic phenotype (Majumdar et al. 2003).

Culture of mouse metanephroi with exogenous Gremlin-1 (*Grem-1*), a specific BMP4 antagonist, results in ectopic ureteric budding morphogenesis and up-regulated expression of *Gdnf* and *Wnt11* within their respective tissues (Michos et al. 2007). Conversely, genetic ablation of *Grem-1* results in decreased *Gdnf* expression within the MM but complete loss of *Wnt11* expression within the ureteric epithelium, suggesting that BMP4 antagonises GDNF signalling by inhibiting epithelial *Wnt11* up-regulation (Figure 1.5) (Michos et al. 2007).

The consequences of perturbations to BMP4 on ureteric budding is illustrated in *Bmp4* heterozygous mice, which display ectopic budding from the Wolffian duct, resulting in a wide range of congenital abnormalities of the kidney and urinary tract (CAKUT), including duplex ureter formation, hydronephrosis, and hypoplastic and dysplastic kidneys (Miyazaki et al. 2000). The association of BMP4 with the development of CAKUT phenotypes was further highlighted by the recent identification of three separate *Bmp4* missense mutations (S91C, T116S, N150K) in five paediatric CAKUT patients (Tabatabaeifar et al. 2009). All three mutations were shown to decrease the level of *Bmp4* mRNA in renal tissues, with S91C and N150K mutations correlating with disruptions in the subcellular localisation of BMP4 protein following translation.

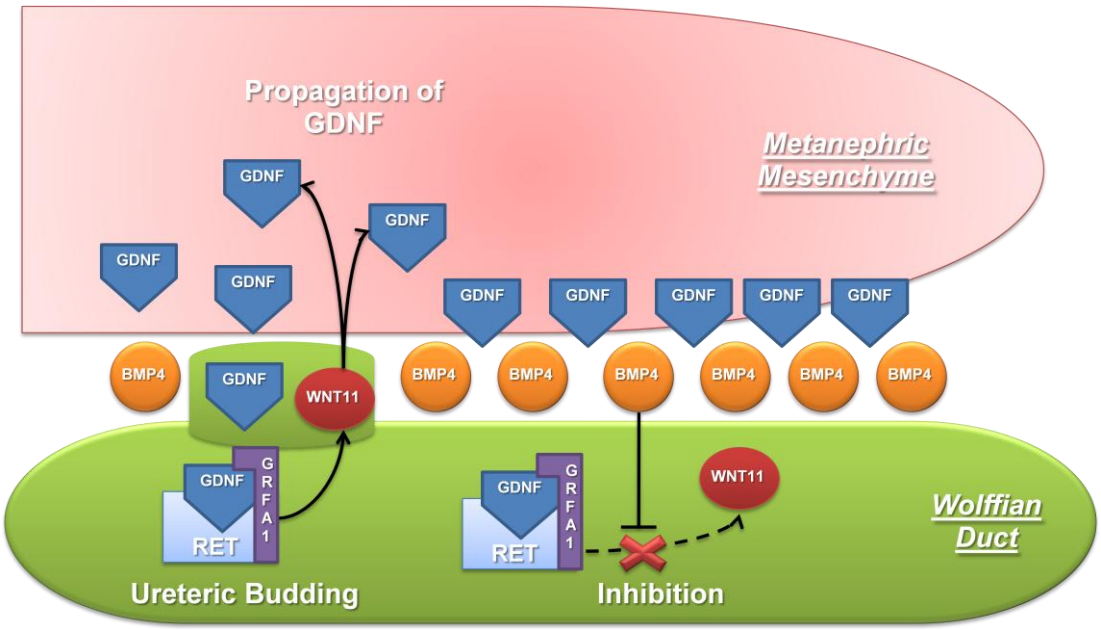

Figure 1.5: Induction of ureteric budding. Emergence of the ureteric bud from the Wolffian duct requires GDNF to bind RET/GFRA1. Transactivation of WNT11 initiates the formation of the ureteric bud. Antagonism of this signalling pathway by BMP4 coordinates the site of bud formation, preventing ectopic ureteric bud formation.

1.4.2 Regulation of *Gdnf* expression

As described above, *Gdnf* is a definitive inducer of metanephric development and a key molecule in the development of nephrons in the metanephros. This finding led to much interest in understanding the signalling network which governs the regulation of *Gdnf* within the MM. As described below, the EYA/SIX/PAX signalling network is evolutionarily conserved, present in a wide range of developing tissues and experimental models, and is believed to be a master regulator of GDNF and consequently metanephric induction (Figure 1.6) (Brodbeck and Englert 2004).

1.4.2.1 EYA1

Eyes absent homologue 1 (*Eya1*) was the first gene identified as necessary for the specification of the MM from the intermediate mesoderm. From e8.5, *Eya1* expression within the intermediate mesoderm becomes progressively restricted to the site of the future defined MM (Sajithlal et al. 2005). Following induction of the

MM by the invading ureteric bud, *Eya1* expression is maintained in the MM. Interestingly, the EYA1 expression profile observed at this stage mirrors that of *Gdnf,* suggesting a possible interaction between *Eya1* and *Gdnf* expression in the MM. This was subsequently confirmed through the characterisation of *Eya1* mutant mice (Xu et al. 1999; Grieshammer et al. 2004; Sajithlal et al. 2005). In mice, *Eya1* haploinsufficiency results in the development of phenotypes similar to an autosomal dominant inherited condition in humans, branchio-oto-renal syndrome, which involves conductive hearing loss and renal defects (Xu et al. 1999; Vervoort et al. 2002; Chang et al. 2004). However, in mice completely lacking *Eya1*, these phenotypes are exacerbated such that mice completely lack ears and exhibit bilateral renal agenesis, both of which are caused by extensive apoptosis of precursor tissues due to deficiencies in inductive signalling during organ development (Xu et al. 1999). Further analysis showed that the renal agenesis in *Eya1*$^{-/-}$ mice was due to a lack of ureteric bud formation, and therefore, a loss of metanephric induction characterised by loss of MM *Gdnf* expression (Xu et al. 1999). This finding highlights that EYA1 is a critical regulator of GDNF and, in turn, metanephric induction.

1.4.2.2 SIX1

EYA1 interacts directly with Sine oculis-related homeobox 1 homologue (SIX1) to regulate the downstream expression of *Gdnf* in the MM (Figure 1.6). *Six1* is expressed in the uninduced MM at e10.5. However, by e11.5 expression is observed in the induced MM proximal to the invading and branching ureteric epithelium (Xu et al. 2003). The major role for SIX1 during metanephric induction is to bind to EYA1 and transport the factor to the nucleus of mesenchymal cells and to then form part of the transcriptional machinery required for the initiation of gene transcription (Ohto et al. 1999).

The requirement for SIX1 is demonstrated in *Six1*$^{-/-}$ mice which display renal agenesis (Xu et al. 2003; Ruf et al. 2004). In *Six1*$^{-/-}$ mouse embryos, both the MM and ureteric bud form. However, both are much smaller than wildtype tissues and fail to satisfactorily induce metanephric development (Xu et al. 2003). As EYA1 expression is unchanged in *Six1*$^{-/-}$ mice, it was believed that a failure to activate downstream transcriptional activator Paired box transcription factor-2 (PAX2) was the cause of

the subsequent renal agenesis. This evidence further strengthens the hypothesis that EYA1 and SIX1 act at the same hierarchical level during the induction of metanephric development (Figure 1.6). Lastly, recent genetic mapping studies of patients with branchio-oto-renal syndrome have discovered mutations in not only *EYA1* but also *SIX1*. The common pathology between both mutant phenotypes suggests that whilst these factors function at a similar level in the hierarchy governing metanephric development, they are neither interchangeable nor able to compensate for the loss of the other (Ruf et al. 2004; Kochhar et al. 2008).

1.4.2.3 PAX2

PAX2 plays a role in the orchestration of gene expression during development of the kidney (Torban et al. 2006). *Pax2* expression is observed in the intermediate mesoderm prior to metanephric development, suggesting it, may play a key role in the specification of the intermediate mesoderm from mesodermal tissue lineages and also early patterning of the subsequent metanephros (Torres et al. 1995). During the initial stages of metanephric development, *Pax2* expression can be observed in both the uninduced MM and the epithelium of the emerging ureteric bud (Torres et al. 1995). This differential tissue expression of *Pax2* is associated with multiple levels of regulation of GDNF signalling (Brophy et al. 2001). Within the MM, *Pax2* acts downstream of *Eya1* and *Six1* to regulate GDNF expression (Figure 1.6), while in ureteric epithelium *Pax2* acts to regulate the expression of the associated GDNF receptors, *c-Ret* and *Gfrα1* (Clarke et al. 2006).

As described in Section 1.3.3, following ureteric branching morphogenesis, MM cells are induced to condense at the tips of the ureteric tree and differentiate to form primitive nephron structures. MM cells committed to nephrogenesis aggregate to form renal vesicles and comma and S-shaped bodies which all exhibit high levels of *Pax2* expression (Dressler and Douglass 1992). However, cells not induced to undergo mesenchymal-to-epithelial transition exhibit down-regulated *Pax2* expression and undergo apoptosis (Dziarmaga et al. 2003). As nephrons and glomeruli in particular continue to mature, *Pax2* expression is attenuated with mature nephrons exhibiting negligible levels of PAX2 expression (Dressler et al. 1990). Co-ordination of both ligand and receptor expression allows tight control over

critical aspects within a developing system. However, this also means that perturbations to *Pax2* can induce severe developmental defects. *Pax2* homozygous null mice exhibit a lack of ureteric budding, bilateral renal agenesis and high levels of apoptosis in a primitive, but defined MM (Torres et al. 1995). In accordance with these murine data, point mutations in the *PAX2* gene in humans is associated with renal hypoplasia and ureter defects in a condition known as Renal-Coloboma syndrome (Sanyanusin et al. 1995; Eccles 1998). However, persistent expression of *Pax2* in mice following normal development can also result in a pathological renal phenotype which resembles congenital nephrotic syndrome in humans (Dressler et al. 1993).

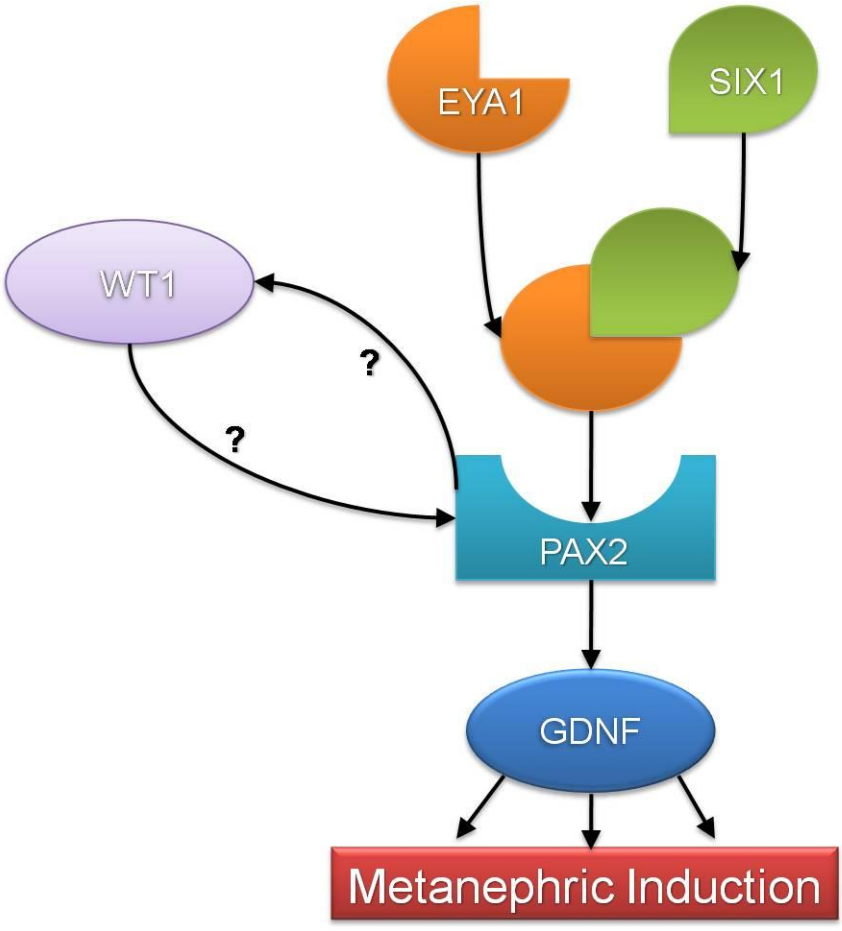

Figure 1.6: Signalling network governing GDNF expression. Transcription factors EYA1 and SIX1 interact directly to form a complex and induce up-regulation of the downstream transcriptional regulator PAX2. WT1 potentially cooperates with PAX2 in an auto-regulatory loop to regulate the expression of both factors. PAX2 further induces the expression of GDNF and the induction of metanephric development.

1.4.2.4 WT1

The final factor of interest that is both critical for the induction of metanephric development and is suggested to be associated with the EYA/SIX/PAX signalling network is Wilm's Tumour-1 (WT1). WT1 is a zinc finger transcription factor expressed at e9.0 in the intermediate mesoderm destined to form the urogenital ridge and, much like *Eya1* and *Pax2,* is believed to define the MM (Kreidberg et al. 1993; Discenza et al. 2003). Initial *Wt1* knockout studies in mice indicated the requirement for WT1 in the induction of metanephric development (Figure 1.6) as all homozygous null mice exhibited bilateral renal agenesis due to apoptosis of the MM (Kreidberg et al. 1993). These findings suggest WT1 is required not only for the development of the ureteric bud but for the survival of the MM during metanephric development.

The molecular profile of *Wt1* null metanephroi indicates that both *Pax2* and *Gdnf* transcripts are detectable at wildtype levels in the MM prior to the onset of apoptosis. However, no protein was detected, suggesting that factors within the signalling network may be regulated at the post-transcriptional stage (Kreidberg et al. 1993; Brodbeck and Englert 2004). Analysis of compound heterozygous mutants for both *Wt1* and *Pax2* genes, $Wt1^{+/-}/Pax2^{1neu/+}$, suggest a cooperative interaction between these factors during metanephric development (Discenza et al. 2003). While both $Wt1^{+/-}$ and $Pax2^{+/-}$ mutant mice exhibit abnormal renal development, compound mutants possess a more severe phenotype, including renal hypodysplasia and decreased nephrogenesis, both believed to be due to increased apoptosis in the MM (Discenza et al. 2003). Further complexity in the relationship between WT1 and PAX2 was revealed from gene profiling of patients with acute myeloid leukaemia (Siehl et al. 2003). Real-time PCR has indicated that a small population of acute myeloid leukaemia patients show a correlation between an upregulation of *PAX2* and *WT1* mRNA (Siehl et al. 2003). It was concluded that PAX2 may be able to upregulate the expression of WT1 within specific tissues and within a specific environment. However, the fact that this correlation was only observed in 11 of 43 samples analysed suggests that additional candidates may need to be investigated to further understand this relationship (Siehl et al. 2003).

Whilst the complex intricacies of the EYA/SIX/PAX/WT1 signalling network have yet to be fully characterised, the use of knockout mouse models has clearly

indicated the importance of the regulation of GDNF for induction, and subsequent normal development, of the metanephros.

1.4.3 Branching inhibition and patterning

Development of the metanephric kidney is reliant not only on induction and propagation of developing structures and tissues but also on the regulation of developmental patterning (Meyer et al. 2004). However, inhibitory signalling is also required during development for harmonious organogenesis to occur. Both *in vitro* and *in vivo* studies have suggested that members of the TGFβ superfamily serve a range of diverse functions during metanephric development, including the inhibition of ureteric branching morphogenesis and the promotion of MM survival during organogenesis. While BMP4 is observed at e10.5, transcripts for the three mammalian TGFβ isoforms (TGFβ1-3) and activin A are detectable in the developing mouse metanephros from e11.5 (Dudley et al. 1995; Sakurai and Nigam 1997; Sanford et al. 1997; Miyazaki et al. 2000; Plisov et al. 2001; Bush et al. 2004; Oxburgh et al. 2004; Hartwig et al. 2005; Michos et al. 2007; Sims-Lucas et al. 2008). The role of these factors will be discussed in turn.

1.4.3.1 BMP4

Following coordination of the site of ureteric budding (Section 1.4.2.1), BMP4 is exclusively expressed by the MM cells surrounding the trunk of the invading ureteric bud and the base of each subsequent branch of the ureteric tree, and at e14.5 expression is observed in developing glomeruli (Miyazaki et al. 2000). Such localised expression is hypothesised to be integral for inhibiting ectopic branching events, thereby maintaining the dichotomous branching pattern observed during normal development, and elongation of the developing branches (Miyazaki et al. 2000; Miyazaki et al. 2003). This complex role was highlighted in mouse metanephric explants exposed to exogenous BMP4 (Cain et al. 2005). While exogenous BMP4 significantly inhibited ureteric branching more greatly in the posterior region of the kidney, branch length in exposed explants was significantly longer when compared to control metanephroi (Cain et al. 2005). BMP4 expression alongside the trunk of the

developing ureteric bud has also been associated with elongation of the ureteric bud itself, in a process which gives rise to early components of the ureteric tree and ureter (Miyazaki et al. 2000; Miyazaki et al. 2003).

1.4.3.2 TGFβ

Much of what we know about the role of TGFβ isoforms during development has come from reverse genetic approaches. However, while all three mammalian isoforms are expressed during metanephric induction and throughout development, the specific role of each isoform during these events remains unclear. *Tgfb1*$^{-/-}$ and *Tgfb3*$^{-/-}$ mice do not exhibit developmental defects of the kidney but have defects of the immune and respiratory systems respectively, both of which result in neonatal death (Letterio et al. 1994; Kaartinen et al. 1995). Nevertheless, explanted metanephroi cultured in the presence of increasing concentrations of human recombinant TGFβ1 were smaller, had arrested ureteric branching morphogenesis and displayed increased apoptosis in the nephrogenic zone when compared to control metanephroi (Clark 1998; Michael and Davies 2004). While these data suggest TGFβ1 is a potent inhibitor of ureteric branching morphogenesis, the lack of an *in vivo* kidney phenotype in the *Tgfb1*$^{-/-}$ mouse suggests that some redundancy in function exists amongst the TGFβ isoforms in the developing kidney (Pelton et al. 1991; Oxburgh et al. 2004).

Interestingly, TGFβ2 appears to have some novel roles during metanephric development. *In vitro* analysis of the direct effect of TGFβ2 on ureteric branching demonstrated that TGFβ2, like TGFβ1, is a potent inhibitor of branching morphogenesis in explanted mouse metanephroi (Sims-Lucas et al. 2010). Also, ureteric trees which developed in the presence of exogenous TGFβ2 exhibited severe distortion of the usual dichotomous branching pattern observed in control metanephroi (Sims-Lucas et al. 2010). These data suggest TGFβ2 functions, like TGFβ1, as an inhibitor of ureteric branching morphogenesis. However, characterisation of the *in vivo* role of TGFβ2 during metanephric development, through the generation of the *Tgfb2* knockout mouse, has brought about much more conjecture as to the specific function of this signalling molecule. *Tgfb2* null (*Tgfb2*$^{-/-}$) mutant mice display variable renal phenotypes, including dysplastic ureteric tree

formation, impaired glomerulogenesis, apoptosis of the ureteric epithelium and MM, and renal agenesis (Sanford et al. 1997; Michael and Davies 2004; Sims-Lucas et al. 2008). The similar phenotypes of impaired ureteric branching morphogenesis seen in *Tgfb2*$^{-/-}$ metanephroi and wildtype metanephroi exposed to exogenous TGFβ2 suggest that a dose-dependent activity gradient for this signalling molecule may function in the developing kidney. This notion was further strengthened by the development of high resolution *in vivo* embryonic metanephric imaging, optical projection tomography, in which it was illustrated that *Tgfb2*$^{+/-}$ mice at e15.5 exhibit a significant reduction in ureteric branching morphogenesis compared to age-matched wildtype embryos (Short et al. 2010). Together these data highlight that the role of TGFβ2 during ureteric branching may be more than simply an inhibitor. Additional research is required to identify those factors responsible for the establishment of this possible TGFβ2 signalling gradient.

1.4.3.3 Activin A

Much like TGFβ2, activin A has been hypothesised to have dual roles in metanephric development. Currently, there are four known activin subunits, activin βA, βB, βC and βE. From these subunits βA and βB can form homodimeric activin A, activin B and the heteromeric A/B, whilst βC and βE have only been shown *in vitro* to form homodimeric activin C, activin E and the heteromeric C/E complexes (Wada et al. 2005). To date, only activin A has been associated with the regulation of metanephric development (Maeshima et al. 2006). *In vitro* analysis has determined that activin A is secreted by the ureteric epithelium and acts on both MM and ureteric epithelium. In MM, activin A directly inhibits the secretion of GDNF and is also required for cellular differentiation within the MM to occur (Maeshima et al. 2006). In the ureteric epithelium, activin A functions in an autocrine manner to down-regulate PAX2 expression and inhibit cell proliferation, together negatively regulating ureteric branching morphogenesis (Maeshima et al. 2006). *In vitro* inhibition of activin A function via either specific activin A antagonists or siRNA directed at the *Inhba* gene, which encodes the activin βA subunit, has been shown to increase sensitivity of ureteric epithelium to both endogenous and exogenous sources of GDNF, resulting in ectopic ureteric budding and altered ureteric bud morphogenesis

(Maeshima et al. 2006). Although activin A was shown to be quite potent *in vitro*, ablation of *Inhba*, which greatly impacts on the production of activin A and inhibin A, did not result in a renal phenotype in *Inhba* null mice, possibly due to functional redundancy between multiple TGFβ superfamily members expressed during kidney formation (Maeshima et al. 2008).

In transgenic mice expressing a dominant-negative truncated type 2 activin receptor (tActR-II), metanephric development was not grossly affected; however, histomorphometric analysis of mature kidneys from these mice at 2 months of age demonstrated an 80% increase in the number of glomeruli per area of kidney tissue (Maeshima et al. 2000). The development of an augmented nephron number phenotype in these mice will be discussed in Section 1.6.2.2. However, Maeshima et al (2000), conceded that disruption of signalling at the receptor level may have impacted the function of multiple factors. More specifically, TGFβ superfamily member BMP7 also binds directly to the type 2 activin receptor. However, *BMP7* null mutant mice develop a dysplastic renal phenotype (Dudley et al. 1995; Yamashita et al. 1995), not an augmented renal phenotype, suggesting that the renal phenotype in tActR-II mice arises due to the loss of activin A function. Together, these data demonstrate the requirement of developmental inhibition for normal kidney organogenesis.

1.4.4 Nephrogenesis

The formation of nephrons is reliant on both the condensation and mesenchymal-to-epithelial transition (MET) of MM, following induction from the adjacent ureteric epithelium. However, while both processes are acknowledged as being vital steps in kidney organogenesis, surprisingly little is known about the cellular populations and factors responsible for regulation of mesenchymal condensation and MET.

1.4.4.1. Cellular Populations: Cap mesenchyme and pretubular aggregates

Following metanephric induction, MM condenses at the tips of the branching ureteric tree and forms the cap mesenchyme from which pretubular aggregates

emerge (Mugford et al. 2008; Mugford et al. 2009). *In situ* hybridisation has shown that key metanephric regulators *Gdnf*, *Pax2* and *Wt1* are expressed throughout the induced cap mesenchyme (Sariola 2002). Cells of the cap mesenchyme in a specific location proximal to the ureteric tip and immediately adjacent to its basement membrane condense to form a ball of cells called the pretubular aggregate (Georgas et al. 2009). Sine oculis-related homeobox 2 homologue (SIX2), a homeodomain transcription factor, and wingless-related MMTV integration site 4 (WNT4), a glycoprotein secreted by the MM, have been identified as the key markers of cap mesenchyme and pretubular aggregate cellular populations, respectively (Kobayashi et al. 2008; Mugford et al. 2009). The induction and formation of pretubular aggregates is a consequence of exposure of cap mesenchyme to epithelially-derived growth factors, in particular wingless-related MMTV integration site 9b (WNT9b), TGFβ2, fibroblast growth factor 2 (FGF2) and leukaemia inhibitory factor (LIF; (Sakurai et al. 1997; Plisov et al. 2001; Carroll et al. 2005). In contrast, as previously mentioned, BMP4 has been hypothesised to inhibit the formation of mesenchymal aggregates within the induced MM (Miyazaki et al. 2000; Miyazaki et al. 2003). Pretubular aggregates continue to differentiate and form renal vesicles, which in turn give rise to all epithelial components of the mature nephron including the renal tubules and the renal corpuscle, with the collecting duct system being derived from the ureteric tree (Oxburgh et al. 2004; Kobayashi et al. 2008).

While the developmental process has been well documented the functionality of the cap mesenchyme and its derivatives is still unclear. However, the recent classification of cellular subpopulations within the cap mesenchyme has provided a change to the prevailing dogma such that this structure is no longer viewed as a homogeneous cellular population. Further, this observation provides some basic genetic markers with which this population and subsequent structures can be investigated.

1.4.4.2 Cellular factors: SIX2 and WNT4

Six2 defines the self-renewing progenitor pool within the cap mesenchyme and is believed to be a key regulator of the period of nephrogenesis (Kobayashi et al. 2008). Recently it was observed that the cap mesenchyme can be further subdivided

into ten distinct subregions based upon genetic marker expression, however *Six2* expression is maintained throughout all regions (Mugford et al. 2009). *Six2* expression is lost during the cellular transition from cap mesenchyme to pretubular aggregate. This loss of expression is accompanied by up-regulated expression of *Fgf8*, *Wnt4*, and *Pax8*, all of which are essential for subsequent renal vesicle formation (Stark et al. 1994; Bouchard et al. 2002; Grieshammer et al. 2005). The importance of *Six2* in the maintenance of the pool of nephron progenitor cells was first illustrated by the generation of the *Six2*$^{-/-}$ knockout mouse (Self et al. 2006). While *Six2*$^{-/-}$ pups die prenatally, metanephroi undergo nephrogenesis but exhibit premature and ectopic differentiation of mesenchymal cells into epithelia, which results in severe renal hypoplasia (Self et al. 2006). While wildtype metanephroi contained renal vesicles on the ventral aspect of ureteric tips, *Six2*$^{-/-}$ metanephroi contained renal vesicles on both dorsal and ventral aspects of ureteric tips. Molecular analysis of these ectopic structures indicated up-regulation of *Wnt4* expression, confirming renal vesicle formation.

Over-expression of *Six2* during metanephric development represses MM differentiation. The importance of regulating *Six2* expression during nephrogenesis was further highlighted by Kobayashi et al. (2008) who showed that as metanephric, and in turn nephron, development continues, the ratio of *Six2+* cells associated with a ureteric tip decreases dramatically from approximately 5,000 cells per tip at E11.5 to approximately 60 cells per tip at P1, an approximate 83-fold change over the course of development (Kobayashi et al. 2008). Finally, five patients with renal hypodysplasia have been shown to carry a heterozygous missense mutation in the *SIX2* gene (Weber et al. 2008). However, due to the variability of the renal hypodysplasia phenotype between patients, Weber et al. (2008) concluded that the development of renal hypodysplasia was not directly linked to *SIX2* function. Instead, they hypothesised that loss of *SIX2* function imbalanced the molecular signalling network which governs metanephric development (Weber et al. 2008).

WNT4, a definitive marker of pre-tubular aggregates and renal vesicles, is first detected at e11.5 in pre-tubular aggregates and is then detected in all subsequent renal vesicles and early glomerular structures (Stark et al. 1994). Wnt4 signals through the canonical Wnt signalling pathway stimulating the trans-nuclear location

of β-catenin to induce downstream gene expression (Iglesias et al. 2007). Culture of isolated MM in the presence of WNT4 induces mesenchymal condensation, renal vesicle formation and the development of renal tubules, demonstrating WNT4 to be a potent developmental inducer (Kispert et al. 1998). Interestingly, in an *in vitro* environment, other members of the Wnt signalling family, WNT1, WNT3a, WNT7a and WNT7b were also able to sufficiently induce similar tubulogenesis in isolated MM, suggesting some functional redundancy between Wnt family members (Kispert et al. 1998).

The requirement for WNT4 for epithelialisation of mesenchymal cells was observed through the generation of *Wnt4* null mice (Stark et al. 1994), which die within 24 hours of birth and display severe renal hypoplasia (Stark et al. 1994). Analysis of *Wnt4* null metanephroi revealed normal ureteric branching morphogenesis but an absence of defined renal vesicles and mesenchymal condensates, believed to be due to an absence of the auto-induction of MM condensation and subsequent MET (Kispert et al. 1998; Torban et al. 2006). The addition of secreted frizzled-related protein 1 (sFRP1), an inhibitor of Wnts, to isolated metanephroi or induced MM did not inhibit mesenchymal condensation but did yield a similar lack of tubule formation to that observed in *Wnt4* null metanephroi (Yoshino et al. 2001). However, in contrast to the *Wnt4* null phenotype, addition of sFRP1 disrupted ureteric branching morphogenesis. This was not believed to be related to the inhibition of WNT4 within the MM but to inhibition of WNT11 in the ureteric epithelium. Finally, addition of secreted frizzled-related protein 2 (sFRP2), a downstream target of WNT4 signalling, along with sFRP1, induced a partial rescue of the tubule deficient phenotype, indicating that while Wnt4 signalling through sFRP2 is a key component of renal vesicle and nephron development, additional downstream targets of WNT4 need to be induced for successful nephrogenesis (Lescher et al. 1998; Yoshino et al. 2001).

1.4.4.3 Induction and epithelialisation of MM

The process of nephrogenesis is reliant on the transition of mesenchymal cells to an epithelial fate (MET). The commencement of this transition is induced by factors secreted from the ureteric epithelium.

As previously mentioned, WNT signalling is critical for many developmental processes during kidney organogenesis. Wnt9b, a glycoprotein secreted by the ureteric epithelium is believed to be a key inducer of renal vesicle formation (Carroll et al. 2005). WNT9b expression is observed throughout the Wolffian duct and ureteric epithelium following ureteric bud morphogenesis; however, from e15.5, expression is restricted to ureteric epithelium-derived structures within the kidney (Carroll et al. 2005). Removal of WNT9b signalling, as observed in *Wnt9b* null mice, prevents mesenchymal condensation and renal vesicle formation. Lack of vesicle formation was confirmed by the absence of expression of definitive markers of MM condensation, *Wnt4*, *Fgf8* and *Pax8,* within the MM. WNT9b was hypothesised to be directly upstream of WNT4 signalling (Carroll et al. 2005). Interestingly, though unlike other members of the WNT family, WNT9b cannot functionally replace loss of WNT4 signalling. However, WNT4 does not require prior WNT9b signalling to induce mesenchymal condensation and tubulogenesis in uninduced MM (Carroll et al. 2005).

Soluble cytokines such as TGFβ2, FGF2 and LIF have also been identified as candidates for the induction and epithelialisation of MM condensates (Sakurai et al. 1997; Plisov et al. 2001). *In vitro* analysis of the direct effect of exogenous FGF2 on MM fate showed that whilst FGF2 is able to induce MM condensation and epithelisation, the process took approximately four times longer than the same process *in vivo,* suggesting that FGF2 requires co-factors for efficient MET (Weller et al. 1991). Through the analysis of conditioned media and the development of reliable *in vitro* approaches, LIF and TGFβ2 were suggested as possible cofactors for the regulation of MM condensation (Karavanova et al. 1996; Barasch et al. 1997; Barasch et al. 1999). Addition of exogenous TGFβ2 and FGF2 together markedly increases the rate of MM condensation above that induced by exogenous FGF2 alone and is sufficient to promote epithelialisation of MM condensates (Plisov et al. 2001). Interestingly, the addition of LIF alone is also able to induce condensation and epithelialisation, showing that multiple secreted factors from the ureteric epithelium regulate aspects of MM cell differentiation during the initial stages of nephrogenesis. MM condensation was confirmed by increased expression of *Wt1* and *Wnt4* whilst populations of cells expressing *Wt1*, *Wnt4* and *Pax2* were noted as undergoing MET.

1.5 TGFβ SIGNALLING AND METANEPHRIC DEVELOPMENT

As described in Section 1.4.3, members of the TGFβ superfamily are critical for normal development of the metanephros (Bush et al. 2004). Superfamily members play integral roles in ureteric bud morphogenesis, ureteric branching morphogenesis, MM condensation and tubulogenesis. As this thesis will focus on the role of particular members of the TGFβ superfamily, TGFβ2 and its co-receptor, TGFβ type III receptor (also known as betaglycan), in the determination of nephron endowment, an understanding of the diversity and functionality of TGFβ superfamily members is critical (Plisov et al. 2001; Bush et al. 2004; Oxburgh et al. 2004; Maeshima et al. 2006).

1.5.1 TGFβ superfamily

Members of the TGFβ superfamily of signalling molecules are secreted polypeptides that regulate a wide range of cellular responses, including cell growth, cell cycle mechanics and cell differentiation. Over 60 family members have been identified, including the following subfamilies: TGFβs, BMPs, activins, inhibins and Growth and Differentiation Factors (GDFs), (Figure 1.7) (Massague et al. 1994; Schmierer and Hill 2007). Peptides of the TGFβ superfamily primarily form homodimers which subsequently activate specific receptor complexes inducing a cascade of intracellular signalling proteins (Cheifetz et al. 1988). Nodal, a member of the BMP subfamily, demonstrates a similar level of binding affinity for both itself and other BMP subfamily members, specifically BMP4 and BMP7, which allows heteromeric protein complexes of Nodal and either BMP to be formed (Yeo and Whitman 2001).

Aside from GDNF which signals directly through a complex of RET and GFRA1 as previously discussed (Section 1.4.1.1), members of the TGFβ superfamily require a heteromeric complex of type I and type II receptor serine-threonine kinase receptors for signalling to occur. There are seven known type I receptors (Activin Like Kinase (ALK) 1 – 7) and five known type II receptors (Figure 1.7) (Shi and Massague 2003). Signal transduction occurs when a ligand brings together type I and type II receptors in a complex, in which the type II receptor phosphorylates and activates the type I

receptor. Whilst this receptor complex assembly is common in signalling of all members of the TGFβ superfamily, subtle differences in the complex assembly between subfamily members exist. For TGFβ receptors, once the ligand has bound to the appropriate type II receptor the type I receptor is recruited and the complex forms through direct interactions between both receptors. However, for BMP receptor complexes, direct interactions between receptors do not occur and instead receptors are only linked through the commonly bound ligand (Groppe et al. 2008).

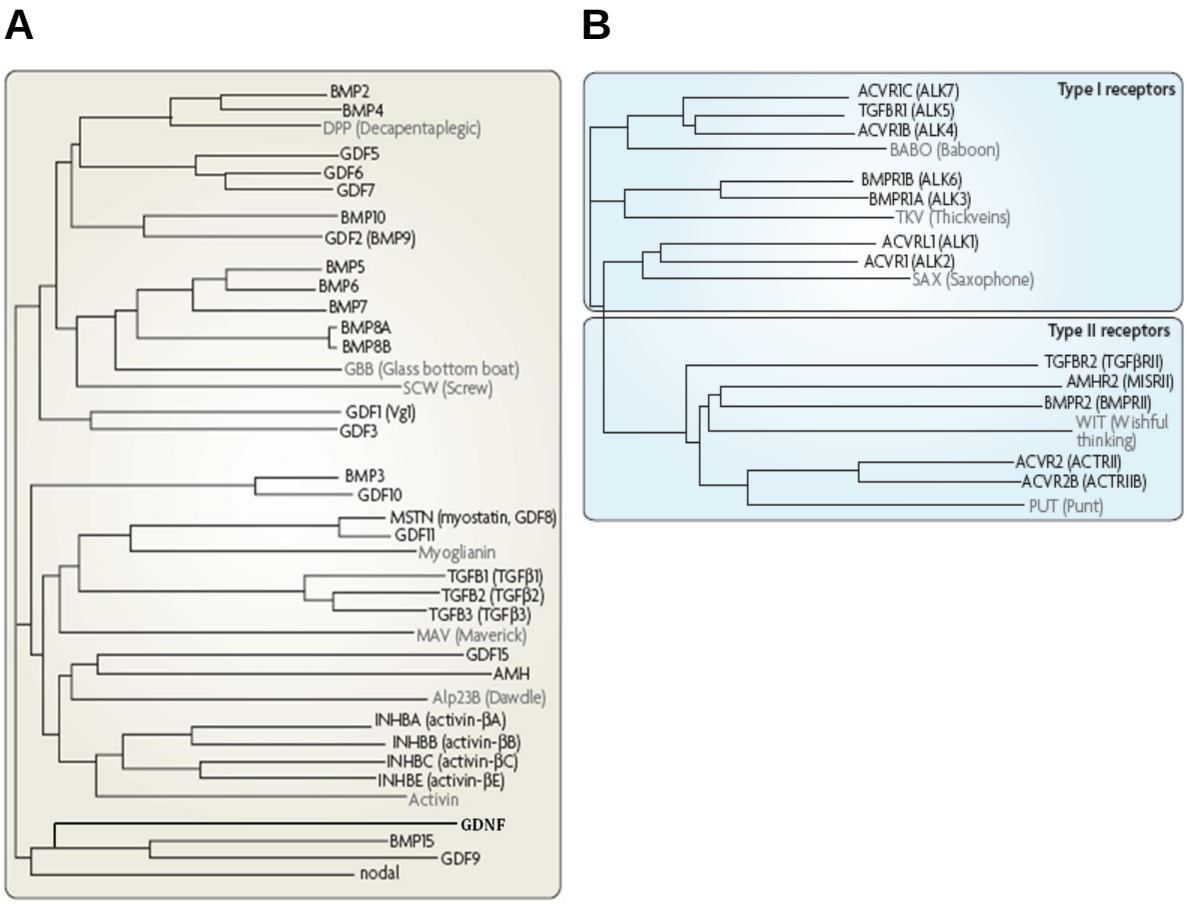

Figure 1.7: Phylogenetic trees of known ligands (A) and type I and II receptors of the TGFβ superfamily (B). Proximity within the tree is determined by protein structural alignment with members demonstrating similar homology represented closer than others. Gray title indicates *Drosophila* only family members. Modified from (Schmierer and Hill 2007).

The diverse functions of TGFβ superfamily members arise in part from the number of different receptor complexes that can be assembled. Previously, it was

believed that BMP and GDF subfamilies signalled through ALK 2, 3 and 6, whereas ALK 4, 5 and 7 were utilised by TGFβs and activins (Schmierer and Hill 2007). However, emerging evidence has indicated that in epithelial cell populations, TGFβ ligands commonly recruit ALK5 to the type II receptor for signal transduction, but complexes containing either ALK2 or ALK3 have also been observed (Massague et al. 1994; Daly et al. 2008). In all tissue types, alternate receptor complex formation can only occur at significantly higher concentrations of TGFβ ligand than those required to form the initial common complexes (Goumans et al. 2003; Bharathy et al. 2008; Daly et al. 2008). Following receptor complex activation, intracellular signalling mediators are phosphorylated and subsequently translocated to the nucleus to modulate targeted gene transcription. The prototypical signalling molecules for the TGFβ superfamily are the SMADs.

1.5.2 SMADS

SMADs are a group of 9 intracellular signalling molecules comprised of receptor-regulated SMADs (R-SMADs – 1,2,3,5,8), inhibitory SMADs (6,7) and the common SMAD, SMAD4 (Shi and Massague 2003). Following phosphorylation by type I receptors, R-SMADs form homomeric or heteromeric complexes which then associate with SMAD4 and are actively translocated to the nucleus. Activated nuclear SMAD complexes then accumulate and, with the aid of cell-specific DNA binding partners, bind to specific DNA sequences to either promote or inhibit gene transcription (Figure 1.8) (Shi and Massague 2003; Groppe et al. 2008).

Interestingly, unlike most transcription factors, SMADs are unable to recruit the basal intranuclear machinery for transcription, indicating that they are only able to transcribe DNA with associated machinery, i.e. chromatin (Ross et al. 2006). As specific SMAD complexes serve specific nuclear functions, the composition of the activated complex is a critical aspect in the regulation of TGFβ superfamily signalling. In much the same way TGFβ superfamily function and signalling diversity was believed to be associated with the large number of possible type I and type II receptor combinations, it was previously thought that SMAD activation was ligand- and receptor-specific with TGFβ/activin signalling predominantly through R-SMADs 2/3 and BMP/GDF signalling predominantly through R-SMADs 1, 5 and 8 (Massague et al.

2005; Schmierer and Hill 2007). However, recent studies have indicated that TGFβ isoforms can activate both SMAD groups in a range of developing, mature and neoplastic tissues, suggesting that an even greater complexity for signal regulation may exist in specific tissues (Bharathy et al. 2008; Daly et al. 2008; Liu et al. 2009).

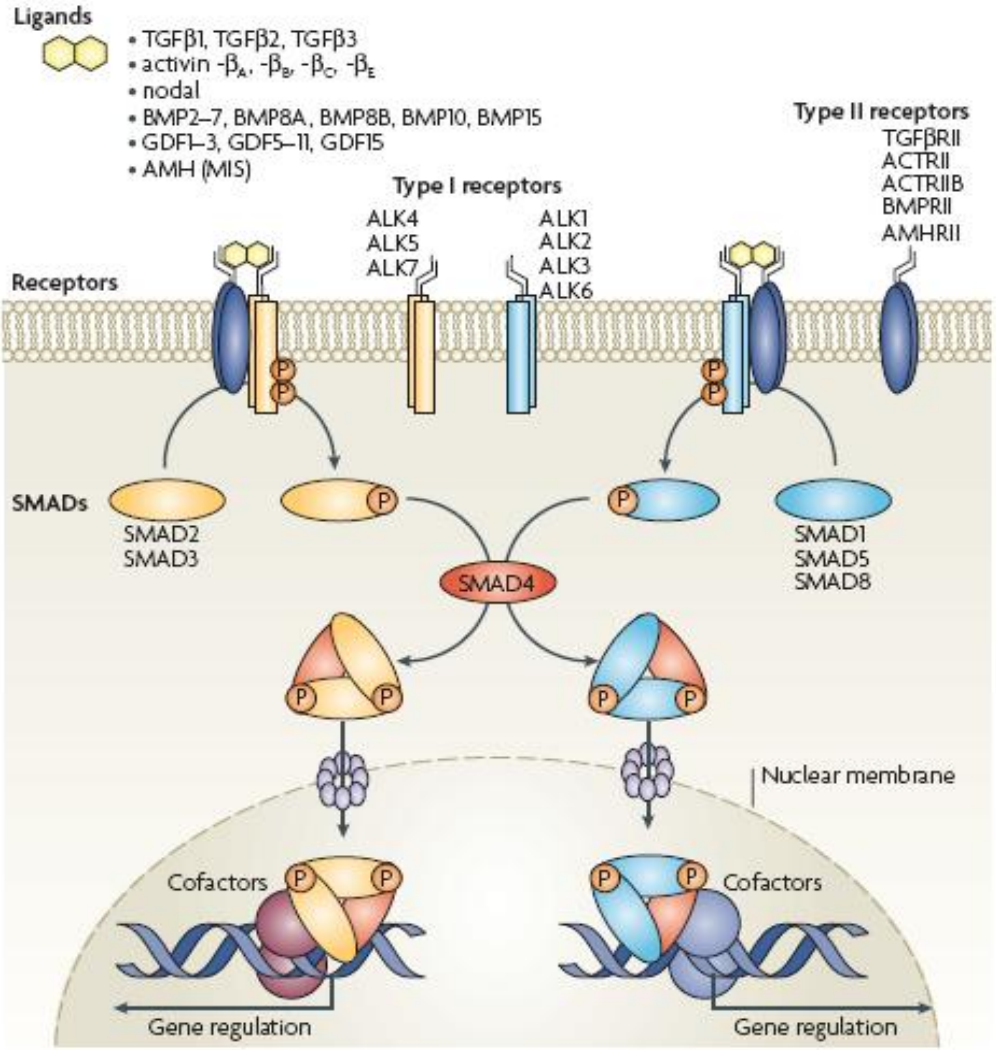

Figure 1.8: TGFβ signal transduction. TGFβ ligand dimers recruit and bind a heteromeric type I/type II receptor complex, inducing phosphorylation of the type I receptor and activation of R-SMADs. Activated SMADs form protein complexes with SMAD4 which are translocated to the nucleus. These complexes interact with transcription factors to regulate gene transcription. Images from (Schmierer and Hill 2007).

1.5.3 Betaglycan

Emerging evidence suggests that TGFβ accessory receptors such as betaglycan are critical for the regulation of TGFβ receptor complex formation and signal transduction. Betaglycan is an 850-amino-acid proteoglycan with heparan sulphate and chondroitin sulphate glycosaminoglycan side chains attached to a core protein (Lopez-Casillas et al. 1991; Wang et al. 1991; Lopez-Casillas et al. 1994). The core protein contains a large extracellular domain, consisting of two putative TGFβ binding sites and two glycosaminoglycan attachment sites as well as a short intracellular tail with no known signalling motif (Lopez-Casillas et al. 1991; Wang et al. 1991; Lopez-Casillas et al. 1994).

Betaglycan is believed to regulate tissue sensitivity to TGFβ isoforms by binding and presenting them to the type II TGFβ receptor, an action of particular importance for TGFβ2 which does not bind to the type II TGFβ receptor with high affinity in the absence of betaglycan (Lopez-Casillas et al. 1993; Esparza-Lopez et al. 2001; Stenvers et al. 2003; Compton et al. 2007). While many studies have focused on the interaction between betaglycan and TGFβ isoforms, other studies have highlighted a more complex role for the co-receptor. Besides TGFβ isoforms, betaglycan has also been shown to directly modulate the activities of inhibins and certain BMP's through binding of these proteins to its core while indirectly influencing BMP and activin function through the regulation of inhibins (Lewis et al. 2000; Kirkbride et al. 2008). Studies have also indicated the potential for betaglycan to modulate FGF function via its glycosaminoglycan side chains, indicating that the role of betaglycan during development may not be limited to the regulation of TGFβ superfamily function (Andres et al. 1992). Whilst the complexity of the role of betaglycan in ligand signalling is still not fully understood, the generation of betaglycan null mutant mice has indicated the requirement of the co-receptor for tissue organogenesis.

Betaglycan heterozygous null (betaglycan$^{+/-}$) mutants appear grossly phenotypically normal, but homozygous null (betaglycan$^{-/-}$) mutants exhibit embryonic lethality between approximately e16.5 and birth, with defects in the developing heart, liver and gonads (Sarraj et al. ; Stenvers et al. 2003; Compton et al. 2007). While severe developmental abnormalities affecting liver and heart

morphogenesis are believed to underlie the lethal phenotype, the presence of gonadal dysgenesis prior to either liver or heart malformations suggests that a global mutation in betaglycan may induce the development of additional, tissue-specific phenotypes (Sarraj et al. 2010). Analysis of embryonic fibroblasts isolated from wildtype and betaglycan$^{-/-}$ embryos indicated a significant decrease in cellular sensitivity to exogenous TGFβ2 protein, suggesting the phenotypic abnormalities seen in betaglycan$^{-/-}$ embryos may in part be due to disruption of TGFβ2-mediated developmental processes (Stenvers et al. 2003). During cardiovascular development in betaglycan$^{-/-}$ mice, perturbed cellular differentiation due to a decreased level of TGFβ signalling activity, specifically through ALK5, is believed to be the possible developmental mechanism driving manifestation of the phenotype (Stenvers et al. 2003; Compton et al. 2007).

The role of betaglycan in metanephric development remains unclear. As previous findings have hypothesised that optimum TGFβ signalling is required for the normal development of specific organs and tissues, it is conceivable that betaglycan may play an important role in kidney development. This thesis will address whether betaglycan plays a role in metanephric development, specifically in the regulation of nephron endowment.

1.6 NEPHRON ENDOWMENT

As previously stated nephron endowment in humans is established at 36 weeks gestation (Solhaug et al. 2004). Interestingly, nephron number in normal adult human kidneys has been shown to vary widely (Nyengaard and Bendtsen 1992; Hoy et al. 2003; Hughson et al. 2003; Keller et al. 2003; McNamara et al. 2008; Zimanyi et al. 2009; McNamara et al. 2010). The largest study to date of 343 human kidneys obtained at autopsy found a 13-fold range in nephron number - from 210,332 to 2,702,076, with the mean nephron number of 876,339 (Figure 1.9) (Puelles et al. 2010). The mechanisms responsible for this large range in human nephron number remain largely unknown, but animal studies have identified numerous environmental

and genetic factors that regulate nephron endowment. Furthermore, such studies have shown that nephron endowment exhibits a high level of developmental plasticity, in that not only can nephron endowment be reduced, but also increased (detailed in Tables 1 and 2).

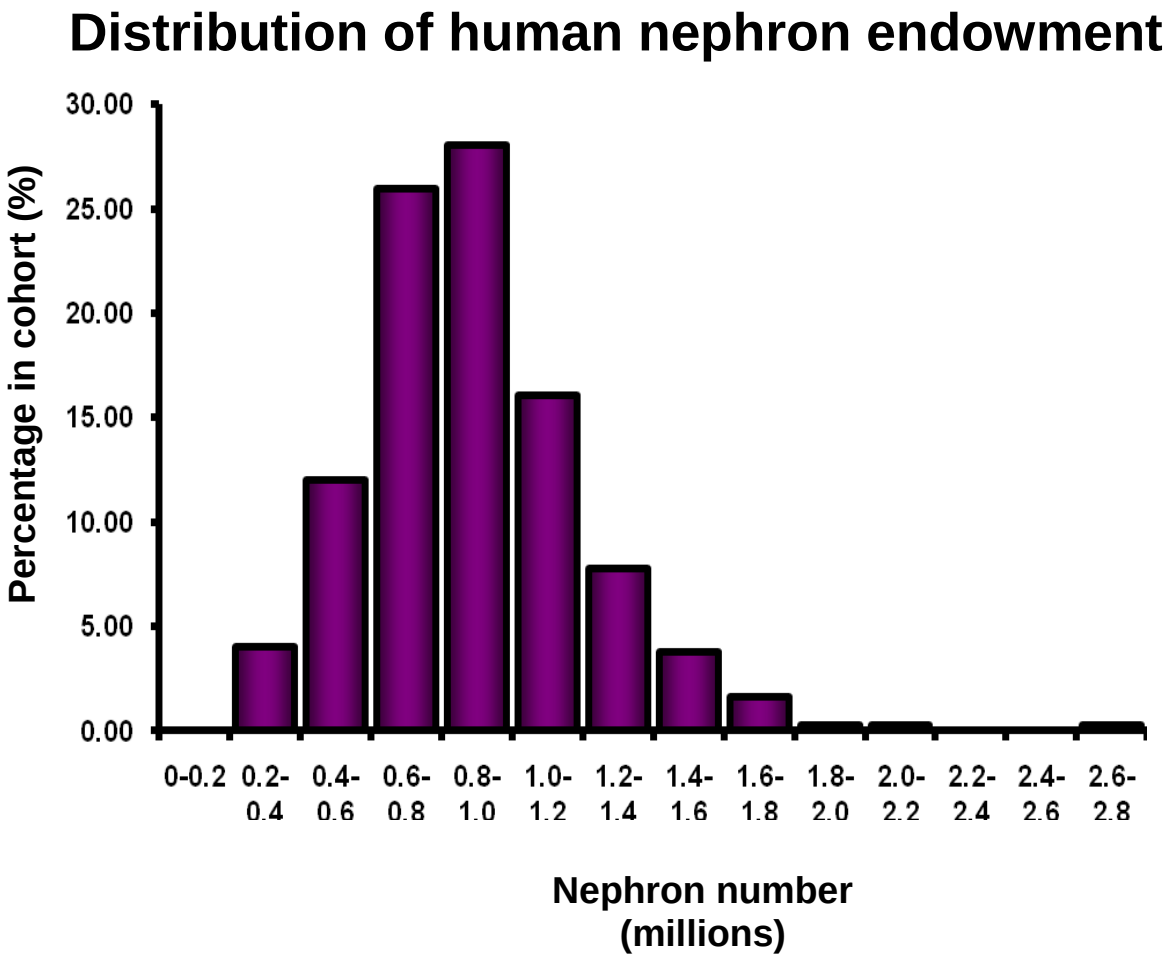

Figure 1.9: Distribution of human nephron number. An approximately 14-fold range in human nephron number (mean, 876,339, highest value, 2,702,079; lowest value, 210,332) has been observed in autopsy studies (n = 343). Data from (Puelles et al. 2010).

1.6.1 Nephron deficient phenotypes

1.6.1.1 Environmental regulation

A range of perturbations to the feto-maternal environment have been shown to limit nephron endowment in a variety of animal models. These models include

global food or nutrient restriction, low protein diet, vitamin deficiency, as well as exposure to natural and synthetic glucocorticoids, environmental toxins and drugs. A brief overview of major findings is provided below (also see Table 1.1).

Numerous studies have reported that global food restriction and low protein diet during pregnancy limit nephron endowment. Offspring of sheep fed 50% of a diet allocated to control animals during pregnancy had 12% fewer nephrons than control offspring (Gilbert et al. 2005). While the precise mechanism for the development of such a phenotype has not been elucidated, gene microarray analysis of baboon kidneys from offspring of mothers fed a 30% nutrient-restricted diet found altered levels of gene expression for such processes as nucleic acid biosynthesis, metabolism, DNA modification, cell cycle mechanics as well as specific factors involved in metanephric development including *Wt1*, *Bmp7* and members of the WNT signalling pathway (Cox et al. 2006).

A maternal low protein diet has been shown in numerous studies to result in a 20 to 30% reduction in nephron endowment in offspring (Welham et al. 2002; Woods et al. 2004; Zimanyi et al. 2004; Hoppe et al. 2007; Hoppe et al. 2007; Villar-Martini et al. 2009). In this model, increased apoptosis within the MM during early glomerulogenesis has been shown to result in a decrease in the number of renal vesicles and in turn glomeruli which develop in the metanephroi of offspring subjected to a low protein *in utero* environment (Villar-Martini et al. 2009).

As with deficiencies in maternal global food and protein intake, deficiency of particular vitamins can also induce decreased nephron endowment in offspring. Retinoic acid (RA), the oxidised form of Vitamin A has previously been shown to be important for normal kidney patterning and ureteric branching morphogenesis through the stimulation of *Ret* expression within the ureteric bud (Vilar et al. 1996; Moreau et al. 1998). Mild deficiency or absence of RA during development results in a range of congenital renal defects including permanent nephron deficit, severe renal hypoplasia or renal agenesis (Wilson et al. 1953; Mendelsohn et al. 1994; Lelievre-Pegorier et al. 1998; Batourina et al. 2001). In human populations with high rates of vitamin A deficiency, the ratio of newborn kidney volume to body size is 40% less than in populations without vitamin A deficiency suggesting experimental models of retinoid deficiency may be truly replicating human phenotypes (Goodyer et al. 2007).

Fetal exposure to maternal glucocorticoids has been identified as another factor capable of inducing reduced nephron endowment across mammalian experimental models. Studies utilising rats, sheep and spiny mice have indicated that embryonic exposure to natural (corticosterone) or synthetic (dexamethasone) glucocorticoids consistently results in an approximately 20% reduction in nephron endowment (Wintour et al. 2003; Dickinson et al. 2007; Dickinson et al. 2007; Singh et al. 2007). Importantly, these phenotypes manifested following just 48 hours of fetal exposure. The most comprehensive of these studies administered intraperitoneal injections of dexamethasone for 48 hours only to pregnant rats on either e11 and e12, e13 and e14, e15 and e16, e17 and e18, e19 and e20, or e20 and e21 (Ortiz et al. 2001). Decreased nephron number was observed in offspring exposed on days e15 – e16, and e17-e18 only, highlighting that timing of a gestational insult can be critical for the development of reduced nephron endowment. The specificity of the timing of the exposure highlighted by Ortiz et al. (2001) may explain the failure of Bramlage et al. (2009) to demonstrate a reduced nephron endowment in marmosets exposed to dexamethasone in either early (7 weeks) or late gestation (13 weeks) (Bramlage et al. 2009).

1.6.1.2 Genetic regulation

Not surprisingly, disruption of the molecular signalling networks that regulate metanephric and nephron development frequently results in kidneys with reduced nephron endowment (Cain et al. 2010). Much attention has focused on mutations which may influence the function of the most potent metanephric inducer, GDNF. Firstly, whilst ablation of GDNF in mice results in a non-viable neonatal lethal phenotype, primarily due to renal agenesis or severe renal dysplasia, *Gdnf* heterozygous mutants are viable and consistently display a range of renal developmental abnormalities including renal hypoplasia and uni- lateral renal agenesis (Moore et al. 1996; Pichel et al. 1996; Sanchez et al. 1996; Cullen-McEwen et al. 2001; Ruta et al. 2010). Further characterisation of *Gdnf* heterozygotes identified a 25 - 30% reduction in nephron number in mice with two kidneys, whilst a 65% decrease in nephron number was observed in *Gdnf* heterozygotes possessing a single kidney compared to age-matched wildtype littermates (Cullen-McEwen et al. 2001;

Cullen-McEwen et al. 2003; Ruta et al. 2010). Surprisingly, however, Zhang et al. (2009) found no effect of GDNF SNPs on kidney size in neonatal children (Zhang et al. 2009).

Secondly, as discussed in Section 1.4.1.1, RET, the epithelially-expressed receptor for GDNF, and PAX2, an upstream MM-expressed transcription factor required for *Gdnf* activation, are critical for GDNF signalling in the developing kidney (Durbec et al. 1996; Clarke et al. 2006; Costantini and Shakya 2006). Heterozygous null mutants for either *Ret* or *Pax2* exhibit severe renal dysplasia, coupled with a significant reduction in the number of nephrons developing within the kidney, a phenotype which is exacerbated in compound heterozygous mutants (Clarke et al. 2006). Polymorphisms in the human genes, *PAX2* and *RET* have been linked to similar renal phenotypes. Quinlan et al. (2007) reported that patients with either a heterozygous or homozygous *PAX2* AAA polymorphism exhibited a 10% decrease in total renal volume compared with age-matched individuals homozygous for the *PAX2* GGG haplotype (Quinlan et al. 2007). *PAX2* AAA polymorphisms were shown to be hypomorphic and were associated with a 40% reduction in the expression of PAX2 (Quinlan et al. 2007). Hypomorphic-inducing polymorphisms in the *RET* gene yield similar results, with individuals possessing a single nucleotide polymorphism exhibiting a 10% decrease in total renal volume at birth (Zhang et al. 2008). Whilst absolute nephron number within these studies was not obtained, the strong correlation between renal volume and nephron number that exists in newborns allowed the authors to hypothesise that a reduction in nephron endowment had occurred (Nyengaard and Bendtsen 1992; Zhang et al. 2008).

Table 1.1: Experimental models of low nephron endowment

ENVIRONMENTAL REGULATION				
Model	**Species**	**% Decrease in Nephron Number**	**Counting Method**	**Author**
50% Restricted Feeding	**Sheep**	12%	Acid Maceration	(Gilbert et al. 2005)
Low Protein Diet (6% or 9% protein diet)	**Rat**	30 % & 41 %	Acid Maceration	(Welham et al. 2002)
Low Protein Diet (9%)	**Mouse**	22 % in males, 16% in females	Physical disector / fractionator	(Hoppe et al. 2007)
Low Protein Diet (9%)	**Rat**	44 %	Physical disector / fractionator	(Woods et al. 2004)
Vitamin A	**Rat**	21 %	Acid Maceration	(Lelievre-Pegorier et al. 1998)
Dexamethasone	**Sheep**	38 %	Physical disector / fractionator	(Wintour et al. 2003)
Dexamethasone	**Spiny Mouse**	13 % in males, 22 % in females	Physical disector / fractionator	(Dickinson et al. 2007)
Dexamethasone	**Rat**	20 % & 30 %	Acid Maceration	(Ortiz et al. 2001)
Alcohol	**Sheep**	11%	Physical disector / fractionator	(Gray et al. 2008)
GENETIC REGULATION				
Gdnf heterozygous	**Mouse**	35 % - HET1K, 25 % HET2K	Physical disector / fractionator	(Cullen-McEwen et al. 2001; Ruta et al. 2010)
Frs2alpha null	**Mouse**	23 %	Physical disector / fractionator	(Sims-Lucas et al. 2009)
Pax2, Ret and compound mutants	**Mouse**	49 %, 37 % and 22 %	Cross-section image analysis *	(Clarke et al. 2006)
$Pax2^{+/-}$ / $Pax8^{+/-}$	**Mouse**	63 %	In situ hybridisation/cross-section image*	(Narlis et al. 2007)

*** biased counting technique used in study**

1.6.2 Augmented nephron endowment phenotypes

Within the nephron endowment literature, experimental models of decreased nephron endowment dominate (reviewed by (Moritz et al. 2008). To date, only nine studies (three *in vitro*, five *in vivo* and one containing both *in vitro* and *in vivo* data) have reported increased nephron endowment in animal models (Table 1.2). In five of these studies, dietary intervention was responsible for the increased nephron endowment, while in the other three studies, manipulation of growth factor signalling was responsible.

1.6.2.1 Environmental regulation

RA was previously discussed in Section 1.6.1.1 as a regulator of nephron endowment, whereby deficiency during metanephric organogenesis decreased nephron endowment. However RA has also been shown to be a potent factor capable of augmenting total nephron number both *in vitro* and *in vivo*. Culture of e13.0 and e14.0 rat metanephroi in the presence of retinoid (derivatives of RA) from 10^{-11} M to 10^{-4} M found that concentrations 10^{-8} M were sufficient to increase the number of developing nephrons (Vilar et al. 1996). As RA induces upregulation of *Ret* mRNA and protein in the ureteric epithelium, it was not surprising that culture in the presence of a combination of RA and GDNF induced even further augmentation of nephron endowment (Moreau et al. 1998).

A single intraperitoneal injection of RA on e11 (20mg/kg) induced a ~20% increase in total nephron endowment (RA-injected: 43,322 ± 1,837 vs. control: 35,911 ± 1,935) in rat offspring at PN14 (Lelievre-Pegorier et al. 1998). While it should be noted that Lelievre-Pegorier et al. (1998) estimated nephron number using acid-maceration methodology and not the gold-standard physical disector approach, the efficacy of this approach in the hands of this group has been shown to produce accurate estimates (Merlet-Benichou et al. 1999). Together these data suggest that understanding the components that influence GDNF-RET signalling during metanephric development may lead to an understanding of the establishment of not only nephron endowment but augmented nephron number phenotypes.

The observation of augmented nephron endowment following RA stimulation has led to much interest in the ability of RA to 'rescue' nephron endowment in offspring predisposed to an impaired nephron endowment. Makrakis et al. (2007) found that rat offspring exposed to maternal low protein diet had a 29% decrease in total nephron endowment. However, maternal intraperitoneal administration of RA prior to the commencement of metanephric development ameliorated the nephron deficient phenotype. If a low protein diet was observed to decrease *Ret* expression in the ureteric epithelium, this could provide a molecular mechanism for the ability of RA to rescue nephron endowment; however this has yet to be described. A recent study from the same group attempted to replicate the 'rescue' of nephrogenesis in a setting of preterm birth in baboons. However, postnatal administration of RA did not influence nephron endowment in the preterm baboon kidney (Sutherland et al. 2009).

Maternal vitamin D deficiency during pregnancy and lactation has previously been shown to induce a 20% increase in nephron endowment in Sprague-Dawley rat offspring at PN30 (Vitamin D deficient: 29,000 ± 1,858 vs. control: 23,330 ± 1,828) (Maka et al. 2008). However, while an unbiased stereological approach was used to determine total nephron number, the values reported must be questioned as those reported are much lower than other published values for Sprague-Dawley rats (Boubred et al. 2007; Hoppe et al. 2007; Gray et al. 2010).

Finally, maternal water restriction during gestation has also been reported to enhance nephrogenesis. Mansano et al. (2007) restricted maternal water intake in pregnant Sprague-Dawley rats at e10.0 (Mansano et al. 2007). Interestingly, water-restricted offspring had 17% more nephrons than age-matched control offspring (Mansano et al. 2007). However, the findings from Mansano et al. (2007) must be questioned as glomerular profiles per unit area of cortex were counted rather than total glomerular number.

Table 1.2: In vivo and in vitro phenotypes of high nephron endowment

In Vivo

ENVIRONMENTAL REGULATION

Model	Species	% Increase in Nephron Number	Counting Method	Author
Vitamin A	**Rat**	21 %	Acid Maceration	(Lelievre-Pegorier et al. 1998)
Vitamin A	**Rat**	29 %	Physical disector / fractionator	(Makrakis et al. 2007)
Vitamin D deficiency	**Rat**	20%	Physical disector / fractionator	(Maka et al. 2008)
Water deprivation	**Rat**	17%	Cross-section image analysis *	(Mansano et al. 2007)
GENETIC REGULATION AND SIGNALLING				
Type 2 Activin receptor truncation	**Mouse**	80 %	Cross-section image analysis *	(Maeshima et al. 2000)
Tgfb2 heterozygous	**Mouse**	63 % in males, 61 % in females	Physical disector / fractionator	(Sims-Lucas et al. 2008)

In Vitro

ENVIRONMENTAL REGULATION

Insult	Model	% increase	Author
Vitamin A	**Rat**	200 %	(Vilar et al. 1996)
Vitamin A + exogenous GDNF	**Rat**	33 %	(Moreau et al. 1998)
GENETIC REGULATION AND SIGNALLING			
IGF-II (100ng/ml, 1000ng/ml)	**Mouse**	25 % & 40 %	(Doublier et al. 2001)
Semaphorin3a (Anti-sense morpholino)	**Mouse**	68%	(Tufro et al. 2008)
Tgfb2 heterozygous	**Mouse**	60 %	(Sims-Lucas et al. 2008)

*** biased counting technique used in study**

1.6.2.2 Genetic regulation and signalling

To date, only four studies have reported mutant mouse models with augmented nephron endowment. The first, as mentioned previously, investigated the effects of over-expression of a dominant-negative truncated form of the type 2 Activin receptor (tActR-II) on metanephric development and nephron endowment (Maeshima et al. 2000). At 2 months of age, tActR-II mutant mice exhibit an 80% increase in glomerular number and a 30% increase in total glomerular volume compared with age-matched wildtype mice. Maeshima et al. (2000) concluded that blockade of the actions of a potent negative regulator such as activin A within the developing kidney, was able to enhance branching morphogenesis and in turn increase nephron endowment (Maeshima et al. 2000). However, much like Mansano et al. (2007), (Section 1.6.2.1) this study adopted a biased nephron number counting approach and the findings need to be verified using gold-standard stereology.

Insulin-like growth factor (IGF) signalling has also been associated with increased nephron number (Doublier et al. 2001). Over-expression of the human insulin-like growth factor binding protein 1 (hIGFBP1) transgene in mice resulted in decreased bioactivity of the IGF ligands IGF-I and IGF-II. Decreased IGF bioavailability was deemed to contribute to impaired nephrogenesis and, in turn, a decreased nephron number in mice carrying the transgene. Following this finding however, Doublier et al. (2001) cultured metanephroi in the presence of either IGF-I or IGF-II to elucidate the direct effect of the ligands on early metanephric development. Surprisingly, while exposure to either ligand promoted metanephric growth, exposure to IGF-II alone significantly increased the number of glomeruli which developed in a dose-dependent manner, with 100ng/ml and 1000ng/ml inducing 25% and 40% increases in the total number of glomeruli respectively (Doublier et al. 2001). However, as this finding has not been recapitulated *in vivo*, a potential mechanism has not yet been proven for the development of this phenotype. Finally, using anti-sense morpholino technologies, Turfo et al. (2007) demonstrated that down-regulation of Semaphorin3a, an inhibitor of ureteric branching morphogenesis, in metanephric cultures increased the number of developing glomeruli present (Tufro et al. 2008). As Semaphorin3a modulates the expression of potent metanephric inducer, GDNF, administration of 10μM of a *Semaphorin3a* anti-

sense morpholino, to e11.5 mouse ureters induced a 68% increase in the number of developing glomeruli, after a 48 hour culture period, possibly through increased *Gdnf* activity. This has been further demonstrated in *Semaphorin3a* null metanephroi which exhibit a trend for augmented ureteric branching, however as these mutants die within 24 hours of birth due to cardiac defects (Behar et al. 1996), no characterisation of *in vivo* nephron endowment has been undertaken.

1.6.2.3 TGFβ2 heterozygous mice

The final and most important model with respect to this thesis is the *Tgfb2*$^{+/-}$ mouse, which to date is the only model of high nephron endowment that has been quantified both *in vitro* and *in vivo* via gold-standard stereological approaches. *Tgfb2*$^{+/-}$ mice exhibit a 60% increase in the number of developing nephrons *in vitro*, as well as a 60% increase in nephron endowment compared with wildtype mice at PN30 (Sims-Lucas et al. 2008). Glomeruli in *Tgfb2*$^{+/-}$ were smaller than in wildtype mice. However, the total volume of all glomeruli in *Tgfb2*$^{+/-}$ mice was 30% greater than in wildtype mice (see Table 1.3). Augmented nephron endowment in *Tgfb2*$^{+/-}$ mice was not associated with renal pathology at P30.

Further analysis of the renal phenotype in *Tgfb2*$^{+/-}$ mice found that while ureteric budding occurred at the same developmental stage as in wildtype mice, upon invading the MM ureteric branching morphogenesis was accelerated. This accelerated ureteric branching appeared phenotypically normal and was not associated with any obvious defects in mesenchymal condensation or glomerulogenesis. Interestingly, complete removal of TGFβ2 as in *Tgfb2*$^{-/-}$ mice severely impacts normal kidney development, demonstrating that TGFβ2 regulates kidney development in a dose-dependent manner (Sims-Lucas et al. 2008). According to this model, removal of some of the inhibitory properties of TGFβ2 on branching morphogenesis in *Tgfb2*$^{+/-}$ mice occurs without any adverse impact on mesenchymal cell condensation, together resulting in augmented nephron endowment (Sanford et al. 1997; Sims-Lucas 2007; Sims-Lucas et al. 2008). Together these studies indicate the importance of TGFβ2 signalling in the establishment of nephron endowment.

In a surprising recent finding, Short et al. (2010) reported reduced ureteric branching morphogenesis in the kidneys of e15.5 *Tgfb2*$^{+/-}$ embryos. Short et al. (2010) used optical projection tomography to image metanephroi and quantitative image analysis to measure the lengths of ureteric branches. The apparent disparate findings between Sims-Lucas et al. (2008) and Short et al. (2010) have yet to be explained, but it must be borne in mind that the two studies measured different parameters - Sims-Lucas et al. (2010) counted glomeruli *in vivo* in postnatal kidneys whilst Short et al. (2010) measured ureteric branches in foetal metanephroi.

Tgfb2$^{+/-}$ mice remain the only postnatal model of congenital augmented nephron endowment verified by gold-standard stereological approaches. They provide a model to investigate the renal and cardiovascular functional consequences associated with augmented nephron endowment. In this thesis, renal and cardiovascular physiology are assessed in *Tgfb2*$^{+/-}$ mice under both basal conditions and following physiological stress.

Table 1.3: Body weights and stereological data for *Tgfb2*$^{+/-}$ mice at PN30

	Wildtype Males	***Tgfb2+/-* Males**	**Wildtype Females**	***Tgfb2+/-* Females**
Body weight (g)	20.3 ± 3.0	21.0 ± 1.5	17.6 ± 2.8	21.0 ± 1.5
Kidney weight (mg)	125 ± 22	143 ± 13	104 ± 19	115 ± 17
Total glomerular number	12283 ± 663	19978 ± 1148***	12748 ± 1438	20501 ± 1793***
Mean glomerular volume ($x10^{-4}mm^3$)	1.81 ± 0.33	1.39 ± 0.14**	1.80 ± 0.42	1.47 ± 0.27
Total glomerular volume (mm^3)	2.22 ± 0.40	2.78 ± 0.27*	2.29 ± 0.60	3.00 ± 0.53*
Mean renal corpuscle volume ($x10^{-4}mm^3$)	2.44 ± 0.50	1.85 ± 0.24*	2.44 ± 0.51	1.90 ± 0.24*
Total renal corpuscule volume (mm^3)	2.99 ± 0.58	3.69 ± 0.41*	3.10 ± 0.69	3.87 ± 0.48*

Values are mean ± SD. N = 7 mice per genotype. * p <0.05, ** p <0.01, *** p <0.001
Table from(Sims-Lucas et al. 2008).

1.7 NEPHRON NUMBER AND DISEASE

The co-morbidity of CVD and CKD throughout the developed and developing world suggests a strong link between these two conditions. However, the nature of this link remains contentious. Nephrons are known to be integral for the maintenance of cardiovascular and renal health. In 1988 Brenner and colleagues proposed a cyclic model linking decreases in glomerular capillary filtration surface area (FSA) due to fewer nephrons (congenital or acquired), to the development of hypertension and CKD (Figure 1.10) (Brenner et al. 1988). They hypothesised that decreases in FSA impaired the ability of glomeruli to filter incoming blood adequately, resulting initially in a state of compensatory glomerular hyperfiltration. Altered glomerular filtrate composition can impair renal tubular function and cause increased retention of sodium within both the renal vasculature and interstitium. As previously mentioned, increased retention of sodium and in turn, water, increases plasma volume and arterial pressure, potentially giving rise to a pre-hypertensive state. However, in this renal setting, increased arterial pressure can induce increases in the intra-glomerular pressure exerted on glomerular capillaries. Compensatory glomerular hypertrophy can also occur in an attempt to adapt to such haemodynamic conditions. However, if high pressure is chronic, it may induce glomerular injury and scarring, both of which in turn can induce nephron loss and further decreases in FSA, perpetuating a devastating cycle (Brenner et al. 1988). Reduced FSA due to fewer and/or smaller glomeruli can be a result of many factors including disease, trauma or age. However, a congenital deficit in FSA through reduced nephron endowment may also underlie an increased risk of CVD and CKD in adulthood (Figure 1.10).

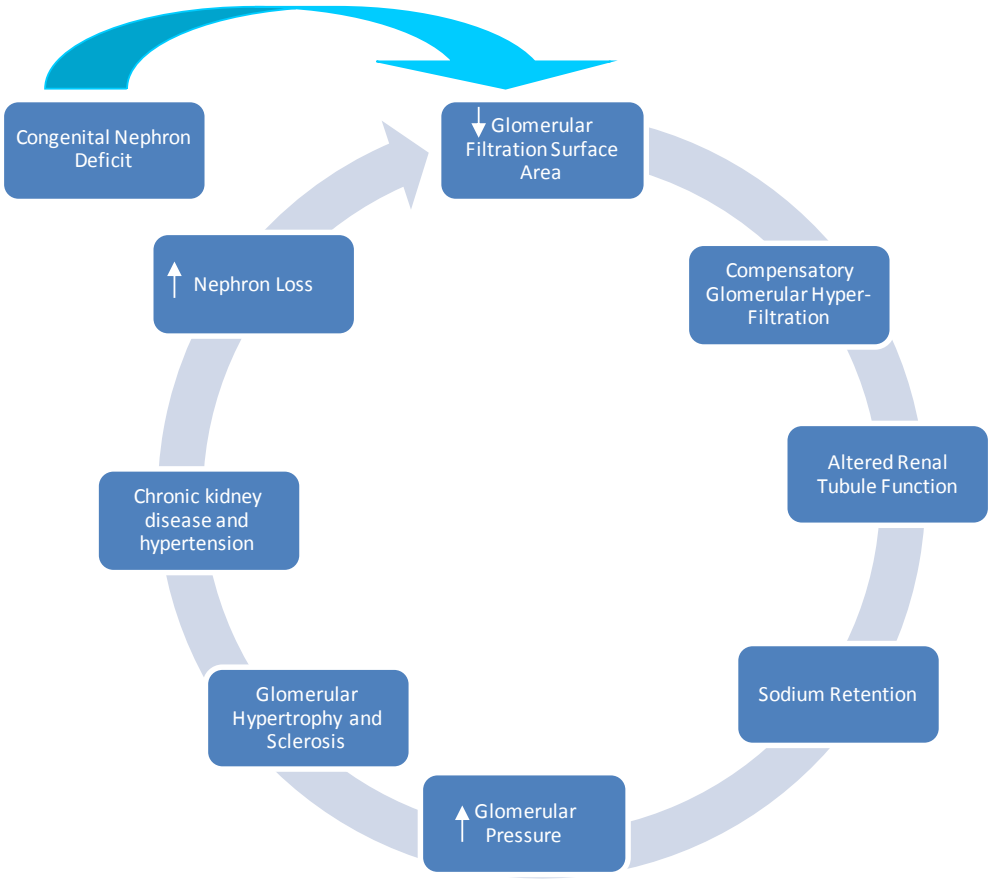

Figure 1.10: The 'Brenner Hypothesis'. Schematic representation of the mechanism through which a congenital nephron deficit is hypothesised to induce further nephron loss and the development of CKD and hypertension.

In 1939, pre-mortem blood pressure readings obtained from individuals with no other detectable pathologies such as oedema or impaired kidney function, were correlated with glomerular number at autopsy with researchers concluding that the lower the glomerular number, the higher the blood pressure (Hayman et al. 1939). This was the first study to propose a link between elevation in blood pressure and glomerular number and to show that glomerular number was not uniform between individuals. Similar findings were reported by Keller at al. (2003) who found that 10 subjects with hypertension had a significantly lower total nephron number than did 10 normotensive matched-control subjects (702,379 vs. 1,429,200 nephrons per kidney) (Keller et al. 2003).

Interestingly, in accordance with the Brenner et al. (1988) theoretical model, Keller et al. (2003) found that the subjects with hypertension also displayed evidence of glomerular hypertrophy. Similar findings were observed in a cohort of Caucasian American adults in whom a decreased nephron number was correlated with an elevation in mean arterial pressure (Hughson et al. 2006). Australian Aborigines, a population with very high rates of hypertension and CKD contain fewer nephrons than white Australians from the same geographical location (Hoy et al. 2008). Aborigines with a history of hypertension have approximately 250,000 fewer nephrons per kidney than Aborigines with no history of hypertension (Hoy et al. 2006).

It is important to acknowledge that not all human studies have provided evidence in support of the Brenner Hypothesis. Considering the human data, Hughson et al. (2006) reported an inverse correlation between nephron number and mean arterial blood pressure in white Americans, but not in African Americans. However, in a subsequent report for more subjects, the association in Whites was no longer observed (Hughson et al. 2008).

Findings of elevated blood pressure in association with low nephron endowment have been reported in many experimental models (Ortiz et al. 2001; Wintour et al. 2003; Woods et al. 2004; Harrison and Langley-Evans 2009; Villar-Martini et al. 2009; Baum 2010). Similarly, as mentioned above in reference to human data, not all animal studies have found an inverse association between nephron endowment and blood pressure (Zimanyi et al. 2006; Dickinson et al. 2007; Hoppe et al. 2007; Bramlage et al. 2009; Ruta et al. 2010). A good example of this is the *GDNF* heterozygous null mutant mouse. Utilising *Gdnf* wildtype and heterozygous mice possessing one (HET1K) or two (HET2K) kidneys, Ruta et al. (2010) eloquently highlighted that moderate or severe impairment in nephron endowment does not result in elevated arterial pressure (Ruta et al. 2010). At 1 year of age, HET2K mice had 19152 ± 1119 (mean $\pm$ standard deviation) nephrons in total, compared to age-matched wildtype mice with 25388 ± 700 nephrons and HET1K mice with just 8952 ± 507 nephrons (Figure 1.11A). However, despite such marked differences in total nephron number, baseline mean arterial pressure was similar in all three groups (Figure 1.11B). These studies indicate that under baseline conditions, perturbations

to nephron number alone may not be sufficient to induce the development of disease, but instead require the presence of other factors, as a secondary insult.

Together with the human findings described above, the findings from experimental models suggest an inverse, albeit complex link, between nephron endowment and the development of CVD and CKD.

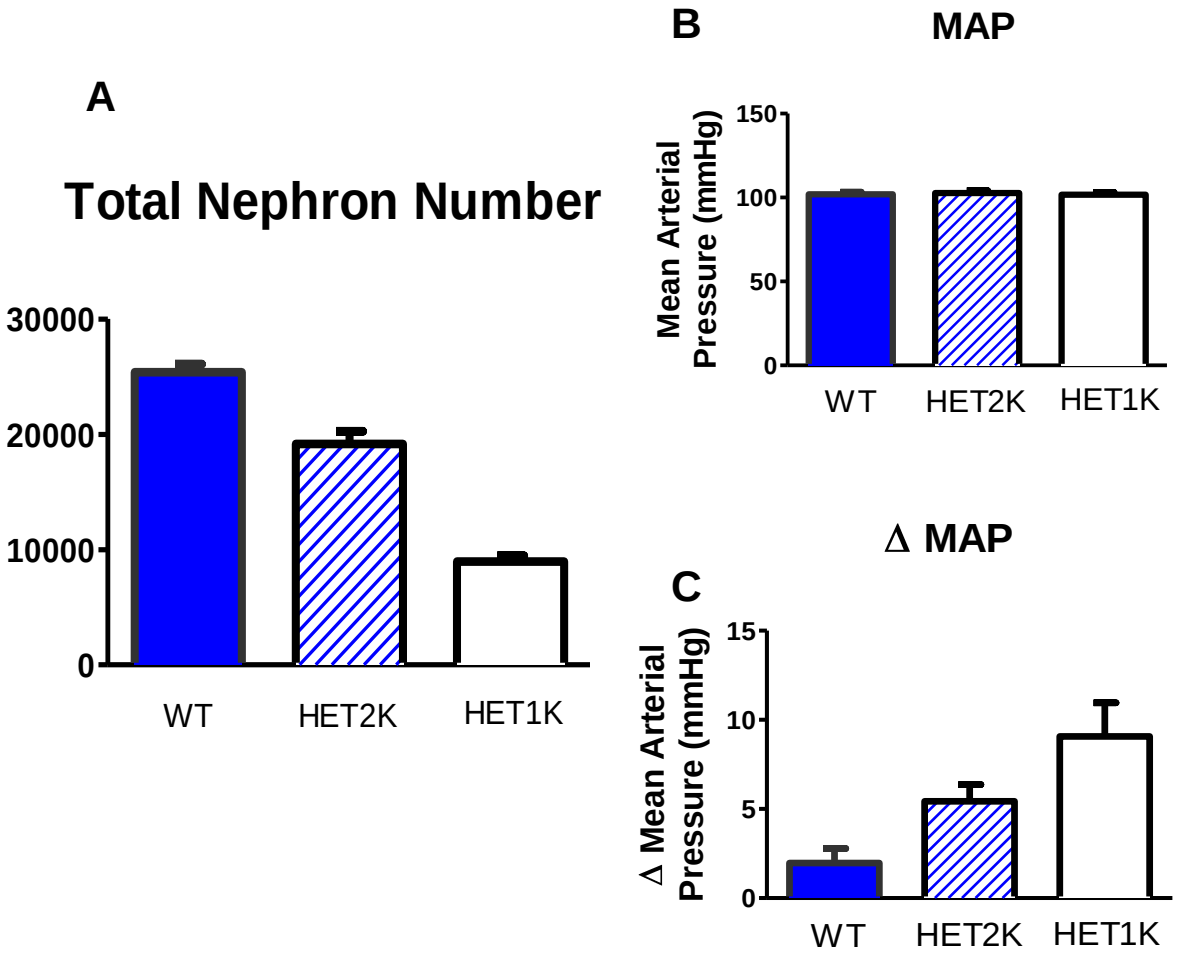

Figure 1.11: Consequences of moderate and low nephron endowment in wildtype (WT) and *Gdnf* heterozygous mice. **(A)** Moderate and low total nephron endowment were observed, respectively, in *Gdnf* heterozygous mice exhibiting renal hypoplasia with two kidneys (HET2K) or one kidney (HET1K). **(B)** Basal mean arterial pressure (MAP) is similar in all three groups of mice. **(C)** Following feeding of a high salt diet, the magnitude of change in MAP correlates strongly with nephron endowment. Data from (Ruta et al. 2010).

1.7.1 'Second Hit Insult'

Although a congenital nephron number deficit may not always be sufficient to induce CVD and CKD, it is believed that the nephron deficit should be regarded as a 'first hit insult' upon which a 'second hit insult' can act, greatly increasing the likelihood of disease development and progression (Nenov et al. 2000). As previously discussed, Ruta et al. (2010) found no direct correlation between mean arterial pressure and nephron endowment (Ruta et al. 2010). However, when these mice were fed a high salt (5% NaCl) diet, mean arterial pressure increased in a manner which correlated strongly with total nephron endowment, with HET1K mice showing the greatest change (Δ 9.1 ± 1.9 mmHg) in arterial pressure, compared to HET2K (Δ5.4 ± 0.9 mmHg) and wildtype (Δ1.9 ± 0.8 mmHg) mice (Figure 1.11C) (Ruta et al. 2010).

In agreement with studies in which a second hit insult is required to induce an elevation in blood pressure in animals with a nephron deficit, Zimanyi et al. (2006) found that rats with a congenital 25% reduction in nephron number had comparable renal morphology to age-matched control rats (Zimanyi et al. 2006). However, following infusion of advanced glycation end-products, a heightened level of renal fibrosis and up-regulation of pro-fibrotic markers was observed in the kidneys of rats with the nephron deficit (Zimanyi et al. 2006).

In humans, the hypothesis of 'first-hit' and 'second-hit' insults is much more difficult to investigate. For example, the prevalence of CVD and CKD is much higher in Australian Aborigines than in Australian whites, and the kidneys of Aborigines contain 30% fewer nephrons. While these associations may exist, the impact of factors such as maternal and postnatal diet, alcohol consumption and socioeconomic status cannot be ignored as contributing factors to the development of chronic disease in Aborigines (Cass et al. 2006; Hoy et al. 2006; McNamara et al. 2010).

Comprehensive reviews of the link between nephron endowment and the development of adult-onset CVD and CKD have generally supported the increased risk for disease associated with a low nephron endowment, and thereby the Brenner hypothesis (Baum 2010; Luyckx and Brenner 2010; Vehaskari 2010). However, low nephron endowment is far from the sole cause of CKD and CVD, and in many cases, a second hit may be required to produce a pathophysiological phenotype. These

second hit phenomena in humans likely include lifestyle choices such as diet, alcohol and tobacco consumption, body size, socioeconomic status, genetic profile and the presence of other disease conditions. Thus, it appears that low nephron endowment may increase the risk of an individual developing hypertension and/or CKD.

However, two key questions remain unaddressed are:

Is a high nephron endowment necessarily beneficial for cardiovascular and renal heath?

What mechanisms give rise to a kidney with high nephron endowment?

Currently, there exists a void in our understanding of the development and consequences of augmented nephron endowment on cardiovascular and renal health and disease development. While the absence of suitable animal models may have been the most significant hurdle to gathering knowledge, a lack of acknowledgment throughout major reviews on the topic of high nephron endowment has done little to raise awareness and stimulate progression of this field. By analysing not only the developmental mechanisms governing augmented nephron endowment but also the functional consequences of such a phenotype in a robust animal model of high nephron number, greater understanding of the role of nephron endowment in health and disease can be achieved.

1.8 HYPOTHESIS AND AIMS OF THE CURRENT PROJECT

1.8.1 Scope of project

The kidney plays a number of critically important homeostatic roles in mammals, including major roles in the regulation of fluid balance, electrolyte balance, acid-base balance, and blood pressure. Total nephron number varies more than 10-fold in the normal human population, and increasing evidence suggests nephron number may

determine an individual's lifetime risk of developing cardiovascular and renal diseases.

The development and functional consequences of a congenital low nephron endowment has been characterised extensively (Woods 1999; Cullen-McEwen et al. 2003; Gilbert et al. 2005; Zimanyi et al. 2006; Narlis et al. 2007; Gray et al. 2008; Villar-Martini et al. 2009; Ruta et al. 2010). However, due to a lack of experimental models, very little is known about the functional consequences of, or the developmental pathways leading to, a high nephron number phenotype. The strikingly augmented nephron number phenotype in *Tgfb2*$^{+/-}$ mice suggests that a greater understanding of TGFβ2 signalling in the developing kidney will provide a potential avenue for understanding the development and, in turn, function, of high nephron number phenotypes. The requirement for the TGFβ accessory receptor, betaglycan, to be present for efficient TGFβ2 signalling suggests that phenotypic similarities may exist between *Tgfb2* and betaglycan knockout mutants, while also providing an environment in which the signalling network governing kidney development can be evaluated in the presence of perturbed TGFβ2 signalling.

The experiments described in this thesis firstly utilise a betaglycan knockout mouse line to characterise the role of betaglycan during metanephric development, and in particular, the establishment of nephron endowment. Second, molecular studies in betaglycan null mutant mice provide an in-depth understanding of the signalling network governing ureteric branching morphogenesis in these mice. Thirdly, the functional consequences of high nephron endowment under basal and physiologically-challenged conditions will be characterised using *Tgfb2*$^{+/-}$ mice. Finally, the potential to augment nephron endowment in wildtype mice via manipulation of the TGFβ2 signalling pathway will be explored.

1.8.2 Overall hypothesis

Mild perturbation of TGFβ2 signalling during metanephric development augments nephron endowment and produces a renal phenotype which is functionally beneficial in the presence of physiological stressors.

1.8.3 Specific aims

1) Determine the role of betaglycan in mouse metanephric development and in the regulation of nephron endowment.

2) Investigate the signalling network governing ureteric branching morphogenesis in betaglycan mutant mouse metanephroi.

3) Characterise arterial pressure and renal functional in a mouse model of high nephron endowment under basal conditions.

4) Investigate cardiovascular and renal function in a mouse model of high nephron number in response to a high salt diet.

5) Characterise renal function during water deprivation in mice with a high nephron endowment.

6) Augment nephron endowment in the developing wildtype mouse kidney through neutralisation of TGFβ2 during late stage nephrogenesis.

CHAPTER 2

GENERAL METHODS

2.1 ANIMAL MODELS

2.1.1 *Tgfb2* mice

All Tgfb2 wildtype and mutant mice used in this thesis were derived from the established *Tgfb2* colony at Mouseworks, Monash University, Clayton, Victoria, Australia. The *Tgfb2* colony was established in 2005 using breeding pairs obtained from Dr. Thomas Doetschman (Department of Molecular Genetics, Biochemistry and Microbiology, University of Cincinnati, OH, USA) (Sanford et al. 1997). Initially, TGFβ2 knockout mice were generated through the disruption of Exon 6 of the *Tgfb2* gene by the insertion of a neomycin-resistance cassette. These gene constructs were injected into embryonic stem cells derived from 129/Ola blastocysts, after which cells expressing the construct were introduced into C57/Bl6J blastocysts. Male germ-line mutants were then out bred with Black Swiss females. The established colony was maintained through non-brother/sister *Tgfb2*$^{+/-}$ matings.

2.1.2 Betaglycan mice

The *Tgfbr3* (betaglycan) knockout mouse was generated on a C57B16/129Sv background (Stenvers et al. 2003). The conventional betaglycan gene knockout was achieved by disruption of Exon 2 of the betaglycan gene by insertion of a PGK-Neomycin cassette. Virtually all betaglycan null (betaglycan$^{-/-}$) mice die between e16.5 and birth (Stenvers et al. 2003). For embryos, adult heterozygous (betaglycan$^{+/-}$) females were time-mated and checked for the presence of vaginal plugs, with the day of plug noted as e0.5. All embryos were Theiler staged by counting tail somites in embryos aged between e11.0-12.5 and by comparing fore and hind limb morphology for embryos aged e13.5 onwards (Section 2.3.2). The established colony was maintained through non-brother/sister betaglycan$^{+/-}$ matings.

2.2 GENOTYPING

To distinguish *Tgfb2* wildtype, *Tgfb2*$^{+/-}$ and *Tgfb2*$^{-/-}$ mice, and betaglycan wildtype, betaglycan$^{+/-}$ and betaglycan$^{-/-}$ mice, tissues from all mice were genotyped

via polymerase chain reaction (PCR). For postnatal mice, tail clips were obtained at weaning. These genotypes were re-confirmed with toe tissue obtained at autopsy. For embryos, portions of the head and tail were collected into separate sterile eppendorf tubes. All tissues were stored at -20 °C until analysis. DNA was extracted from tissues using a Sigma-Aldrich REDExtract-N-Amp^{tm} tissue PCR kit (Sigma-Aldrich, Saint Louis, MO, USA). Tissues were incubated at room temperature in a 125 µl of 1:4 extraction solution:tissue preparation solution (Sigma-Aldrich) for 10 min. Tissues were then heated to 95 °C for 3 min, before being neutralised by the addition of 100 µl of neutralisation solution B (Sigma-Aldrich). Samples were stored at 4 °C until required.

2.2.1 *Tgfb2* genotyping

Each PCR tube contained the follow: PCR grade H_20 (2 µl); REDExtract-N-Amp PCR Reaction Mix (10 µl; Sigma-Aldrich); 2 µM Forward Primer (2µl); 2 µM Reverse Primer (2 µl); DNA extract (4 µl) for a total volume of 20 µl. Previously genotyped embryo DNA was used as a positive control, and water was used as negative control. Separate reactions were carried out for the identification of *Tgfb2* wildtype allele (TGFβ2) and *Tgfb2* neo cassette allele (NEO). The specific primer sequences were as follows:

TGFβ2-Forward 5'-GGCCATCATCACTGACTTAGG-3'
TGFβ2-Reverse 5'-ATGGTGCTCGAGGTTAATGG-3'
NEO-Forward 5'-TCCTGTCATCTCACCTTGCTC-3'
NEO-Reverse 5'-GTAGCCAACGCTATGTCCTG-3'

Step-down PCR amplification conditions were as follows: initial denaturing step 95 °C for 3 min (1 cycle), first denaturing, annealing and extension step 95 °C for 20 sec, 63 °C for 30 sec, 72 °C for 30 sec (2 cycles), second denaturing, annealing and extension step 95 °C for 20 sec, 61 °C for 30 sec, 72 °C for 30 sec (2 cycles), third denaturing, annealing and extension step 95 °C for 20 sec, 59 °C for 30 sec, 72 °C for 30 sec (2 cycles), final denaturing, annealing and extension step 95 °C for 20 sec, 57 °C for 30 sec, 72 °C for 30 sec (2 cycles), further extension step 72 °C for 5 min (1 cycle) and an infinite hold at 4 °C. PCR products were resolved on a 2% agarose gel at

90 V for approximately 30 min and viewed with a Kodak Image Station 4000 M (Carestream Molecular Imaging, Woodbridge, CT, USA). The wildtype TGFβ2 primers generated a 300 bp fragment while the NEO primers generated a 320 bp fragment.

2.2.2 Betaglycan genotyping

The genotype of each embryo was determined using primers designed against either the wildtype Exon 2 or the Neomycin cassette in the targeted allele in a multiplex PCR reaction. The total PCR reaction volume used was 25 μl containing 1 μl of tested DNA sample, 10.5 μl of 2X GoTaq® Green Master Mix, 0.6μl forward primer (10 μM), 0.6 μl reverse primer (10 μM), 0.5 μl Neo2 primer (10 μM) and 11.8 μl water. Specific primers used were:

Exon 2 Forward - 5'- ATTGTGTTCATAGGTCCAGA-3'
Exon 2 Reverse - 5'- CCTAQGTCCTTGGTCTGTACT -3'
Neo Reverse - 5'- TAGGGTTCCGATTTAGTGCT -3'

These primer pairs yielded a single 200 bp band for wildtype embryos; 200 bp and 700 bp bands for heterozygous embryos and a single 700 bp band for knockout embryos. Previously genotyped embryo DNA was used as a positive control, and water was used as negative control. The thermal conditions used for genotyping PCR were: initial denaturing step 95 °C for 4 min (one cycle), denaturing at 94 °C for 1 min (35 cycles), annealing at 58 °C for 1 min (35 cycles), extension at 72 °C for 1 min (35 cycles), further extension at 72 °C for 5 min and hold temperature at 15 °C. The PCR products were run at 65 V for approximately 50 min in a 2% agarose gel.

2.3 TISSUE COLLECTION

2.3.1 Embryonic dissection

Pregnant dams were euthanised via inhalation of carbon dioxide gas (>70% in air or with oxygen) in an induction chamber. A transverse incision was made in the abdomen to expose the uterus, allowing the decidua to be visualised. Embryos were

dissected from the uterine horns and placed in a Petri dish containing sterile phosphate buffered saline (PBS) before dissection. Mouse tails or heads were dissected and stored in a clean eppendorf tube at 4 °C for later genotyping. Metanephroi were dissected from the urogenital ridge and either: 1) stored in a clean 1.5ml eppendorf tube at -80 °C for later real-time PCR analysis (Section 2.5)**;** 2) fixed for 30 min at 4 °C in 4% paraformaldehyde in PBS (PFA), before being transferred into 70% ethanol and stored at 4°C for subsequent stereological (Section 2.4) or immunolabelling analysis (Section 2.7); or 3) transferred into a 24-well culture plate for metanephric culture studies (Section 2.6).

2.3.2 Theiler staging

As multiple developmental ages were utilized during these studies, Theiler staging, the approach by which embryonic age is determined via the presence or absence of morphological structures was used to ensure consistency in the determination of embryonic development.

(http://www.emouseatlas.org/Databases/Anatomy/new/)

Embryonic age was determined in accordance with the number of tail somites present. Tail somites were defined as those that exist between the end of the tail and the intercept of the hind limb (Table 2.1). Embryos were Theiler staged prior to dissection. If any stages were unclear from tail somite number (e.g. in embryos e13.5 and greater), other morphological traits such as limb and face development were assessed in accordance with Theiler staging protocol.

(http://www.emouseatlas.org/Databases/Anatomy/new/)

Table 2.1: Tail somite number and equivalent embryonic age

Tail Somites	Embryonic Age
8 – 11	10.5
12 – 16	11
17 – 21	11.5
22 – 26	12
27 – 31	12.5
32 – 36	13
37 – 41	13.5
42 – 46	14.0
47 - 51	14.5

Modified from Hacker et al. (1995) and
http://www.emouseatlas.org/Databases/Anatomy/new/

2.2.3 Embryonic tissue processing

Embryonic tissues dissected for stereological or immunolabelling analysis were fixed in 4% PFA for 30 min and then transferred into 70% ethanol solution and stored at 4°C. Tissues were then placed in individually labelled multi-chambered histological processing cassettes. Entire cassettes were then sequentially immersed in the following solutions for 20 min each: 50% - 50% butanol / ethanol, 70% - 30% butanol / ethanol, 95% - 5% butanol / ethanol, 100% butanol solution, and finally fresh 100% butanol solution. At the completion of the final step, the entire cassette was placed in a 60°C paraffin wax bath for 30 min. Tissues were then taken from the multi-chambered cassette, placed in individual steel embedding moulds and embedded in paraffin wax.

2.3.4 Postnatal tissue collection

Postnatal mice were euthanized via cervical dislocation and tissues collected. Body weights were recorded and organs dissected, cleaned of fat and blood vessels,

decapsulated and weighed. All organs were immersion-fixed in 4% PFA overnight at 4°C, and then washed for 24 hours in 70% ethanol. Right kidneys were then immersed in 100% butanol for 72 hours with butanol solutions changed every 24 hours in preparation for glycolmethacrylate (GMA) processing. Left kidneys and aortas were halved, with one fragment snap frozen in liquid nitrogen and stored at -80°C for subsequent molecular analysis, while remaining portions of the left kidney, aorta, lungs and cardiac ventricles were processed into paraffin wax for histological analysis.

2.4 STEREOLOGY

All stereological analyses were conducted in a blind manner with the candidate unaware of sample genotypes. Uncoding of samples was conducted at the completion of sterological experiments.

2.4.1 Glycolmethacrylate processing

Tissues were infiltrated with infiltration solution at room temperature (Technovit 7100 kit, Kulzer & Co. GmbH, Friedrichsdorf, Germany). Tissue was left in infiltration solution for 3 days on a roller. Once infiltration was complete, tissue was placed cut surface down in the centre of a mould and covered with embedding solution (Kulzer & Co). Embedding solution was allowed to set for 30 minutes and labels were inserted into the front of blocks to allow for sample identification. Once labels were positioned, blocks were left to sit for 2-3 days. After embedding, backing blocks were poured and allowed to set for 30 min (Kulzer & Co). Once blocks had set, excess backing solution was used to 'glue' the backing block and embedded tissue together. Glue was allowed to set for 1 h.

2.4.2 Sectioning and staining

Tissues embedded in GMA were exhaustively sectioned at 20 μm using a Leica RM2165 microtome (Leica Microsystems, Nussloch GmbH, Germany) fitted with a

glass Ralph knife. The first section chosen was randomly selected via the use of a random number table, between the first and the tenth cut section. Every tenth ("reference") and eleventh ('look up') section was then floated on a cold water bath, mounted on glass slides and dried on a 90 °C hot plate. Once sections had dried, they were stained with Period Acid Schiff's (PAS) stain (Section 2.12.1).

2.4.3 Postnatal stereology

Once staining was completed, stereological analysis was conducted. The total number of glomeruli within each kidney was estimated using the unbiased physical disector/fractionator principle (Bertram 1995; Cullen-McEwen et al. 2001). Paired sections were placed on two Olympus BX50F4 light microscopes fitted with projection arms. Every tenth ("reference") section was placed on a motorised stage (Autoscan EL300, Autoscan System P/L, Melbourne, Australia) on the right hand microscope, whilst every eleventh ('look up') section was placed on a manually rotating stage on the left hand microscope. The motorised stage was operated with the aid of TRAKSCAN software (TRAKSCAN V7.0.0, Autoscan Systems P/L, Melbourne, Australia). A 20 mm x 20mm, 64 point test grid was used to analyse sections. Any point on the grid which landed on tissue was graded P_{kid}. When the point landed on a glomerulus, it was graded P_{glom}. When the point landed on the renal corpuscle, it was graded P_{corp}. Using unbiased counting frames (1300 µm x 1300 µm) superimposed on both the reference and look up sections, glomeruli present in the reference section but not in the look up section were counted as Q^-_L, whereas glomeruli present within the look up section but not the reference section were counted as Q^-_R. Next, a 30 mm x 30 mm grid was placed over each reference section, with all points landing on kidney tissue graded as P_s, whilst points only landing on complete tissue sections (with no artificial tissue edges) were graded P_f. The following equation was then used to determine the total number of glomeruli (nephrons) per kidney ($N_{glom, kid}$):

$$N_{glom,\,kid} = 10 \times (P_s / P_f) \times 1 / 2\,FA \times Q^-$$

Where:

10 is the reciprocal of the section sampling fraction,

$\mathbf{P_s}$ is the total number of grid points overlying the kidney sections, both complete and incomplete,

$\mathbf{P_f}$ is the total number of grid points overlying only the complete sections,

1 / 2 FA is the fraction of the total section area used to count glomeruli, and

$\mathbf{Q^-}$ **is** the combined values of Q^-_L and Q^-_R giving the actual number of glomeruli counted.

The total volume of the embedded kidney (V_{kid}) was estimated using the Cavalieri principle (Gundersen and Jensen 1987):

$$V_{kid} = 2 \times 10 \times t \times a(p) \times P_s$$

Where:

2 is the inverse of the slice sampling fraction,

10 is the inverse of the section sampling fraction,

t is average section thickness (0.02 mm),

a(p) is the area associated with each grid point at a magnification of 24.25 on the microfiche (1.5304 mm^2), and

$\mathbf{P_s}$ is the total number of grid points overlying the kidney sections, both complete and incomplete.

For estimation of mean glomerular volume (V_{glom}) and mean renal corpuscle volume (V_{corp}), the following formulae were used:

$$V_{glom} = (P_{glom} / P_{kid}) / N_{Vglom,\,kid}$$

$$V_{corp} = (P_{corp} / P_{kid}) / N_{Vglom,kid}$$

Where, $N_{Vglom,kid}$ is the number of glomeruli per unit volume of kidney.

Finally, the total volume of all glomeruli in kidneys ($V_{glom,kid}$) and the total volume of all renal corpuscles in kidney ($V_{corp,kid}$) were determined using the following formulae:

$$\mathbf{V_{glom,kid} = V_{glom} \times N_{glom,kid}}$$

$$\mathbf{V_{corp,kid} = V_{corp} \times N_{glom,kid}}$$

2.4.4 Embryonic nephron number estimation

To determine total nephron number in embryonic kidneys, metanephroi collected from e15.5 mouse embryos were immersion fixed in 4% PFA for 30 min, embedded in paraffin wax and exhaustively sectioned at 5 µm. All sections were dewaxed, rehydrated and blocked in 2% bovine serum albumin (BSA) in PBS with 0.3% Triton-X for 30 mins at room temperature. Sections were then digested with 0.1% neuraminidase (Sigma Aldrich) in 1% $CaCl_2$ in PBS, and incubated overnight at 4°C with biotinylated peanut agglutinin (PNA; Sigma-Aldrich) diluted at 20 µg/ml in 2% BSA/PBS and 0.3% Triton-X with 1 mmol/L $CaCl_2/MnCl_2/MgCl_2$. Following incubation, sections were rinsed twice with PBS. The biotinylated PNA was visualized using the Elite streptavidin/biotin amplification ABC kit (Vector Laboratories Inc., Burlingame, CA, USA). The ABC solution was applied for 1 hour at room temperature, after which slides were washed and the stain developed with diaminobenzidine (DAB; Sigma Aldrich) /0.01% H_2O_2/PBS. Sections were counterstained with hematoxylin. Absolute volume of metanephroi and total nephron number were calculated using previously described equations and the Cavalieri principle (Section 2.4.3).

2.4.5 Ureteric epithelium volume estimation

To identify ureteric epithelium within developing metanephroi, whole metanephroi dissected from e13.5 mouse embryos were immersion fixed in 4% PFA, embedded in paraffin wax and exhaustively sectioned at 5 µm. All sections were dewaxed, rehydrated and blocked in 2% BSA in PBS with 0.3% Triton-X for 30 min at room temperature. Sections were then incubated overnight at 4°C with biotinylated *dolichus biflorus* agglutinin (DBA; Sigma-Aldrich) diluted at 20µg/ml in 2% BSA/PBS

and 0.3% Triton-X with 1 mmol/L $CaCl_2$/$MnCl_2$/$MgCl_2$. Following incubation, sections were rinsed twice with PBS. The biotinylated DBA was visualized using the Elite streptavidin/biotin amplification ABC kit (Vector Laboratories Inc., Burlingame, CA, USA). The ABC solution was applied for 1 hour at room temperature, after which slides were washed and the stain developed with DAB (Sigma Aldrich)/0.01% H_2O_2/PBS. Sections were counterstained with haematoxylin. The absolute volumes of metanephroi were estimated as described in Section 2.4.3. To estimate absolute ($\mathbf{V_{ue}}$) relative ($\mathbf{V_{ue,kid}}$) volumes of ureteric epithelium in metanephroi, a 1 cm x 1 cm counting grid was projected over DBA labelled sections. All points interesecting metanephric tissue as well as points intersecting DBA positive structures were counted. Metanephric ($\mathbf{V_{kid}}$) and ureteric epithelial volumes were estimated using the Cavalieri principle, and the described formulae.

For estimation of metanephric volume and absolute ureteric epithelial volume the following formulae was used:

$$\mathbf{V_{kid} = \Sigma\ Points \times a(p) \times t \times 5}$$

$$\mathbf{V_{ue} = \Sigma\ Points \times a(p) \times t \times 5}$$

Where:

Σ Points is the total number of points overlying positive structures

a(p) is the area associated with each grid point at a magnification of 298 (0.00281 mm^2)

t is average section thickness (0.005 mm),

5 is the inverse of the section sampling fraction,

For estimation of relative ureteric epithelial volume for following formula was used:

$$\mathbf{V_{ue,kid} = (V_{ue} / V_{kid}) \times 100}$$

2.5 REAL-TIME PCR

2.5.1 RNA extraction

The total RNA was extracted from frozen tissues (e11.5-e14.5 metanephroi) using the RNeasy kit (Qiagen GmbH, Germany) according to manufacturer's instructions. Tissues were disrupted using 21, 24, 27 and 30 Gauge needles and homogenized with guanidine thiocyanate (RLT) buffer containing 0.01% β-Mercaptoethanol (β-ME), which prevents RNA degradation. The resulting lysates were mixed with 70% ethanol and passed through an RNeasy mini spin column (Qiagen) after which samples were DNase treated after a series of centrifugation and washes. DNase treatment was performed directly after RNA extraction to remove traces of DNA that would interfere with PCR if non-intron spanning primers were used. DNase treatment was performed using the DNA-*free*™ kit (Ambion, TX, USA). A mixture of 3 μl 10X DNase I buffer and 1 μl DNase (2 Units/μl) was first added to 30 μl RNA and incubated at 37 °C for 25 min. Upon addition of DNase inactivation reagent and 2 min incubation, RNA was eluted by addition of 30 μl RNase free water into an RNeasy free eppendorf tube (Qiagen) and stored at -80 °C.

2.5.2 RNA quantification

The concentration and quality of the RNA was subsequently quantified using a NanoDrop® ND-1000 UV-Vis Spectrophotometer (Nanodrop Technologies Inc, Wilmington, DE, USA) in which a 2μl aliquot (1μl RNA and 1μl DEPC water) is sufficient to give reproducible readings at wavelengths of 260nm and 280nm. Pure RNA preparations have a A_{260}/A_{280} ratio normally between 1.8-2.0. The integrity of RNA samples was confirmed by electrophoresis on a 2% agarose gel with addition of RNA loading dye. The concentration of RNA was determined by this equation:

$$\textbf{[RNA sample] (ng/μl) = (OD } A_{260} \textbf{ x 40) x dilution factor}$$

2.5.3 Reverse-Transcription

Total RNA (1 μg for adult tissue; 250 ng for embryonic tissue) was converted into cDNA prior to real-time analysis. The initial reaction contained the following reagents: 9 μl of RNA, 1 μl of 40 U/μl RNA Inhibitor (Roche, Basal, Switzerland), 1 μl of 50 μM oligo Random Hexamer (Applied Biosciences, Mumbai, India) and 1 μl of 0.25μg Oligo dT (Roche). The mixture was heated to 37 °C for 10 min and mixed with a master mix containing the following: 4 μl of 5X Expand reverse transcriptase buffer, 2 μl of 0.1 M DTT, 1 μl 10 mM dNTP and 1 μl of 50 U/μl Expand Reverse Transcriptase (Roche) which made up a final reaction volume of 20 μl. The final mixture was then incubated at 30°C for 10 min, followed by 42°C for 50 min. The RT reaction was inactivated by heating to 70 °C for 15 min. All reaction steps were carried out in a PCR machine.

2.5.4 Primer design

Sense and antisense oligonucleotide primers were designed from the reported mouse gene sequence. Primers were checked to span at least one intron in order to eliminate genomic DNA contamination in the final product using the Genome Browser Gateway (http://genome.ucsc.edu/cgi-bin/hgGateway) and Primer 3: WWW primer software (http://biotools.umassmed.edu/bioapps/primer3_www.cgi). Specific primers were designed with the following criteria: PCR product size less than 350 bp, primer size between 18-20 nucleotides long, annealing temperature between 58-63 °C, approximately 50% GC content, maximum 3' stability equal to 9 and no mismatches and self-priming.

NetPrimer software (http://www.premierbiosoft.com/netprimer/index.html) was used to determine primer dimer formation and any complementary sequences within or between primers, which were to be avoided. Finally, the desired primer sequence was "blasted" (http://www.ncbi.nlm.nih.gov/blast/Blast.cgi) against the sequence database to confirm that the primers only amplify one specific product. All primers were custom made by Sigma Genosys (Sydney, Australia).

2.5.5 Primer optimisation

Synthesized cDNA of adult tissue was initially amplified by normal PCR using the designed primers. A temperature gradient PCR was performed for all primers to determine optimum annealing temperatures. PCR reactions were carried out over a range of annealing temperatures of 56 - 61 °C. PCR was repeated again at the optimum annealing temperature to reconfirm the result (Table 2.2).

Table 2.2: Table of primer sequences

Gene Name	Gene Bank Number	Primer Sequence (5' – 3')	Product Size (bp)	Annealing Temperature (°C)
Bmp4	NM_007554	Forward AGGAGGAGGAGGAAGAGCAG Reverse GAGGAAACGAAAAGCAGAGC	149	61
Ret	NM_001080780	Forward TAAAGCAGGCTACGGCATCT Reverse GTGGTGGCAGACACAGAAGA	172	61
Eya1	NM_010164	Forward ACAAGTCAGGCGGTCACAG Reverse CCAGGTCCCAGATGAACACT	193	61
Gdnf	NM_010275	Forward AATGTCCAACTGGGGGTCTA Reverse GCCGAGGGAGTGGTCTTC	180	55
Pax2	NM_011037	Forward CTGCCCACATTAGAGGAGGT Reverse TGGAAGACATCGGGATAGGA	199	55
Six1	NM_009189	Forward AACCCCTACCCCTCACCG Reverse AGAGAGTTGATTCTGCTTGTT	177	55
Tgfb1	NM_011577.1	Forward AGCCCGAAGCGGACTACTAT Reverse TTCCACATGTTGCTCCACAC	215	55
Tgfb2	NM_009367	Forward TTTAAGAGGGATCTTGGATGGA Reverse AGAATGGTCAGTGGTTCCAGAT	197	55
Tgfb3	NM_009368	Forward CGCACAGAGCAGAGAATTGA Reverse GTGACATGGACAGTGGATGC	204	55
Wnt4	NM_009523	Forward CCGGGCACTCATGAATCTT Reverse ACGTCTTTACCTCGCAGGAG	113	61
Wt1	NM_144783	Forward GAGAGCCAGCCTACCATCC Reverse CAACTGTCAGTAGGGGTGTGG	212	61
18s	NR_003278.1	Forward GTAACCCGTTGAACCCCATT Reverse CCATCCAATCGGTAGTAGCG	151	61

2.5.6 Real - Time PCR

Real-time PCR was utilized to determine gene expression in foetal metanephroi. Duplicate pools of foetal metanephroi (e11.5, e12.5, e13.5 and e14.5)

from both male and female embryos, and of all three genotypes (+/+, +/- and -/-) were tested (n = 4 - 6 embryos per pool). All real-time PCR experiments were carried out in either 96 or 384 well plates (Applied Biosystems, Australia) with each well contained a 10 μl reaction mixture. The reaction mixture was comprised of 2 μl cDNA sample (12.5 ng) or standards, 5 μl SYBR® Green PCR Master Mix (Applied Biosystems), 1 μl of 10 μM forward and 1 μl of 10 μM reverse primer of interest each, and 1 μl dH_2O. A water sample was used as negative control in every real-time run, and a "negative RT" control (lack of reverse transcriptase during RT reaction) was also used to ensure the absence of DNA contamination at the reverse transcription step of cDNA synthesis. All reactions were set up in triplicate and performed by the ABI 7900 HT Fast Real-time PCR machine (Applied Biosystems) with the following thermal conditions: initial denaturation at 95 °C for 10 min, repeat 55 cycles of 95 °C for 15 sec, 61 °C for 5 sec, 72 °C for 10 sec and three final denaturation steps of 95 °C for 15 seconds, 60 °C for 15 seconds, 95 °C for 15 seconds. The final amplified products were confirmed by sequencing.

2.5.7 Preparation of standards

To ensure that similar amounts of RNA were being utilised between experimental pools, a standard curve was generated. Standards for all RNA investigated were prepared from 1 μg of adult kidney cDNA and sterile water to make up serial masses of 50 ng, 25 ng, 12.5 ng, 6.25 ng and 3.125 ng. The standard curve generated by real-time PCR confirmed the quantity of tested cDNA to be 12.5 ng by assuring all sample values fell between the 25 ng and 6.25 ng mass points.

2.5.8 Sequencing

All real-time PCR products were sequenced by the Gandel Charitable Trust Sequencing Centre (Monash Health Research Precinct) using the 16-capillary 3130x/Genetic Analyzer (Applied Biosystems, USA). The reaction mixtures contained 3.2 pmol of either forward or reverse primer (1 μl), 40 ng DNA template and dH_2O made up to a final volume of 16 μl. Samples were first incubated at 96 °C for 1 min, followed by 25 cycles of denaturing at 96 °C for 10 sec, annealing at 50 °C for 5 sec

and extension at 60 °C for 4 min. The sequencing result was verified against the nucleotide database using the nucleotide-nucleotide BLAST search engine provided by the National Institutes of Health (http://www.ncbi.nlm.nih.gov/blast/Blast.cgi).

2.6 METANEPHRIC DEVELOPMENT

2.6.1 Metanephric organ culture

Whole metanephroi were isolated from e12.5 mouse embryos and placed on polycarbonate filters (3 μm pores) in wells containing serum-free culture medium (350 μl) at 37°C and 5% CO_2. Culture media consisted of 50:50 Dulbecco's modified Eagle's medium (DMEM): Ham's F12 liquid medium (Trace Biosciences, Castle Hill, Australia) supplemented with transferrin (5 μg/ml); Sigma-Aldrich), L-glutamine (2.5 mmol/L; Trace Biosciences), penicillin (100 μg/ml) and streptomycin (100 μg/ml). Metanephroi were cultured for 48 hours. At the conclusion of the culture period, metanephroi were fixed with methanol (-20°C) and stored at -20°C until required.

2.6.2 Analysis of metanephric development

Immunohistochemistry for Calbindin-D_{28K} and Wilm's Tumor-1 (WT1) was performed to identify ureteric epithelium and developing glomeruli, respectively. Whole metanephroi on polycarbonate inserts previously fixed with 100% methanol at -20 °C were washed in PBS at room temperature (2 x 10 min), permeabilised using 0.3% Triton-X 100 in PBS (10 min) and then blocked in 10% normal goat serum, 2% BSA, in PBS solution at room temperature (30 min). Metanephroi were then incubated with monoclonal mouse anti-calbindin-D_{28K} (1:200; Sigma-Aldrich) and rabbit anti-mouse anti-WT1 (1:100; Santa Cruz, CA, USA) antibodies at a dilution of 1:100, at 37 °C for 1 hour. Metanephroi were washed in PBS before the addition of the secondary antibodies, Alexa Fluor ® 488 goat anti-mouse (Molecular Probes, Inc, Eugene, OR) and Alexa Fluor ® 594 goat anti-rabbit (Molecular Probes), at a dilution of 1:500, at 37 °C for 1 hour. Metanephroi were then washed in PBS for several hours prior to visualization. Branch tips and glomeruli were viewed and counted with the

aid of an Olympus Provis epifluoresence microscope and images obtained using a Leica DC digital camera (Leica Microsystems Ltd).

2.6.3 Ureteric bud analysis

Whole mount Calbindin D_{28k} immunofluorescence was performed (Section 2.6.2) on gonadal ridges isolated from e11.0 (14 – 17 tail somites), e11.5 (18 – 22 tail somites) and e12.0 embryos (23 – 26 tail somites). Gonadal ridges were visualized with the aid of an Olympus Provis epifluoresence microscope and images obtained using a Leica DC digital camera (Leica Microsystems Ltd). The presence and morphology of the ureteric bud was correlated with the number of developing somites.

2.7 IMMUNOSTAINING

2.7.1 Betaglycan immunofluorescence labelling

Metanephroi from e12.5 – e16.5 wildtype mouse embryos were fixed in 4% PFA at 4 °C for 10 min, incubated in 20% sucrose overnight at 4 °C, then processed for embedding in OCT and sectioned at 5 μm. For immunofluorescence, sections were treated with 1% Triton-X in PBS for 10 min at room temperature and rinsed with PBS. Sections were blocked with 5% donkey serum in PBS, and incubated overnight at 4°C with a polyclonal antibody against betaglycan raised in goat (1:50; R&D Systems, Minneapolis, USA). Sections were then washed with PBS then incubated with a donkey anti-goat Alexa Fluor 488-conjugated secondary antibody for detection (1:400; Molecular Probes). Cell nuclei were visualized with TO-PRO (Invitrogen, Carlsbad, CA, USA). Slides were mounted in Fluorosave Mounting Medium (Calbiochem, San Diego, CA, USA) and visualized via standard fluorescence microscopy using an Olympus Provis epifluoresence microscope fitted with a Leica DC digital camera.

2.7.2 SMAD immunohistochemistry

Metanephroi were dissected, fixed, and hand processed to paraffin as previously described (Section 2.2.3). Paraffin sections (5 μm) were microwave oven-heated in a 10 mmol/L citrate buffer (pH 6.0) for 10 min. To improve the efficiency and specificity of staining, Dako Envision System-HRP (Dako North American, Carpinteria, CA) was utilised as per manufacturer's instructions. All sections were washed in PBS, blocked with 10% normal goat serum plus 10% fetal calf serum in PBS for 30 min at room temperature, and then incubated overnight at 4 °C with either primary antibodies specific for the phosphorylated (p) form of SMAD1 (pSMAD1; 1:100; Santa Cruz) or pSMAD3 (1:100; Abnova, Redfern, NSW, Australia) antibodies in 1% BSA in PBS. For each slide, an irrelevant isotype rabbit IgG_1 was used as the negative control. Sections were subsequently washed in PBS, treated with 3% H_2O_2 in methanol for 20 min to inactivate endogenous peroxidases, and incubated with biotin-conjugated goat anti-rabbit IgG (Dako) for 25 min. Sections were then developed via a 5 min incubation with 3, 3'-diaminobenzidine (DAB) and substrate-chromogen (Dako), which resulted in a brown-coloured precipitate at the antigen site. Finally 4', 6-diamidino-2-phenylindole (DAPI) was applied to slides for 5 min to counterstain nuclei (1:10,000). Slides were mounted in Fluorosave Mounting Medium (Calbiochem) and visualized via standard fluorescence microscopy using an Olympus Provis epifluoresence microscope fitted with a Leica DC digital camera.

Quantitative assessment of pSMAD1 and pSMAD3 expression in developing metanephroi was performed. Fluorescent nuclear profiles with overlapping localized pSMAD1 or pSMAD3 staining were counted in approximately six non-overlapping high-power (×400 magnification) fields per metanephric section. Entire metanephric sections were analysed, with results expressed as the percentage of cells expressing per total number of metanephric cells. SMAD immunohistochemistry was performed by Dr. Jinhua Li from the Department of Anatomy and Developmental Biology, Monash University, Clayton, Victoria. All labelled tissues were quantified by Kenneth Walker.

2.7 ASSESSMENT OF BLOOD PRESSURE, HEART RATE AND ACTIVITY IN CONSCIOUS MICE

2.7.1 Dietary salt intake

Currently much conjecture surrounds what percentage of salt should be contained in 'normal' rodent chow. Previous studies have suggested that 0.05% sodium is sufficient for normal growth and reproduction of rodents (Martus et al. 2005). However, recent studies have demonstrated that 'normal' can range between 0.1 – 0.7% sodium (Sandberg et al. 2006; Carlstrom et al. 2007; Chi et al. 2008). Curiously, the description as to whether this concentration refers to sodium chloride (NaCl) or sodium alone is unclear. For all physiological studies in this thesis, 0.26% (w/w) NaCl diet was adopted as a 'normal' salt diet (Specialty Feeds, Glen Forrest, WA, Australia). This diet is based on requirements from the American Society of Nutritional Sciences, and satisfies the nutritional requirements of rodents (Reeves et al. 1993; Reeves et al. 1993). While 0.26% NaCl is higher than the required 0.05% sodium, this diet is at the lower end of the 'normal' concentrations previously published.

In selecting appropriate high salt diets, previous examinations of the renal physiology of mice and rats fed high salt diets ranging from 4 – 10 % w/w NaCl were taken into consideration (Ruta 2009). Briefly, short term administration of 5% NaCl (w/w) diet (Specialty Feeds) was shown to induce moderate increases in water intake (2-fold) and urine volume excretion (4-fold), without any evidence of renal histopathology (Ruta et al. 2010). Returning mice to a normal salt diet was shown to completely restore baseline renal function. 5% NaCl (w/w) was therefore deemed as sufficient for analysing cardiovascular and renal function in the presence of a physiological stressor.

Concentrations of 8% NaCl (w/w) and higher have previously been shown to induce widespread myocardial and renal fibrosis in rodents (Yu et al. 1998). As a primary aim of the present study was to determine whether augmented nephron number provides protection against a pathological stressor, 8% (w/w) NaCl diet was selected as an appropriate factor for inducing a pathological environment (Specialty Feeds).

2.7.2 PA-C10 radiotelemetry transmitter

For the measurement of mean arterial, systolic and diastolic pressures, heart rate, pulse pressure and physical activity, radiotelemetry was utilised. This approach is the gold standard for blood pressure recording in small rodents firstly, as mice are free to roam in their home cages, and are not subjected to restraint or tethering (Kurtz et al. 2005; Van Vliet et al. 2006). Secondly, data are continuously obtained for conscious animals over multiple days. Mice underwent brief surgery for the implantation of transmitters which telemeter blood pressure and other parameters from within the animal being measured. A receiver, placed below the mouse home box, detects the radio frequency signal from the transmitter and converts the signal into a serial bit stream.

The TA11PA-C10 (Data Sciences International, St Paul, MN, USA) blood pressure transmitter used in the present study consists of a thin walled catheter tip, main catheter and sealed body which contains the electronics, sensor and battery, together weighing 1.4 g (Figure 2.1). Arterial pressure is transferred to the sensor via a 5 cm long catheter. The catheter is constructed of urethane with a 0.1 mm wall and a 0.2 mm lumen which is filled with a low-viscosity fluid. The distal 4 mm of the catheter is composed of a thin-walled pressure sensing tip, coated in an antithrombotic coating and the final 2 mm of the tip is filled with a biocompatible silicone gel (Figure 2.1). This prevents blood from entering the catheter lumen and clotting, while allowing efficient transmission of blood pressure to the main catheter.

Ambient pressure was measured and subtracted from telemetered pressure by the data collection software (Dataquest A.R.T., Data Sciences International, St Paul, MN, USA). Data were collected and stored to disk using the Dataquest A.R.T system.

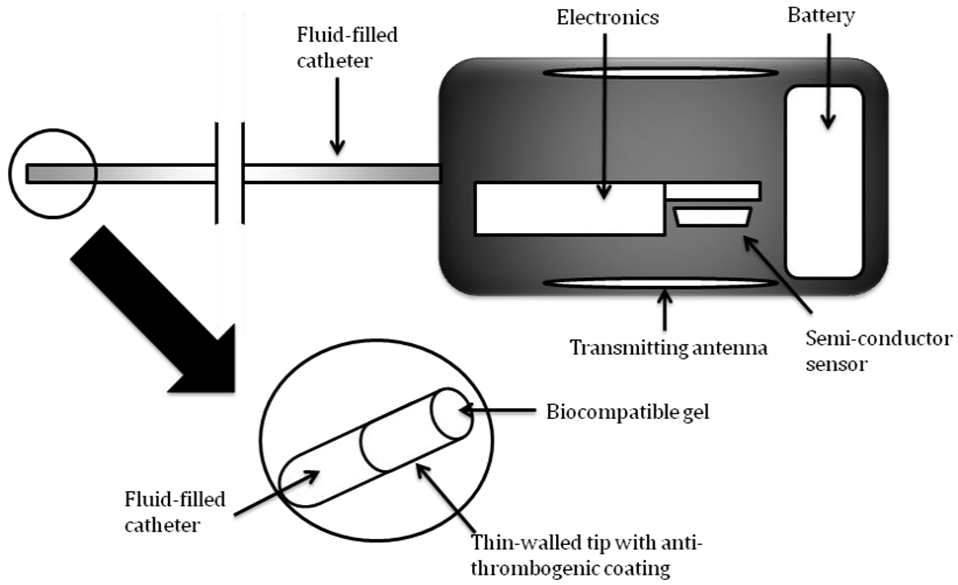

Figure 2.1: PA-C10 radiotelemetry transmitter. When implanted, blood pressure, heart rate and activity are recorded by the transmitter. Pressure is detected by the thin walled tip and transmitted to the transmitter body via the fluid filled catheter. Modified from (Mills et al. 2000)

2.7.3 Surgery

Male wildtype and *Tgfb2*$^{+/-}$ mice were anaesthetised with isoflurane inhalation anaesthetic (Rhodia Australia Pty. Ltd.) mixed with 40% O_2 and 60% N_2 (BOC-Gases Australia Pty. Ltd.). Isoflurane was delivered using a Univentor 400 anaesthesia unit (Univentor Ltd, Zejtun, Malta) at a concentration of 4.5% for induction and reduced to 2.2 – 2.6% for maintenance of anaesthesia during surgery. Following induction mice were placed in a supine position on a heated operating surface designed to maintain core body temperature at 37°C throughout surgery. The region around the neck was swabbed with 70% ethanol to clean the area and prevent fur from interfering with the procedure. Chloroptsone eye ointment (Delta Laboratories Pty Ltd, Mt Kuring-Gai, NSW, Australia) was administered to the conjunctiva to prevent damage due to drying during surgery.

An initial ventral incision (~2 cm) was made in the neck, slightly to the left of the midline. This facilitated subsequent isolation of the left carotid artery. Following the incision, a subcutaneous pouch along the animal's right flank was made using a pair of blunt dissecting scissors. Skin was blunt-dissected gently away from

underlying tissue, starting from the neck region and progressing downwards toward the right hind limb (Figure 2.2A). The pouch was large enough to house the telemetry probe without stretching the skin, to avoid pressure necrosis.

Through the initial incision, the left carotid artery was located and isolated. Blood flow was inhibited with the aid of curved forceps. Particular care was taken not to disturb the vagus nerve running parallel with the carotid artery. Once isolated, three silk ties (6-0 suture, Dysilk: Dynek Pty Ltd, SA, Australia) were passed under the artery. One silk tie was used to ligate the artery at the bifurcation of the exterior and interior carotid arteries. This tie was then retracted towards the head. The second silk tie was loosely placed as distal as possible to the carotid bifurcation, and then retracted towards the core to temporally occlude the artery and allow catheter insertion. The final tie was placed distal to the designated point of incision in the carotid artery to be used to secure the catheter within the artery.

The telemetry probe was turned on at this point to assess signal quality and remained on until the completion of the surgery. An incision in the carotid artery was made with micro scissors. Fine tipped forceps were used to further open the incision in the artery and allow the catheter to be slowly inserted and loosely secured with the tie to prevent the catheter from slipping out of the vessel. The most distal tie was then released and the catheter fed through the artery until the plastic notch (10 mm from the tip of the catheter) was in line with the final tie and the carotid bifurcation. This point was used as guidance to ensure the tip of the catheter was correctly positioning in the aortic arch. Finally, the most distal tie was secured around the notch of the catheter, and forceps were removed, allowing blood flow to return.

The telemetry probe body was inserted into the subcutaneous pouch through the initial incision. To assist the probe into the pouch, 1 ml of saline was flushed into the pouch, and then the probe was gently pushed along the right flank and into the pouch. To prevent infection, antibiotics were then administered subcutaneously (trimethoprim 80mg/ml, sulfadiazine 400mg/ml, Tribactral, Jurox, NSW, Australia). The incision was then closed with 5-0 suture and anaesthetic removed allowing the mouse to breathe room air. Analgesia was given subcutaneously at this point to assist with recovery (Rimadyl (carprofen) 0.75mg/ml, Pfizer, West Ryde, NSW, Australia) The mouse was observed until motor control returned, after which it was returned to

its home cage, on a heated operating surface, and monitored closely for signs of bleeding or distress for approximately 1 hour. During surgery, the mouse was anaesthetised for approximately 30 min, with recovery taking place within 5 min of isoflurane cessation. Mouse behaviour and wound appearance were monitored daily for the following 10 day recovery period. Baytril® 25 antibiotic oral solution (Bayer Australia, Pymble, NSW, Australia) was administered orally in drinking water (3 ml per 200 ml of H_20), 1 day after surgery for 48 hours to prevent post-operative infection.

Telemetry probes were switched on with the aid of a magnet, and signal trace quality was confirmed using the Dataquest system, with a pulse pressure of greater than 20 mmHg deemed acceptable. Once the probe was switched on, diastolic, systolic and mean arterial pressures, heart rate and physical activity were continuously sampled for 10 sec every 10 min, until probes were switched off.

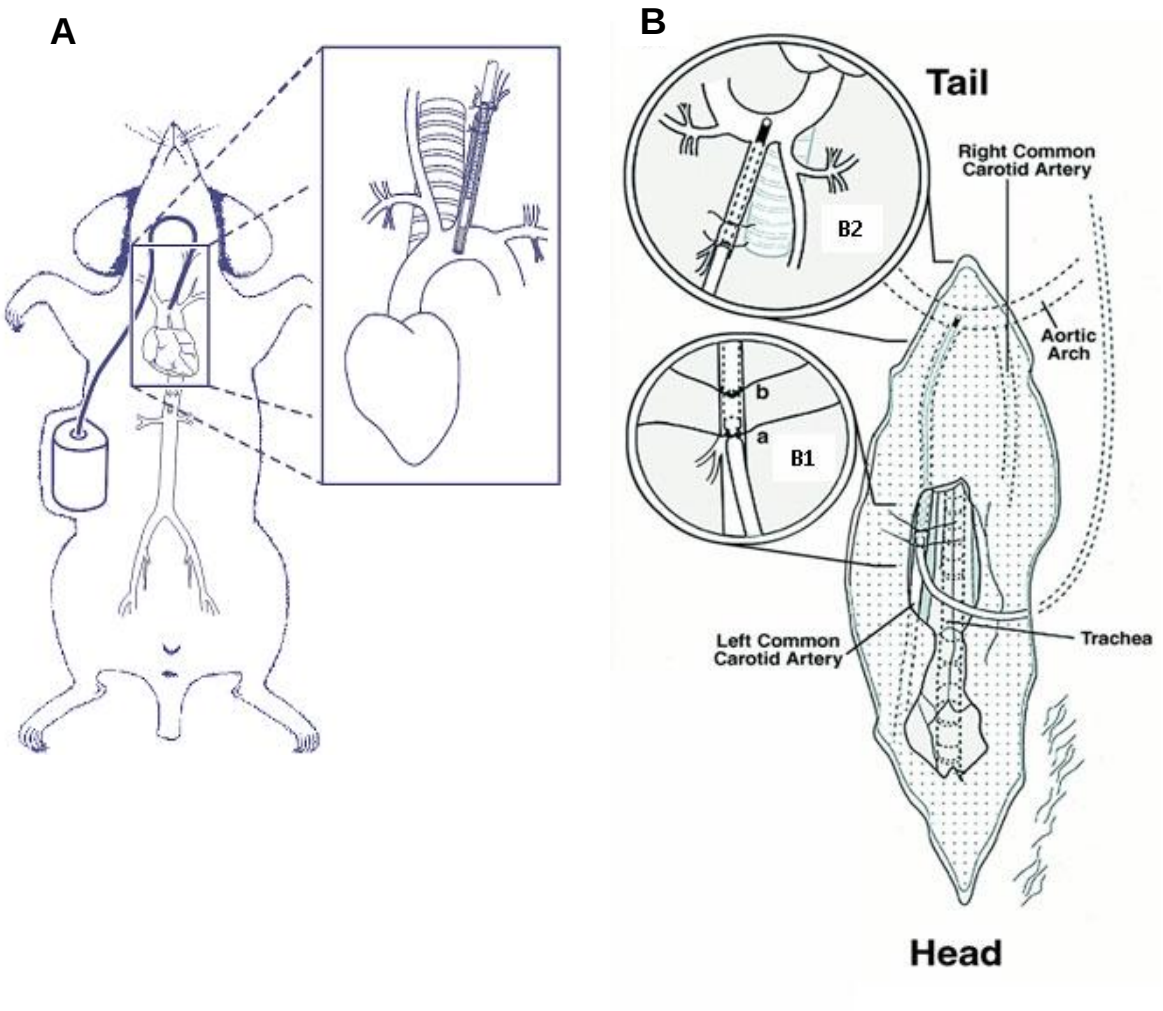

Figure 2.2: Implantation of the radiotelemetry transmitter. (A) Subcutaneous position of the probe body near the right hind limb. Transmitter probe catheter is seen feeding into the right carotid artery, with the tip positioned within the aortic arch (insert), image from http://www.datasci.com/products/implantable-telemetry/Mouse-Implantable-Telemetry/Blood-Pressure-Transmitter.asp.
(B) Surgical site for telemetry probe surgery, highlighting insertion point of catheter into left carotid artery (Insert B1) and the positioning of catheter tip and silk ties (Insert B2). Modified from (Butz and Davisson 2001).

2.8 ASSESSMENT OF RENAL FUNCTION IN CONSCIOUS MICE

2.8.1 Metabolic cages

To allow for the collection of urine and analysis of conscious renal function in mice, purpose-built metabolic cages were used. Each metabolic cage consisted of a glass housing chamber (10 cm in diameter) with a fine steel grate floor,

accompanying peripheral chambers housing food and water, and a splitter associated with the base of the chamber, functioning to separate urine and faecal wastes. Collection vials beneath food, water and splitter allowed for food and water intake, as well as urine and faeces excretion, to be recorded. The sealed nature of the system minimised evaporation of urine and water, while at the same time allowing adequate ventilation.

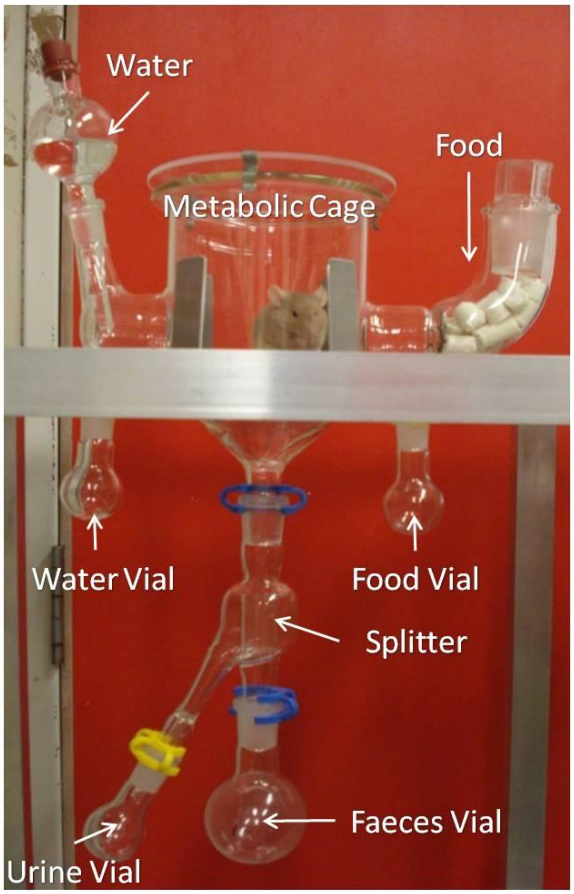

Figure 2.3: Metabolic cage. Glass metabolic cage utilised to measure food and water consumed, and urine and faeces excreted, during a 24 hour period.

2.8.2 Training

Metabolic cages can be stressful for mice as they are an unfamiliar environment. Stress can manifest in abnormal behaviour and confound experimental data. To minimise stress, mice were subjected to metabolic cage training periods approximately 2 days prior to actual data collection. Training involved placement of mice in individual metabolic cages with *ad libitum* access to food and water for 8

hours, during which time behaviour was monitored every few hours. During periods within the metabolic cages, cardboard screens were set around the central chamber to reduce the sense of exposure. Additional training periods in the presence of water deprivation were adopted for all water deprivation experiments to minimise aberrant behaviour.

2.8.3 24 hour urine collection

Following successful training periods, mice were weighed and placed in individual metabolic cages for a 24 hour period. The amount of food and volume of water supplied were recorded, and urine and faeces collection vials were weighed. At the completion of the 24 hour period, observations assessing mouse stress were documented, and then mice were weighed and returned to their home cage. If mice showed signs of stress such as major weight loss (>0.5 g) or significant shredding of food, results were excluded. Remaining food and water, as well as excreted urine and faeces, were weighed and recorded. Urine was transferred into 2 ml eppendorf tubes, clarified by centrifugation and frozen at -20 °C for subsequent analysis of urinary ion concentration, osmolality, microalbuminuria and creatinine. At the end of the collection period, a retro-orbital bleed was taken when required to obtain a blood sample for analysis of haematocrit and plasma creatinine.

2.8.4 Measurement of conscious GFR

Measurement and analysis of urinary and plasma creatinine concentrations by high performance liquid chromatography (HPLC) were performed by Associate Professor Merlin C. Thomas at the Baker IDI Heart and Diabetes Institute, Melbourne, Australia. Analysis was conducted in accordance to the animal models of diabetic complications consortium (AMDCC) guidelines (Dunn et al. 2004). Creatinine clearance (Ccre), and in turn GFR, was calculated using:

$$\text{Ccre} = \frac{\text{Urinary creatinine concentration (µmol/L) x Urine volume (ml/min)}}{\text{Plasma Creatinine concentration (µmol/L)}}$$

2.9 PLASMA AND URINE ANALYSIS

2.9.1 Urinary electrolytes and osmolality

Urinary electrolytes were analysed using a Bayer RapidChem 744 (Sysmed Lab, Inc. Chicago, IL, USA). Samples were diluted 1:10 in RapidChem buffer, aspirated, and via the use of ion-selective electrode detection, the concentration of urinary sodium, potassium and chloride was determined. Urinary osmolality was measured by freezing-point depression using the Advanced Osmometer 2020 (Advanced Instruments, Needham Heights, MA, USA).

2.9.2 Microalbuminuria

Urinary albumin concentration and excretion was determined using a murine specific microalbuminuria ELISA kit (Exocell Inc., Philadelphia, PA, USA). Serial dilutions of enzyme immunoassay (EIA) diluent (10, 5, 2.5, 1.25, 0.625, 0.313 and 0.016 μg/ml, respectively), were added to the 96-well plate in triplicate (10 μg/ml: A1, 2, 3; 5 μg/ml: B1, 2, 3; 2.5 μg/ml: C1, 2, 3; 1.25 μg/ml: D1, 2, 3; 0.625 μg/ml: E1, 2, 3, 0.313 μg/ml: F1, 2, 3; 0.016 μg/ml: G1, 2, 3) and used to construct standard curves. The mean of the curves was graphed and the equation of the line obtained.

Urine samples from metabolic cage collections were thawed and allowed to come to room temperature without heating. Samples were diluted 1:13 in EIA and loaded into the remaining wells of the 96-well plate in duplicates. Rabbit anti-murine albumin antibody was added to all wells except A1 as this was used as a negative control to blank the microplate reader. Wells A2 and A3 were set as positive controls. After 30 min incubation at room temperature and a series of vigorous washes with ddH_20, anti-rabbit HRP conjugate was added to all wells and the plate was left to incubate for 30 min at room temperature. After another series of ddH_20 washes, colour developer was added to each well and allowed to develop for 6 min before colour stopper was added. Absorbance of experimental wells was determined at 450 nm using a microplate reader (BioRad 3350, Tokyo, Japan) with all values normalised to the standard curve.

The concentration of murine serum albumin was determined using:

$$\mathbf{Log_{10}[MSA] = m\ (A_{450}) + b,}$$

where [MSA] is the concentration of murine serum albumin, 'm' is the gradient of the standard curve, A_{450} is the absorbance reading of each well at 450 nm and 'b' is where the standard curve intersects the y axis. The concentration of murine serum albumin was determined by multiplying by 13 to correct for the dilution factor, and then multiplied again by the initial volume of urine sample to determine albumin excretion in a 24 hour period.

2.10 POST-MORTEM

At the conclusion of the physiology experiments, post-mortems were performed to collect tissues and final blood samples. Mice were anaesthetised (isoflurane), placed on a heated operating surface and a ventral incision made in the neck, as described previously (Section 2.7.3). The right carotid artery was isolated, and blood flow was restricted with the aid of curved forceps. Microscissors were used to make several small incision in the carotid artery and a blood sample was collected into a 100 µl heparinised microhaematocrit tube for determination of haematocrit. Blood flow was then returned to the vessel, and blood was collected directly into a chilled eppendorf tube containing 4 µl of heparin (10 IU/ml), to prevent clotting. Into a separate chilled eppendorf tube containing 12.5 µl of BAL (British Anti-Lewisite Reagent, 2, 3-Dimercapto-1-propanol, Sigma Chemical Company, MO, USA) to inhibit activity of angiotensin converting enzyme, approximately 200 µl of blood was collected. Blood samples were immediately spun in a refrigerated centrifuge for 5 min and plasma collected. Plasma samples were then transferred into fresh eppendorf tubes. A 20 µl plasma sample from the heparin tube was collected into a separate eppendorf tube for analysis of plasma creatinine concentration. All samples were then stored at -20 °C until required.

A midline incision was then made and the kidneys rapidly excised and weighed. The left kidney was cut in half by a transverse section through the hilum, and subsequent halves either immersion fixed in 10% buffered formalin for histological analysis or snap frozen by immersion in liquid nitrogen for gene expression analysis. The right kidney was decapsulated and immersion fixed in 10% buffered formalin for stereological analysis. The thoracic cage was then opened giving access to the lungs, heart and aorta. Lung lobes were removed, weighed and immersion fixed in 10% buffered formalin. The heart was removed and weighed, with the right ventricle then dissected from the left and both ventricles weighed separately. The left ventricle was transversely sectioned and both ventricles were immersion fixed in 10% buffered formalin. The thoracic and abdominal portions of the aorta were then visualised and reflected from the posterior body wall. Fine-tipped forceps were used to dissect adipose tissues away from the vessel wall. The aorta was held and cut at the most inferior portion of the vessel. A second cut was made approximately 1 cm rostral to the first, with this tissue then snap frozen in liquid nitrogen for gene expression analysis. An incision was then made through the most superior point of the thoracic aorta, slightly inferior to the aortic arch, with special care taken not to distort the shape of the vessel. This portion was immersion fixed in 10% buffered formalin for histological analysis. Finally, toes were collected into a fresh eppendorf for subsequent analysis of genotype. All frozen tissues and toes were stored at -80 °C until required.

2.11 INTRAPERITONEAL INJECTIONS

2.11.1 Timed matings

Six week old male 129sv mice were mated with six week old female C57Bl6 mice to generate hybrid (129sv/C57Bl6) offspring of a similar genetic background to the *Tgfb2*$^{+/-}$ mice. Two female mice were placed with one male for 4 hours, after which female mice were checked for vaginal plugging and returned to their own individual 'home' box. This small time window for mating was adopted to allow littering down to occur between 9:00 a.m. and 11:00 a.m. on the morning of birth and

to ensure all subsequent injections could be administered promptly. Over the following 21 days, female mice were removed from their home box at 9:00 a.m. and 11:00 a.m. and placed in a 'secondary' box for 30 min. This was to acclimatize mice to being handled and to being transferred daily at a specific time to a specific place. Female mice were monitored for pregnancy over the following 21 days and allowed to litter down naturally.

2.11.2 Intraperitoneal injections of new born pups

Once the dams had littered down, they were moved from their 'home' box to their 'secondary' box. The time of littering down, litter size, and body weights of all pups were recorded. This was designated PN0. Pups from each litter were then tattooed for identification purposes and randomly allocated to one of four experimental groups:

1) Vehicle (saline);
2) Immunological control (IgG; CAT No: AB-108-BC Goat IgG; R&D systems);
3) 5μg/g body weight; or
4)10 μg/g body weight anti-TGFβ2 neutralising antibody (CAT No: AB-112-NA - R&D Systems)

Once allocated, pups were removed from the 'home' box and administered 20 μl per gram of body weight of the relevant compound via intraperitoneal (ip) injections. Once the solution was injected, the wound was coagulated with BleedEx (Tag Medical, Canterbury, Victoria, Australia), and the pups were returned to their 'home' box. Once all pups in the litter had undergone their allocated injections, urine was collected from the mother and swabbed over all pups in the litter with particular attention given to the injection site. This was done to mask any foreign scent pups acquired during handling. Once all pups had been swabbed, the mother was returned to the 'home' box. This protocol was repeated over subsequent days (PN0 – 3). Pups were allowed to remain with their mother in the 'home' box, being monitored and weighed until PN14, when they were culled and tissues collected for analysis.

2.12 HISTOLOGY

2.12.1 Periodic acid schiff's (PAS)

GMA sections (20 μm) were rinsed in distilled water for approximately 1 min and then placed in 1% Periodic Acid (30 min). Slides were rinsed in distilled water for 5 min, with water changes at 2.5 min. Sections were then placed in Schiff's solution (30 min), and then placed under running tap water for 15 min, or until water ran clear. Sections were then counterstained with Harris's haematoxylin (30 min). Excess haematoxylin was removed by rinsing sections in running tap water for 5 min. Sections were immersed in Scott's tap water (3 min). Once this was complete, slides were incubated at 40°C overnight, and then coverslipped with polystyrene mounting medium, allowed to dry, and viewed using light microscopy.

2.12.2 Haematoxylin and eosin

Cross sections (5 μm) of paraffin-embedded kidneys were mounted onto slides. Sections were dewaxed with 3 changes (3 min, 3 min, 1 min) of xylene. Xylene was then removed with 3 changes (1 min each) of absolute alcohol and rinsed in tap water for 30 sec to remove excess alcohol. Sections were then placed in Harris's haematoxylin for 5 min to stain cell nuclei and washed 3 times (30 sec each) in tap water to remove excess haematoxylin. Sections were then treated with acid alcohol (1 sec) to differentiate cell nuclei. Excess acid alcohol was removed with 3 rinses in tap water (30 sec) followed by incubation with Scott's tap water for 10 sec to further differentiate nuclei. Remaining Scott's tap water was removed with 3 rinses in tap water (30 sec). Sections were then counterstained with aqueous eosin for 3 min. This allowed cell cytoplasm and other tissue structures to be observed. Excess eosin was removed with 3 rinses in tap water (30 sec). Sections were then dehydrated with 3 changes of absolute alcohol (10 sec) and cleared with 3 changes of xylene (10 sec). All slides were then coverslipped and allowed to dry before viewing.

2.12.3 Gomori's one-step trichrome

Cross sections (5 μm) of paraffin-embedded kidney were mounted onto slides. Sections were dewaxed with 3 changes (3 min, 3 min, 1 min) of xylene. Xylene was

then removed with 3 changes (1 min each) of absolute alcohol and rinsed in tap water for 30 sec. Sections were then placed in Gomori's Trichrome Solution for 10 min. Sections were then treated with 0.2% acidified water (2ml acetic acid in 1000 ml distilled water; 5 sec) to differentiate stain. Sections were then dehydrated with 3 changes of absolute alcohol, 1 min each change, and cleared with 3 changes of xylene, 10 sec each, then coverslipped and allowed to dry before viewing.

2.12.4 Picrosirius red

Cross sections (5 μm) of paraffin-embedded kidney were mounted onto slides. Sections were dewaxed with 3 changes (3 min, 3 min, 1 min) of xylene. Xylene was then removed with 3 changes (1 min each) of absolute alcohol and rinsed in tap water for 30 sec to remove excess alcohol. Sections were then placed in 0.01% saturated Picric acid solution for 1 hour. Sections were then treated with 0.5% acidified water (2 ml acetic acid in 1000ml distilled water; 5 sec) to differentiate stain. Sections were then dehydrated with 3 changes of absolute alcohol, 1 min each change, and cleared with 3 changes of xylene, 10 sec each, then coverslipped and allowed to dry before viewing.

2.13 STATISTICAL ANALYSIS

Unpaired student's t-tests, one-way ANOVA, two-way ANOVA, two-way repeated measures ANOVA and linear regression analyses, and corresponding Bonferroni's, Dunnett's and Tukey's post-hoc analyses were conducted using GraphPad Prism™ 5 (Prism 5 for Windows, GraphPad Software Inc, 1992-2007). See individual Chapters for specifications of particular tests used in each study. All values expressed are in accordance with figure legends. A probability of 0.05 or less was accepted as statistically significant.

CHAPTER 3

ROLE OF BETAGLYCAN IN METANEPHRIC DEVELOPMENT AND THE REGULATION OF NEPHRON ENDOWMENT

3.1 INTRODUCTION

The development of the metanephros and the subsequent establishment of nephron endowment begins when an outgrowth from the Wolffian duct known as the ureteric bud extends towards and invades a mass of intermediate mesoderm, the metanephric mesenchyme (Saxen and Sariola 1987). Reciprocal interactions between the epithelial ureteric bud and the surrounding metanephric mesenchyme result in branching and extension of the ureteric tree, which generates the framework of the collecting duct system of the adult kidney. At the tips of the ureteric tree, mesenchymal condensation and mesenchymal-to-epithelial transition occur giving rise to nephrons, the functional units of the kidney (Costantini 2006).

The many processes involved in metanephric development are tightly regulated by complex molecular regulatory networks (Meyer et al. 2004). Members of the TGFβ superfamily of signalling molecules have previously been shown both *in vitro* (Plisov et al. 2001; Bush et al. 2004; Sims-Lucas et al. 2008) and *in vivo* to regulate key aspects of metanephric development (Dudley et al. 1995; Sakurai and Nigam 1997; Sanford et al. 1997; Esquela and Lee 2003; Oxburgh et al. 2004; Michos et al. 2007). At e11.5, transcripts for the three TGFβ isoforms (*Tgfb1–3*), the type I (*Tgfbr1*) and II (*Tgfbr2*) TGFβ signalling receptors as well as transcripts for many other related factors of the TGFβ superfamily are present in the mouse kidney (Oxburgh et al. 2004). Of the TGFβ isoform null mouse lines, only *Tgfb2* mutant mice exhibit defects in kidney development (Letterio et al. 1994; Kaartinen et al. 1995; Sanford et al. 1997; Sims-Lucas et al. 2008). These include dysplastic ureteric tree formation, impaired glomerulogenesis and agenesis (Sanford et al. 1997; Sims-Lucas et al. 2008). In contrast, *Tgfb2*$^{+/-}$ mice exhibit accelerated metanephric development (Sims-Lucas et al. 2008). These data indicate that TGFβ2 plays complex, non-redundant roles in the developing metanephros, and further understanding of the factors that control TGFβ2 action in the foetal kidney is required.

Recent evidence suggests that the efficacy of TGFβ isoforms on tissue development, in particular TGFβ2, may be dependent on the presence or absence of specific TGFβ superfamily co-receptors such as the type III TGFβ receptor (TGFBR3), commonly referred to as betaglycan (Stenvers et al. 2003; Compton et al. 2007). Betaglycan is believed to regulate tissue sensitivity to TGFβ isoforms by binding and

presenting ligand to the type II TGFβ receptor, an action of particular importance for TGFβ2, which does not bind to the type II TGFβ receptor with high affinity in the absence of betaglycan (Lopez-Casillas et al. 1993; Esparza-Lopez et al. 2001; Stenvers et al. 2003). However, while many studies have focused on the interaction between betaglycan and TGFβ isoforms, other studies have highlighted a more complex role for the co-receptor. Besides TGFβ isoforms, betaglycan has also been shown to directly modulate the activities of inhibins and certain BMPs through binding of these proteins to its core, while indirectly influencing BMP and activin function through the regulation of inhibins (Lewis et al. 2000; Kirkbride et al. 2008).

While very little is known about the role of betaglycan in the development of the metanephros, one finding has suggested that the co-receptor is important in the determination of nephron endowment. Similar to the augmented nephron endowment phenotype observed in *Tgfb2*$^{+/-}$ mice, stereological analysis of the kidneys of PN30 betaglycan$^{+/-}$ mice found a 23% increase in nephron endowment (+/+: 11,395 ± 921; +/-: 13,960 ± 693) compared with age-matched wildtype littermates (Sims-Lucas 2007). Augmented nephron endowment was accompanied by a significant decrease in mean glomerular volume (+/+: 1.678 ± 0.151 x10^{-4} mm^3; +/-: 1.316 ± 0.226 x10^{-4} mm^3); however, total glomerular volume was similar in the two genotypes (+/+: 1.844 ± 0.370 mm^3; +/-:1.910 ± 0.375 mm^3). Finally, no renal pathology was observed in the betaglycan$^{+/-}$ mice.

While the finding of augmented nephron endowment in postnatal betaglycan$^{+/-}$ mice was striking, neither the mechanism for the development of this phenotype nor the role of betaglycan in metanephric development was addressed. The aim of the experiments described in this Chapter was to determine the role of betaglycan in metanephric development and the establishment of nephron endowment. Morphological and molecular studies were conducted in wildtype, betaglycan$^{+/-}$ and betaglycan$^{-/-}$ kidneys.

3.2 METHODS

3.2.1 Animal Models

All animal handling and experimental procedures were approved by the Monash Medical Centre Animal Ethics Committee. Wildtype, betaglycan$^{+/-}$ and betaglycan$^{-/-}$ mouse embryos were obtained from timed mating of betaglycan$^{+/-}$ mice, with noon on the day of vaginal plugging designated as e0.5 (Section 2.1). All embryos obtained were Theiler staged (Section 2.3.2), sexed by morphology and genotyped as previously described (Section 2.2). Briefly, metanephroi were dissected from e11.0-e16.5 embryos and either: 1) stored in a clean 1.5ml eppendorf tube at -80 °C for later real-time PCR analysis (Section 2.5); 2) fixed for 30 min at 4 °C in 4% PFA, before being transferred into 70% ethanol and stored at 4°C for subsequent stereological (Section 2.4) or immunolabelling analysis (Section 2.7); or 3) transferred into a 24-well culture plate for metanephric culture studies (Section 2.6). Postnatal tissues were collected and processed into paraffin as previously described (Section 2.3.4).

3.2.2 Betaglycan immunofluorescence

For betaglycan localisation, metanephroi from e11.5 – e16.5 wildtype mouse embryos were fixed in 4% PFA at 4 °C for 30 min, embedded in paraffin wax and sectioned at 5 μm. Immunofluorescence detection of betaglycan was conducted as previously described (Section 2.7.1).

3.2.3 Embryonic stereology

3.2.3.1 Estimation of embryonic nephron number

Total nephron endowment was determined in the developing kidneys of e15.5 wildtype, betaglycan$^{+/-}$ and betaglycan$^{-/-}$ embryos (Section 2.4.4). Briefly, serially sectioned paraffin-embedded metanephroi were digested with 0.1% neuraminidase in 1% $CaCl_2$ in PBS, and incubated overnight at 4°C with biotinylated PNA. PNA-positive structures were then detected via the Elite streptavidin/biotin amplification ABC kit (Section 2.4.4). Only PNA-positive structures were determined as developing

nephrons, with total nephron number calculated using previously described equations and the Cavalieri principle (Section 2.4.3).

3.2.3.2 Volume of ureteric epithelium

Ureteric epithelial volume was determined in e13.5 wildtype, betaglycan$^{+/-}$ and betaglycan$^{-/-}$ metanephroi (Section 2.4.5). Paraffin-embedded metanephroi were exhaustively sectioned at 5 μm, after which all sections were dewaxed, rehydrated and blocked in 2% BSA in PBS with 0.3% Triton-X for 30 min at room temperature. Sections were then incubated overnight at 4°C with biotinylated DBA. DBA-positive structures were visualized using the Elite streptavidin/biotin amplification ABC kit. Unbiased stereology was then used to determine total and relative epithelial volumes, as well as total metanephric volumes as previously described (Section 2.4.3).

3.2.4 Metanephric organ culture and analysis

Whole metanephroi from e12.5 wildtype, betaglycan$^{+/-}$ and betaglycan$^{-/-}$ mouse embryos were placed on polycarbonate filters (3 μm pores) in wells containing serum-free culture medium (350 μl) at 37°C and 5% CO_2, for 48 hours (Section 2.6.1). The total number of ureteric branch points, branch tips (Green: Calbindin D_{28K}) and developing glomeruli (Red: WT1) were quantified as previously described (Section 2.6.2). Embryo development was determined via Theiler staging criteria and the total number of tail somites present, with e12.5 determined as equivalent to 26 - 30 somites extending from tail to hind limb (Table 2.1).

3.2.5 Ureteric bud analysis and cessation of nephrogenesis

For analysis of ureteric buds, whole mount Calbindin D_{28k} immunofluorescence was performed (as detailed in Section 2.6.3) on gonadal ridges isolated from e11.0 (14 – 17 tail somites), e11.5 (18 – 22 tail somites) and e12.0 embryos (23 – 26 tail somites; Table 2.1). The presence and morphology of the ureteric bud was correlated with the number of developing somites observed.

To assess postnatal renal morphology, kidneys collected from wildtype and betaglycan$^{+/-}$ mice at PN4 and PN5 were immersion-fixed in 10% neutral buffered

formalin, processed and embedded in paraffin wax (Section 2.3.4). Sections (5 μm) were stained with haematoxylin and eosin (Section 2.12.2) and assessed in a blind manner. The absence of a nephrogenic zone and developing glomerular structures was acknowledged as cessation of nephrogenesis.

3.2.6 Quantitative real-time PCR

Sense and antisense oligonucleotide primers were designed against published mouse sequences and verified as previously described (Section 2.5.4). Total RNA was isolated from pooled e11.5 – e14.5 metanephroi using the RNeasy Micro Kit (QIAGEN®). All findings were observed across four separate, independently collected pools of kidneys for each genotype (wildtype, betaglycan$^{+/-}$ and betaglycan$^{-/-}$) and age (n = 4-6/pool). Complementary DNA was synthesized using Superscript III Reverse Transcriptase (Life Technologies) using random hexamer and oligo d(T)20 primers and total RNA (300 ng), as previously described (Section 2.4.3). Real-time PCR was performed using the Applied Biosystems ABI 7900 HT Fast real-time machine with all reactions performed in triplicate. Yields were converted to femtograms (fg) based on the standard curve for each PCR product, and the resultant mRNA levels were normalized to the *18S* mRNA level per sample, as previously described (Bilandzic et al. 2009). Genes selected for analysis are described in Table 2.2. Cycling conditions for *Gdnf, Pax2, Six1, Tgfb1, Tgfb2* and *Tgfb3* comprised a 10 min initial denaturation step at 95°C, then 55 cycles of denaturing (95°C for 15 sec), annealing (55°C for 5 sec) and elongation (72°C for 8 sec and 79°C for 8 sec). PCR products were detected at 16 - 30 cycles; the extra cycles (i.e. 55 cycles) ensured that the water control was clean and no contamination was detected. For *Ret, Eya1, Wnt4, Wt1* and *18S* primers, the annealing temperature was modified to 61°C. All PCR products were initially verified by sequencing.

3.2.7 SMAD immunohistochemistry

Metanephroi were dissected, fixed, and hand processed to paraffin as previously described (Section 2.2.3). Paraffin sections (5 μm) underwent antigen retrieval via immersion in 10 mmol/L citrate buffer (pH 6.0) and microwave

radiation for 10 minutes. Subsequent sections were blocked with 10% normal goat serum plus 10% foetal calf serum in PBS and then incubated overnight at 4 °C with either phosphorylated SMAD1 (pSMAD1) or phosphorylated SMAD3 (pSMAD3) antibodies (1:100) in 1% BSA (Section 2.7.2). Sections were developed via 5 min incubation with 3, 3'-diaminobenzidine (DAB) and substrate-chromogen (Dako), which resulted in a brown-coloured precipitate at the antigen site. Finally 4', 6-diamidino-2-phenylindole (DAPI; 1:10,000) was applied to slides to counterstain nuclei. Slides were mounted in Fluorosave Mounting Medium (Calbiochem) and visualized via standard fluorescence microscopy using an Olympus Provis epifluorescence microscope fitted with a Leica DC digital camera (Section 2.7.2).

Quantitative assessment of pSMAD1 and pSMAD3 expression in developing metanephroi was performed. Fluorescent nuclear profiles with overlapping localized pSMAD1 or pSMAD3 staining were counted in approximately six non-overlapping high-power (×400 magnification) fields per metanephric section. Entire metanephric sections were analysed, with results expressed as the percentage of pSMAD1 or pSMAD3 immunopositive cells per total number of metanephric cells.

3.2.8 Statistical analysis

Unpaired Student's *t*-tests, one-way ANOVA and two-way ANOVA, and Tukey's post-hoc analysis were conducted using GraphPad Prism™ 5 (Prism 5 for Windows, GraphPad Software Inc, 1992-2007). Values are mean ± SD. A probability of 0.05 or less was accepted as statistically significant.

3.3 RESULTS

3.3.1 Betaglycan is expressed in the developing mouse kidney

At e11.5, betaglycan protein was localised to the ureteric epithelium, with no specific immunostaining detected in the metanephric mesenchyme (Figure 3.1A, B). By e14.5, betaglycan was detected in developing pre-glomerular structures while remaining strongly expressed in ureteric epithelium (Figure 3.1C, Ci, Cii, Ciii). At this developmental stage, expression was also observed in the interstitium (Figure 3.1Ci, Cii) ,but was absent from the mesenchyme in the nephrogenic zone (Figure 3.1Ciii). At e16.5, betaglycan immunolocalisation was similar to that seen at e15.5 (Figure 3.1D, E). Betaglycan protein expression was not detected in the negative control, e14.5 betaglycan null kidney (Figure 3.1F, G, H). Embryonic wild type mouse gut epithelium served as a positive control for this experiment as prior work has demonstrated betaglycan mRNA to be expressed by the epithelium of developing mouse intestine (Stenvers, K.L., unpublished data). In gut, betaglycan was highly expressed in the epithelium as expected (Figure 3.1I-K).

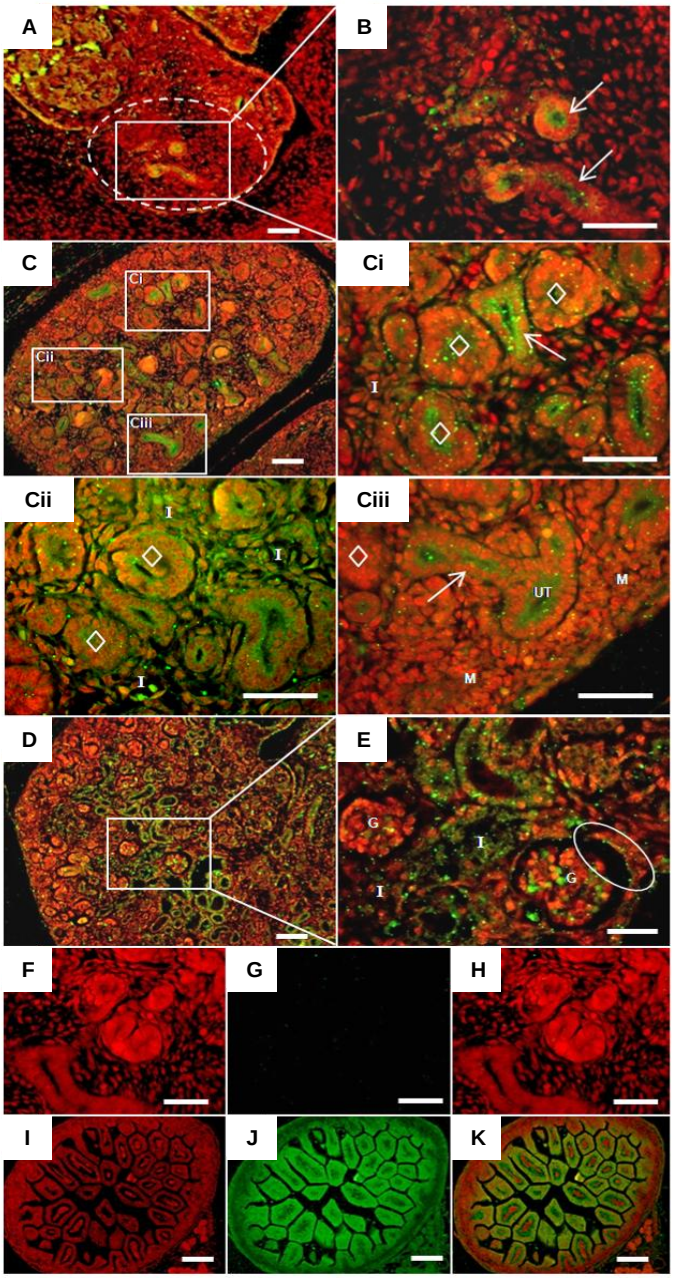

Figure 3.1: Localisation of betaglycan in the developing mouse kidney. Betaglycan immunostaining (*green fluorescence*) in mouse kidney at e11.5 (A, B); e14.5 (C, Ci, Cii, Ciii) and e16.5 (D, E). Negative control, e14.5 betaglycan null metanephros (TO-PRO: F, Betaglycan: G, Merge: H) and positive control, e16.5 wildtype mouse intestine (TO-PRO: I, Betaglycan: J, Merge: K). Arrows, ureteric epithelium; M, metanephric mesenchyme; I, interstitial mesenchyme; diamonds, pre-glomerular structures; G, glomeruli; Oval, Bowman's capsule; Red fluorescence, TO-PRO nuclear staining. Scale bars = 100 μm.

3.3.2 Contrasting developmental phenotypes in betaglycan mutant metanephroi

To determine the direct role of betaglycan in early kidney morphogenesis, metanephroi from e12.5 wildtype, betaglycan$^{+/-}$ and betaglycan$^{-/-}$ mutant embryos were cultured for 48 hours (Figure 3.2A-C). Interestingly, at the competition of the culture period, betaglycan$^{+/-}$ metanephroi appeared more developed than wild type metanephroi, while betaglycan$^{-/-}$ metanephroi appeared less developed than age-matched wildtype metanephroi**.** Quantitative analysis indicated that branch (p<0.01) and tip number (p<0.01) were both significantly greater in betaglycan$^{+/-}$ mice (27.43 ± 5.08: 34.29 ± 5.68) than in wildtype mice (21.83 ± 4.69: 27.42 ± 5.11; Figure 3.2D, E). The increased ureteric tree development in betaglycan$^{+/-}$ mice correlated with a significant increase (p<0.01) in the number of developing glomeruli (38.64 ± 4.22) compared with wildtype metanephroi (29.42 ± 5.26). In contrast, betaglycan$^{-/-}$ metanephroi exhibited a dysplastic ureteric tree which further analysis indicated contained significantly fewer ureteric branches (11.20 ± 2.94; p<0.01), tips (14.40 ± 3.72; p<0.01) and glomeruli (15.20 ± 4.92; p<0.01) than both wildtype and betaglycan$^{+/-}$ metanephroi (Figure 3.2C, F).

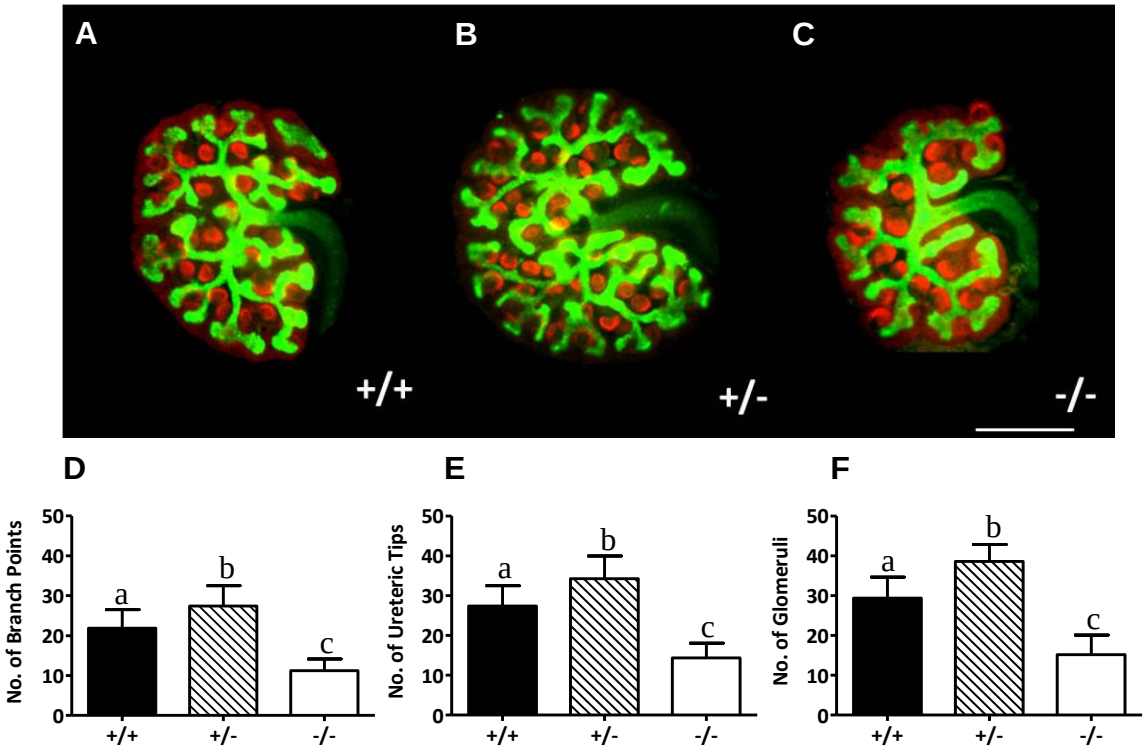

Figure 3.2: Effect of decreased endogenous betaglycan expression on metanephric development and glomerulogenesis. (A-C) Wholemount immunofluorescent labelling of the ureteric tree (Calbindin D28K, *green fluorescence*) and developing glomeruli (WT1, *red fluorescence*) in e12.5 betaglycan wildtype (+/+), heterozygous (+/-) and null (-/-) metanephroi following 48 hours culture. (D-F) Quantification of ureteric branch points, ureteric tips and glomeruli in betaglycan wildtype, heterozygous and null mice (n) = +/+ (12), +/- (14), -/- (10). Values are mean ± S.D. Data were analysed via one-way ANOVA followed by a Tukey's post-hoc analysis. Those groups not sharing a common letter are significantly different (p<0.01). Scale bar = 250 μm.

3.3.3 Total metanephric volume is altered in betaglycan mutant mice

Stereological analysis of e13.5 betaglycan wildtype, betaglycan$^{+/-}$ and betaglycan$^{-/-}$ metanephroi found a significant 30-40% decrease in metanephric volume in null embryos compared to wildtype and betaglycan$^{+/-}$ embryos (Table 3.1). Likewise, absolute ureteric epithelial volume was significantly decreased in betaglycan$^{-/-}$ mice compared to wildtype and betaglycan$^{+/-}$ mice. However, the relative volume of the ureteric volume was comparable in all three groups. At e15.5,

metanephric volume in betaglycan$^{+/-}$ was significantly greater (30%) than in wildtype embryos, which in turn were 49% larger than the kidneys of null embryos (Table 3.1).

3.3.4 Betaglycan heterozygous mice have augmented nephron endowment at e15.5

Analysis of nephron number at e15.5 revealed that the kidneys of betaglycan$^{+/-}$ mice contained approximately 32% more PNA-positive structures than the kidneys of wildtype metanephroi (Table 3.1). In contrast, betaglycan$^{-/-}$ metanephroi contained 31.6% fewer PNA-positive structures than wildtype kidneys, and approximately half the number as betaglycan$^{+/-}$ kidneys (Table 3.1).

Table 3.1: Stereological data for betaglycan wildtype (+/+), heterozygous (+/-) and null (-/-) mouse kidneys at e13.5 and e15.5.

		+/+	+/-	-/-	*p*
e13.5	V_{kid} (mm^3)	0.109 ± 0.018^a	0.103 ± 0.021^a	0.077 ± 0.011^b	<0.001
	V_{ue} (mm^3)	0.015 ± 0.003^a	0.015 ± 0.003^a	0.010 ± 0.001^b	0.0013
	% V_{ue} of V_{kid}	13.50 ± 1.67^a	13.56 ± 0.39^a	12.58 ± 0.26^a	0.3
e15.5	V_{kid} (mm^3)	0.261 ± 0.034^a	0.340 ± 0.055^b	0.187 ± 0.005^c	<0.001
	No. of PNA^{+ve} Structures	68 ± 11^a	90 ± 12^b	47 ± 8^c	<0.001

Values are mean ± S.D. e13.5: (n) = +/+ (5), +/- (9), -/- (6); e15.5: (n) = 7 mice / genotype. Data were analysed via one-way ANOVA followed by a Tukey's post-hoc analysis. Those groups not sharing a common letter are significantly different (p<0.01).

3.3.5 The nephrogenic period is normal in betaglycan heterozygote mice

Analysis of e11.0 – e12.0 gonadal ridges indicated that metanephric development (characterised by the emergence of the ureteric bud from the Wolffian duct) commenced in all three genotypes at the same embryonic stage (e11.0; Figure 3.3A, B). Between e11.5 (18–22 tail somites) and e12.0 (Figure 3.3A, B), the ureteric bud from betaglycan$^{-/-}$ embryos exhibited the same number of branches as wildtype ureteric bud. However, betaglycan$^{+/-}$ metanephroi consistently exhibited an augmented number of ureteric tips at this time, indicating extra ureteric branching had occurred (Figure 3.3A, B). Cessation of nephrogenesis occurred at the same postnatal age in betaglycan$^{+/-}$ and wildtype littermates. Histological analysis revealed that nephrogenesis was complete in both genotypes by PN5, as indicated by absence of a nephrogenic zone (Figure 3.4).

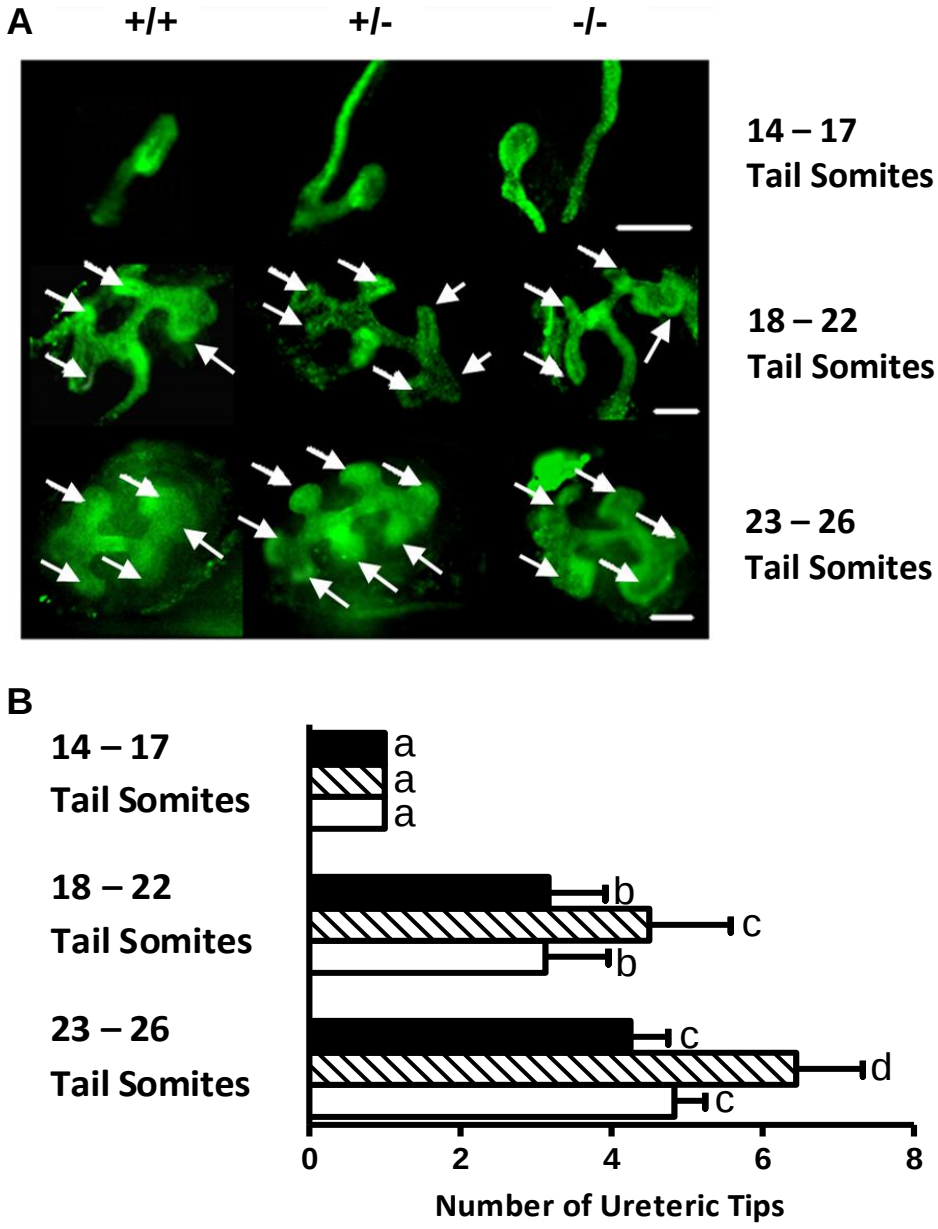

Figure 3.3: Commencement of metanephric development. **(A)** Representative images of developing metanephroi from wildtype (+/+), betaglycan heterozygous (+/-) and null (-/-) embryos with 14 – 17 tail somites (e11.0), 18 - 22 tail somites (e11.5) and 23 - 26 tail somites (e12.5). Arrows, ureteric tips; scale bars = 150 μm. **(B)** Total number of ureteric tips present in +/+ (solid bars), +/- (striped bars) and -/- (clear bars) developing metanephroi, at progressive developmental stages. Values are mean ± SD. n = ≥5 genotype/stage. Analysis via one-way ANOVA followed by Tukey's post-hoc analysis, across all genotypes and ages. Significant differences (p<0.05) between groups are represented by different letters.

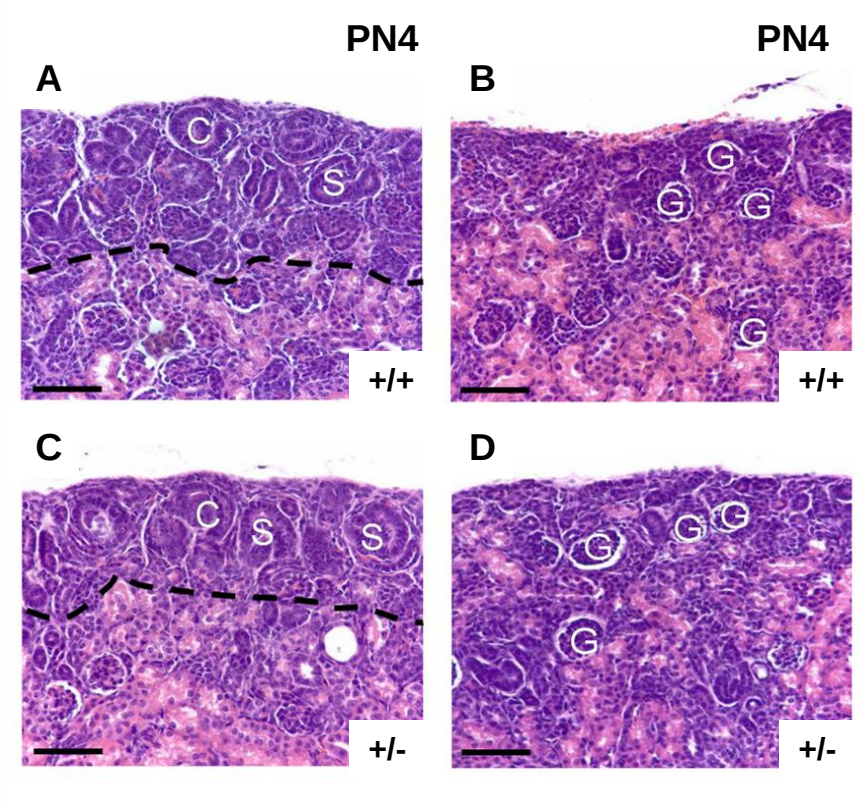

Figure 3.4: Cessation of nephrogenesis. (A-D) Representative histological images of PN4 and PN5 kidneys from wildtype (+/+) and betaglycan heterozygous (+/-) mice containing comma-shaped (C) and S-shaped (S) bodies in a clearly defined nephrogenic zone (dotted line; A,C), or displaying mature glomeruli (G) and no nephrogenic zone indicating cessation of nephrogenesis (B,D). Scale bars = 100 μm.

3.3.6 Metanephric signalling networks are disrupted in betaglycan mutant mice

3.3.6.1 Early Ureteric Branching Morphogenesis

BMP4 and GDNF, both members of the TGFβ superfamily, play important roles in regulating ureteric budding and ureteric branching morphogenesis. Formation of the ureteric bud at approximately e11.0 and subsequent ureteric branching morphogenesis both require secreted GDNF from the metanephric mesenchyme to bind with its cognate receptor RET, as well as inhibition of BMP4 at the ureteric bud site and around the ureteric tips. In accordance with the increased ureteric branching observed in wholemount urogenital ridges, betaglycan heterozygous mice exhibited significant changes in the expression of *Gdnf* and *Bmp4* mRNA during early metanephric development. Betaglycan$^{+/-}$ metanephroi displayed significantly

decreased *Bmp4* mRNA expression at e11.5 ($p<0.01$) while *Gdnf* mRNA expression was significantly upregulated at e12.5 in comparison to age-matched wildtype metanephroi (Figure 3.5 A, B). These changes in betaglycan$^{+/-}$ were accompanied by consistent increases in *Ret* mRNA expression from e12.5 (Figure 3.5C). In contrast, betaglycan$^{-/-}$ metanephroi displayed wildtype-like mRNA expression profiles for *Bmp4*, *Gdnf* and *Ret* at e11.5 (Figure 3.5A-C). However, from e12.5-e14.5, significant decreases in the expression of both the inhibitory (*Bmp4*) and stimulatory pathways (*Gdnf/Ret*) controlling renal branching morphogenesis were detected in betaglycan$^{-/-}$ kidneys (Figure 3.5A-C).

3.3.6.2 Regulation of the Ret and GDNF Expression Profile

GDNF signalling through RET is viewed as the critical positive factor in branching morphogenesis (Schuchardt et al. 1996; Majumdar et al. 2003). Multiple studies have identified upstream transcriptional regulators of *Gdnf* such as *Pax2*, *Eya1* and *Six1* as integral to the induction of GDNF expression and in turn early metanephric development (Brodbeck and Englert 2004). Mutant mice lacking *Pax2*, *Eya1* or *Six1* exhibit no ureteric bud formation (Xu et al. 1999; Brophy et al. 2001; Xu et al. 2003). However, while *Eya1* and *Pax2* mutants exhibit no *Gdnf* mRNA expression, *Six1* mutants exhibit wildtype levels of *Gdnf* mRNA expression (Xu et al. 1999; Brophy et al. 2001; Xu et al. 2003), indicating that *Eya1* and *Pax2* but not *Six1* are upstream of *Gdnf* in a major regulatory pathway controlling metanephric development. The most important of these factors appears to be *Pax2*, as *Pax2* is not only critical for the initiation of *Gdnf* expression but also in the enhancement of *Ret* expression in the developing ureteric tree (Clarke et al. 2006).

At e11.5, *Pax2* mRNA expression was significantly increased in betaglycan$^{+/-}$ mutants. However, at this time point no difference in *Eya1* mRNA expression was observed between genotypes (Figure 3.5D, E). At e12.5 and e13.5, betaglycan$^{+/-}$ metanephroi displayed significant increases in both *Pax2* and *Eya1* mRNA compared with age-matched wildtype, with mRNA expression for both genes returning to wildtype levels at e14.5 (Figure 3.5D, E). Betaglycan$^{-/-}$ metanephroi displayed wildtype-like expression profiles of *Pax2* and *Eya1* mRNA until e13.5, after which time significant decreases in expression of these genes was observed in betaglycan$^{-/-}$

metanephroi compared to age-matched wildtype metanephroi. Such changes in *Pax2* and *Eya1* mRNA expression at e12.5 and e13.5 correlate with previously described changes in *Gdnf* mRNA expression, suggesting a possible mechanism for increased *Gdnf* expression and development of the morphological phenotypes observed. *Six1* mRNA expression was similar in all genotypes across all time points observed (Figure 3.5F).

3.3.6.3 Nephrogenesis

Wilm's Tumor 1 (WT1) and Wingless-related MMTV integration site 4 (WNT4) are both essential for nephrogenesis (Stark et al. 1994; Davies et al. 2004; Kim et al. 2007; Valerius and McMahon 2008). Changes in mRNA expression for *Wt1* were observed from e12.5 with betaglycan$^{+/-}$ metanephroi displaying consistently increased *Wt1* mRNA expression and betaglycan$^{-/-}$ metanephroi consistently decreased *Wt1* mRNA expression from e13.5, compared with age-matched wildtype metanephroi (Figure 3.5H). Similar changes were observed in *Wnt4* mRNA expression levels (Figure 3.5G). These data suggest that dysregulation of glomerular formation in betaglycan mutant mice is present from the commencement of glomerulogenesis.

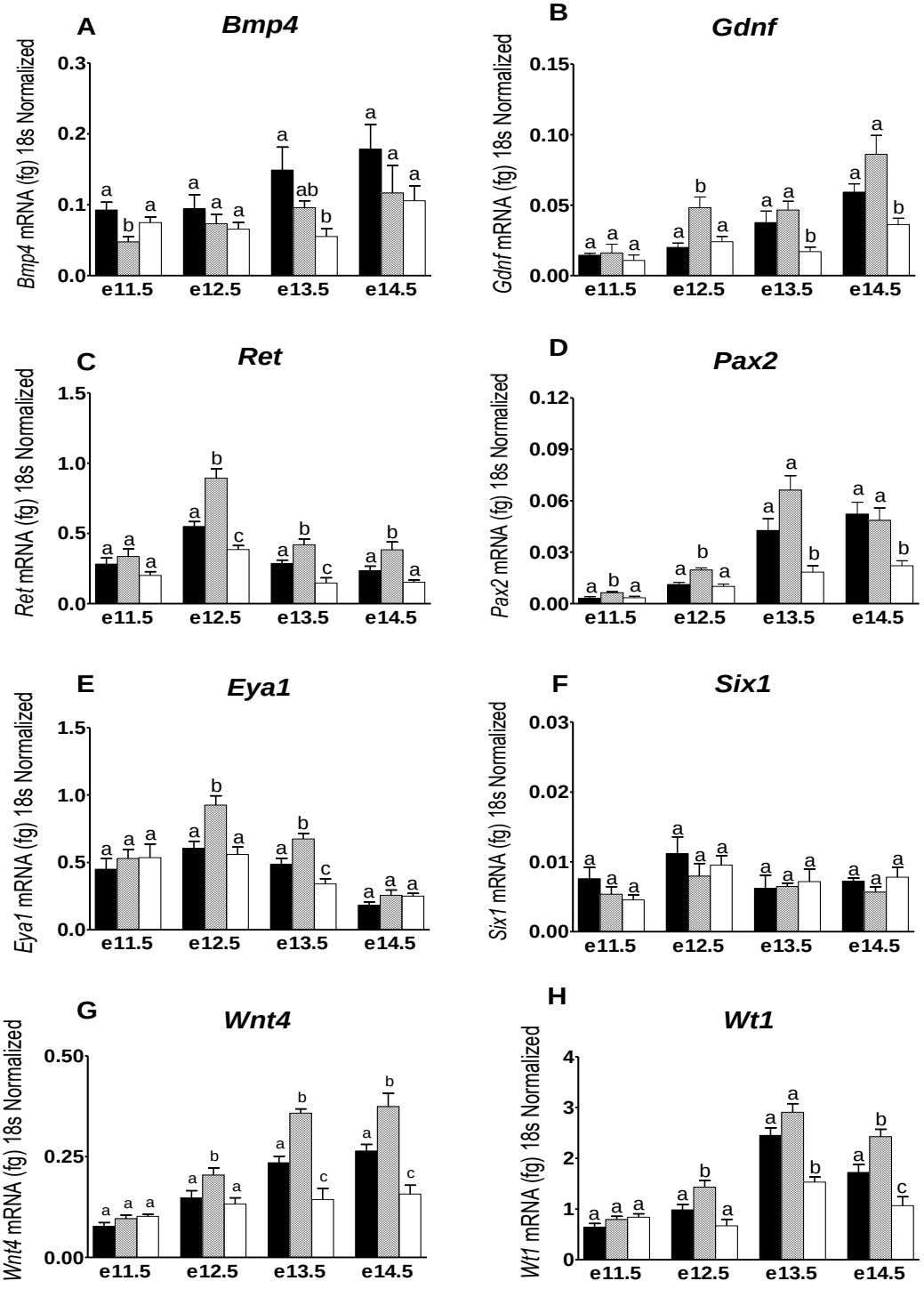

Figure 3.5: Betaglycan mutant renal mRNA expression. Quantitative real time PCR assessment of genes involved in metanephric development using RNA derived from age-matched wildtype (solid bars), betaglycan$^{+/-}$ (striped bars) and betaglycan$^{-/-}$ (clear bars) metanephroi. Values are mean + SEM. n = 4 - 6 RNA pools/genotype/age. Analysis via one-way ANOVA followed by Tukey's post-hoc analysis conducted separately for each gene at each time point. Significant differences (p<0.05) between genotypes are represented by different letters.

3.3.6.4 TGFβ Isoforms

Betaglycan directly binds all three TGFβ isoforms expressed in mammals and modulates their activities differentially (Lopez-Casillas et al. 1993). All three TGFβ isoforms were detected in wildtype metanephroi from e11.5, with an upregulation in *Tgfb1* and *Tgfb2* expression detected at e13.5-e14.5 (Figure 3.6A, B). This upregulation in *Tgfb1* and *Tgfb2* mRNA was not observed in betaglycan mutant metanephroi, with both betaglycan$^{+/-}$ and betaglycan$^{-/-}$ mutants displaying decreased mRNA expression levels of these genes compared to wildtype littermates ($p<0.01$; Figure 3.6 A, B). Interestingly, the levels of *Tgfb2* and betaglycan mRNA expression appeared to be directly correlated, as *Tgfb2* expression at e13.5 and e14.5 was less in betaglycan$^{+/-}$ mutants than in wildtype mice, and less again in betaglycan$^{-/-}$ mutants (Figure 3.6B). *Tgfb3* mRNA expression was similar in all three genotypes at all ages examined (Figure 3.6C).

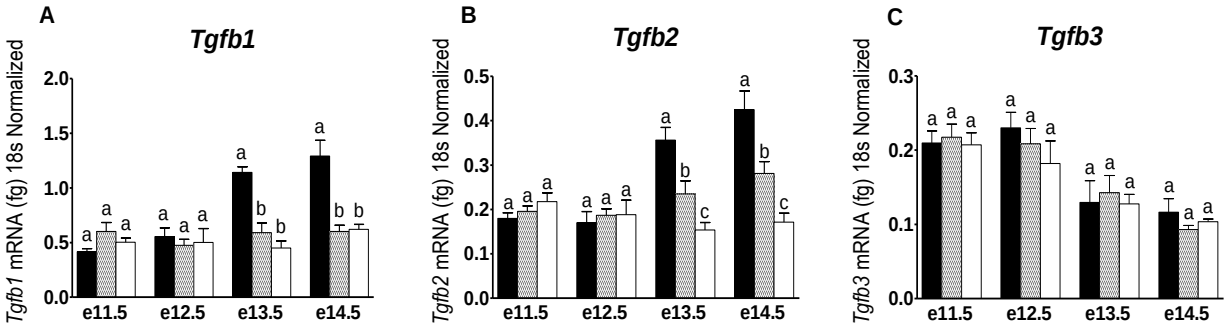

Figure 3.6: Expression of TGFβ isoforms in kidneys of betaglycan mutant mice. Quantitative real time-PCR assessment of (A) *Tgfb1*; (B) *Tgfb2*; and (C) *Tgfb3* using RNA derived from age-matched wildtype (solid bars), betaglycan$^{+/-}$ (striped bars), and betaglycan$^{-/-}$ (clear bars) metanephroi. Values are mean + SEM. n = 4 - 6 RNA pools/genotype/age. Analysis via one-way ANOVA followed by Tukey's post-hoc analysis conducted separately for each gene at each time point. Significant differences ($p<0.05$) between genotypes are represented by different letters.

3.3.7 SMAD1 and SMAD3 signalling is unchanged in betaglycan mutants

Transduction of TGFβ superfamily signals involves the phosphorylation of intracellular receptor associated proteins known as SMADs. SMAD 2/3 are

predominantly associated with activation of TGFβ/activin signalling pathways, while BMP/GDF signalling predominantly utilises SMADs 1, 5 and 8 (Massague et al. 2005; Schmierer and Hill 2007). As betaglycan can bind both TGFβ and BMP ligands, the altered expression of the co-receptor has the potential to disrupt both pathways (Wiater et al. 2006; Kirkbride et al. 2008). To determine whether TGFβ or BMP signal transduction was altered in betaglycan mutants, pSMAD immunohistochemistry was performed. Quantification of pSMAD1 (Figure 3.7A) and pSMAD3 (Figure 3.7B) immunohistochemistry in e13.5 metanephroi from betaglycan wildtype, betaglycan$^{+/-}$ and betaglycan$^{-/-}$ embryos illustrated that far fewer cells exhibited pSMAD1 than pSMAD3 in all three genotypes. However, no differences in the percentages of cells containing activated pSMAD1 or pSMAD3 were found between genotypes (Figure 3.7A, B).

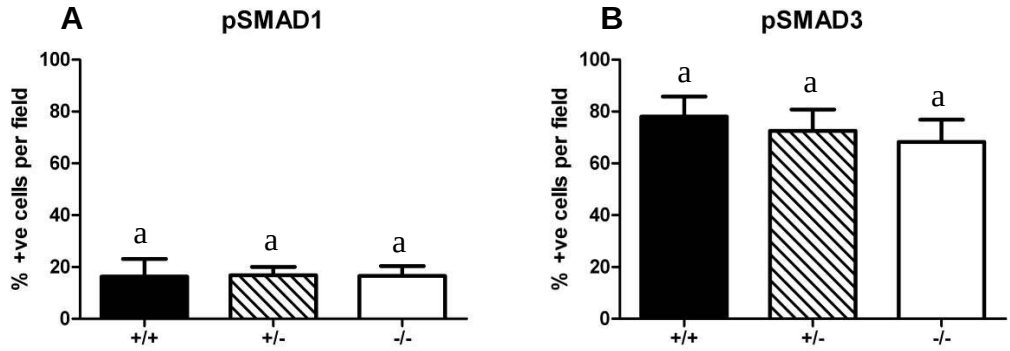

Figure 3.7: SMAD1 and SMAD3 activation in betaglycan mutant metanephroi. Quantitative analysis of nuclear pSMAD1 and pSMAD3 expression per microscopic field in wildtype (solid bars), betaglycan$^{+/-}$ (striped bars) and betaglycan$^{-/-}$ (clear bars) metanephroi. n = 4 metanephroi per genotype, with a minimum of 5 fields of view per metanephros. Values are mean + SD. Analysis via one-way ANOVA followed by Tukey's post-hoc analysis. No significant differences were found between genotypes for either pSMAD.

3.4 DISCUSSION

The aim of the experiments described in this Chapter was to investigate the role of betaglycan in metanephric development and to determine the impact of the co-receptor on establishing nephron endowment. The major findings from these experiments were: 1) betaglycan expression during metanephric development is temporally and spatially dynamic; 2) tightly controlled betaglycan expression is essential for normal metanephric development as partial or complete ablation of expression results in opposing renal phenotypes; 3) betaglycan$^{+/-}$ mice display accelerated ureteric branching morphogenesis following metanephric induction, which gives rise to augmented nephron endowment sustained into adulthood; and 4) transient changes in the expression profiles of *Bmp4* and the upstream regulators of *Gdnf* suggest a potential mechanism for altered metanephric development in betaglycan mutant embryos.

3.4.1 Betaglycan is a TGFβ co-receptor and regulator of nephron endowment

Betaglycan is a multifunctional proteoglycan that acts as a co-receptor for several members of the TGFβ superfamily (Lopez-Casillas et al. 1993; Lewis et al. 2000; Wiater and Vale ; Kirkbride et al. 2008). *In vitro*, both ligand-dependent and ligand-independent roles for betaglycan have been discovered in different cell types (Eickelberg et al. 2002; Finger et al. 2008; Bilandzic et al. 2009; Wiater et al. 2009). As foetal metanephroi express several potential ligands of betaglycan, the specific mechanisms by which diminished betaglycan expression impacts kidney development are not yet clear. However, several pieces of evidence from this thesis suggest that betaglycan is serving an essential role as a TGFβ2 co-receptor during early kidney development.

Firstly, betaglycan expression is coincident with the previously published expression pattern of TGFβ2 in murine metanephroi (Pelton et al. 1991; Plisov et al. 2001; Oxburgh et al. 2004). Betaglycan was localised in the ureteric epithelium from the earliest stages of ureteric bud formation, and from e14.5 was also detected in metanephric mesenchyme and the epithelium of developing nephrons. TGFβ2 is similarly expressed by the ureteric epithelium, with expression also detected in

neighbouring tissues after e14.5 (Pelton et al. 1991). These overlapping expression patterns of TGFβ2 and its co-receptor suggest that betaglycan helps mediate the autocrine and paracrine actions of TGFβ2 within the ureteric epithelium and the metanephric mesenchyme. The expression of betaglycan in the ureteric epithelium at e11.0-e11.5 and the increased branching of the ureteric tree at e11.5-e12.0 suggests that TGF2 initially acts directly upon ureteric epithelium to inhibit branching. Subsequent expression of betaglycan in interstitial cell populations from e14.5 suggests that after this age, TGFβ2/betaglycan signalling is involved in the development of both the epithelial and interstitial cell populations of the metanephros.

Secondly, betaglycan and *Tgfb2* mutant renal phenotypes share several similarities. Like betaglycan$^{+/-}$, *Tgfb2*$^{+/-}$ develop normally and possess more nephrons than wildtype mice at PN30, displaying an even greater enhancement of nephron number than betaglycan$^{+/-}$ (Sims-Lucas 2007; Sims-Lucas et al. 2008). This suggests that TGFβ2/betaglycan signalling is required to negatively regulate nephrogenesis, possibly through the regulation of ureteric branching morphogenesis. This observation is in agreement with previous work that suggests abrogation of endogenous betaglycan *in vitro* attenuates endogenous autocrine and/or paracrine TGFβ-mediated negative regulation of lung branching morphogenesis (Zhao et al. 1998).

In contrast to the renal phenotype in betaglycan$^{+/-}$ mice, *in vivo* stereological analysis and *in vitro* culture of betaglycan$^{-/-}$ metanephroi revealed a hypoplastic renal phenotype that closely resembled the defective development of *Tgfb2*$^{-/-}$ explants (Sims-Lucas et al. 2008). These contrasting phenotypes in betaglycan$^{+/-}$ and betaglycan$^{-/-}$ kidneys suggest that the TGFβ2/betaglycan signalling pathway plays dual roles *in vivo*, both limiting the growth of the ureteric tree while supporting the maintenance of the newly-formed nephron tubules. However, the presence of a subtle hypomorphic renal phenotype in betaglycan$^{-/-}$ metanephroi, in contrast to the renal degeneration which occurs in *Tgfb2*$^{-/-}$ kidneys (Sanford et al. 1997), suggests that sufficient TGFβ2 signalling may occur in foetal kidneys in the absence of betaglycan, as has previously been suggested to occur during bone patterning (Stenvers et al. 2003). This conclusion is supported by the greater augmentation of

both branching morphogenesis and nephron number in *Tgfb2*$^{+/-}$ (Sims-Lucas et al. 2008) relative to betaglycan$^{+/-}$, suggesting the inhibitory actions of TGFβ2 may be present in betaglycan mutants.

The involvement of other betaglycan ligands in the development of the renal phenotype in betaglycan mutant mice cannot be completely ruled out, as we and others have shown that a number of potential ligands for betaglycan are expressed in foetal kidney (Cancilla et al. 1999; Godin et al. 1999; Maeshima et al. 2006; Bates 2007; Cain et al. 2008). However, several lines of evidence argue against significant contributions by ligands in addition to TGFβ2. For example, despite the expression of both *Tgfb1* and *Tgfb3* in foetal kidney as shown in Figure 3.6 and also by Oxburgh et al. (2004), these isoforms clearly do not fully compensate for the loss of TGFβ2 signalling in *Tgfb2* mutant mice (Sanford et al. 1997; Sims-Lucas et al. 2008). Similarly, although certain activins and BMPs are also negative regulators of ureteric branching (Maeshima et al. 2000; Miyazaki et al. 2003; Maeshima et al. 2006) and betaglycan is known to counter activin and BMP function by increasing the efficacy of inhibins (Lewis et al. 2000; Wiater and Vale), no renal phenotype was noted in *Inha* null mice, which are null for the inhibin-α subunit, common to all inhibins (Matzuk et al. 1992). Thus, it is believed that the inhibin/betaglycan pathway is not involved in the mechanisms underlying the renal phenotypes observed in the present study.

3.4.2 TGFβ2/betaglycan signalling is temporally required for normal metanephric development

The contrasting renal phenotypes in betaglycan$^{+/-}$ and betaglycan$^{-/-}$ mice suggests that TGFβ2/betaglycan signalling is required at more than one stage of kidney development and in more than one cell type, with specific developmental processes in the kidney having higher thresholds for TGFβ2 signalling than others. Specifically, the data suggest that greater TGFβ2 signalling is necessary to limit the branching of the ureteric tree, and that betaglycan is the determining component of the TGFβ2 signalling complex that allows critical thresholds of TGFβ2 signalling to be met during this process. Interestingly, TGFβ2-mediated survival of ureteric epithelium during late gestation appears to occur at a lower threshold of TGFβ2 signalling. This conclusion is based on the observation that newly-formed epithelial

structures are maintained when the level of either the ligand or the accessory receptor is reduced, as in *Tgfb2*$^{+/-}$ or betaglycan$^{+/-}$, respectively. Conversely, ablation of TGFβ2 signalling in *Tgfb2*$^{-/-}$ metanephroi results in degeneration of these newly-formed structures, an effect that could be hypothesised to be due to insufficient pro-survival signalling attributed to TGFβ2 (Tomoda et al. 1996; Sanford et al. 1997; Sims-Lucas et al. 2010). As degeneration of renal tissues was not observed in betaglycan$^{-/-}$ metanephroi, this suggests that the relatively low, but still present TGFβ2 signalling in betaglycan$^{-/-}$ metanephroi is sufficient to satisfy a threshold necessary for cell survival. This further suggests that the processes of ureteric branching morphogenesis and cell/tissue survival have differing TGFβ2 concentration-dependent signalling thresholds.

Concentration-dependent actions of TGFβ2 have previously been demonstrated in renal cell culture. In cultured podocytes, autocrine TGFβ2 (but not TGFβ1) production was associated with TGFβ/SMAD3 signal transduction and cell-cycle arrest and differentiation; in contrast, higher doses of TGFβ2 activated an alternative p38 signalling pathway and caused podocyte apoptosis (Wu et al. 2005). A similar paradigm has been proposed to address the development of specific phenotypes in the presence of differing concentrations of specific factors, proposing that transcription factors regulate commitment to specific cell fates at distinct protein expression levels (Seymour et al. 2008). Seymour et al. (2008) found that *Sox9* ablation resulted in severe pancreatic hypoplasia, while *Sox9* haploinsufficiency resulted in an opposing phenotype which favoured the enhanced commitment of multipotent progenitor cells to an endocrine lineage compared to wildtype controls.

3.4.3 Distinct renal phenotypes in betaglycan mutants were mirrored by distinct molecular profiles from e11.5-e14.5

Previous studies have shown that altered expression of any of a multitude of factors can compromise kidney development (Cullen-McEwen et al. 2001; Xu et al. 2003; Sajithlal et al. 2005; Narlis et al. 2007; Skinner et al. 2008). In the betaglycan$^{+/-}$ kidney, changes in gene expression were observed as early as e11.5. Notably, a decrease in *Bmp4* expression at this time was observed in betaglycan heterozygous kidneys, compared with wildtype, and betaglycan$^{-/-}$ kidneys. This period of

development occurs shortly after the ureteric bud has invaded the metanephric mesenchyme, when branching morphogenesis is beginning. Although BMP4 appears to have multiple roles throughout kidney development (Miyazaki et al. 2003), at the time of ureteric bud outgrowth, BMP4 activity in the sleeve of metanephric mesenchyme surrounding the Wolffian duct must be antagonized by an endogenous inhibitor, gremlin 1, for budding to occur. While the timing of ureteric budding appears similar in the three genotypes, BMP4 can also act as an inhibitor of GDNF/RET/WNT-mediated branching morphogenesis (Michos et al. 2007). Therefore, the reduced expression of *Bmp4* at e11.5 is in accordance with the observed increase in ureteric branching at this time. Interestingly, the level of renal *Bmp4* mRNA expression in betaglycan$^{+/-}$ after this time was not different to that of age-matched wildtype mice. However, a cascade of changes in the gene regulatory network governing metanephric development followed in the betaglycan$^{+/-}$ kidney, including significant increases in expression levels of *Pax2*, *Eya1, Gdnf, Ret, Wnt4,* and *Wt1*. Of these genes, *Pax2* was the first to be upregulated in the betaglycan$^{+/-}$ kidney (at e11.5), in keeping with its role in inducing expression of downstream mediators of branching morphogenesis such as *Gdnf* and *Ret* (Brophy et al. 2001; Clarke et al. 2006).

In contrast to betaglycan$^{+/-}$ kidneys, the rate of early branching morphogenesis in betaglycan$^{-/-}$ metanephroi resembled that in wildtype metanephroi. Accordingly, no differences in levels of gene expression were found between betaglycan$^{-/-}$ and wildtype kidneys at e11.5. At e12.5, betaglycan$^{-/-}$ kidneys exhibited only small decreases in *Bmp4* and *Ret* expression compared to the wildtypes. However, by e13.5, expression levels of several genes were significantly reduced in betaglycan$^{-/-}$ kidneys compared to wildtype, including *Bmp4, Gdnf, Ret, Pax2, Eya1, Wnt4*, and *Wt1*. These findings correlate with the reduced kidney volume observed in betaglycan$^{-/-}$ embryos compared with wildtype embryos at this time. These findings indicate that a complete loss of betaglycan results in an uncoupling of the reciprocal inductive signalling pathways that operate between the metanephric mesenchyme and ureteric epithelium to drive the progression of branching morphogenesis and nephrogenesis. In particular, genes that drive the *Gdnf/Ret* regulatory pathway, such as *Pax2,* fail to be upregulated in the null kidney, which may be a possible mechanism for the

development of the hypoplastic renal phenotype which this study first identified at e13.5.

3.4.4 Betaglycan may impact local TGFβ ligand gene expression

Finally, it was demonstrated that loss or reduction of betaglycan expression results in decreased *Tgfb1* and *Tgfb2* expression in the foetal kidney. This may be due to reduced TGFβ sensitivity in the betaglycan mutant kidneys, as TGFβs are well-recognized to auto-induce their own expression by both transcriptional and post-transcriptional mechanisms (Kim et al. 1990; Tang et al. 1998). As a TGFβ co-receptor, a loss or reduction in betaglycan on the cell surface would lead to decreased sensitivity to the TGFβs, which could in turn reduce the level of TGFβ auto-induction and compound the effects of the loss of betaglycan. Indeed, in betaglycan$^{-/-}$ kidneys, the collective reduction of several TGFβ superfamily inputs (TGFβ1, TGFβ2, BMP4) coupled with the complete absence of betaglycan, a key determinant of cellular TGFβ sensitivity, may result in sub-threshold levels of TGFβ superfamily signalling, which may explain why betaglycan$^{-/-}$ kidneys exhibit hypoplasia rather than an even greater rate of kidney development than the betaglycan$^{+/-}$. While quantification of TGFβ superfamily signalling through analysis of pSMAD1 and pSMAD3 immunohistochemistry identified no differences in activity between the three genotypes, this approach may not have been sufficiently sensitive to detect changes in signal transduction. Furthermore, only the activity of pSMAD1 and pSMAD3 were investigated in the present study due to the lack of specific mouse antibodies against the remaining receptor associated SMADs (2,5,7). Future studies should examine whether these remaining SMADS are critical for intracellular signal regulation in betaglycan mutant mice.

3.5 CONCLUSION

In summary, despite considerable functional redundancy amongst TGFβ superfamily members in the developing kidney (Oxburgh et al. 2004), morphological and molecular defects were detected in betaglycan$^{+/-}$ and betaglycan$^{-/-}$ kidneys. These phenotypes largely resemble their *Tgfb2* mutant counterparts, suggesting that a major role for betaglycan in the foetal murine kidney is as a determinant of TGFβ2 efficacy. Furthermore, the opposing phenotypes in both *Tgfb2* and betaglycan null and heterozygote kidneys indicate that the TGFβ2/betaglycan signalling pathway has dose-dependent actions and that activity of this pathway must be tightly controlled for normal branching morphogenesis and nephrogenesis to occur. Molecular analysis of betaglycan mutant kidneys indicated that the distinct morphological phenotypes in the betaglycan$^{+/-}$ and betaglycan$^{-/-}$ kidneys were mirrored at the molecular level. In particular, specific temporal changes in the expression of certain TGFβ superfamily members (for example *Bmp4* during the initiation of ureteric branching morphogenesis in betaglycan$^{+/-}$) may underlie the contrasting phenotypes. These findings may be of considerable importance to human health in that renal hypodysplasia is a recognized cause of paediatric renal failure and a risk factor for hypertension in adults.

CHAPTER 4

FUNCTIONAL CONSEQUENCES OF A HIGH NEPHRON ENDOWMENT

4.1 INTRODUCTION

In 1988, Brenner et al. hypothesized a link between nephron endowment and the risk for developing hypertension and CKD (Brenner et al. 1988). The 'Brenner hypothesis' suggested a decreased glomerular filtration surface area, acquired through a decreased nephron endowment or glomerular size, altered renal sodium and handling, inducing increased local (renal and glomerular) and systemic arterial pressures, and ultimately glomerular sclerosis (Section 1.7). Since the publication of this seminal paper, a large body of experimental data has been produced to support the role of nephron number in determining an individual's risk for the development of CVD and CKD (Ortiz et al. 2001; Wintour et al. 2003; Woods et al. 2004; Harrison and Langley-Evans 2009; Villar-Martini et al. 2009; Baum 2010). Interestingly, while this data is compelling, it must be noted that some models of moderate or severe congenital reduction in nephron endowment do not exhibit CVD or CKD (Martins et al. 2003; Zimanyi et al. 2006; Dickinson et al. 2007; Ruta et al. 2010). This has led to suggestions that a low nephron endowment alone does not induce disease, but rather predisposes the kidney to a second insult which, in turn, exacerbates the influence of this insult on cardiovascular and renal function ultimately resulting in the development of disease (Nenov et al. 2000).

To date, no study has characterized the consequences of augmented nephron endowment on cardiovascular and renal function; or whether such a phenotype provides cardiovascular or renal protection against the impact of secondary insults. Currently, only five *in vivo* models of augmented nephron endowment have been published (Lelievre-Pegorier et al. 1998; Maeshima et al. 2000; Mansano et al. 2007; Maka et al. 2008; Sims-Lucas et al. 2008). Of these five reports, only the study of *Tgfb2*$^{+/-}$ mice used gold-standard unbiased stereology to estimate glomerular number in a mouse model (Sims-Lucas et al. 2008). *Tgfb2*$^{+/-}$ mice contain 60% more nephrons than wildtype (WT) littermates (19978 ± 1148; 12283 ± 663, respectively) (Sims-Lucas et al. 2008). Whilst mean glomerular volume of *Tgfb2*$^{+/-}$ mice is approximately 30% less than WT mice, total glomerular volume is 30% greater (Table 1.3). Further, *Tgfb2*$^{+/-}$ mice appear phenotypically normal and renal size and morphology is comparable with WT mice, despite the dramatic augmentation in nephron number.

These characteristics suggest a robust model for determining the functional consequences, and potential benefits, of augmented nephron endowment.

Thus, the aims of the experiments described in this chapter were to firstly characterize baseline arterial pressure, heart rate and renal function in adult male *Tgfb2*$^{+/-}$ mice; secondly, to determine the renal functional response of *Tgfb2*$^{+/-}$ mice to a period of 24 hour water deprivation; and thirdly to characterize arterial pressure, heart rate and renal function in *Tgfb2*$^{+/-}$ mice in response to an acute and a chronic period of exposure to the secondary stressor of a high salt diet.

4.2 METHODS

4.2.1 Animal model:

16 week old male WT and *Tgfb2*$^{+/-}$ mice were obtained from the *Tgfb2* colony at Mouseworks, Monash University (see Section 2.1.1). All genotypes were determined prior to mice being selected for experimentation, and confirmed at autopsy via PCR (Section 2.2.1). Mice were housed individually in the experimental facility for 1 week prior to the commencement of experiments. All mice had *ad libitum* access to water and normal salt diet (0.26% NaCl w/w, Specialty Feeds) unless otherwise stated. The experimental room was maintained at ~25°C with a 12 hour light-dark cycle.

4.2.2 Baseline arterial pressure, heart rate, activity and renal function

24 hour baseline conscious renal function was determined in all WT and *Tgfb2*$^{+/-}$ mice from samples collected using glass metabolic cages (Section 2.8). Body weight was recorded, as well as the volume of food and water consumed, and excretion of urine and faeces. Urine samples were spun and frozen at -20°C for subsequent analysis. Mice were then implanted with radiotelemetry probes (PA-C10) for the measurement of conscious arterial pressure and heart rate (Section 2.7). During this time a blood sample (~60 µl) was collected for measurement of haematocrit and plasma creatinine. Post-surgery, mice were given a 10 day recovery period, during which behaviour, mobility and body weights were closely monitored. During this period body weight was observed to return to, and stabilize at, pre-implantation levels. Following the recovery period, probes were activated and conscious mean arterial, systolic and diastolic pressures, heart rate and activity values were then recorded in unrestrained mice for 7 days, sampling for 10 sec every 10 min.

4.2.3 Water Deprivation

A subset of mice (WT=6; *Tgfb2*$^{+/-}$=6) that underwent analysis of baseline renal function were used to determine the renal functional response to 24 hours of water deprivation. These mice did not undergo telemetry implantation. WT and *Tgfb2*$^{+/-}$ mice were placed in glass metabolic cages for 24 hours with the usual *ad libitum*

access to food; however water deprivation was induced by using an empty water vial. Immediately following the 24 hour period, a retro-orbital blood sample was taken (haematocrit and plasma creatinine), before mice were returned to their home box and water. Following the water deprivation experimental protocol, mice were maintained on a 0.26% NaCl diet and designated age-matched control mice for those mice allocated to the investigation of the effects of high salt diet on WT and *Tgfb2*$^{+/-}$ blood pressure, heart rate and renal function.

4.2.4 High salt diet

Following characterization of baseline cardiovascular and renal function, the effect of exposure to a high salt diet on cardiovascular and renal function was determined.

Chronic High Salt: To determine the functional response to a chronic high salt diet, a subset of mice (WT=7; *Tgfb2*$^{+/-}$ =7) were fed a 5% NaCl diet for 4 weeks. During the second week of this diet, blood pressure and heart rate were recorded, with renal function characterized (as above) during the third week. A retro-orbital blood sample was taken at the completion of renal function measurements to determine haematocrit and plasma creatinine. One week later (to allow for recovery post retro-orbital bleed) the diet of these mice was changed to an 8% NaCl diet for 4 weeks with blood pressure and heart rate recorded during the third week and renal function characterized during the fourth week of the diet. In total, mice fed a chronic high salt diet were fed a 5% NaCl diet for 4 weeks, followed by an 8% NaCl diet for 4 weeks, (total of 8 weeks) before tissues were collected and analysed.

Acute high salt: To determine the functional response to an acute 8% high salt diet, a separate cohort of mice (WT=6; *Tgfb2*$^{+/-}$=6) had arterial pressure measured for 5 days before being fed the 8% NaCl for 7 days. Arterial pressure and heart rate were recorded continuously throughout this 8% NaCl diet, and averages for the last 5 days are presented. At the completion of arterial pressure recording, renal function (urine volume excretion, Na^+ and creatinine excretion) was determined from urine collected

in the glass metabolic cages (Section 2.8). In total, mice were fed an 8% diet for 2 weeks before tissues were collected and analysed.

4.2.5 Tissue Collection

At the experimental end point, all mice were anaesthetized to collect a terminal blood sample and a post-mortem conducted to collect tissues (kidneys, heart, aorta) for analysis (Section 2.10). Left kidneys were transversely sliced in half, and one-half frozen in liquid nitrogen, while the remaining half of the left kidney, right kidneys, left and right ventricles were collected and immersion-fixed in 10% buffered formalin.

4.2.6 Urine and Plasma Analysis

All urine samples were analysed for electrolyte concentration (Na^+, K^+, Cl^-) and osmolality, as described in Section 2.9.1, and 24 hour excretions calculated. Urinary albumin concentration was determined using a murine-specific microalbuminuria ELISA kit (Exocell Inc; Section 2.9.2). Urinary and plasma creatinine concentration was determined using high performance liquid chromatography (HPLC) with creatinine clearance (Ccre) determined as an estimate of glomerular filtration rate (GFR; Section 2.8.4). All renal values are presented per gram of body weight.

4.2.7 Histology

Paraffin-embedded kidney sections (5μm) were dewaxed and stained with either haematoxylin and eosin (Section 2.12.2) or Picrosirius red (for visualization of collagen deposition; Section 2.12.4). Images were obtained with the aid of an Olympus Provis epifluorescence microscope and Leica DC digital camera (Leica Microsystems Ltd).

4.2.8 Statistical analysis

One-way ANOVA and two-way ANOVA (repeated measures where appropriate), and Dunnett's post-hoc analysis were conducted where appropriate, using GraphPad Prism™ 5 (Prism 5 for Windows, GraphPad Software Inc, 1992-2007). Values are mean ± SEM. A probability of 0.05 or less was accepted as statistically significant.

4.3 RESULTS

4.3.1 Basal arterial pressure, heart rate and activity

Under basal conditions, *Tgfb2*$^{+/-}$ mice showed normal circadian rhythms and all measures of arterial pressure, heart rate and activity were similar in WT and *Tgfb2*$^{+/-}$ mice (Table 4.1). 24 hour mean arterial (WT 107.8 ± 1.4; *Tgfb2*$^{+/-}$ 107.9 ± 1.3 mmHg), systolic and diastolic pressures and heart rate were all comparable between both genotypes. WT and *Tgfb2*$^{+/-}$ mice also had comparable arterial pressures and heart rate during the day and night periods (Table 4.1).

Table 4.1: Baseline arterial pressures, heart rate and activity of adult male WT and *Tgfb2*$^{+/-}$ mice fed a normal salt diet.

		WT	*Tgfb2*$^{+/-}$	*p*
MAP (mmHg)	**24 h**	107.8 ± 1.4	107.9 ± 1.3	0.9
	Night	114.7 ± 1.7	114.6 ± 1.4	0.9
	Day	101.1 ± 1.5	101.3 ± 1.3	0.9
Systolic (mmHg)	**24 h**	122.2 ± 1.6	122.6 ± 1.2	0.8
	Night	129.5 ± 2.0	129.9 ± 1.4	0.9
	Day	114.8 ± 1.5	115.3 ± 1.1	0.8
Diastolic (mmHg)	**24 h**	91.8 ± 2.1	91.9 ± 1.9	0.9
	Night	97.7 ± 2.1	97.7 ± 2.0	0.9
	Day	85.9 ± 2.3	86.2 ± 1.9	0.9
Heart Rate (BPM)	**24 h**	538 ± 7	532 ± 7	0.5
	Night	593 ± 9	579 ± 9	0.3
	Day	482 ± 8	485 ± 8.	0.8
Activity	**24 h**	7.6 ± 1.4	6.8 ± 0.8	0.6
	Night	11.8 ± 2.7	10.4 ± 1.3	0.6
	Day	3.3 ± 0.3	3.2 ± 0.3	0.8
N		14	15	

Values are mean ± SEM. Data analysed using one-way ANOVA.

4.3.2 Basal renal function

On the basal sodium diet (0.26%), WT and *Tgfb2*$^{+/-}$ mice demonstrated similar 24 hour food and water intake, and urine and faecal excretion (Table 4.2). Na^+ excretion was comparable in the two genotypes (Table 4.2), as was K^+ and Cl^- excretion (data not shown). Urine osmolality and osmolar excretion were also similar in the two genotypes (Table 4.2). 24 hour creatinine clearance and albumin excretion was both similar between the genotypes (Table 4.2).

Table 4.2: 24 hour baseline renal function in adult male WT and *Tgfb2*$^{+/-}$ mice fed a normal salt diet.

	WT	***Tgfb2*$^{+/-}$**	***p***
Body weight (g)	34.1 ± 1.0	32.6 ± 1.3	0.3
Food intake (µg gBW^{-1})	121.7 ± 8.8	98.4 ± 6.6	0.2
Water intake (µl gBW^{-1})	103.2 ± 5.2	104.7 ± 6.9	0.7
Urine volume (µl gBW^{-1})	45.8 ± 2.6	40.2 ± 2.7	0.2
Faecal weight (µg gBW^{-1})	26.8 ± 2.6	23.1 ± 1.6	0.1
Osmolality (mOsmol kgH_20^{-1})	1619 ± 62	1535 ± 59	0.3
Osmolar excretion (µOsmol gBW^{-1})	71.7 ± 3.2	62.0 ± 4.6	0.1
Na^+ excretion (µmol gBW^{-1})	6.23 ± 0.27	5.38 ± 0.43	0.2
***Creatinine clearance** (µg ml gBW^{-1})	9.87 ± 0.46	9.33 ± 1.06	07
Albumin excretion (µg gBW^{-1})	0.74 ± 0.13	0.88 ± 0.19	0.6
Haematocrit (%)	48.7 ± 0.6	48.1 ± 0.8	0.9
N	23	22	

Values are mean ± SEM. *N = WT=3; *Tgfb2*$^{+/-}$=4. Data analysed using a one-way ANOVA.

4.3.3 Water deprivation induces comparable renal responses in both genotypes

In this cohort of animals, WT mice were significantly heavier than *Tgfb2*$^{+/-}$ mice. However, water deprivation (WD) induced similar relative falls in body weight in both genotypes (WT -6.8%; *Tgfb2*$^{+/-}$ -6.4%; *p*Water <0.001; Table 4.3). Plasma haematocrit was elevated by a similar amount in both WT and *Tgfb2*$^{+/-}$ mice following water deprivation (*p*Water <0.001), and urine volume was significantly reduced in both genotypes by approximately 35% (*p*Water <0.001) indicating that 24 hour WD was sufficient to push all mice into a state of dehydration (Table 4.3).

WD significantly reduced the faecal weight excreted (*p*Water = 0.03) by both WT and *Tgfb2*$^{+/-}$ mice over the 24 hour period, however food intake and osmolar excretion were unaffected and remained comparable to values obtained when water was supplied to mice. Analysis of 24 hour urine samples indicated significant (*p*Water <0.001) but similar (*p*Int = 0.2) elevations in urine osmolality in both WT and *Tgfb2*$^{+/-}$ mice with WD. Urinary Na^+ excretion and albumin excretion were unaffected by 24 hour WD (Table 4.3).

Table 4.3: 24 hour renal function of adult male WT and *Tgfb2*$^{+/-}$ mice during basal and 24 hour water deprivation (WD) conditions.

	WT		*Tgfb2*$^{+/-}$		*p*		
	Basal	**WD**	**Basal**	**WD**	**G'type**	**Water**	**Int**
Starting body weight (g)	35.7 ± 1.0	34.7 ± 0.8	31.0 ± 0.7	31.4 ± 0.7	<0.001	0.8	0.5
Δ Body weight (%)	1.4 ± 0.5	-6.6 ± 0.6	1.1 ± 0.4	-6.3 ± 0.8	0.8	<0.001	0.8
Food intake (µg gBW^{-1})	104.8 ± 4.0	90.1 ± 9.0	106.8 ± 10.7	92.0 ± 6.1	0.9	0.2	0.6
Urine volume (µl gBW^{-1})	56.0 ± 3.3	37.1 ± 2.1	52.8 ± 5.6	33.3 ± 2.4	0.3	<0.001	0.9
Faecal weight (µg gBW^{-1})	22.2 ± 2.3	16.7 ± 2.7	23.8 ± 2.6	16.8 ± 1.7	0.9	0.03	0.9
Osmolality (mOsmol kgH_20^{-1})	1312 ± 70	1707 ± 92	1434 ± 85	2057 ± 151	0.03	<0.001	0.2
Osmolar excretion (µOsmol gBW^{-1})	73.3 ± 3.7	63.8 ± 6.0	75.0 ± 8.4	67.1 ± 3.3	0.6	0.1	0.8
Na^+ excretion (µmol gBW^{-1})	6.39 ± 0.34	6.65 ± 0.60	7.03 ± 0.99	6.75 ± 0.44	0.6	0.9	0.9
Albumin excretion (µg gBW^{-1})	0.93 ± 0.38	0.73 ± 0.30	1.22 ± 0.50	1.09 ± 0.44	0.2	0.4	0.9
Haematocrit (%)	46.8 ± 1.2	52.3 ± 0.4	48.8 ± 0.9	52.1 ± 1.0	0.1	<0.001	0.2
N	**6**		**6**				

Values are mean ± SEM. Data analysed by two-way repeated ANOVA, with factors of genotype (*p*G'type), water (*p*Water) and interaction between these factors (*p*Int).

4.3.4 High Salt Study

4.3.4.1 Chronic high salt

Arterial pressures were increased in both WT and *Tgfb2*$^{+/-}$ mice following the administration of a chronic high salt diet (*p*Diet <0.001). However, the effects of the diet on arterial pressures were significantly different between the genotypes (*p*Int <0.05; Fig 4.1A-F). Feeding of a 5% NaCl diet for 14 days led to similar and significantly elevated 24 hour mean arterial pressure in both genotypes (WT +3.5 ± 1.6 mmHg; *Tgfb2*$^{+/-}$ +3.4 ± 0.8 mmHg) above that of established baseline pressure (Figure 4.1A,B). 24 h mean systolic (WT +2.7 ± 1.2 mmHg; *Tgfb2*$^{+/-}$ +2.9 ± 1.0 mmHg) and diastolic (WT +4.9 ± 2.6 mmHg; *Tgfb2*$^{+/-}$ +4.0 ± 1.2 mmHg) pressures were also similarly elevated in both WT and *Tgfb2*$^{+/-}$ mice (Figure 4.1C-F). Heart rate and animal activity remained similar to baseline levels in both genotypes (Figure 4.1 G-J).

In WT mice, a further increase in dietary salt concentration to 8% induced dramatic elevations in mean arterial (Δ from 5% diet +15.9 ± 5.1 mmHg; Δ from baseline +19.4 ± 5.3 mmHg), systolic (Δ from 5% diet +15.5 ± 6.8 mmHg; Δ from baseline: +18.2 ± 6.2 mmHg) and diastolic (Δ from 5% diet: +18.4 ± 3.4 mmHg; Δ from baseline: +23.3 ± 5.0 mmHg) pressures (Figure 4.1A-D). Interestingly, on the same dietary regime, *Tgfb2*$^{+/-}$ mice did not exhibit any further elevations in MAP (Δ from 5% diet -0.1 ± 1.0 mmHg; Δ from baseline +4.2 ± 1.4 mmHg; Figure 4.1A,B) or systolic or diastolic pressures (Figure 4.1C–F) above those reached on a 5% NaCl diet. Heart rate and activity remained comparable on all diets for all mice (Figure 4.1G-J).

Following feeding of chronic high salt diets, water intake and urine excretion both significantly increased in accordance with increasing levels of salt in the diet (*p*Diet <0.001; Figure 4.2A,B). Similarly, Na^+ excretion was elevated in both genotypes (Figure 4.2C) when fed a high salt diet (*p*Diet = 0.005). Urinary osmolar excretion was elevated consistently in both genotypes on high salt diets and correlated strongly with increasing dietary salt intake (Figure 4.2D) Urinary osmolality was decreased in the presence of chronic high salt diets, but appeared to plateau as no further decrease was observed between the administration of 5% and 8% NaCl diets (Figure 4.2E). Also urinary albumin excretion was consistently elevated in both genotypes in the presence of a chronic high salt diet (Figure 4.2F). None of these renal responses to high salt diet differed between the genotypes.

Chronic high salt diet increased creatinine clearance in both WT and *Tgfb2*$^{+/-}$ mice (Figure 4.2G). However, once elevated in mice fed 5% NaCl diet, creatinine clearance did not increase further between 5% and 8% NaCl diets (WT: p = 0.6, *Tgfb2*$^{+/-}$: p = 0.9) (Figure 4.2 G).

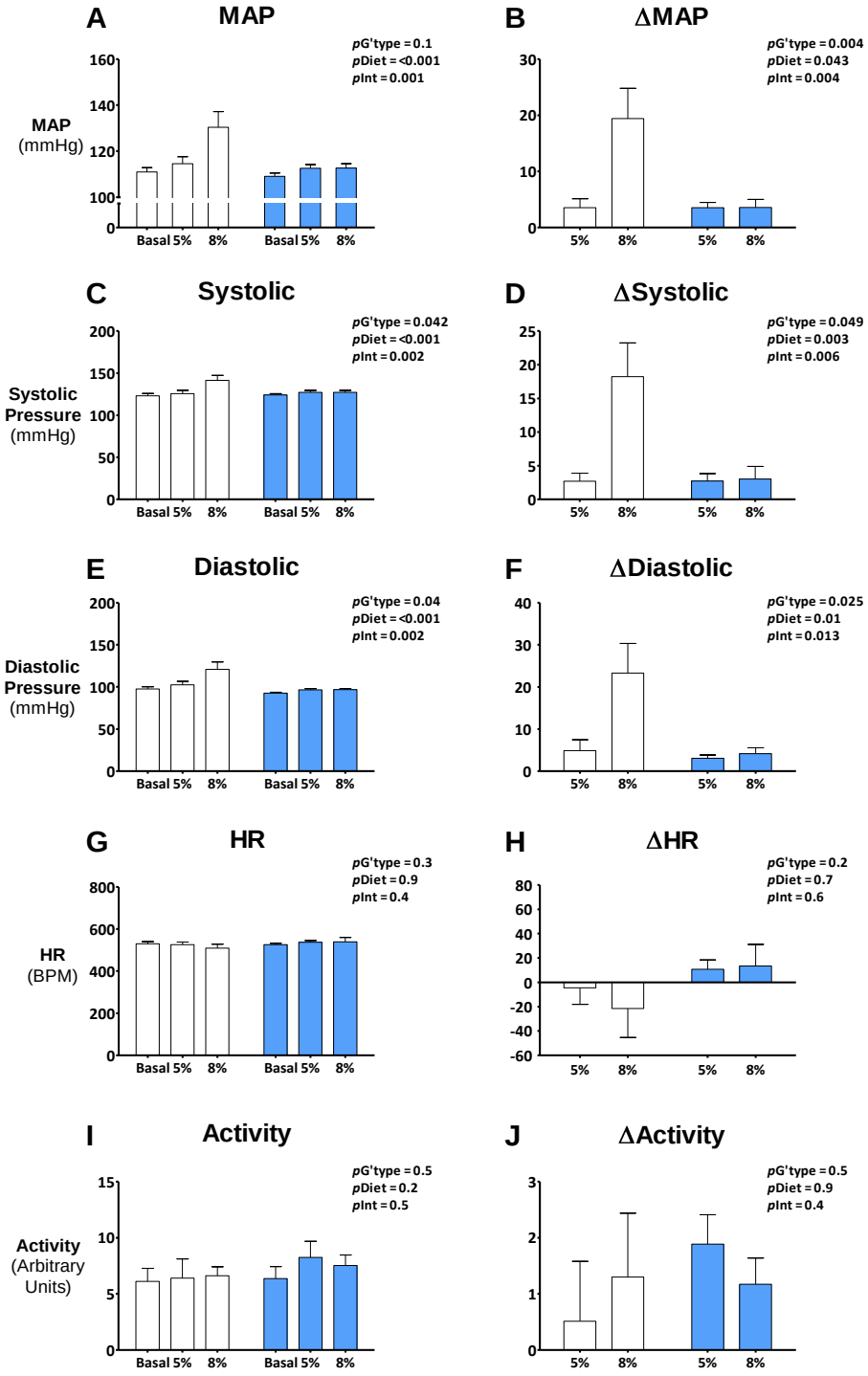

Figure 4.1: 24 hour arterial pressure, heart rate and activity in adult male WT and *Tgfb2*$^{+/-}$ mice under basal conditions, and when fed chronic 5% and 8% NaCl diets. Absolute values for WT (white bars) and *Tgfb2*$^{+/-}$ (blue bars) mice are presented in the left panels whilst deltas (Δ) calculated from basal measurements are presented in the right panels for A, B 24 h mean arterial pressure (MAP); C, D Systolic arterial pressure; E, F Diastolic arterial pressure; G, H 24 h heart rate (HR); and I, J Activity. Values are mean ± SEM. N = WT=7; *Tgfb2*$^{+/-}$=7. Data analysed by two-way repeated ANOVA, with factors of gentoype (*p*G'type), diet (*p*Diet) and interaction between these factors (*p*Int).

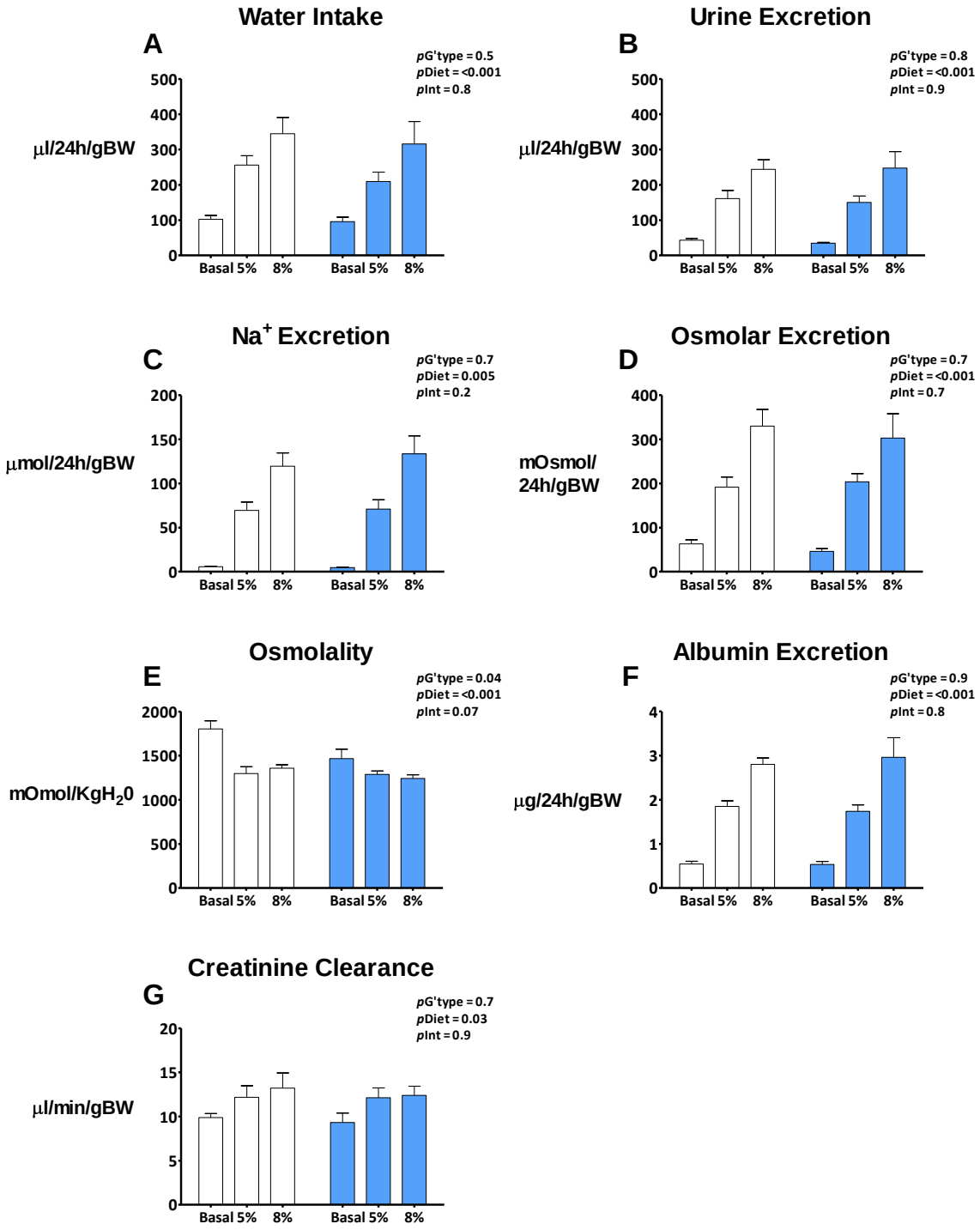

Figure 4.2: 24 hour renal function in adult male WT and *Tgfb2*$^{+/-}$ mice under basal conditions and on chronic 5% and 8% NaCl diets. WT (white bars) and *Tgfb2*$^{+/-}$ (blue bars). Values are mean ± SEM. N = WT=7; *Tgfb2*$^{+/-}$=7. However, for creatinine clearance N = WT=3; *Tgfb2*$^{+/-}$=4. Data analysed by two-way repeated ANOVA, with factors of gentoype (*p*G'type), diet (*p*Diet) and interaction between these factors (*p*Int).

4.3.4.2 Acute high salt

Given that a marked elevation in arterial pressure was observed in WT mice fed an 8% NaCl diet as part of the chronic high salt diet protocol, it was important to determine whether this was a response to the 8% high salt diet *per se* or cumulative effects of the 8 weeks of chronic 5% and then 8% salt diet. Therefore, in a separate cohort of mice, the acute effects of an 8% high salt diet were assessed. WT and *Tgfb2*$^{+/-}$ mice were fed the 8% high salt diet for 7 days immediately following baseline measurements and the data from the final 5 days of 8% high salt were analysed (see Figure 4.3). Mean arterial (ΔWT +3.6 ± 0.7 mmHg; Δ *Tgfb2*$^{+/-}$ +4.8 ± 1.1 mmHg), systolic (ΔWT +3.6 ± 0.7 mmHg; Δ *Tgfb2*$^{+/-}$ +4.7 ± 1.4 mmHg) and diastolic (ΔWT +3.4 ± 0.8 mmHg; Δ *Tgfb2*$^{+/-}$ +4.5 ± 0.8 mmHg) pressures were significantly elevated in the presence of the 8% NaCl diet (pDiet <0.001; Figure 4.4 A-F). However, the rise in arterial pressure was similar in WT and *Tgfb2*$^{+/-}$ mice (pInt > 0.3; Figure 4.5). Heart rate and activity were also increased in response to the 8% NaCl diet (pDiet <0.01), but again the effects were similar in the two genotypes (Figure 4.4 G-J).

WT and *Tgfb2*$^{+/-}$ mice fed an 8% NaCl diet exhibited comparable renal function (Table 4.4). Water intake and urine excretion volumes were both significantly increased (3-fold and 6-fold respectively; p<0.001), while food intake and faecal excretion were similar to baseline measurements (Table 4.4). Further, with increased dietary Na^+ intake, urinary excretion of Na^+ was significantly elevated in both genotypes (pDiet <0.001) as was osmolar excretion (pDiet <0.001), however these increases were similar in the two genotypes (Table 4.4). Urine osmolality was significantly decreased (pDiet <0.001) in both genotypes when fed the acute high salt diet. Albumin excretion (pDiet = 0.01) was also elevated in both genotypes when fed an acute high salt diet, with values comparable in both genotypes (Table 4.4).

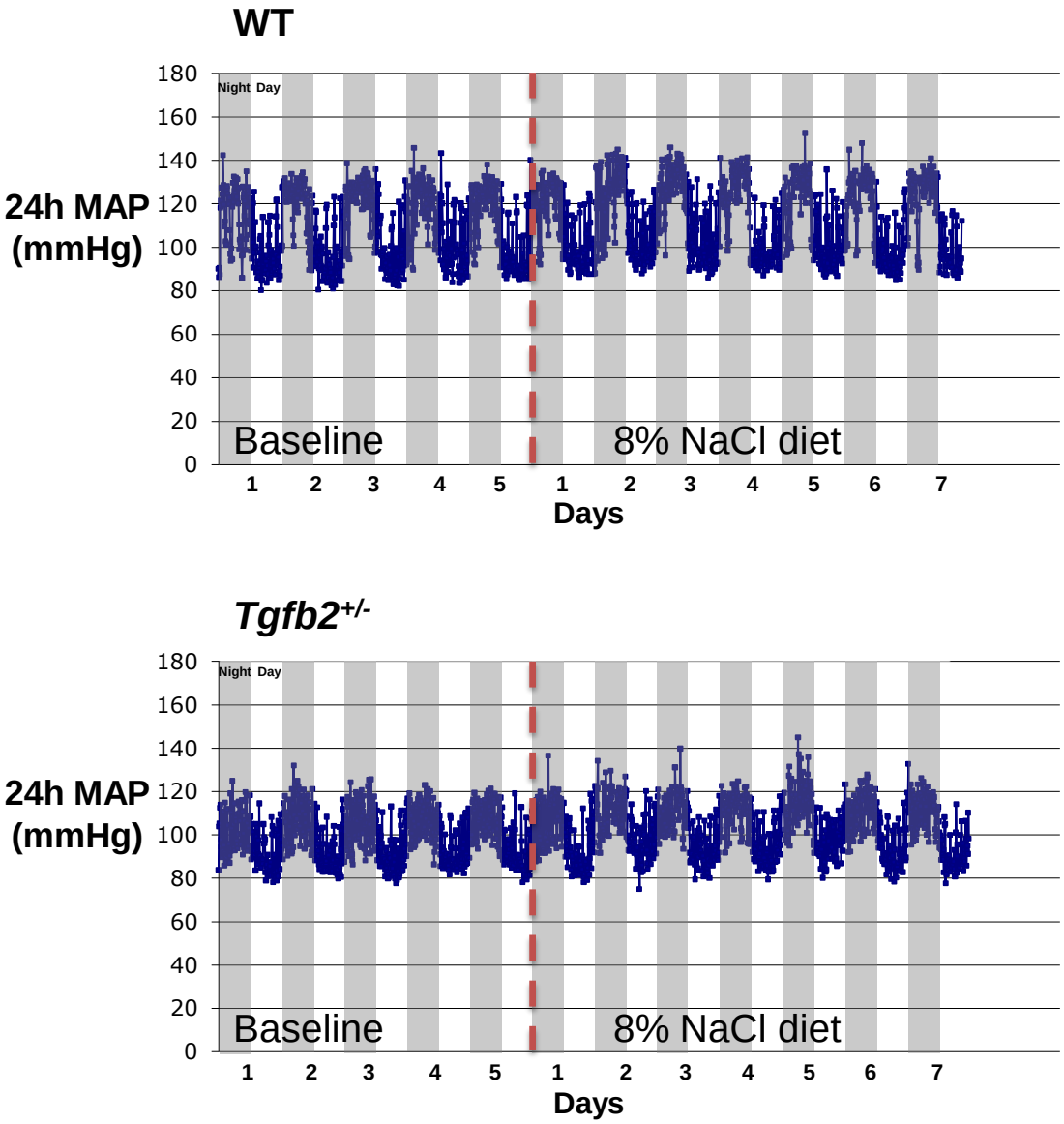

Figure 4.3: Examples of radiotelemetry recordings of the blood pressure response of WT and *Tgfb2*$^{+/-}$ mice to 7 days of 8% high salt diet. Traces show 24 hour mean arterial pressure (MAP) over the baseline period on normal salt diet, followed by 7 days on 8% NaCl diet. The last 5 days of recordings were compared to baseline measurements. Both genotypes display elevations in MAP after being fed the 8% NaCl diet. Gray and white panels indicate night and day periods, respectively.

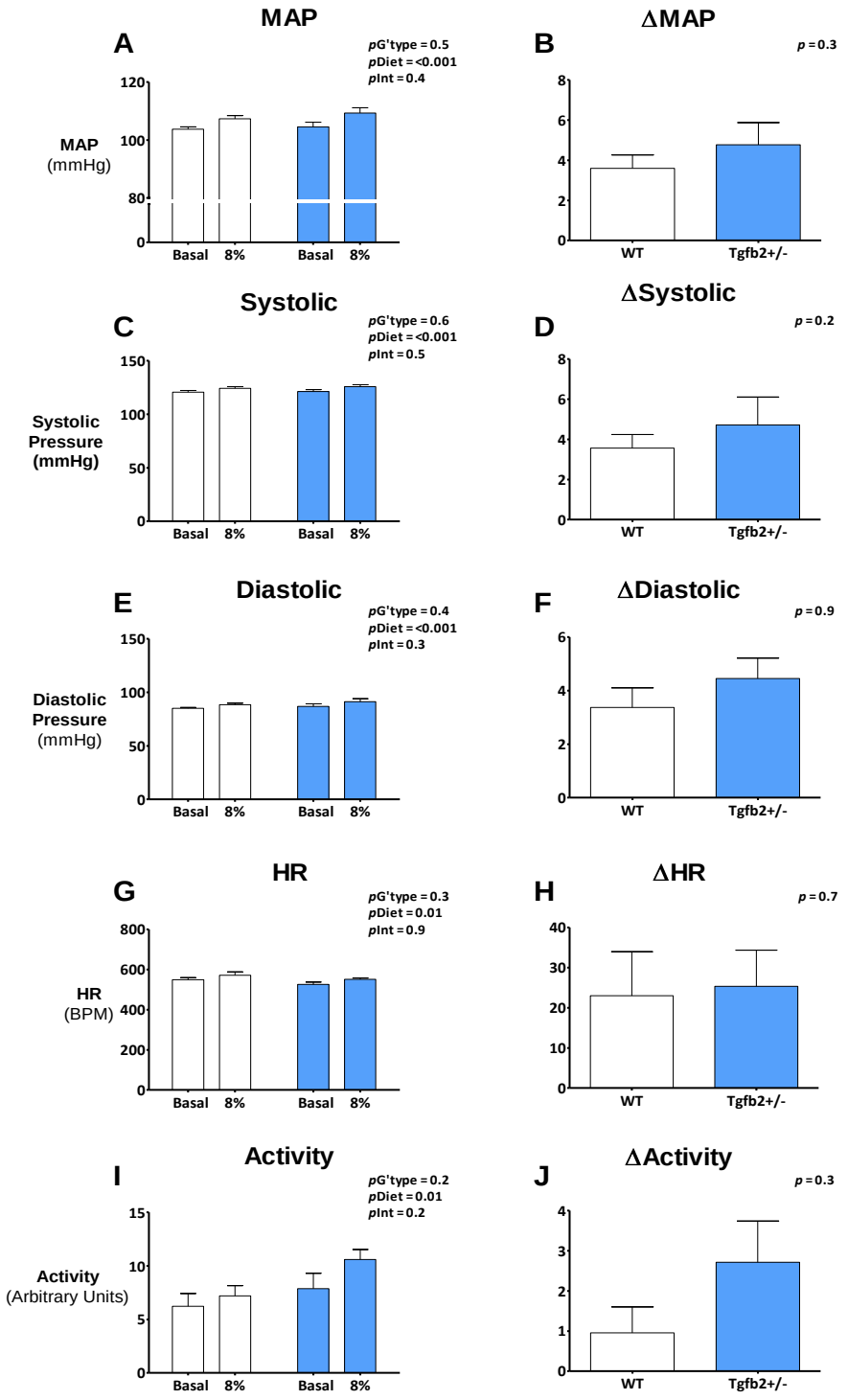

Figure 4.4: Effects of acute 8% salt diet on arterial pressure, heart rate and activity. Absolute values for WT (white bars) and *Tgfb2*$^{+/-}$ (blue bars) mice are presented in the left panels whilst deltas (Δ) calculated from basal measurements are presented in the right panels for: A, B, 24 hour mean arterial pressure (MAP); C, D, Systolic arterial pressure; E, F, Diastolic arterial pressure; G, H Heart rate (HR); and I, J Activity. Values are mean + SEM. N = WT=6; *Tgfb2*$^{+/-}$=7. Data analysed by two-way repeated measures ANOVA with factors of gentoype (*p*G'type), diet (*p*Diet) and interaction between these factors (*p*Int). All delta's were analysed by one-way ANOVA.

Table 4.4: Effect of 8% NaCl diet on 24 hour renal function in adult male WT and *Tgfb2*$^{+/-}$ mice.

	WT		*Tgfb2*$^{+/-}$		*p*		
	Basal	**8%**	**Basal**	**8%**	**G'type**	**Diet**	**Int**
Body weight (g)	31.2 ± 0.6	32.7 ± 0.4	30.2 ± 0.6	31.6 ± 0.5	0.2	0.003	0.8
Food intake (µg gBW^{-1})	117.2 ± 13.7	104.5 ± 5.6	126.6 ± 11.4	136.1 ± 13.0	0.2	0.9	0.3
Water intake (µl gBW^{-1})	93.8 ± 9.8	287.2 ± 22.9	102.8 ± 8.9	335.0 ± 25.5	0.1	<0.001	0.4
Urine volume (µl gBW^{-1})	41.3 ± 3.7	232.9 ± 22.8	40.0 ± 4.1	263.0 ± 17.5	0.3	<0.001	0.3
Faecal weight (µg gBW^{-1})	18.5 ± 1.5	18.00 ± 1.5	20.9 ± 1.7	20.9 ± 1.8	0.2	0.8	0.9
Osmolality (mOsmol kgH_20^{-1})	1841 ± 80	1309 ± 78	1658 ± 119	1215 ± 35	0.2	<0.001	0.5
Osmolar excretion (µOsmol gBW^{-1})	75.2 ± 5.4	296.5 ± 15.0	67.3 ± 9.4	317.7 ± 16.9	0.6	<0.001	0.3
Na^+ excretion (µmol gBW^{-1})	5.73 ± 0.65	108.1 ± 6.1	5.31 ± 0.8	118.7 ± 7.3	0.3	<0.001	0.3
Albumin excretion (µg gBW^{-1})	0.66 ± 0.26	1.42 ± 0.39	0.88 ± 0.29	1.08 ± 0.37	0.6	0.01	0.1
Haematocrit (%)	47.2 ± 1.9	43.1 ± 2.5	48.1 ± 0.8	45.8 ± 1.3	0.5	0.047	0.5
N	**6**	**6**	**6**	**6**			

Values are mean ± SEM. Analysis was conducted using a two-way repeated measures ANOVA; factors were genotype (*p*G'type), diet (*p*Diet) and interaction between these factors (*p*Int).

4.3.4.3 Pressure-Natriuresis

Arterial pressure and renal function are also presented in classical pressure-natriuresis format (Figure 4.5). In the current high salt study, *Tgfb2*$^{+/-}$ mice display a steep relationship, with little change in arterial pressure following a ~45-fold increase in Na^+ intake (Figure 4.5A). WT mice initially display a similar steep relationship, however this flatterns greatly indicating a marked change in arterial pressure with increasing Na^+ intake (Figure 4.5A). This suggests WT mice may display a heightened arterial response sensitivity to high salt diet than *Tgfb2*$^{+/-}$ mice. Interestingly, when fed the 8% high salt diet acutely, which resulted in similar sodium excretions seen in the chronic study, WT and *Tgfb2*$^{+/-}$ mice exhibited similar steep pressure-natriuresis relationships (Figure 4.5B). Together, these data indicate that the cumulative effect of a chronic high salt diet may be driving the marked elevation in arterial pressure observed in WT mice and not the 8% NaCl diet *per se*.

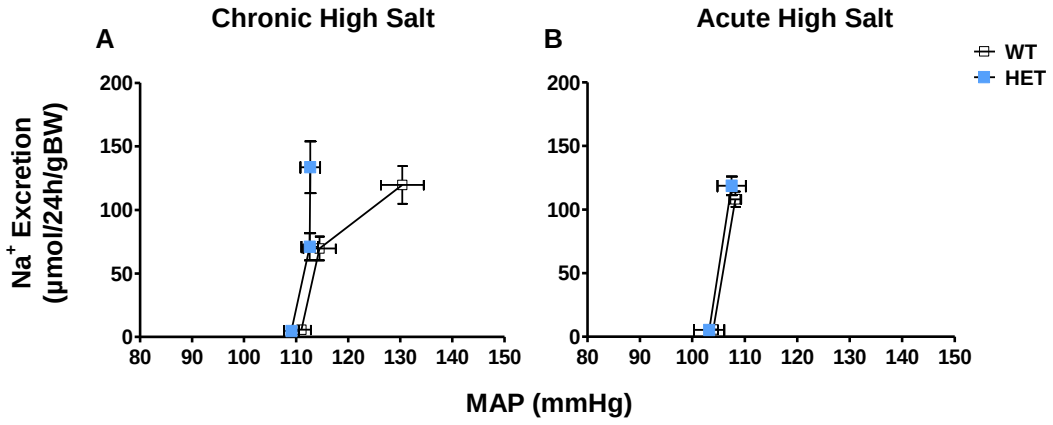

Figure 4.5: Pressure-natriuresis curves for WT and *Tgfb2*$^{+/-}$ mice fed either a chronic or acute high salt diet. Values are mean ± SEM. Chronic high salt N = WT=7; *Tgfb2*$^{+/-}$=7. Acute high salt N = WT=6; *Tgfb2*$^{+/-}$=6.

4.3.5 Body weights, organ weights and organ-to-body weight ratios

Baseline body weights were comparable in WT and *Tgfb2*$^{+/-}$ mice on a normal salt diet (Table 4.5). In the cohort of mice analysed, WT mice fed a normal salt diet had significantly greater weights for the left (p = 0.03) and right kidneys (p = 0.01) and also a greater total kidney weight (p = 0.01) compared to age-matched *Tgfb2*$^{+/-}$ mice. However, these differences were not present when values were normalized to body weights (Table 4.5). Cardiac weights were also similar between genotypes on a normal salt diet (Table 4.5).

Interestingly, a chronic high salt diet did not significantly affect wet organ weight or organ-to-body weight ratios in WT mice (Table 4.5). In contrast, *Tgfb2*$^{+/-}$ mice fed a chronic high salt diet exhibited greater left, right and total kidney organ weights when compared to age-matched mice fed a normal salt diet (Table 4.5). These changes in *Tgfb2*$^{+/-}$ mice were further highlighted by a significantly greater (p<0.05) total kidney-to-body weight ratio following a chronic high salt diet. Ventricular weights and ratios were similar in mice of both genotypes when fed a normal or chronic high salt diet.

WT and *Tgfb2*$^{+/-}$ mice fed an acute 8% high salt diet, exhibited significantly greater left kidney weight (p<0.05), but not right kidney weight than their normal salt controls (Table 4.5). Interestingly, while total kidney weights for WT and *Tgfb2*$^{+/-}$ mice fed an acute high salt diet were comparable to normal salt controls, WT mice only displayed a greater total kidney-to-body weight ratio (p<0.05) when compared to normal salt fed control mice. Furthermore, while no changes in absolute ventricular weights were observed in mice of either genotype when fed an acute salt diet, these mice had significantly greater left ventricle-to-body weight ratios than their respective normal salt controls (p<0.05; Table 4.5).

Table 4.5: Body weights and organ weights for adult male WT and *Tgfb2*$^{+/-}$ mice in the three dietary groups.

	WT			***Tgfb2*$^{+/-}$**		
	NS	**Chronic**	**Acute**	**NS**	**Chronic**	**Acute**
Body Weight (g)	35.4 ± 1.5	35.7 ± 1.3	32.5 ± 0.5	34.0 ± 0.8	33.5 ± 1.2	31.8 ± 0.6
Left Kidney Weight (mg)	199 ± 5	210 ± 7	212 ± 10*	178 ± 6$^{\#}$	208 ± 9*	204 ± 11*
Right Kidney Weight (mg)	232 ± 6	250 ± 9	237 ± 3	203 ± 6$^{\#}$	237 ± 9*	196 ± 37
Total Kidney Weight (mg)	432 ± 10	460 ± 15	449 ± 9	380 ± 10$^{\#}$	445 ± 17*	400 ± 47
TK / BW (mg/g)	12.3 ± 0.7	13.0 ± 0.5	13.9 ± 0.2*	11.2 ± 0.4	13.4 ± 0.8*	12.6 ± 1.4
Left Ventricle Weight (mg)	137.4 ± 7.9	136.0 ± 5.3	142.8 ± 8.7	123.0 ± 6.9	131.7 ± 11.3	139.8 ± 7.3
LV/BW (mg/g)	3.88 ± 0.13	3.83 ± 0.16	4.41 ± 0.22*	3.62 ± 0.21	3.98 ± 0.40	4.40 ± 0.22*
Right Ventricle Weight (mg)	25.8 ± 2.7	28.1 ± 2.5	28.7 ± 2.5	23.0 ± 1.5	27.9 ± 2.2	22.3 ± 1.3
RV/BW (mg/g)	0.73 ± 0.06	0.79 ± 0.06	0.89 ± 0.08	0.68 ± 0.05	0.82 ± 0.08	0.70 ± 0.04
N	**6**	**8**	**6**	**6**	**7**	**6**

Values are mean ± SEM. NS: Normal salt diet; Chronic: 5% salt diet followed by 8% salt diet; Acute: 8% salt diet. LK/BW indicates left kidney to body weight ratio, RK/BW indicates right kidney to body weight ratio, LV/BW indicates left ventricle to body weight ratio, RV/BW indicates right ventricle to body weight ratio. WT and *Tgfb2*$^{+/-}$ fed a NS diet compared using Student's T-test, $^{\#}p<0.05$ vs. WT NS mice. Analysis was conducted within genotype using a one-way ANOVA followed by Dunnett's post-hoc analysis $^{*}p<0.05$, vs. NS genotype control.

4.3.6 Renal histology after being fed a normal salt, chronic high salt or acute high salt diet.

Renal histology was similar in WT and *Tgfb2*$^{+/-}$ mice fed a normal salt diet throughout life (Figure 4.6 A-H). WT and *Tgfb2*$^{+/-}$ mice fed a chronic salt diet displayed similar renal cortical morphology (Figure 4.6 I, J, M, N). Interestingly, WT mice fed a chronic high salt diet appeared to display hypercellularity at the vascular pole of in small number of glomeruli in the juxtamedullary region of the kidney (Figure 4.6 L). In contrast, renal histology in *Tgfb2*$^{+/-}$ mice fed a chronic high salt diet was indistinguishable from that in age-matched *Tgfb2*$^{+/-}$ mice fed a normal salt diet (Figure 4.6 E-H, M-P). Similarly, renal histology in mice of both genotypes fed an acute high salt diet was similar to renal histology of age and genotype-matched mice fed a normal salt diet (Figure 4.6 Q-X).

Collagen deposition was similar in WT and *Tgfb2*$^{+/-}$ mice fed a normal salt diet throughout life (Figure 4.7 A-H). However, a chronic high salt diet appeared to increase perivascular collagen deposition in WT mice (Figure 4.7 K-L), which was not apparent in *Tgfb2*$^{+/-}$ mice fed the same diet (Figure 4.7 O-P). This increased deposition was more prominent in the cortico-medullary region and included markedly increased peritubular collagen deposition; however these changes were only present in the vicinity of renal vasculature. Collagen deposition appeared normal in *Tgfb2*$^{+/-}$ mice fed a chronic high salt diet (Figure 4.7 M-P). The acute high salt diet did not appear to alter collagen deposition in the kidneys of WT or *Tgfb2*$^{+/-}$ mice (Figure 4.7 Q-X).

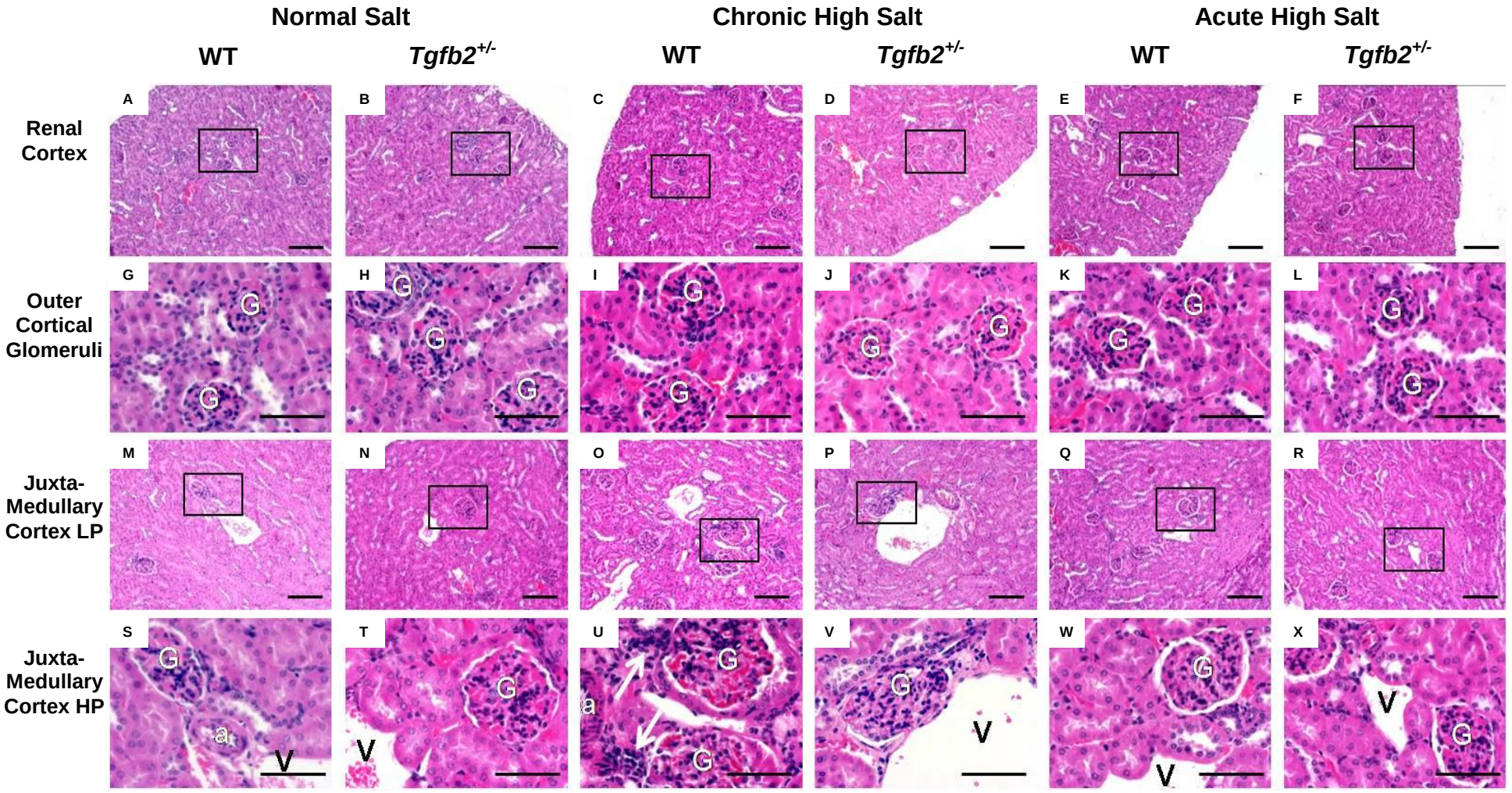

Figure 4.6: Photomicrographs of kidneys stained with haematoxylin and eosin. LP: low power, HP: high power. Arrows indicate hypercellularity, (a) artery, (G) glomerulus, (V) vein. All scale bars = 100µm.

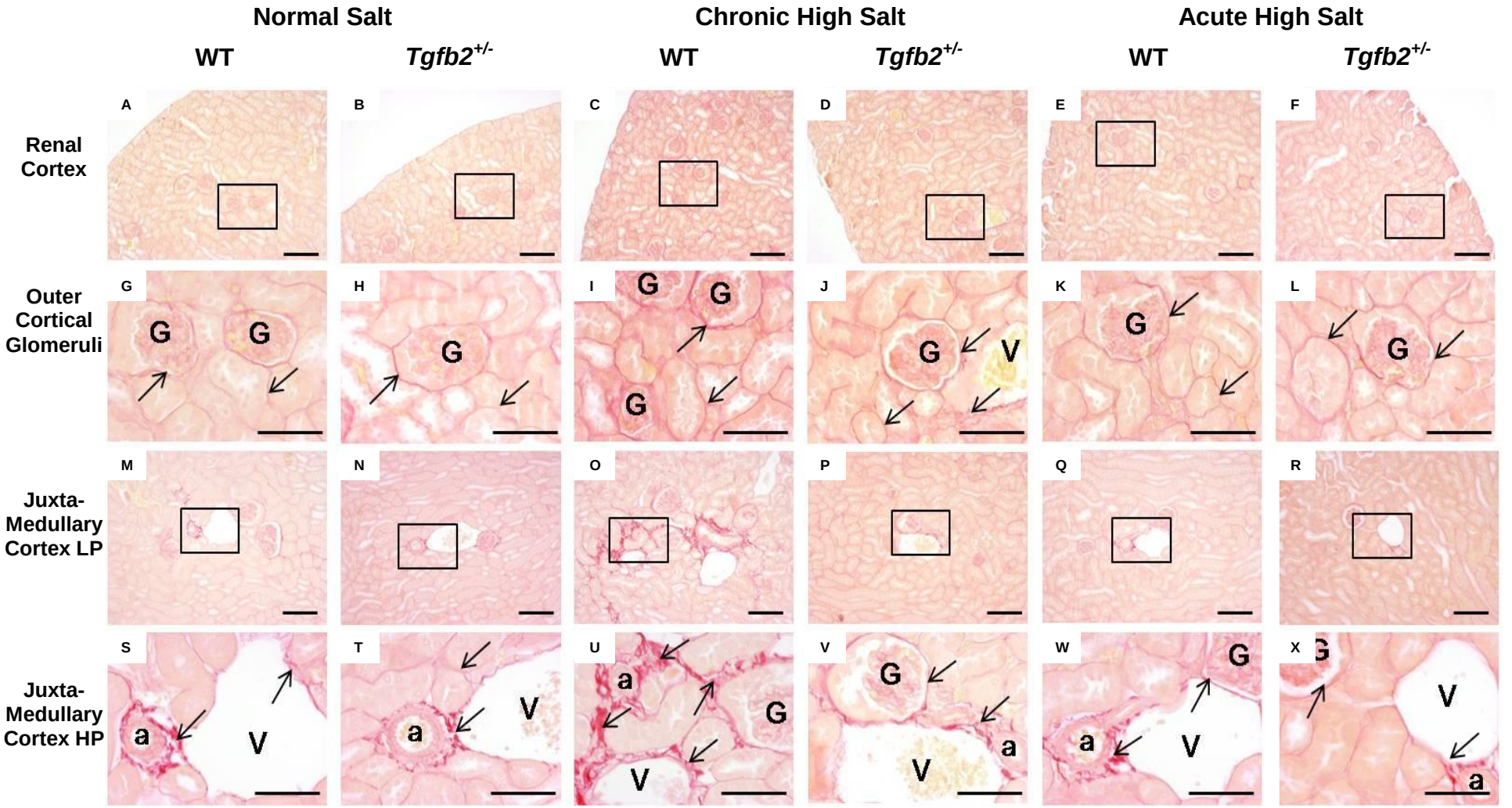

Figure 4.7: Photomicrographs of kidneys stained with picrosirius red. LP: low power, HP: high power. Arrows indicate collagen deposition, (a) artery, (G) glomerulus, (V) vein. Scale bars = 100µm.

4.4 DISCUSSION

The aims of the experiments described in this Chapter were to characterize cardiovascular and renal function in adult male *Tgfb2*$^{+/-}$ mice under basal, physiologically stimulated, and pathologically stressed conditions. The major findings were: 1) baseline blood pressure, heart rate and renal function were similar in adult male *Tgfb2*$^{+/-}$ and WT mice; 2) *Tgfb2*$^{+/-}$ mice appear protected from the large impact of a chronic high salt diet on arterial pressure; and 3) exposure to acute and chronic high salt diets, as well as water deprivation induced comparable renal functional responses in both genotypes. Taken together, these findings suggest that a high nephron endowment does not influence baseline arterial pressure or generate an alternate response to an acute period of physiological or pathological stress. However, the findings are consistent with the hypothesis that a high nephron endowment provides cardiovascular protection against a prolonged chronic stressor.

4.4.1 High nephron number does not affect baseline arterial pressure or renal function

This is the first study to date to characterize both arterial pressure and renal function in a model of high nephron endowment. Comparable arterial pressure and renal function in adult male WT and *Tgfb2*$^{+/-}$ mice under basal conditions suggests that an augmented nephron number does not impact the baseline function of either system. All arterial pressure and renal parameters measured including mean arterial pressure, heart rate and activity, as well as urine volume excretion, creatinine clearance, urinary osmolality, urinary albumin and electrolyte excretion were similar in the two genotypes. Two previous studies have examined urinary excretion volumes, osmolality and albumin in WT and *Tgfb2*$^{+/-}$ mice (Pietri et al. 2002; Sims-Lucas et al. 2008). Whilst quantitatively the values recorded in previous studies differ from those in this current study (due largely to different composition of normal diets consumed), all studies have concluded that WT and *Tgfb2*$^{+/-}$ mice have similar values for those parameters measured. Importantly, the indistinguishable baseline arterial pressure, renal function and body weights of *Tgfb2*$^{+/-}$ and WT mice further

highlight the robust nature of this model for the characterization of the functional consequences of high nephron endowment.

There is now considerable conjecture as to the role of nephron number in the regulation of baseline arterial pressure. Brenner et al. (1988) hypothesized that a low nephron endowment contributes to the development of essential hypertension, suggesting a strong inverse relationship between nephron number and arterial pressure (Brenner et al. 1988). The seminal study by Keller et al. (2003), which demonstrated that hypertensive subjects exhibited a significantly lower nephron endowment at autopsy than matched normotensive subjects further substantiated the 'Brenner' hypothesis (Keller et al. 2003). However, while some experimental models of congenital low nephron endowment have displayed elevations in arterial pressure, this has not been a consistent finding, particularly when radiotelemetry has been used to limit stress-associated arterial pressure increases (Ortiz et al. 2001; Wintour et al. 2003; Woods et al. 2004; Brennan et al. 2008; Harrison and Langley-Evans 2009; Villar-Martini et al. 2009; Baum 2010; Ruta et al. 2010). This issue was highlighted by Ruta et al. (2010) who found that neither moderate nor severe reductions in nephron endowment impact on baseline mean arterial pressure (Ruta et al. 2010). Firstly, Ruta et al. (2010) found that *Gdnf* heterozygous mice with one or two kidneys exhibit a 65% and 25% reduction in nephron number respectively, when compared to age-matched WT mice. Ruta et al. (2010) then demonstrated that despite these reductions in total nephron number, baseline mean arterial pressure was comparable between all groups even when examined at 1 year of age. Data from the present study has further highlighted that under baseline conditions nephron number may not be an important factor for the regulation of arterial pressure.

4.4.2 WT and *Tgfb2*$^{+/-}$ mice demonstrate similar responses to water deprivation

When nephron endowment was initially characterized in *Tgfb2*$^{+/-}$ mice, augmented nephron endowment was associated with decreased mean glomerular and renal corpuscle volumes with comparable kidney weight to age-matched WT mice (Sims-Lucas et al. 2008). While stereological analysis of the nephron tubular and collecting duct systems of *Tgfb2*$^{+/-}$ mice has not been conducted, it is possible to hypothesize that, changes in length of nephron tubular segments or collecting ducts

may be present in *Tgfb2*$^{+/-}$ kidneys to accommodate for the augmented nephron endowment. A primary function of the kidney and in particular the nephron is the maintenance of fluid homeostasis, a process which is particularly important during periods of water deprivation (Guyton 1991). Briefly, filtrate collected in the urinary space passes through the proximal tubule where 65% of water reabsorption occurs (see Section 1.2.2). Remaining filtrate then passes through the thin descending, thin ascending and finally thick ascending limbs of the loop of Henle where a sophisticated countercurrent system concentrates urinary sodium and regulates both urinary and interstitial osmolality (Guyton 1991). Importantly, the lengths of the loops of Henle differ between juxtamedullary and outer cortical nephrons. Juxtamedullary nephrons, which are believed to comprise between 20 - 30% of total nephron number, contain much longer thin descending and ascending limbs compared to outer cortical nephrons, which allows for greater concentrating abilities (Jamison 1973; Guyton 1991). From the loop of Henle, filtrate passes through the collecting duct system where a final stage of water reabsorption occurs under hormonal control. Should an augmented nephron endowment be associated with changes in the length or proportion of tubular/collecting duct segments, or the proportion of cortical or juxtamedullary nephrons within the kidney, the ability of the kidney to regulate water homeostasis and respond to periods of water deprivation may be compromised. Thus the current study aimed to determine whether an augmented nephron endowment impacts upon the response of the kidney to a period of water deprivation.

Tgfb2$^{+/-}$ mice demonstrated a similar response to a 24 hour period of water deprivation as age-matched WT mice with both urine volume decreasing and haematocrit increasing significantly. This finding correlates with a previous study in which the response of *Tgfb2*$^{+/-}$ mice to an 82 hour period of water deprivation was shown to be similar to that of WT mice (Pietri et al. 2002). While Pietri et al. (2002) and the present study reached similar conclusions, it is important to acknowledge the major differences in experimental approaches adopted. Firstly, in the present study, a 24 hour period of water deprivation was shown to be sufficient to induce a physiological state of dehydration in mice, as indicated by elevated haematocrit levels (approximately 5 percentage points) (Guyton 1991). This suggests that extending the period of water deprivation beyond 24 hour may be excessive as mice are already in a

physiologically challenged state. Indeed, although Pietri et al. (2002) did not measure changes in haematocrit 82 hour period of water deprivation resulted in a marked 22% reduction in body weight compared with a 6% change in body weight in both genotypes in the present study. However, irrespective of the differences in experimental design, these studies both highlight that *Tgfb2*$^{+/-}$ and WT mice respond similarly to water deprivation. Thus, these data suggest that nephron number and global TGFβ2 expression are not important in determining an individual's response to a period of water deprivation.

4.4.3 Chronic high salt diets differentially affect arterial pressure in WT and *Tgfb2*$^{+/-}$ mice

The most striking finding from the present study was the arterial pressure response of mice fed a chronic high salt diet. WT and *Tgfb2*$^{+/-}$ mice fed a high salt diet for a total period of 8 weeks (5% NaCl diet for 4 weeks followed by 8% NaCl diet for 4 weeks) exhibited similar changes in urine volume, Na^+ and albumin excretion, and creatinine clearance; however on this diet regime WT and *Tgfb2*$^{+/-}$ mice exhibited significantly different responses in arterial pressure. While both genotypes demonstrated mild elevations in MAP when fed a 5% NaCl diet, when these mice were then fed an 8% NaCl diet, only WT mice exhibited a further elevation in MAP whilst blood pressure in *Tgfb2*$^{+/-}$ mice remained stable at the level seen with 5% NaCl diet. To determine whether this rise in WT MAP on the 8% diet was due to an acute response to the higher 8% diet or a result of the cumulative response to 8 weeks on a high salt diet (5% + 8%), separate studies to examine the acute affects of an 8% high salt diet were performed. Interestingly, when both genotypes were fed the 8% NaCl diet for an acute period of 7 days, WT and *Tgfb2*$^{+/-}$ mice exhibited mild elevations in arterial pressure, similar to those observed in mice fed a 5% NaCl diet. When renal function was characterized, urine volume as well as osmolar, albumin and Na^+ excretion were all elevated in both genotypes when fed a chronic or acute high salt diet, but remained comparable between genotypes. This suggests that the duration of the dietary stressor is important for unmasking a protective effect of the *Tgfb2*$^{+/-}$ genotype and/or high nephron number on arterial pressure.

As a high salt diet was the selected physiological stressor for this study, it is important to acknowledge that the sensitivity of different strains of mice to high salt diets can be a confounding factor when investigating alterations in arterial pressure (McLoone et al. 2009). In this current study WT and *Tgfb2*$^{+/-}$ mice on a mixed 129/OLa - Black Swiss background were utilized. To date, no study has shown either of these strains to be salt sensitive. Previously, 8% NaCl diets fed for 7 days to WT mice of varying background strains has been shown to induce a 4 - 8 mmHg elevation in MAP when measured using radiotelemetry (Carlson and Wyss 2000; Carlson et al. 2002; Shindo et al. 2002; Kim et al. 2008). However, when salt-sensitive mice were fed the same diet for 7 days, arterial pressure was elevated >10 mmHg (Kim et al. 2008). While both genotypes in the present study exhibited significant elevations in MAP when fed an acute 8% NaCl diet, these elevations were quite moderate (~ 5mmHg) and consistent with previous studies, suggesting that the background strain is not contributing to the observed changes in arterial pressure.

Finally, this is the first study to provide experimental evidence that an augmented nephron endowment may be protective for arterial pressure in the presence of a chronic pathological stressor. Yet as the *Tgfb2*$^{+/-}$ mice exhibit a global reduction in TGFβ2 expression as well as an augmented nephron endowment, the possible mechanism for the inferred protective effective observed in *Tgfb2*$^{+/-}$ remains unclear. Therefore, it is important that these two separate, but non-mutually exclusive factors are discussed.

4.4.3.1 Role of augmented nephron endowment in arterial pressure regulation

The hypothesis that a high nephron endowment is potentially beneficial to cardiovascular and renal health has come from much work focusing on the consequences of a low nephron endowment. It is quite conceivable that if a low nephron endowment is associated with an increased risk for hypertension and its associated pathologies, as originally hypothesized by Brenner et al. (1988), then a high nephron endowment may act in an opposing, protective manner. Human nephron endowment has been shown to be highly variable, with the most recent data indicating a 13-fold range (range 210,332 to 2,702,079; mean, 876,339) (Puelles et al. 2010). In an exciting recent autopsy study, the probability of Caucasian and African

Americans developing hypertension based on their nephron number (Puelles et al. 2010). Puelles et al. found that Caucasian Americans with a nephron endowment greater than 876,300 have a decreased probability of presenting with hypertension compared with those subjects with a lower nephron endowment (Figure 4.8). Interestingly, this relationship did not hold for African Americans, whose probability of hypertension was not dependent on nephron endowment

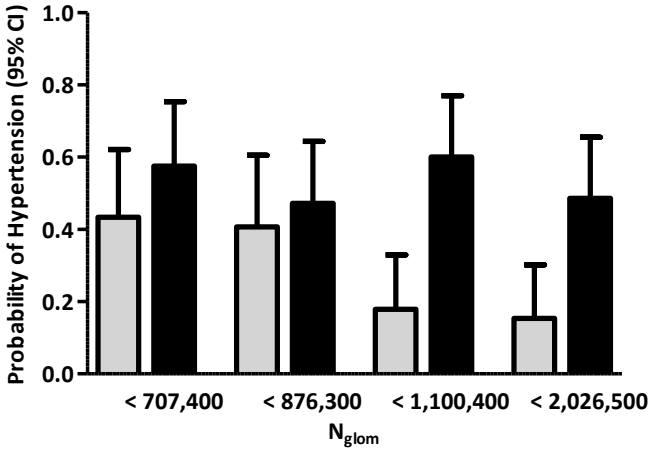

Figure 4.8 Probability of Hypertension by Glomerular Number Quartiles in African and Caucasian Americans. Probability of hypertension by total glomerular number (N_{glom}) quartiles and race, where □ Caucasian Americans and ■ African Americans. All +18 years old (N=252). Figure from (Puelles et al. 2010)

No study to date has characterized arterial pressure and renal function in a known animal model of high nephron endowment. However, the potential benefit of increased renal mass and, in turn, nephron number has been explored. An important study by Ots et al. (2004) demonstrated that supplementation of renal mass through transplantation of an entire kidney into an experimental model, of renal insufficiency (5/6 nephrectomy), significantly lowered systolic blood pressure and slowed the progression of glomerular injury in the remnant kidney. They concluded that an increase in nephron endowment in hypertensive individuals may provide greater control of arterial pressure, and potentially slow the development and progression of hypertensive associated pathologies. Ots et al. (2004) further suggested that augmentation of nephron endowment may be a possible means by which the risk for developing disease can be decreased, a concept reiterated by data obtained in the present study.

4.4.3.2 Protective nature of global TGFβ deficiency

The model of high nephron endowment used in the current study also exhibits a global reduction in TGFβ2 protein expression. Previously, it has been shown that *Tgfb2*$^{+/-}$ mice consistently express approximately 50% of the WT levels of TGFβ2 protein in their tissues, including the kidney (Sanford et al. 1997; Dunker and Krieglstein 2000; Pietri et al. 2002). All three TGFβ isoforms are expressed in the adult murine kidney and their function is predominantly associated with the regulation of ECM accumulation and turnover. In the presence of renal injury, TGFβ isoforms are upregulated and contribute to the progression of renal fibrosis (Hill et al. 2000; Bottinger 2007). It is due to these roles in disease development, that anti-TGFβ based approaches have been adopted to inhibit the adverse effects of TGFβ function on renal function (Border et al. 1992; Hill et al. 2000; Gagliardini and Benigni 2007).

Of significance to the present study, neutralisation of TGFβ function has been shown to not only slow the progression of renal fibrosis, but also ameliorate the hypertensive effects of a high salt diet. Dahly et al. (2002) fed Dahl salt-sensitive (S) rats an 8% NaCl diet for 21 days to induce elevations in arterial pressure and increased proteinuria. In a subset of rats, a pan-specific TGFβ neutralising antibody was administered i.p. every second day during the second and third weeks of the 8% NaCl diet. Anti-TGFβ treatment ameliorated elevations in arterial pressure compared with control rats maintained on the 8% NaCl diet. However, it must be noted that while arterial pressure was 13 mmHg lower than control rats following anti-TGFβ treatment, systolic pressure remained high at the end of the third week of 8% NaCl. Anti-TGFβ treatment in Dahl S rats also significantly decreased proteinuria, reduced type III collagen and fibronectin mRNA expression and reduced glomerular injury and the formation of protein casts. Dahly et al. (2002) concluded that the significantly reduced renal *Tgfb1* and *Tgfb2* mRNA expression observed in anti-TGFβ treated Dahl S rats was renoprotective as it limited production of TGFβ proteins which in turn decreased the deposition of ECM within the kidney. These findings of Dahly et al. (2002) correlate strongly with the present findings of a protective phenotype in *Tgfb2*$^{+/-}$ mice compared to the increased collagen deposition and elevated arterial pressures in WT mice fed a chronic high salt diet.

A possible mechanism for the renoprotective effect of the pan-specific TGFβ neutralising antibody observed by Dahly et al. (2002) may involve disruption of TGFβ

expression levels by the high salt diet. Previously, high salt diets have been shown to increase intrarenal expression and urinary excretion of TGFβ1 (Ying and Sanders 1998; Sanders 2009). Upregulated TGFβ1 expression induces increased ECM deposition as well as decreased vascular compliance and increased peripheral resistance, all of which contribute to the development of hypertension (Bruijn et al. 1994; Kopp et al. 1996; Mozes et al. 1999; Bottinger and Bitzer 2002; Ying et al. 2008). Such correlations have led to elevated TGFβ1 excretion being targeted as a possible biomarker of renal disease (Lee et al. 2009). It is possible that administration of the pan-specific TGFβ neutralising antibody by Dahly et al. (2002) provided protection against high salt induced elevations in arterial pressure by either reducing endogenous TGFβ expression or by impairing upregulated expression of TGFβ1 specifically. However, while it is unknown as to whether TGFβ2 is upregulated by a high salt diet in a similar manner to TGFβ1, both isoforms have been shown to mirror each other's expression in the presence of disease (Bruijn et al. 1994; Bottinger and Bitzer 2002). Importantly, Dahly et al. (2002) concluded that disruption of the positive feedback loop associated with TGFβ signalling and protein expression may be the mechanism for the renoprotective effect observed. As *Tgfb2*$^{+/-}$ mice exhibit global deficiency in TGFβ2 expression, this conclusion may also explain the similar effects observed in the current study in *Tgfb2*$^{+/-}$ mice fed a chronic high salt.

The importance of 'normal' TGFβ paracrine signalling in the kidney in the presence of a renal insult has recently been highlighted. Gewin et al. (2010) selectively ablated TGFβ type II receptor from the developing and, in turn, mature collecting ducts. As this receptor is critical to the formation of the TGFβ signalling complex, it was hypothesized that a renoprotective effect would be associated with impaired TGFβ signalling. Paradoxically however, renal fibrosis was exacerbated in mice in which the TGFβ type II receptor was absent from collecting ducts. Gewin et al. (2010) concluded that absence of TGFβ type II receptor in the collecting ducts enhanced TGFβ paracrine signalling between epithelial and interstitial cells, potentially enhancing the progression of renal fibrosis. Importantly, while Dahly et al. (2002) and Gewin et al. (2010) observed contrasting phenotypes in the presence of perturbed TGFβ function, both concluded that a greater understanding of the regulation of TGFβ paracrine signalling during renal injury was required. However,

while most studies have focused on the pro-fibrotic attributes of TGFβ isoforms, the mechanism by which decreased TGFβ expression ameliorates elevations in arterial pressure is unknown. Findings by Dahly et al. (2002) strongly agree with the present findings, however while Dahly et al. (2002) targeted all TGFβ isoforms, the present study demonstrated that a similar protective effect on arterial pressure can be achieved through decreasing the expression of TGFβ2 alone. By separating the influence of specific TGFβ isoforms on arterial pressure, greater understanding of their function will be achieved. Therefore, what remains to be known is whether neutralisation of TGFβ2 alone in a Dahl S rat would be sufficient to replicate the protective effect on arterial pressure and renal function previously observed.

4.4.4 Is nephron endowment or TGFβ2 more important for the regulation of arterial pressure?

While the current model of augmented nephron endowment, the *Tgfb2*$^{+/-}$ mouse, has provided insight into the potential protective nature of an augmented nephron endowment on arterial pressure, the previously described studies have highlighted potential issues with the current model. As *Tgfb2*$^{+/-}$ mice exhibit both augmented nephron endowment and decreased TGFβ2 expression, models which separate these key factors are required to better understand how *Tgfb2*$^{+/-}$ mice are protected from a chronic stressor.

4.4.4.1 Suitable models of augmented nephron endowment

A model of augmented nephron endowment which has been characterized using unbiased stereological approaches and does not contain confounding factors such as a global impairment of growth factor signalling is required to investigate the direct role of augmented nephron endowment on the regulation of arterial pressure. Currently only five models of augmented nephron endowment *in vivo*, including *Tgfb2*$^{+/-}$ mice, have been described (see Table 1.2). However, there are several factors limiting their use in the investigation of the significance of high nephron endowment for cardiovascular and renal physiology.

In the first model, Mansano et al. (2007) demonstrated that exposure of pregnant rat dams to periods of dehydration induced a 17% increase in nephron

endowment in offspring. As assessment of nephron number was conducted using a biased morphometric approach, this model requires confirmation using unbiased methods before persevering further. Secondly, vitamin D deficiency during pregnancy and lactation was concluded to increase nephron endowment by 20% in rat offspring. However, while an unbiased stereological approach was utilized, the values reported are questionable, as they do not correlate other studies investigating nephron endowment in Sprague-Dawley rats.

The tActR-II mouse carries a truncated 'dominant-negative' variant of the activin type II receptor and has an 80% augmentation of nephron endowment (Maeshima et al. 2000). However, like *Tgfb2*$^{+/-}$ mice, tActR-II mice exhibit global disruption of TGFβ superfamily signalling, which may confound any data pertaining to cardiovascular and renal physiology. More recently, Sims-Lucas et al. found using gold-standard unbiased stereological techniques that betaglycan$^{+/-}$ mice have a 23% increase in nephron endowment at PN 30 compared to age-matched WT mice (Sims-Lucas 2007). While further characterization of these mice has indicated they are a robust model of augmented nephron endowment (see Chapter 3), the confounding factors of global lifelong deficiency and impaired TGFβ superfamily signalling remain.

Aside from *Tgfb2* and betaglycan heterozygous mice, there is only one other *in vivo* model of augmented nephron endowment that has been characterized appropriately. Lelievre-Pegorier et al. (1998) demonstrated that following intraperitoneal injection of retinoic acid (RA) to pregnant rat dams on e11, nephron endowment was augmented in offspring by 21% at PN14. No other phenotypic changes were observed in offspring of RA-treated mothers. Unfortunately, Lelievre-Pegorier et al. (1998) conducted no mechanistic or functional analysis of the augmented nephron endowment phenotype generated. However, RA has recently been utilized in attempts to enhance and rescue nephron endowment in experimental models susceptible to nephron deficits. Administration of RA at e11.5 to pregnant rat dams fed a low protein diet resulted in offspring with nephron endowment greater than low protein alone, and similar to that of control offspring (Makrakis et al. 2007). A recent study however attempted to recapitulate the augmented nephron endowment observed by Lelievre-Pegorier et al. (1998) in neonatal baboons (Sutherland et al. 2009). However, nephron endowment was similar in the RA-treated and control experimental groups. However, the successful findings of

Lelievre-Pegorier et al. (1998) suggest that further titration and characterization of the ability of RA to induce augmented nephron endowment in murine experimental models is required for the approach to be successfully translated into higher order species. Moreover, the transient period of intervention and manipulation, coupled with phenotypically 'normal' offspring suggests that RA administration during gestation may be an appropriate model in which the role of an augmented nephron number on the regulation of arterial pressure can be investigated.

4.4.4.2 TGFβ2, a target for arterial pressure regulation

A possible mechanism by which arterial pressure is protected in the presence of TGFβ2 deficiency may involve a reduction in renal or systemic fibrosis. Increased perivascular collagen deposition in WT mice fed a chronic high salt diet only, suggests that in the presence of a pathological stressor *Tgfb2*$^{+/-}$ mice may poses an altered renal fibrotic response, which in turn may contribute to protective phenotype observed. Currently, anti-TGFβ2 neutralising agents are in use in experimental models and pre-clinical trials, for the manipulation of fibrosis and wound healing in a variety of organs including the kidney (Hill et al. 2001; Benigni et al. 2003; Bandyopadhyay et al. 2005; Xiao et al. 2009; Bottoms et al. 2010). Renal disease is often associated with elevated blood pressure and the development of cardiovascular disease (Sarnak et al. 2003; Coresh et al. 2004). It has been hypothesized that increased vascular and interstitial fibrosis due to chronic dietary or environmental stressors may act to increase total peripheral resistance, a key factor in the development of hypertension (Briones et al. 2010). Interestingly, administration of an anti-TGFβ1 neutralising antibody to angiotensin-II infused hypertensive or streptozotocin-treated diabetic mice partially ameliorated arterial stiffness (Belmadani et al. 2008). It is therefore possible that disruption of TGFβ2 activity may ameliorate elevations in arterial pressure by preventing fibrosis in the kidney and systemic vasculature. Future studies should focus on whether administration of an anti-TGFβ2 agent to WT mice is sufficient to induce the protective phenotype observed in *Tgfb2*$^{+/-}$ mice in response to a high salt diet. It will also be important to determine whether administration of the anti-TGFβ2 agent is capable of ameliorating elevations in arterial pressure or if the agent must be administered prior to the high

salt diet. The clinical application of such findings could help in the development of pharmaceuticals for the treatment of hypertension and renal disease progression.

4.5 CONCLUSION

In conclusion, augmented nephron endowment in *Tgfb2*$^{+/-}$ mice does not impact baseline arterial pressure or renal function. Consistent with the hypothesis for this study, the high nephron endowment in *Tgfb2*$^{+/-}$ mice was associated with a protective effect on arterial pressure in the presence of a chronic physiological stressor. However, the mechanism by which arterial pressure is protected in *Tgfb2*$^{+/-}$ mice is unclear. The findings of the present study need to be confirmed in another model of high nephron number such as the RA model. In addition, the role of global TGFβ2 deficiency and its association with a protective effect on arterial pressure needs to be fully elucidated as this may identify TGFβ2 as a potential target for therapeutic interventions to regulate arterial pressure, particularly in hypertensive individuals.

CHAPTER 5

EFFECTS OF AN ANTI-TGFβ2 NEUTRALISING ANTIBODY ON TOTAL NEPHRON NUMBER IN THE MOUSE

5.1 INTRODUCTION

Nephron endowment and nephron number vary widely in human kidneys (Section 1.6). Animal studies have demonstrated that dietary, environmental and genetic perturbations can either increase or decrease nephron endowment in offspring (Woods et al. 2004; Hoppe et al. 2007; Singh et al. 2007; Singh et al. 2007; Gray et al. 2008; Sims-Lucas et al. 2009). Currently, the literature is dominated by reports of low nephron endowment, with only five studies reporting augmented nephron endowment *in vivo* (Table 1.2). Of these five studies, the only mouse model in which the kidneys have been analysed using gold-standard stereological approaches are those of *Tgfb2*$^{+/-}$ mice (Sims-Lucas et al. 2008). Sims-Lucas et al. (2008) demonstrated that the kidneys of *Tgfb2*$^{+/-}$ mice contain 60% more nephrons than their wild type littermates (Table 1.3).

TGFβ2 is a multifunctional growth factor previously shown to be critical for the development of the metanephros. In contrast to the observed phenotype in *Tgfb2*$^{+/-}$ mice, *Tgfb2*$^{-/-}$ mutant mice exhibit severe renal dysplasia (Sanford et al. 1997). These opposing phenotypes indicate that the development of the metanephric kidney and the establishment of nephron endowment are sensitive to alterations in the activity or availability of TGFβ2, and suggest direct manipulation of this signalling network during kidney organogenesis may provide an avenue for therapeutic augmentation of nephron endowment.

Manipulation of TGFβ isoform activity for therapeutic means has previously been pursued, though more commonly for the purpose of slowing the progression of adult renal disease. In the adult kidney, TGFβ isoforms (TGFβ1, -β2, -β3) are detectable in mature glomeruli and function to maintain renal homeostasis through the regulation of extracellular matrix (ECM) turnover (MacKay et al. 1990; Bruijn et al. 1994; Wilson et al. 2000; Bottinger and Bitzer 2002). Consistent with this finding, systemic inhibition of TGFβ activity with the natural non-specific TGFβ inhibitor, decorin, limited the accumulation of ECM proteins within glomeruli in an experimental model of glomerulonephritis (Border et al. 1992). Similarly, decreased mesangial matrix production and down-regulation of pro-fibrotic gene expression were observed when a pan-specific anti-TGFβ antibody was administered to rats with streptozotocin-induced diabetic nephropathy (Sharma et al. 1996). Hill et al. (2001) found that neutralisation of TGFβ2 bioactivity through the use of a specific anti-

TGFβ2 neutralising antibody provided protection from the renal pathological changes observed in streptozotocin-induced diabetes. Together these studies indicate that the endogenous activity of TGFβ isoforms can be manipulated through the use of isoform-specific antibodies.

Unlike humans, nephrogenesis in the mouse continues after birth, with cessation of nephrogenesis occurring by PN5 (Kuure et al. 2000; Sims-Lucas et al. 2008). This brief period of postnatal nephrogenesis provides the opportunity to manipulate nephron endowment without the confounding effect of the maternal intrauterine environment (Vize et al. 1997; Kuure et al. 2000; Loria et al. 2007; Saez et al. 2007; Wlodek et al. 2008). The presence of analogous molecular signalling systems during kidney development and disease, coupled with the postnatal window of nephrogenesis in mice, suggests that partial inhibition of TGFβ2 signalling in the developing kidney may augment nephron endowment. In this Chapter, the effect of early postnatal administration of a TGFβ2 neutralising antibody on nephron endowment in the mouse was investigated.

5.2 METHODS

5.2.1 Animal model

All animal handling and experimental procedures were approved in advance by the Monash University Animal Ethics Committee. As described in Section 2.11.1, 6 week old male 129sv mice were mated with 6 week old female C57Bl6 mice to generate hybrid (129sv/C57Bl6) offspring. Hybrid offspring of this strain have previously been shown to be highly robust for the analysis of blood pressure and renal function and therefore were selected for this study to allow for subsequent physiological characterisation should this be warranted (Hoppe et al. 2009). Briefly, to generate offspring two female mice were placed with one male for 4 h, after which female mice were checked for vaginal plugging. When a plug was detected, gestational day 0 was defined. Over the following 21 days, female mice were moved from their home box to a 'secondary' box for 30 min each day to acclimatise to handling and moving. At the end of pregnancy females littered down naturally in their home box.

5.2.2 Intraperitoneal injections of newborn pups

Once the dams had littered down (PN0), they were moved from their 'home' box to their 'secondary' box. The time of littering down, litter size and body weights of all pups were recorded. Pups were then tattooed and randomly allocated to one of four experimental groups: 1) vehicle (saline; n = 13); 2) isotype control antibody (IgG; R&D Systems; n = 8); 3) 5μg/g body weight; or 4) 10 μg/g body weight anti-TGFβ2 neutralising antibody (n = 11 for each experimental group; R&D Systems). CAT: AB-112-NA anti-TGFβ2 antibody was selected for this study due to its high specificity for TGFβ2 protein (Tsang et al. 1995). This antibody effectively neutralises TGFβ2 biological activity *in vitro* at a concentration of 1μg/ml, and has a 100-fold higher affinity for TGFβ2 than the other TGFβ isoforms. A total of eight litters were used in the study, with each litter represented in each experimental group. Intraperitioneal (ip) injections were performed once daily for four days from PN0 – 3 as described in Section 2.11.2. Pups were allowed to remain with their mother in the 'home' box, being monitored and weighed daily until PN14.

5.2.3 Tissue collection

At PN14, pups were euthanized via cervical dislocation and tissues were collected as described in Section 2.3.4. Right kidneys were processed for embedding in GMA as described in Section 2.4.1. Left kidneys and remaining tissues were processed for embedding in paraffin wax.

5.2.4 Sectioning and ataining

Due to the small size of kidneys at PN14 (~ 60 mg), tissues embedded in GMA were exhaustively sectioned at 15 μm using a Leica RM2165 microtome (Leica Microsystems). In accordance with the stereology protocol described in Section 2.4.2, the first section was randomly selected in the interval 1 to 10 using a random number table. Thereafter, every tenth (reference) and eleventh ('look up') section was floated on a cold water bath, mounted on glass slides, dried on a 90°C hot plate and stained with PAS (Section 2.12.2).

5.2.5 Histological analysis

Paraffin-embedded kidney sections (5 μm) were dewaxed and stained with haematoxylin and eosin (Section 2.12.2), Gomori's one-step trichrome stain (Section 2.12.3) or picrosirius red (Section 2.12.4). Images were obtained with the aid of an Olympus Provis epifluorescence microscope fitted with a Leica DC digital camera (Leica Microsystems Ltd).

5.2.6 Stereology

Total glomerular (nephron) number and kidney volumetric parameters were estimated using the physical disector/fractionator combination and the Cavalieri principle as described in Section 2.4. Kidney volume (V_{kid}) was estimated using the Cavalieri principle (Gundersen and Jensen 1987) with the formula:

$$V_{kid} = 2 \times 10 \times t \times a(p) \times P_s$$

Where:

2 is the inverse of the slice sampling fraction,

10 is the inverse of the section sampling fraction,

t is average section thickness (0.0015 mm),

a(p) is the area associated with each grid point on the microfiche grid following adjustment for magnification of 24.25 (1.5304 mm^2), and

P_s is the total number of grid points overlying the kidney in the first section of each pair of sections.

To estimate total glomerular number, mean glomerular and renal corpuscle volumes, paired sections were placed on two Olympus BX50F4 light microscopes fitted with projection arms. Every tenth (reference) section was placed on a motorised stage (Autoscan System) on the right microscope, whilst every eleventh ('look up') section was placed on a manually rotating stage on the left microscope. Images were projected at a final magnification of 298X on to a table with a stereological point grid (20 mm x 20mm grid with 64 points). Grid points overlying kidney (P_{kid}), glomeruli (P_{glom}), renal corpuscles (P_{corp}), as well as glomeruli present and no longer present in a section (Q^-), in all kidney sections used for counting, were counted as described in Section 2.4.3. The total number of glomeruli per kidney (N_{glom}) was determined using the following formula:

$$\mathbf{N_{glom,\,kid} = 10 \times (P_s / P_f) \times (1 / 2\ FA) \times Q^-}$$

Where:

10 is the reciprocal of the section sampling fraction,

P_s is the total number of grid points overlying the kidney sections, both complete and incomplete,

P_f is the total number of grid points overlying only the complete sections,

1 / 2 FA is the fraction of the total section area used to count glomeruli, and

Q^- is the combined values of Q^-_L and Q^-_R giving the actual number of glomeruli counted.

Mean glomerular volume (V_{glom}), mean renal corpuscle volume (V_{corp}), total glomerular volume ($V_{glom,kid}$) and total renal corpuscle volume ($V_{corp,kid}$) were estimated as described in Section 2.4.3.

5.2.7 Statistical analysis

Growth charts were analysed using a Two-way repeated measures ANOVA followed by Tukey's post-hoc analysis, while all remaining data were analysed using a One-way ANOVA followed by Tukey's post-hoc test. These statistical tests were performed using GraphPad Prism™ 5 (GraphPad Software Inc). Values are presented as mean ± standard deviation (SD). A probability $p<0.05$ was accepted as statistically significant.

5.3 RESULTS

5.3.1 Pup growth and survival was not affected by antibody administration

Daily ip administration of saline (vehicle), control antibody (IgG) or anti-TGFβ2 neutralising antibody (anti-TGFβ2) from PN0 – P3 did not affect survival of mouse pups (Table 5.1). Furthermore, body weights of mice in the four groups were similar throughout the study (Figure 5.1), and body dimensions at the completion of experimentation (Table 5.2) were also similar in the four groups. At PN14, the absolute and relative (to body weight) wet weights of the heart, lungs, and left and right kidneys were also similar in the four groups (Table 5.2).

Table 5.1: Survival rate of neonatal pups in the four treatment groups.

Experimental Group	Injected / Survived
Vehicle	12 / 13
IgG	8 / 8
5 μg / g Anti-TGFβ2 antibody	11 / 11
10 μg / g Anti-TGFβ2 antibody	11 / 11

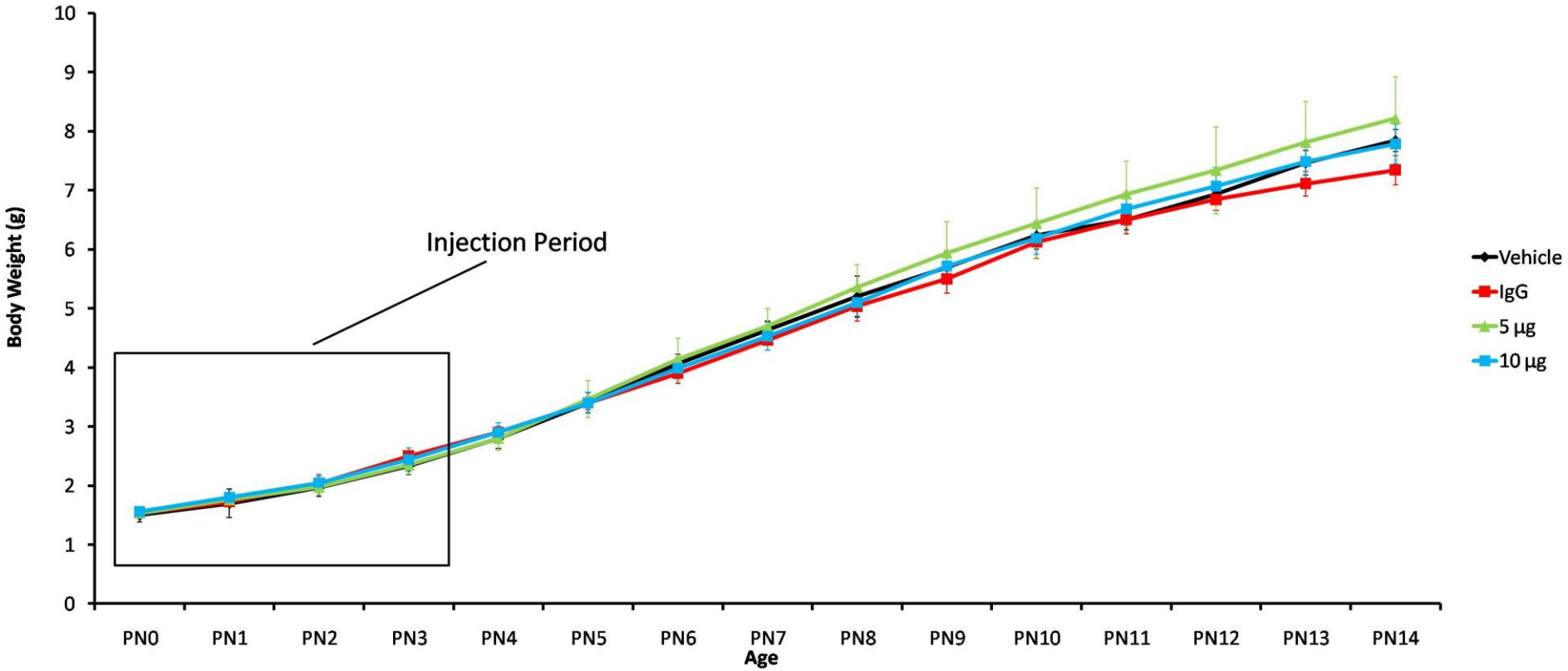

Figure 5.1: Growth of mice during and following neonatal intraperitoneal injections. No significant differences in mouse pup body weight were observed between experimental groups at any time point. Values are presented as mean ± S.D. (n) = Vehicle (12), IgG (8), 5µg/g anti-TGFβ2 neutralising antibody (11) and 10µg/g anti-TGFβ2 neutralising antibody (11). Analysis via a two-way repeated measures ANOVA followed by Tukey's post-hoc analysis.

Table 5.2: Body dimensions and organ weights of mice at postnatal day 14.

	Vehicle	IgG	5μg/g TGFβ2 antibody	10μg/g TGFβ2 antibody	*p*
Body Weight (g)	7.85 ± 0.16^{ab}	7.56 ± 0.30^{a}	8.12 ± 0.62^{bc}	7.81 ± 0.30^{abc}	0.3
Crown-Rump Length (cm)	5.52 ± 0.26^{a}	5.66 ± 0.21^{a}	5.45 ± 0.24^{a}	5.55 ± 0.29^{a}	0.3
Thoracic Girth Length (cm)	1.95 ± 0.17^{a}	1.91 ± 0.19^{a}	2.05 ± 0.19^{a}	1.98 ± 0.13^{a}	0.4
Head-Snout Length (cm)	1.94 ± 0.12^{a}	1.91 ± 0.08^{a}	2.06 ± 0.15^{a}	2.03 ± 0.16^{a}	0.1
Left Kidney Wt (mg)	59.9 ± 4.1^{ab}	61.1 ± 3.1^{ab}	65.0 ± 7.5^{b}	58.5 ± 4.3^{ac}	0.3
LK / BW (mg/g)	7.63 ±0.48^{a}	8.01 ±0.57^{a}	8.00 ±0.67^{a}	7.49 ±0.49^{a}	0.1
Right Kidney Wt (mg)	62.4 ± 5.5^{a}	64.9 ± 3.0^{a}	68.0 ± 8.7^{a}	61.5 ± 6.0^{a}	0.1
RK / BW (mg/g)	7.95 ± 0.67^{a}	8.59 ± 0.57^{a}	8.36 ± 0.75^{a}	7.88 ± 0.67^{a}	0.1
Total Kidney Wt (mg)	122.3 ± 8.5^{ab}	126.0 ± 5.3^{ab}	133.0 ± 15.8^{bc}	120.0 ± 9.0^{ac}	0.3
TKW / BW (mg)	15.6 ± 1.0^{a}	16.7 ± 1.1^{a}	16.4 ± 1.3^{a}	15.4 ± 1.0^{a}	0.2
Heart Wt (mg)	59.4 ± 4.4^{ab}	55.9 ± 4.1^{ab}	63.2 ± 7.7^{bc}	56.1 ± 6.5^{ac}	0.3
Heart / BW (mg/g)	7.58 ± 0.55^{a}	7.41 ± 0.72^{a}	7.80 ± 0.90^{a}	7.21 ± 1.00^{a}	0.4
Lung Wt (mg)	117.5 ± 27.1^{a}	109.3 ± 5.2^{a}	109.3 ± 18.6^{a}	123.4 ± 33.1^{a}	0.5
Lung Wt / BW (mg/g)	15.0 ± 3.5^{a}	14.5± 1.0^{a}	13.5 ± 2.10^{a}	15.8 ± 4.3^{a}	0.4
N	12	8	11	11	

LK/BW indicates left kidney to body weight ratio, RK/BW indicates right kidney to body weight ratio, TKW / BW indicates total kidney to body weight ratio, Values are mean ± S.D. Analysed using One-way ANOVA followed by a Tukey's post-hoc test. Those groups not sharing a common letter are significantly different (p<0.05).

5.3.2 Nephron number was unaltered by administration of TGF-β2 antibody

At PN14, total nephron number in mouse pups administered 5 μg/g or 10 μg/g body weight of TGFβ2 neutralising antibody was 12787 ± 677 and 12440 ± 414, respectively. These values were not significantly different to nephron numbers in both vehicle (12708 ± 534) and IgG control (12474 ± 529) mice (Figure 5.2A).

5.3.3 Effect of the TGF-β2 neutralising antibody on kidney and glomerular size

No significant differences were observed in either kidney volume or mean and total glomerular and renal corpuscle volumes at PN14 between mice which received ip injections of vehicle, IgG or 5 μg/g body weight of the TGFβ2 neutralising antibody (Figure 5.2B-F). However, mice that received 10 μg/g body weight of anti-TGFβ2 had smaller kidneys (17%; p = 0.041) than mice that received vehicle (Figure 5.2B). These mice that received 10 μg/g body weight of TGFβ2 neutralising antibody also had larger mean glomerular (15%; p = 0.004) and renal corpuscle volumes (14%; p = 0.003; Figure 5.2C, D). These changes resulted in larger total glomerular (12%; p = 0.003) and total renal corpuscle volumes (11%; p = 0.002) when compared to mice that received ip injections of vehicle (Figure 5.2E, F).

5.3.4 Renal histology was not changed by administration of TGF-β2 antibody

Renal histology at PN14 was similar in the four experimental groups (Figures 5.3 – 5.5). There was no evidence of glomerular, tubular, interstitial or vascular changes in any of the kidneys.

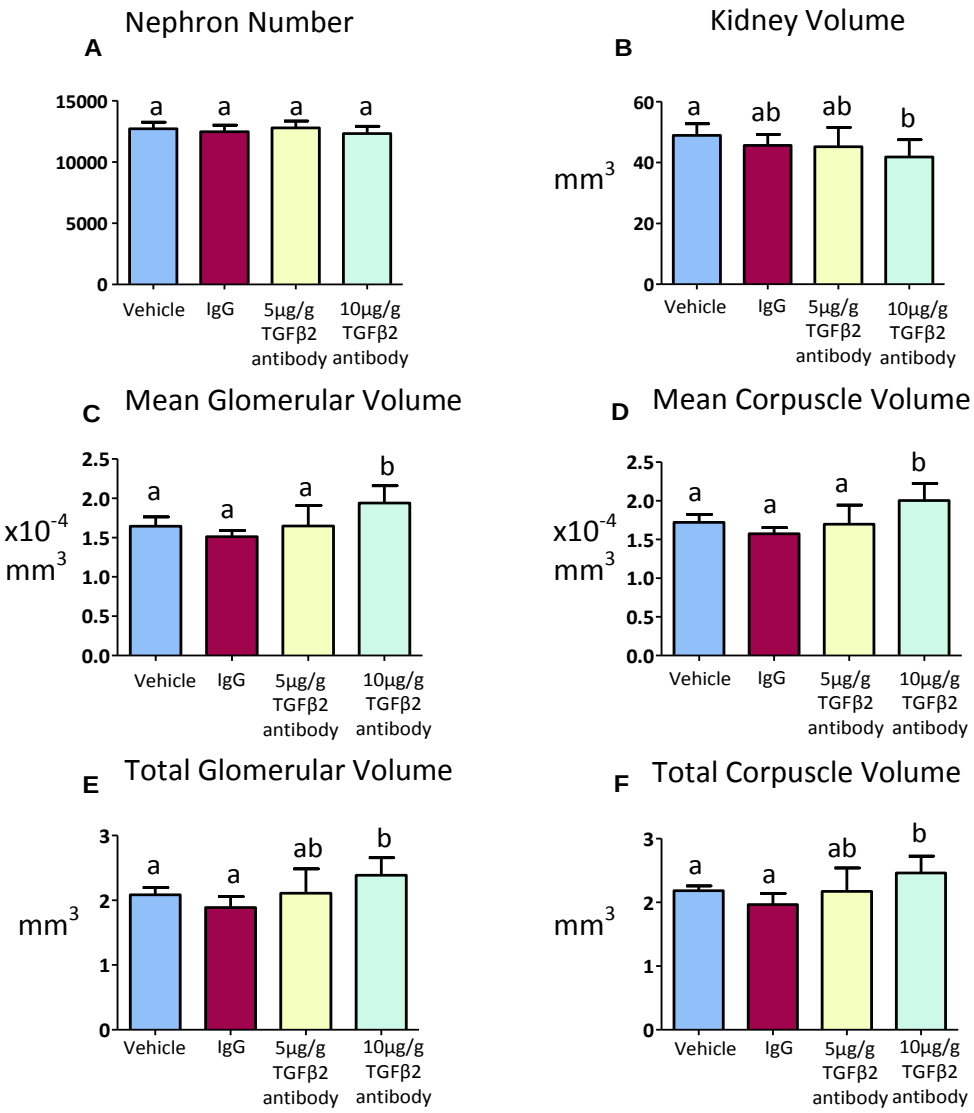

Figure 5.2: Stereological data for PN14 kidneys from each of the four treatment groups. (A) Total nephron endowment, (B) total kidney volume, (C,E) mean and total glomerular volumes, (D, F) mean and total renal corpuscle volumes in mice at PN14 following intraperitoneal injections of vehicle, IgG, 5µg/g anti-TGFβ2 neutralising antibody or 10µg/g body weight anti-TGFβ2 neutralising antibody. (n) = Vehicle (9), IgG (7), 5µg/g anti-TGFβ2 neutralising antibody (5) and 10µg/g anti-TGFβ2 neutralising antibody (8). Values are mean + S.D. Analysis via One-way ANOVA followed by a Tukey's post-hoc test. Those groups not sharing a common letter are significantly different (p<0.05).

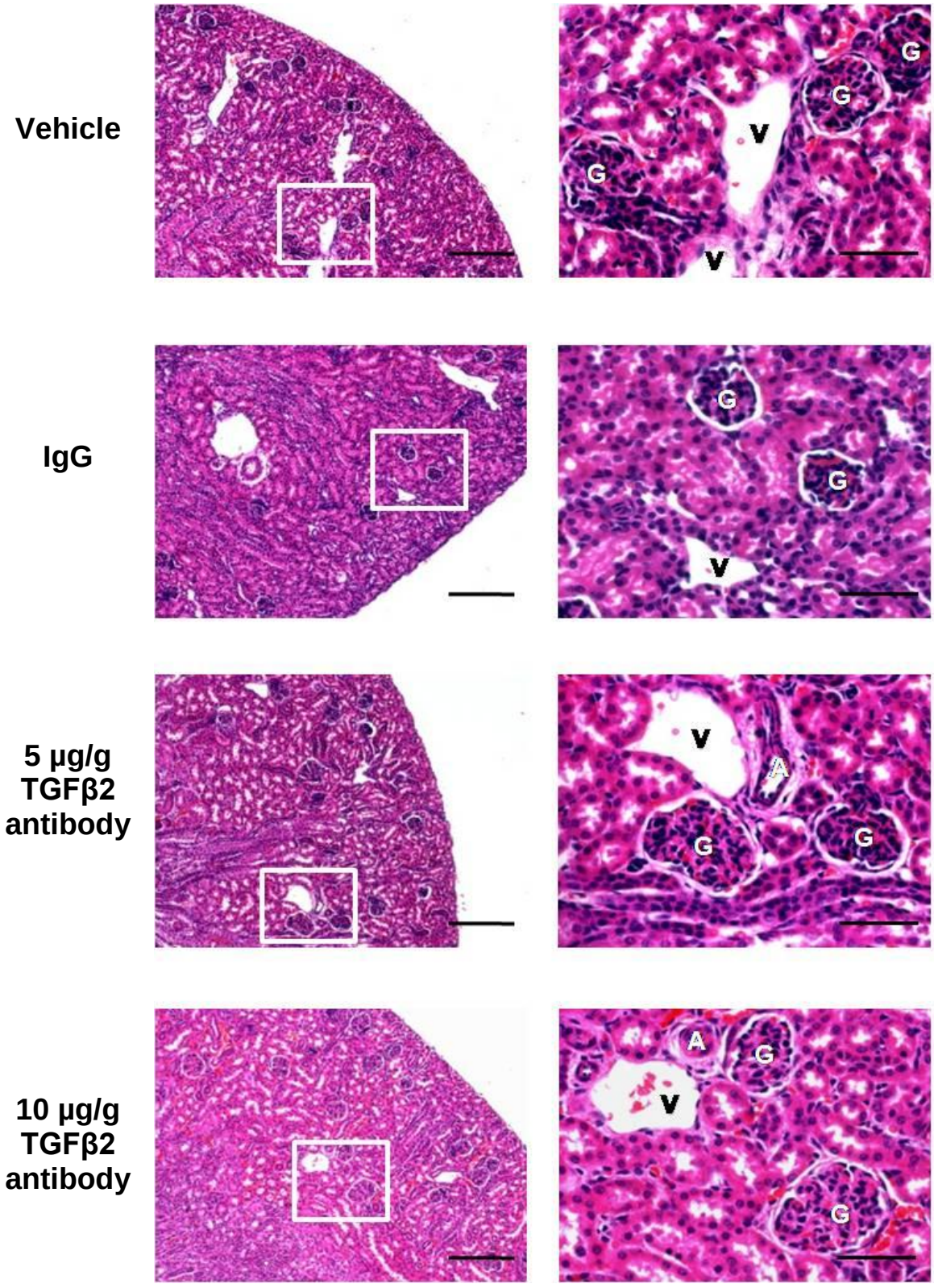

Figure 5.3: Photomicrographs of PN14 kidney sections stained with haematoxylin and eosin. Renal histology was similar in all experimental groups at PN14. (A) artery, (G) glomerulus, (V) vein; scale bar: Left panels = 100µm; Right panels = 50µm.

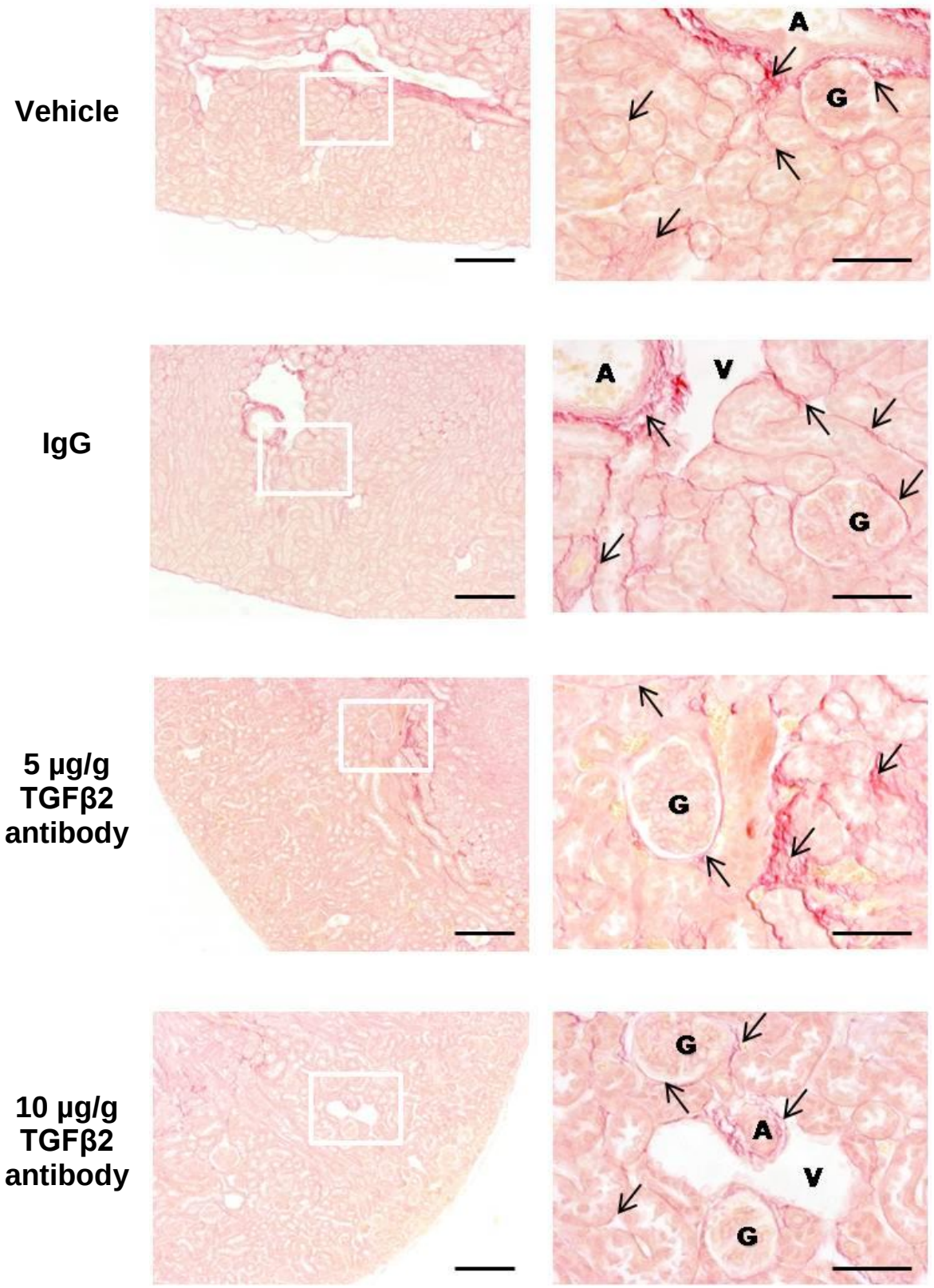

Figure 5.4: Photomicrographs of PN14 kidney sections stained with picrosirius red. Collagen deposition was similar in all four experimental groups at PN14. Arrows indicate collagen deposition, (A) artery, (G) glomerulus, (V) vein; scale bar: Left panels = 100µm; Right panels = 50µm.

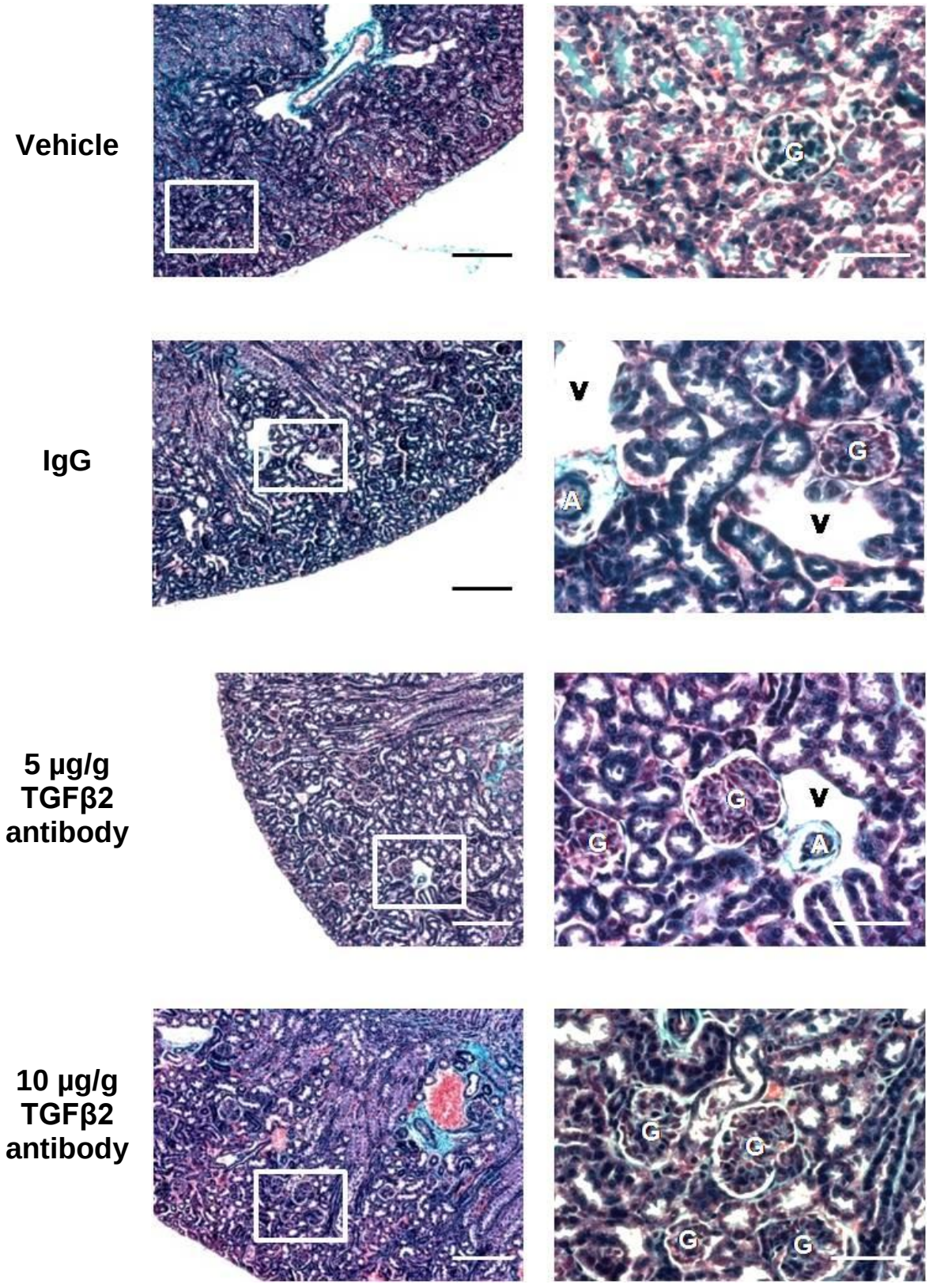

Figure 5.5: Photomicrographs of PN14 kidney sections stained with Gomori's One-Step Trichrome. No differences in ECM deposition were observed between the four experimental groups at PN14. (A) artery, (G) glomerulus, (V) vein; scale bar: Left panels = 100µm; Right panels = 50µm.

5.4 DISCUSSION

TGFβ2 is a potent negative regulator of kidney development and has been shown to regulate nephron endowment (Ritvos et al. 1995; Sanford et al. 1997; Sims-Lucas et al. 2008). Complete ablation of TGFβ2 in *Tgfb2*$^{-/-}$ mice results in dysplastic ureteric branching morphogenesis *in vitro* and renal dysgenesis (Sanford et al. 1997; Oxburgh et al. 2004; Sims-Lucas et al. 2008). Conversely, *Tgfb2*$^{+/-}$ mice exhibit increased ureteric branching morphogenesis and 60% augmentation in total nephron number at PN30 compared to wild type littermates (Sims-Lucas et al. 2008). The aim of the experiments described in this Chapter was to determine if administration of an anti-TGFβ2 neutralising antibody during a period of active nephrogenesis could augment nephron endowment in wildtype mice. The major findings were: (1) nephron number was unchanged following administration of the TGFβ2 neutralising antibody; and (2) administration of the higher concentration (10μg/g body weight) of TGFβ2 neutralising antibody increased glomerular and renal corpuscle volumes while decreasing total kidney volume.

5.4.1 Nephron number in mice receiving anti-TGFβ2 neutralising antibody is normal

The neonatal period of metanephric development selected for experimentation in the present study has previously been shown to be an important period in the establishment of nephron endowment. At birth the normal mouse kidney contains approximately 8000 formed nephrons (Cebrian et al. 2004), which is approximately 65% of the nephron endowment observed in adult mice (Cullen-McEwen et al. 2003) and vehicle-treated mice at PN14 in the present study. The importance of the neonatal period in the establishment of nephron endowment in rodents has been demonstrated by several groups (Loria et al. 2007; Saez et al. 2007; Wlodek et al. 2008). Wlodek et al. (2008) found that an adverse lactational environment in rats resulted in postnatal growth restriction and a 27% reduction in nephron endowment. Further, Salazar and colleagues have shown that administration of an angiotensin II receptor antagonist to rat pups during the neonatal nephrogenic period induced a subsequent 37% reduction in nephron

number (Saez et al. 2007). These findings demonstrate the developmental plasticity of the developing metanephros, at least in terms of nephrogenesis, in this early neonatal period. A major advantage of studies aimed at manipulating nephrogenesis and nephron endowment in the early neonatal period is that complications associated with administering an agent (the anti-TGFβ2 neutralising antibody in this case), to the pregnant mother is removed. Such complications include issues associated with crossing the placental barrier and dosage to the foetus.

In the present study, administration of an anti-TGFβ2 neutralising antibody to wild type mice at two doses during postnatal nephrogenesis did not alter nephron endowment. This lack of effect may be due to multiple factors. First, the timing of antibody administration is likely an important factor. While the plasticity of nephrogenesis in the early postnatal period was demonstrated by Wlodek et al. (2008) and Saez et al. (2007), these studies were performed in rats which demonstrate a longer period of neonatal nephrogenesis than mice. Other studies have suggested that the early stages of nephrogenesis are more susceptible to environmental manipulation, while some stages appear more resistant. For example, Ortiz et al. (2001) reported that 48 hour administration of dexamethasone to pregnant rats at e15.0 and e17.0, lead to a 30% and 20% nephron deficit respectively, whereas administration on days e11.0, e13.0, e19.0 or e20.0 had no effect on nephron endowment. Interestingly, this period of sensitivity observed by Ortiz et al. (2001) coincides with the induction of ureteric budding and early nephrogenesis. These findings suggest that future studies with the aim of augmenting nephron endowment should explore multiple periods of nephrogenesis. Optimal timing may well vary depending on the species under investigation as well as the agent being tested to augment nephron endowment.

A second possible reason for why the TGFβ2 neutralising antibody did not augment nephron endowment in the present study concerns the route of antibody administration, namely intraperitoneal injection. This route of administration raises the issue of how much antibody actually reached the developing foetal kidneys. Previous studies have successfully directed a TGFβ1 neutralising antibody to the neonatal rat kidney at PN3 through injections into the suprarenal aorta (Liu et al. 1999). While this approach provides a more direct route to the kidney, it has not previously been employed in neonatal mice due mainly to the size difference between

PN3 rat pups (body weight of ~7 g) and PN0 mouse pups (body weight of ~1.3 g). Issues of pup size, surgical success and maternal rejection of pups would likely limit the efficacy of this approach in mice.

A third issue is the concentration of neutralising antibody required to achieve TGFβ2 neutralisation. Concentrations of 5 μg/g and 10 μg/g body weight of anti-TGFβ2 were used in the present study, in accordance with previous studies showing that 5 μg/g of anti-TGFβ2 was sufficient to neutralise 100% of biologically active TGFβ2 protein *in vitro* (Tsang et al. 1995). As *in vitro* and *in vivo* systems are vastly different, and given the issue of route of administration discussed above, the present study also employed a concentration of 10 μg/g body weight of anti-TGFβ2. Similar concentrations of anti-TGFβ2 neutralising agents have previously been used to successfully neutralise TGFβ2 activity in the kidney *in vivo* (Hill et al. 2001; Juarez et al. 2007). Also, previous studies have indicated that to sufficiently neutralise TGFβ2 activity, ip injections must be performed at least once every 2 days during the selected injection period. However, due to the window of neonatal nephrogenesis in mice being brief, daily ip injections were used in the present study. The observed effects of 10 μg/g of the antibody on renal and glomerular volumes suggest this concentration is effectively influencing kidney development. Clearly, further optimisation of the *in vivo* protocol characterising antibody stability *in vivo*, neutralisation half-life, and antibody clearance are required to fully analyse the effects of partial TGFβ2 neutralisation on kidney development.

Finally, while neutralising antibodies have been successfully utilised in other systems to neutralise the function of TGFβ2 (Sharma et al. 1996; Hill et al. 2001; Mead et al. 2003; Elvers et al. 2005), ligand sequestration also shows significant potential as an alternative approach for inhibiting the biological function of TGFβ2. The type III TGFβ receptor, betaglycan, binds all TGFβ isoforms but displays highest binding affinity for TGFβ2 (Bandyopadhyay et al. 2002). A soluble form of betaglycan has previously been adopted to sequester TGFβ2 ligand in the kidney to limit the progression of renal fibrosis in a model of diabetes (Esparza-Lopez et al. 2001; Juarez et al. 2007). Intraperitoneal administration of soluble betaglycan to 8 week old *db/db* diabetic mice attenuated renal structural damage. Betaglycan administration was associated with significant decreases in the mRNA expression of all three TGFβ isoforms, COL4A1 and fibronectin (Juarez et al. 2007). These data correlate strongly

with the phenotypic changes previously discussed in regards to the administration of pan-TGFβ and TGFβ2-specific neutralising antibodies to diabetic phenotypes (Hill et al. 2000; Benigni et al. 2003; Gagliardini and Benigni 2006), suggesting a viable alternative agent to neutralising antibodies.

5.4.2 Anti-TGFβ2 neutralising antibody alters glomerular and kidney volumes

An unexpected finding from the present study was that administration of the higher dose of TGFβ2 neutralising antibody (10 μg/g body weight) during the brief period of postnatal nephrogenesis resulted in increases in glomerular and renal corpuscle volumes, and a decrease in kidney volume. In contrast to kidney volume, kidney weight was not altered by TGFβ2 neutralising antibody administration. This disparity between findings for wet kidney weight and fixed and embedded kidney volume may be due to the level of kidney hydration at weighing, or possibly the effects of tissue processing for embedding in glycolmethacrylate. Increased glomerular and renal corpuscle volumes in mice administered the highest concentration of TGFβ2 antibody may be due to altered TGFβ regulation of angiogenesis and ECM remodelling as now discussed.

5.4.2.1 TGFβ and endothelial cells

TGFβ isoforms have been previously implicated as critical regulators of angiogenesis in both normal and neoplastic tissues (Yang and Moses 1990; Dickson et al. 1995; Liu et al. 1999; Bandyopadhyay et al. 2002; Holifield et al. 2004; Ferrari et al. 2009). Recently, TGFβ1 was implicated as the predominant isoform stimulating the growth and migration of endothelial cells (Ferrari et al. 2009). In the kidney, neutralisation of TGFβ1 during postnatal nephrogenesis in rats delays vascularisation of glomerular tufts through the inhibition of endothelial cell migration (Liu et al. 1999). Previously, angiogenesis and cellular migration have been shown to require expression of multiple TGFβ isoforms at specific concentrations for normal development (Holifield et al. 2004). In the functional absence of an isoform, such as TGFβ2, local renal paracrine TGFβ signalling may be disrupted and result in upregulated expression of TGFβ1 to compensate for the loss of activity (Bottinger 2007; Gewin et al. 2010). This upregulation of a potent angiogenic promoter may

have facilitated the augmented glomerular volumes observed in mice receiving 10 μg/g body weight of anti-TGFβ2 neutralising antibody. To further explore this hypothesis, analyses of glomerular cellular populations including absolute and relative cellular numbers and glomerular capillary length (Guo et al. 2005), total collagen levels within the tissue (Cochrane et al. 2005), endothelial cell proliferation and TGFβ isoform expression following antibody treatment would need to be undertaken.

5.4.2.2 TGFβ and ECM remodelling

Considering evidence from previous studies focusing on the role of TGFβ signalling in ECM remodelling, increased glomerular volume following anti-TGFβ2 antibody administration is an unexpected finding. As mentioned previously, all TGFβ isoforms are present in mature glomeruli, with TGFβ1 and TGFβ2 both shown to be critical in maintaining renal homeostasis through the regulation of ECM (MacKay et al. 1990; Bruijn et al. 1994; Wilson et al. 2000; Bottinger and Bitzer 2002). The influence of TGFβ isoforms on ECM remodelling has become a major research focus in recent years due to the potential for treating diseases such as asthma, renal disease and wound healing (Wright et al. 2000; Gagliardini and Benigni 2006; Gagliardini and Benigni 2007; Xiao et al. 2009; Bottoms et al. 2010). In the kidney, neutralisation of TGFβ isoforms has previously been shown to alter renal volume (Sharma et al. 1996; Hill et al. 2001). Administration of either a 'pan-TGFβ specific' neutralising antibody, directed against all TGFβ isoforms or a specific TGFβ2 neutralising antibody partially attenuated diabetic-induced renal hyperplasia. Administration of the pan-specific TGFβ neutralising antibody also significantly decreased mRNA transcripts for the profibrotic factors fibronectin and collagen type IV alpha 1 (*COL4A1*) as well as TGFβ1 and TGFβ type II receptor mRNAs in diabetic mice (Sharma et al. 1996). The authors concluded that attenuation of renal hyperplasia was directly linked to the reduction of TGFβ signalling and in turn ECM deposition. Furthermore, Hill et al. (2001) showed that specific targeting of TGFβ2 during the initial stages of kidney disease can greatly impact renal volume and ECM deposition. Again using a model of streptozotocin-induced diabetes, anti-TGFβ2 neutralising antibody infused via a jugular vein catheter was shown to inhibit increases in total renal volume and renal

expression of procollagen-1 protein previously attributed to the onset of diabetes. In contrast, in the present study, histological analysis revealed no differences in the amount or distribution of ECM in kidneys or glomeruli from the four experimental groups. It must be noted, however, that longer term studies may be required to produce alterations in ECM deposition. In addition, more sensitive assays such as studies of gene and protein expression and measurement of collagen deposition may be required to detect ECM accumulation (Mimura et al. 2010).

5.5 CONCLUSION

In conclusion, administration of a TGFβ2 neutralising antibody during an active period of nephrogenesis did not augment nephron endowment at PN14 in wildtype mice. However, mean and total glomerular volumes were increased in mice administered the highest concentration of the antibody. Given the importance of TGFβ2 dosage in kidney development and in the regulation of nephron endowment, and the possible therapeutic benefits of nephron number rescue in foetuses at risk of being born with a nephron deficit, future studies are warranted. These studies must take into consideration such technical issues as the nature of the agent (neutralising antibody, soluble betaglycan, other), the timing of administration, agent concentration and route of administration.

CHAPTER 6

GENERAL DISCUSSION

6.1 SUMMARY OF MAJOR FINDINGS

The developmental regulation of nephron endowment has been widely investigated through the use of animal models. Most studies have involved perturbations to metanephric development in order to understand the role of specific environmental or genetic factors (see Tables 1.1 and 1.2), and the predominant phenotype generated has been low nephron endowment, after which cardiovascular and/or renal function was characterised. These experimental approaches have provided a wealth of data on the development and functional role of low nephron endowment in health and disease. However, very little is known about high nephron endowment phenotypes from either developmental or functional perspectives.

This thesis addressed three separate but not mutually exclusive concepts regarding kidneys with high nephron endowment: 1) how does high nephron endowment develop?; 2) what are the functional consequences of a high nephron endowment?; and 3) can the present findings be used as a basis for designing a therapeutic approach for augmenting nephron endowment?

The findings from this thesis have firstly highlighted that TGFβ signalling is critical for early kidney development and thereby the establishment of nephron endowment. Perturbed TGFβ signalling in betaglycan mutant mice was found to result in either renal hypoplasia (betaglycan$^{-/-}$ embryos) or augmented nephron endowment (betaglycan$^{+/-}$ embryos). Coupled with previous data characterising renal development in *Tgfb2* mutant mice (Sims-Lucas et al. 2008), these data suggest that the TGFβ2 signalling pathway is critical not only for the establishment of nephron endowment but overall metanephric development.

Secondly, findings from this thesis demonstrate that augmented nephron endowment does not influence baseline renal function or arterial pressure, at least in the *Tgfb2*$^{+/-}$ model. However, the augmented nephron number in this model was associated with a protective effect on arterial pressure in the presence of a chronic stressor. Arterial pressure and renal functional responses to water deprivation and an acute period of a high salt diet were similar in wildtype and *Tgfb2*$^{+/-}$ mice. However, when fed a chronic high salt diet, wildtype mice exhibited a 19.4 mmHg elevation in MAP from baseline, as well as increased perivascular collagen deposition. In contrast, *Tgfb2*$^{+/-}$ mice fed a chronic high salt diet exhibited only a 4.2 mmHg

increase in MAP compared with control mice, and had normal renal histology. Together, these data indicate that a high nephron number is not detrimental to basal cardiovascular and renal function, and appears to be a beneficial phenotype in the presence of chronic stressors. Also, this study has highlighted the potential of TGFβ2 as a therapeutic target for antihypertensive treatments.

Finally, based on the findings discussed above, an attempt was made to augment nephron endowment in the developing kidney. Although administration of an anti-TGFβ2 neutralising antibody during postnatal nephrogenesis was unsuccessful in generating an augmented nephron phenotype, total glomerular volumes were altered by antibody administration. The approach developed provides a model upon which future studies can be based.

6.2 HOW DOES A HIGH NEPHRON ENDOWMENT DEVELOP?

This thesis has shown that betaglycan, an accessory TGFβ superfamily receptor, is expressed throughout early stages of metanephric development and that perturbation of betaglycan expression levels can result in varying metanephric phenotypes (Figure 6.1). Complete ablation of betaglycan, as highlighted by betaglycan$^{-/-}$ mice (Stenvers et al. 2003), did not alter the induction of ureteric budding. However, ureteric branching morphogenesis was significantly decreased and, in turn, renal hypoplasia with an accompanying nephron deficit was evident at e15.5. In contrast, betaglycan$^{+/-}$ mice exhibited accelerated ureteric branching morphogenesis, which was detected directly following ureteric bud invasion of the metanephric mesenchyme. This early phenotype may underlie the augmented nephron endowment observed at e15.5. These findings correlate strongly with a previous study in which antisense oligonucleotides were utilised to down-regulate betaglycan expression in lung explants resulting in a dose-dependent augmentation of branching morphogenesis (Zhao et al. 1998). Together these data demonstrate a conserved developmental pathway for the regulation of epithelial branching morphogenesis, in which reduced expression of betaglycan stimulates branching.

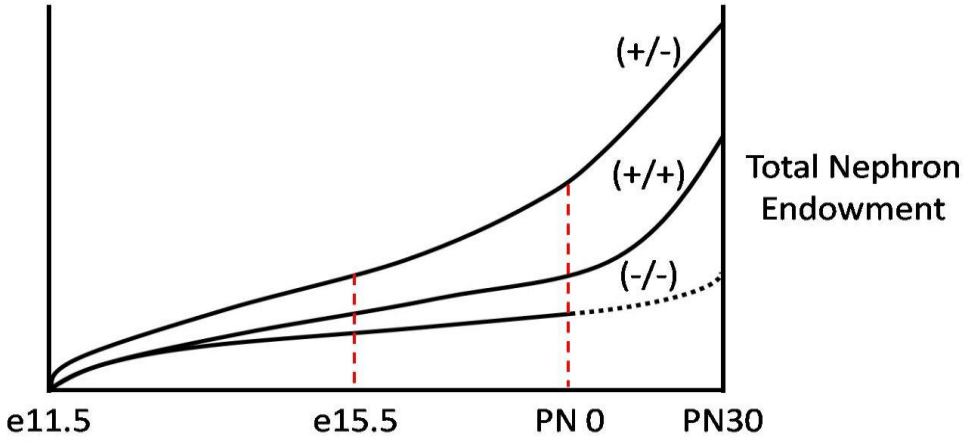

Figure 6.1: Theoretical model of metanephric development in wildtype (+/+), betaglycan heterozygous (+/-) and betaglycan null (-/-) offspring. All genotypes commence metanephric development at the same time point. Early changes in the developmental trajectory appear to give rise to adult phenotypes of nephron endowment. Betaglycan$^{+/-}$ offspring exhibit accelerated ureteric branching morphogenesis and metanephric development following initial ureteric budding. Betaglycan$^{-/-}$ metanephroi initially exhibit comparable development to wildtype metanephroi, however this is not maintained.

6.2.1 Disrupted TGFβ superfamily signalling may underpin the renal phenotypes in betaglycan$^{+/-}$ and betaglycan$^{-/-}$ mice.

Betaglycan$^{+/-}$ and betaglycan$^{-/-}$ metanephroi showed marked reductions in *Tgfb1* and *Tgfb2* mRNA expression, however this was only evident from e13.5. Interestingly, while *Tgfb1* expression profiles were similar in both mutants, a greater reduction in *Tgfb2* was observed in betaglycan$^{-/-}$ metanephroi. These findings agree with those from previous lung culture experiments in which down-regulation of betaglycan expression induced a reduction in endogenous paracrine signalling of TGFβ isoforms (Zhao et al. 1998). The distinct dysregulation of TGFβ isoforms and the onset of phenotypic abnormalities such as altered metanephric volume and impaired branching morphogenesis at the same time point, suggest that the mechanism driving the renal phenotype in betaglycan mutant mice is linked with insufficient TGFβ2 expression. While deficiency in TGFβ2 alone is a possible mechanism, a disruption of the ratio of TGFβ isoforms, particularly TGFβ1:TGFβ2, has also been shown to perturb tissue development (Holifield et al. 2004). However, while this hypothesis reconciles developmental differences between betaglycan$^{+/-}$

and betaglycan$^{-/-}$ metanephroi at later stages of development, the mechanism driving initial differences remains unclear. An example of these initial differences is that a reduction in betaglycan expression in betaglycan$^{+/-}$ embryos was associated with accelerated ureteric branching morphogenesis following ureteric bud invasion, yet total ablation of betaglycan in betaglycan$^{-/-}$ embryos was associated with normal ureteric branching at the same stage. It is possible that further analysis of local TGFβ signalling networks and intracellular signalling may indicate a potential molecular mechanism. However, TGFβ isoform mRNA levels were first found to be altered in mutant metanephroi from e13.5. The branching promoter, *Gdnf*, a distant member of the TGFβ superfamily also appears to be a candidate factor in the development of both phenotypes, as significant changes in *Gdnf* mRNA expression were observed in betaglycan$^{+/-}$ and betaglycan$^{-/-}$ metanephroi from e12.5 and e13.5, respectively.

6.2.2 A new model of augmented nephron endowment

The current study has highlighted the requirement of stringent molecular regulation during metanephric development to achieve a 'normal' kidney. Dysregulated betaglycan expression initiated a chain of events leading to dramatic phenotypic changes. The highly plastic nature of the developing kidney means that alterations in only a handful of key regulatory factors can have a dramatic impact on the final phenotype. The opposing renal phenotypes in betaglycan$^{+/-}$ and betaglycan$^{-/-}$ mice also demonstrated the importance of dose-dependent responses in kidney development. Also, concurrent morphological and stereological examination of betaglycan$^{+/-}$ metanephroi has lead to the characterisation of a new model of augmented nephron endowment. While previous stereological analysis of PN 30 wildtype and betaglycan$^{+/-}$ kidneys identified a 23% increase in nephron endowment in betaglycan$^{+/-}$ at PN30 (Sims-Lucas 2007), the current study has provided insight into the developmental origin and potential mechanism driving this phenotype.

Lastly, the identification of altered betaglycan expression being linked to alternative renal phenotypes suggests that polymorphisms in this co-receptor could be associated with changes in human nephron endowment. Previously, single nucleotide polymorphisms (SNPs) identified in key metanephric molecular genes such as *EYA1, RET* and *PAX2* have been linked with hypomorphic function of the allele

and generated phenotypes of renal dysgenesis in children (Clarke et al. 2006; Weber et al. 2006; Quinlan et al. 2007; Zhang et al. 2008). As betaglycan has now been demonstrated to be critical in the determination of nephron endowment, the present findings suggest betaglycan as a new candidate for SNP analysis in humans. However, one would hypothesise that a betaglycan SNP would induce hypomorphic expression of betaglycan, similar to that of betaglycan$^{+/-}$, and would be associated with higher nephron endowment in humans. Thus, the present study has identified a new candidate gene to screen either in children with renal hypodysplasia or post-mortem in individuals who possess a high nephron endowment.

6.2.3 Strengths and limitations of the present study of nephron endowment

A significant strength of this study has been the correlation of metanephric phenotypes observed both *in vitro* and *in vivo* with real-time PCR analyses of potential molecular mechanisms responsible for high nephron endowment in the betaglycan$^{+/-}$ mouse. While each approach has inherent limitations, a combined experimental design is required for an appropriate interpretation of the developing phenotypes. Also, these multiple approaches allow one to partially overcome the confounding factor of using a model with a global deficiency in TGFβ superfamily signalling. As betaglycan is expressed in other developing tissues, many of which develop contemporaneously with the kidney, it is hard to entirely rule out the impact of these developing systems on kidney development (Stenvers et al. 2003; Compton et al. 2007; Sarraj et al. 2007; Sarraj et al. 2010). Of greatest concern in this regard is the renal phenotype observed in betaglycan$^{-/-}$ mice. *In vivo,* betaglycan$^{-/-}$ embryos display defects in heart and liver development, both of which compromise embryonic survival (Stenvers et al. 2003). While metanephric culture allows the direct role of betaglycan in metanephric development to be analysed, the system itself presents a number of concerns. Metanephroi in culture develop at a slower rate to those *in vivo*, are avascular and typically lose much of their three-dimensional morphology, all of which can impact on tissue development. However, the complementation of approaches used in the present study greatly increases the strength of the data and observations recorded. Finally, incorporation of comprehensive real-time PCR analysis of the developmental stages covered by the *in vivo* and *in vitro* analyses has

highlighted potential molecular mechanisms for the observed phenotypes. This provides a more comprehensive view of the role of betaglycan in metanephric development.

6.3 FUNCTIONAL CONSEQUENCES OF A HIGH NEPHRON ENDOWMENT

In 1988, Brenner and colleagues hypothesised that a low nephron endowment is associated with an increased risk of developing hypertension and CKD. Extrapolation of this hypothesis has led to a consensus that a high nephron number would be associated with a degree of protection from the aforementioned pathologies. However, no study to date has characterised arterial pressure or renal function in a model of high nephron endowment under basal or physiologically challenged conditions, or in the presence of a pathological stressor.

This thesis hypothesised that augmented nephron endowment would not influence baseline arterial pressure or renal function but would be associated with a protective effect on arterial pressure in the presence of a chronic stressor. To test this hypothesis, arterial pressure and renal function were characterised in wildtype mice and mice with augmented nephron endowment (*Tgfb2*$^{+/-}$) under basal, physiologically stimulated, and pathologically stressed conditions. Gold-standard and clinically relevant measures of arterial pressure and renal function were obtained. Augmented nephron endowment did not influence baseline arterial pressure or renal function in the *Tgfb2*$^{+/-}$ model. Also, responses to both water deprivation and an acute period of a high salt diet were similar in wildtype and *Tgfb2*$^{+/-}$ mice. However, in the presence of a chronic high salt diet, high nephron endowment was associated with a protective effect on arterial pressure. These findings are consistent with the hypothesis that high nephron endowment is associated with a protective effect on arterial pressure in the presence of a chronic stressor, and constitute the first evidence directly associating high nephron endowment with a protective phenotype.

6.3.1 High nephron endowment is associated with a protective effect on arterial pressure and renal histology

An important finding from the present study was that baseline arterial pressure and renal function were similar in wildtype and *Tgfb2*$^{+/-}$ mice. This suggests that the hypothesised inverse relationship between nephron endowment and renal function only holds true in the setting of low nephron endowment (Keller et al. 2003; Hughson et al. 2006; Hoy et al. 2008). However, a limitation of the current study is that global renal function was assessed, rather than the function of individual nephrons. The question therefore remains, do all nephrons in *Tgfb2*$^{+/-}$ mice function at a lower rate than nephrons in the wildtype kidney? Or alternatively, are there distinct functional populations of nephrons within the kidney, with some functioning at wildtype levels and others functioning at a decreased capacity? Or finally, is there a functional gradient that extends throughout the kidney that is tightly regulated to deal with changes in cardiovascular and renal functional demands? Micropuncture studies to assess single nephron GFR in *Tgfb2*$^{+/-}$ mice are required to answer these questions.

The protective nature of augmented nephron endowment on arterial pressure was demonstrated when wildtype and *Tgfb2*$^{+/-}$ mice were fed a chronic high salt diet. Marked increases in arterial pressure and increased renal collagen deposition were observed in wildtype mice after 8 weeks of a chronic high salt diet (4 weeks on a 5% NaCl diet, followed by 4 weeks on 8% NaCl diet), but no such changes were observed in *Tgfb2*$^{+/-}$ mice. Thus, in this study, the protective nature of the high nephron number phenotype was only observed in the presence of a pathological stressor.

6.3.2 What is the protective mechanism: High nephron endowment or decreased TGFβ2?

The mechanism driving the protective phenotype observed in *Tgfb2*$^{+/-}$ mice when fed a chronic high salt diet remains unclear. While *Tgfb2*$^{+/-}$ mice represent one of only three animal models of congenital high nephron endowment in which nephron number has been accurately quantified, the combination of augmented nephron number and global TGFβ2 deficiency makes interpretation of functional outcomes difficult (Lelievre-Pegorier et al. 1998; Sims-Lucas 2007; Sims-Lucas et al.

2008). Both high nephron endowment and reduced TGFβ isoform expression have previously been hypothesised to prevent elevations in arterial pressure and to limit renal fibrosis. While previous studies have shown positive outcomes for arterial pressure and renal function through the use of pan-specific TGFβ neutralisation, this thesis demonstrated comparable outcomes with a global deficiency in TGFβ2 alone. Importantly, the present findings have identified TGFβ2 as a potential therapeutic target for antihypertensive treatments.

6.3.3 Strengths and limitations of the present study

Both a strength and limitation of this current study has been the methodology utilised. Gold-standard recording of arterial pressure, heart rate and animal activity via radiotelemetry enabled characterisation of function and response in *Tgfb2*$^{+/-}$ mice, free of confounding factors. Unlike other approaches for measuring arterial pressure such as tail-cuff and indwelling arterial catheters, radiotelemetry allows data to be recorded from unrestrained, conscious animals that can freely move about their environment. Previous studies investigating arterial pressure in models of altered nephron endowment have utilised tail-cuffs, indwelling arterial catheters or anaesthetised approaches, all of which have been shown to confound experimentation (Cullen-McEwen et al. 2003; Zimanyi et al. 2004; Hoppe et al. 2009; Ruta et al. 2010).

Selecting an appropriate method for estimating GFR in mice has become a contentious issue. In the current study, GFR was determined by measuring plasma creatinine and creatinine clearance using HPLC (Dunn et al. 2004). In 2004, the National Institute of Diabetes and Digestive and Kidney Diseases (NIDDK) concluded that HPLC is a highly accurate method for measuring both plasma creatinine and creatinine clearance in mice (Dunn et al. 2004). Creatinine is an endogenous protein derived from the breakdown of skeletal muscle (Guyton 1991). Circulating creatinine, termed plasma creatinine, is freely filtered by the glomerulus and excreted in the urine. Measurement of creatinine clearance by the glomerulus allows global GFR to be determined. Importantly, creatinine clearance is a clinically relevant and common method for determining human GFR. A major benefit of using creatinine clearance in the current study to estimate GFR was that the endogenous nature of

creatinine allows renal function to be determined repeatedly in conscious mice at multiple time points. As mice were challenged with various stimuli for differing periods of time, being able to repeatedly analyse renal function within the same mouse added power to the experimentation.

However, it is widely acknowledged that estimation of GFR via creatinine clearance has limitations. Firstly, tubular secretion of creatinine into the post-glomerular filtrate results in overestimation of GFR (Miller and Winkler 1938; Guyton 1991; Eisner et al. 2010). Recently, Eisner et al. (2010) directly compared estimates of GFR obtained using creatinine clearance with estimates obtained using the acknowledged gold-standard measurement of inulin, a freely-filtered exogenous molecule. The GFR estimates based on creatinine clearance were three to five times greater than estimates based on inulin clearance (Eisner et al. 2010). Secondly, it is generally assumed that plasma creatinine concentrations are constant in an individual. However, various states of disease have been shown to alter creatinine clearance without the presence of impaired GFR or renal disease (MacAulay et al. 2006; Barraclough et al. 2009). Therefore, the reliability of creatinine clearance data obtained in the present study in mice under physiologically or pathologically stimulated conditions must be questioned. Further studies evaluating GFR in *Tgfb2*$^{+/-}$ and wildtype mice fed a chronic high salt diet using inulin based approaches are required to fully understand the protective role, if any, of high nephron number.

6.4 AUGMENTATION OF NEPHRON ENDOWMENT IN THE 'NORMAL' KIDNEY

In the present study, administration of an anti-TGFβ2 neutralising antibody during postnatal nephrogenesis in mice was non-lethal but did not alter nephron endowment. Nevertheless, administration of the highest concentration of antibody did induce mild changes in mean glomerular volume. Stringent handling of female mice prior to and during pregnancy, the systematic injection of neonatal pups during the first 4 days of life, and the use of gold-standard stereological approaches to estimate glomerular number constituted a robust experimental design. While the overall significance of this study is lessened by the 'null' result in regards to nephron endowment, this study represents one of the first attempts to augment nephron

endowment *in vivo*. Should a successful method be developed for optimising or augmenting nephron endowment in an individual at risk of developing kidneys with a nephron deficit, the impact upon rates of CVD and CKD are likely to be significant.

The overarching aim of this study was to utilise knowledge of TGFβ2 function in the developing kidney to manipulate the developmental environment of a wildtype mouse to replicate the augmented nephron endowment phenotype observed in *Tgfb2*$^{+/-}$ mice. To reduce TGFβ2 activity, a TGFβ2-specific neutralising antibody (AB-112-NA; R&D Systems) which inhibited the binding of the ligand with the TGFβ type I/II receptor complex was selected. Previous metanephric culture experiments had indicated that this antibody neutralises the inhibitory effects of exogenous TGFβ2 on ureteric branching (Sims-Lucas 2007). However, the antibody had not been shown to neutralise endogenous TGFβ2 in explant cultures (Sims-Lucas 2007).

6.4.1 Options for neutralising TGFβ2 activity

A variety of strategies are available for neutralising TGFβ2 activity *in vivo*. Several studies have used CAT-152, a monoclonal anti-TGFβ2 neutralising antibody also known as Lerdelimumab. Mead et al. (2003) and Bottoms et al. (2010) used CAT152 to reduce post-operative fibrosis and inhibit sub-epithelial collagen deposition in airways following exposure to an allergen. In the kidney, systematic intravenous administration of CAT-152 to rats with streptozotocin-induced diabetes successfully reduced fibrosis (Hill et al. 2001). However, it is important to note that CAT-152, a product of Cambridge Antibody Technologies, was unfortunately not available for the present study. Nevertheless, the findings of Hill et al. (2001), Mead et al. (2003) and Bottoms et al. (2010) clearly indicate that anti-TGFβ2 neutralising antibodies can successfully neutralise endogenous TGFβ2 *in vivo*.

RNA-based technologies such as antisense morpholinos and interference RNA may also provide options for inhibiting TGFβ2 signalling *in vivo,* although the clinical translation of these approaches may be difficult (Saulnier et al. 2002; Hu et al. 2010). An alternate approach involves the use of soluble betaglycan to prevent TGFβ ligands from binding to the type I/II receptor complex (Vilchis-Landeros et al. 2001; Eickelberg et al. 2002). Much like CAT-152, soluble betaglycan has been shown to reduce renal fibrosis in a model of diabetic nephropathy. *db/db* mice administered

soluble betaglycan ip exhibited significant reductions in renal pathology and improved renal function compared to mice administered vehicle (Juarez et al. 2007). Interestingly, all TGFβ isoform mRNAs were significantly down-regulated following soluble betaglycan administration, suggesting the co-receptor was able to disrupt the auto-induction of TGFβ isoforms in the presence of disease. A possible limitation of the use of soluble betaglycan is the high binding affinity of the protein for TGFβ isoforms, inhibins and some BMPs, and the likelihood therefore of broad and varied effects. However, while soluble betaglycan has not been utilised in developing tissues, no adverse affects or immune responses were reported in studies in adult animals suggesting it does not induce pathology and is tolerated by the immune system. A final advantage of soluble betaglycan is that the protein occurs naturally as a cleavage product of the membrane-bound form of the receptor and has been detected in human, porcine and rat milk (Cheung 2002; Cheung et al. 2003). While the physiological significance of this finding has not been elaborated, it leaves open the possibility that soluble betaglycan may be suitable for future translational studies with the aim of augmenting nephron endowment.

6.4.2 Strengths and limitations of the present study

The major limitations of this current study were the timing of antibody administration and the inability to direct the neutralising antibody specifically to the kidney. While rodent models provide a postnatal window of nephrogenesis in which nephron development may potentially be manipulated, this window may be too late in kidney development for changes in nephron number to be induced (Cebrian et al. 2004; Gubhaju et al. 2009). Previous studies of metanephric development have suggested the presence of "developmental windows" in which environmental factors have their greatest impact (Ortiz et al. 2001; Wintour et al. 2003; Gray et al. 2010). These "windows" predominantly coincide with early ureteric branching. Based on these previous findings, one can hypothesize that an anti-TGFβ2 agent may have its greatest impact on renal development in the mouse at approximately e11.5 – e12.0. However, this is a time in development when many other organs are developing quickly. Moreover, considering translational issues, e11.5 – e12.0 corresponds to week 5 of human gestation, a time when many women do not know they are pregnant

and certainly do not know if their foetus will develop the normal complement of nephrons. Consequently, while early administration of an anti-TGFβ2 agent may augment nephron endowment, the safety and practical issues appear significant.

The use of ip injections to deliver the anti-TGFβ2 agent appeared to be the most appropriate method for the present study considering pup size, the need to minimise pup handling, and the volume of antibody to be administered. However, ip administration does not direct the antibody specifically to the kidney. To overcome this hurdle, Liu et al. (1999) administered neutralising antibody directly into the renal artery. However, this approach is unrealistic for neonatal mice. Targeted administration of a specific agent to the kidney remains a major obstacle for the progression of this research into clinical practice.

6.5 FUTURE DIRECTIONS

6.5.1 How does a high nephron endowment develop?

The current findings have implicated betaglycan and, in turn, TGFβ superfamily signalling as critical regulators of nephron endowment. However, we currently lack understanding of the metanephric molecular profile in *Tgfb2* mutant mice. Comprehensive analysis of gene expression during early kidney development in *Tgfb2* mutant mice would reveal whether a conserved mechanism for augmented nephron endowment is shared between betaglycan and *Tgfb2* mutant mice. Moreover, the intracellular signalling components responsible for elucidating the dramatic changes in metanephric gene profiles observed in betaglycan$^{+/-}$ and betaglycan$^{-/-}$ metanephroi remain unclear. Through investigating pSMAD1 and pSMAD3, the present study briefly touched upon this issue. However, the contribution of other SMADs and other non-SMAD regulated TGFβ signalling pathways such as mitogen-activated protein kinase (MAPK) driven pathways in the development of the observed phenotypes remain unknown. Whether these pathways are conserved in *Tgfb2* mutants also remains to be determined.

A valuable complement to such a study would be analysis of the sensitivity of betaglycan mutant metanephroi to ranging concentrations of TGFβ isoforms, and other superfamily members such as BMP4 and GDNF. In an approach mirroring those

used in lung culture studies (Zhao et al. 1998), the precise TGFβ ligand most responsible for the altered renal development in betaglycan mutant mice could be discovered. While much data and literature suggest that TGFβ2 is the most important ligand, the multiple roles of betaglycan and its ability to influence the function of multiple proteins make this experiment essential for understanding the role of betaglycan in metanephric development.

6.5.2 Functional consequences of a high nephron endowment

To further understand the mechanism and extent of the protective phenotype observed in *Tgfb2*$^{+/-}$ mice, a comprehensive analysis is required of the renal expression and localisation of TGFβ superfamily members and pro-fibrotic factors in mice fed normal and chronic salt diets. Such an analysis would provide insight into potential signalling pathways or homeostatic processes which are disrupted in *Tgfb2*$^{+/-}$ mice, and possibly suggest additional therapeutic targets.

It is also important to characterise both cardiovascular and renal physiology in additional models of augmented nephron endowment. The use of *Tgfb2*$^{+/-}$ mice in this thesis has provided first insights into the potentially beneficial effects of a high nephron endowment. However, as these mice possess a global TGFβ2 deficiency, it is unclear whether high nephron endowment or decreased TGFβ2 expression, or possibly both, were responsible for the protective phenotype observed. The previously published RA-induced model of augmented nephron endowment appears to be the most suitable experimental model for the characterisation of physiology in a setting of high nephron endowment (Lelievre-Pegorier et al. 1998).

To elucidate the role of decreased TGFβ2 activity in the regulation of arterial pressure, specific anti-TGFβ2 neutralising agents could be administered to wildtype animals fed a chronic high salt diet. Subsequent molecular analysis of kidneys from these mice would provide insights into the specific role of TGFβ2 in the kidney in the setting of a pathological stressor. Also, molecular profiles from these wildtype mice administered an anti-TGFβ2 agent could be directly compared with that of *Tgfb2*$^{+/-}$ mice, in order to identify the protective mechanism observed in the current study.

Of significant interest would be the functional response of *Tgfb2*$^{+/-}$ mice to other cardiovascular and renal stressors such as diabetes mellitus and obesity. The

epidemic prevalence of both conditions worldwide coupled with the economic burden of treatment of their associated pathologies highlights a requirement for preventative-based approaches. Both stressors are associated with elevations in arterial pressure, impaired renal function and vascular pathology, most of which *Tgfb2*$^{+/-}$ mice display protection against. Were *Tgfb2*$^{+/-}$ mice to show some degree of resistance to the pathologies associated with diabetes and/or obesity, then anti-TGFβ2 therapies should be comprehensively studied for their clinical potential.

Finally, the present findings suggest that SNPs in either *Tgfb2* or betaglycan genes may be associated with high nephron endowment in humans. Of interest would be whether an associated SNP correlates with protection against elevated arterial pressure, or impaired renal function in the presence of dietary stressors.

6.5.3 Augmentation of a nephron endowment in a 'normal' kidney

The most important issue for any future study with the aim of augmenting nephron endowment remains the selection of an adequate anti-TGFβ2 neutralising agent. As mentioned above, anti-TGFβ2 neutralising antibodies have shown great promise and are highly selective for the particular isoform. However, much of the success to date has come through the use of CAT-152, an antibody unavailable to the present investigation. Should this antibody not be available to future researchers, soluble betaglycan is perhaps the next best candidate due to its potential translational relevance. Once an agent is selected, extensive optimisation and characterisation of the effects on metanephric development must be undertaken.

6.6 CONCLUSION

Increasing evidence suggests that nephron endowment is a critical factor in the development of CVD and CKD. While low nephron endowment has been associated with an increased risk for hypertension and associated pathologies, little is known about the development or functional consequences of a high nephron endowment. This thesis has demonstrated that betaglycan, a TGFβ superfamily co-

receptor, is critical for normal kidney development and the establishment of nephron endowment. Betaglycan$^{-/-}$ mice display renal hypoplasia with decreased nephron development; in contrast, betaglycan$^{+/-}$ mutant mice exhibit increased nephron endowment. Functional characterisation of *Tgfb2*$^{+/-}$ mice, a previously identified model of augmented nephron endowment demonstrated that high nephron endowment does not influence cardiovascular or renal function under basal or physiologically-stimulated conditions. However, high nephron number in this model was associated with a protective effect on arterial pressure in the presence of a chronic stressor. Importantly, the present findings suggest that manipulation of TGFβ2 signalling may provide a potential avenue for both the augmentation of nephron endowment in the developing kidney, and the development of TGFβ2 targeted anti-hypertensive therapeutics.

CHAPTER 7

REFERENCE LIST

Andres, J. L., D. DeFalcis, M. Noda and J. Massague (1992). "Binding of two growth factor families to separate domains of the proteoglycan betaglycan." J Biol Chem **267**(9): 5927-5930.

Bandyopadhyay, A., F. Lopez-Casillas, S. N. Malik, J. L. Montiel, V. Mendoza, J. Yang and L. Z. Sun (2002). "Antitumor activity of a recombinant soluble betaglycan in human breast cancer xenograft." Cancer Res **62**(16): 4690-4695.

Bandyopadhyay, A., L. Wang, F. Lopez-Casillas, V. Mendoza, I. T. Yeh and L. Sun (2005). "Systemic administration of a soluble betaglycan suppresses tumor growth, angiogenesis, and matrix metalloproteinase-9 expression in a human xenograft model of prostate cancer." Prostate **63**(1): 81-90.

Bandyopadhyay, A., Y. Zhu, S. N. Malik, J. Kreisberg, M. G. Brattain, E. A. Sprague, J. Luo, F. Lopez-Casillas and L. Z. Sun (2002). "Extracellular domain of TGFbeta type III receptor inhibits angiogenesis and tumor growth in human cancer cells." Oncogene **21**(22): 3541-3551.

Barasch, J., J. Qiao, G. McWilliams, D. Chen, J. A. Oliver and D. Herzlinger (1997). "Ureteric bud cells secrete multiple factors, including bFGF, which rescue renal progenitors from apoptosis." Am J Physiol **273**(5 Pt 2): F757-767.

Barasch, J., J. Yang, C. B. Ware, T. Taga, K. Yoshida, H. Erdjument-Bromage, P. Tempst, E. Parravicini, S. Malach, T. Aranoff and J. A. Oliver (1999). "Mesenchymal to epithelial conversion in rat metanephros is induced by LIF." Cell **99**(4): 377-386.

Barraclough, K., L. Er, F. Ng, M. Harris, J. Montaner and A. Levin (2009). "A comparison of the predictive performance of different methods of kidney function estimation in a well-characterized HIV-infected population." Nephron Clin Pract **111**(1): c39-48.

Bates, C. M. (2007). "Role of fibroblast growth factor receptor signaling in kidney development." Pediatr Nephrol **22**(3): 343-349.

Batourina, E., S. Gim, N. Bello, M. Shy, M. Clagett-Dame, S. Srinivas, F. Costantini and C. Mendelsohn (2001). "Vitamin A controls epithelial/mesenchymal interactions through Ret expression." Nat Genet **27**(1): 74-78.

Baum, M. (2010). "Role of the kidney in the prenatal and early postnatal programming of hypertension." Am J Physiol Renal Physiol **298**(2): F235-247.

Behar, O., J. A. Golden, H. Mashimo, F. J. Schoen and M. C. Fishman (1996). "Semaphorin III is needed for normal patterning and growth of nerves, bones and heart." Nature **383**(6600): 525-528.

Belmadani, S., M. Zerfaoui, H. A. Boulares, D. I. Palen and K. Matrougui (2008). "Microvessel vascular smooth muscle cells contribute to collagen type I deposition through ERK1/2 MAP kinase, alphavbeta3-integrin, and TGF-beta1 in response to ANG II and high glucose." Am J Physiol Heart Circ Physiol **295**(1): H69-76.

Benigni, A., C. Zoja, D. Corna, C. Zatelli, S. Conti, M. Campana, E. Gagliardini, D. Rottoli, C. Zanchi, M. Abbate, S. Ledbetter and G. Remuzzi (2003). "Add-on anti-TGF-beta antibody to ACE inhibitor arrests progressive diabetic nephropathy in the rat." J Am Soc Nephrol **14**(7): 1816-1824.

Bertram, J. F. (1995). "Analyzing renal glomeruli with the new stereology." Int Rev Cytol **161**: 111-172.

Bharathy, S., W. Xie, J. M. Yingling and M. Reiss (2008). "Cancer-associated transforming growth factor beta type II receptor gene mutant causes activation of bone morphogenic protein-Smads and invasive phenotype." Cancer Res **68**(6): 1656-1666.

Bilandzic, M., S. Chu, P. G. Farnworth, C. Harrison, P. Nicholls, Y. Wang, R. M. Escalona, P. J. Fuller, J. K. Findlay and K. L. Stenvers (2009). "Loss of betaglycan contributes to the malignant properties of human granulosa tumor cells." Mol Endocrinol **23**(4): 539-548.

Border, W. A., N. A. Noble, T. Yamamoto, J. R. Harper, Y. Yamaguchi, M. D. Pierschbacher and E. Ruoslahti (1992). "Natural inhibitor of transforming growth factor-beta protects against scarring in experimental kidney disease." Nature **360**(6402): 361-364.

Bottinger, E. P. (2007). "TGF-beta in renal injury and disease." Semin Nephrol **27**(3): 309-320.

Bottinger, E. P. and M. Bitzer (2002). "TGF-beta signaling in renal disease." J Am Soc Nephrol **13**(10): 2600-2610.

Bottoms, S. E., J. E. Howell, A. K. Reinhardt, I. C. Evans and R. J. McAnulty (2010). "Tgf-Beta isoform specific regulation of airway inflammation and remodelling in a murine model of asthma." PLoS One **5**(3): e9674.

Boubred, F., C. Buffat, J. M. Feuerstein, L. Daniel, M. Tsimaratos, C. Oliver, M. Lelievre-Pegorier and U. Simeoni (2007). "Effects of early postnatal hypernutrition on nephron number and long-term renal function and structure in rats." Am J Physiol Renal Physiol **293**(6): F1944-1949.

Bouchard, M., A. Souabni, M. Mandler, A. Neubuser and M. Busslinger (2002). "Nephric lineage specification by Pax2 and Pax8." Genes Dev **16**(22): 2958-2970.

Bramlage, C. P., C. Schlumbohm, C. R. Pryce, S. Mirza, C. Schnell, K. Amann, V. W. Amstrong, F. Eitner, A. Zapf, J. Feldon, M. Oellerich, E. Fuchs, G. A. Muller and F. Strutz (2009). "Prenatal dexamethasone exposure does not alter blood pressure and nephron number in the young adult marmoset monkey." Hypertension **54**(5): 1115-1122.

Brennan, K. A., S. Kaufman, S. W. Reynolds, B. T. McCook, G. Kan, I. Christiaens, M. E. Symonds and D. M. Olson (2008). "Differential effects of maternal nutrient restriction through pregnancy on kidney development and later blood

pressure control in the resulting offspring." Am J Physiol Regul Integr Comp Physiol **295**(1): R197-205.

Brenner, B. M., D. L. Garcia and S. Anderson (1988). "Glomeruli and blood pressure. Less of one, more the other?" Am J Hypertens **1**(4 Pt 1): 335-347.

Briones, A. M., S. M. Arribas and M. Salaices (2010). "Role of extracellular matrix in vascular remodeling of hypertension." Curr Opin Nephrol Hypertens **19**(2): 187-194.

Brodbeck, S. and C. Englert (2004). "Genetic determination of nephrogenesis: the Pax/Eya/Six gene network." Pediatr Nephrol **19**(3): 249-255.

Brophy, P. D., L. Ostrom, K. M. Lang and G. R. Dressler (2001). "Regulation of ureteric bud outgrowth by Pax2-dependent activation of the glial derived neurotrophic factor gene." Development **128**(23): 4747-4756.

Bruijn, J. A., A. Roos, B. de Geus and E. de Heer (1994). "Transforming growth factor-beta and the glomerular extracellular matrix in renal pathology." J Lab Clin Med **123**(1): 34-47.

Bush, K. T., H. Sakurai, D. L. Steer, M. O. Leonard, R. V. Sampogna, T. N. Meyer, C. Schwesinger, J. Qiao and S. K. Nigam (2004). "TGF-beta superfamily members modulate growth, branching, shaping, and patterning of the ureteric bud." Dev Biol **266**(2): 285-298.

Butz, G. M. and R. L. Davisson (2001). "Long-term telemetric measurement of cardiovascular parameters in awake mice: a physiological genomics tool." Physiol Genomics **5**(2): 89-97.

Cacalano, G., I. Farinas, L. C. Wang, K. Hagler, A. Forgie, M. Moore, M. Armanini, H. Phillips, A. M. Ryan, L. F. Reichardt, M. Hynes, A. Davies and A. Rosenthal (1998). "GFRalpha1 is an essential receptor component for GDNF in the developing nervous system and kidney." Neuron **21**(1): 53-62.

Cain, J. E., S. Hartwig, J. F. Bertram and N. D. Rosenblum (2008). "Bone morphogenetic protein signaling in the developing kidney: present and future." Differentiation **76**(8): 831-842.

Cain, J. E., T. Nion, D. Jeulin and J. F. Bertram (2005). "Exogenous BMP-4 amplifies asymmetric ureteric branching in the developing mouse kidney in vitro." Kidney Int **67**(2): 420-431.

Cain, J. E., D. I. G. V, J. Smeeton and N. D. Rosenblum (2010). "Genetics of renal hypoplasia: insights into the mechanisms controlling nephron endowment." Pediatr Res **68**(2): 91-98.

Cancilla, B., M. D. Ford-Perriss and J. F. Bertram (1999). "Expression and localization of fibroblast growth factors and fibroblast growth factor receptors in the developing rat kidney." Kidney Int **56**(6): 2025-2039.

Carlson, S. H., S. Oparil, Y. F. Chen and J. M. Wyss (2002). "Blood pressure and NaCl-sensitive hypertension are influenced by angiotensin-converting enzyme gene expression in transgenic mice." Hypertension **39**(2): 214-218.

Carlson, S. H. and J. M. Wyss (2000). "Long-term telemetric recording of arterial pressure and heart rate in mice fed basal and high NaCl diets." Hypertension **35**(2): E1-5.

Carlstrom, M., J. Sallstrom, O. Skott, E. Larsson and A. E. Persson (2007). "Uninephrectomy in young age or chronic salt loading causes salt-sensitive hypertension in adult rats." Hypertension **49**(6): 1342-1350.

Carroll, T. J., J. S. Park, S. Hayashi, A. Majumdar and A. P. McMahon (2005). "Wnt9b plays a central role in the regulation of mesenchymal to epithelial transitions underlying organogenesis of the mammalian urogenital system." Dev Cell **9**(2): 283-292.

Cass, A., S. Chadban, J. Craig, H. Howard, S. McDonald, G. Salkeld and S. White (2006). The Economic Impact of End-Stage Kidney Disease in Australia. T. G. I. o. I. Health. Melbourne, Kidney Health Australia.

Cebrian, C., K. Borodo, N. Charles and D. A. Herzlinger (2004). "Morphometric index of the developing murine kidney." Dev Dyn **231**(3): 601-608.

Chang, E. H., M. Menezes, N. C. Meyer, R. A. Cucci, V. S. Vervoort, C. E. Schwartz and R. J. Smith (2004). "Branchio-oto-renal syndrome: the mutation spectrum in EYA1 and its phenotypic consequences." Hum Mutat **23**(6): 582-589.

Cheifetz, S., A. Bassols, K. Stanley, M. Ohta, J. Greenberger and J. Massague (1988). "Heterodimeric transforming growth factor beta. Biological properties and interaction with three types of cell surface receptors." J Biol Chem **263**(22): 10783-10789.

Chen, J. (2010). "Epidemiology of hypertension and chronic kidney disease in China." Curr Opin Nephrol Hypertens **19**(3): 278-282.

Cheung, H. K., J. Mei and R. J. Xu (2003). "Quantification of soluble betaglycan in porcine milk." Asia Pac J Clin Nutr **12 Suppl**: S61.

Cheung, H. K., Mei, J., Xu, R.J (2002). "Detection of betaglycan in porcine and human milk." Proceedings of the Nutrition Society of Australia(26): S317.

Chi, X., O. Michos, R. Shakya, P. Riccio, H. Enomoto, J. D. Licht, N. Asai, M. Takahashi, N. Ohgami, M. Kato, C. Mendelsohn and F. Costantini (2009). "Ret-dependent cell rearrangements in the Wolffian duct epithelium initiate ureteric bud morphogenesis." Dev Cell **17**(2): 199-209.

Chi, Y., M. L. Pucci and V. L. Schuster (2008). "Dietary salt induces transcription of the prostaglandin transporter gene in renal collecting ducts." Am J Physiol Renal Physiol **295**(3): F765-771.

Clark, A. T. (1998). Studies on the role of transforming growth factor-B1 and its receptors in the kidney. Anatomy and Cell Biology. Melbourne, University of Melbourne. **PhD:** 177.

Clarke, J. C., E. M. Honey, E. Bekker, L. C. Snyman, R. M. Raymond, Jr., C. Lord and P. D. Brophy (2006). "A novel nonsense mutation in the EYA1 gene associated with branchio-oto-renal/branchiootic syndrome in an Afrikaner kindred." Clin Genet **70**(1): 63-67.

Clarke, J. C., S. R. Patel, R. M. Raymond, Jr., S. Andrew, B. G. Robinson, G. R. Dressler and P. D. Brophy (2006). "Regulation of c-Ret in the developing kidney is responsive to Pax2 gene dosage." Hum Mol Genet **15**(23): 3420-3428.

Cochrane, A. L., M. M. Kett, C. S. Samuel, N. V. Campanale, W. P. Anderson, D. A. Hume, M. H. Little, J. F. Bertram and S. D. Ricardo (2005). "Renal structural and functional repair in a mouse model of reversal of ureteral obstruction." J Am Soc Nephrol **16**(12): 3623-3630.

Compton, L. A., D. A. Potash, C. B. Brown and J. V. Barnett (2007). "Coronary vessel development is dependent on the type III transforming growth factor beta receptor." Circ Res **101**(8): 784-791.

Coresh, J., B. Astor and M. J. Sarnak (2004). "Evidence for increased cardiovascular disease risk in patients with chronic kidney disease." Curr Opin Nephrol Hypertens **13**(1): 73-81.

Costantini, F. (2006). "Renal branching morphogenesis: concepts, questions, and recent advances." Differentiation **74**(7): 402-421.

Costantini, F. and R. Shakya (2006). "GDNF/Ret signaling and the development of the kidney." Bioessays **28**(2): 117-127.

Cox, L. A., M. J. Nijland, J. S. Gilbert, N. E. Schlabritz-Loutsevitch, G. B. Hubbard, T. J. McDonald, R. E. Shade and P. W. Nathanielsz (2006). "Effect of 30 per cent maternal nutrient restriction from 0.16 to 0.5 gestation on fetal baboon kidney gene expression." J Physiol **572**(Pt 1): 67-85.

Cullen-McEwen, L. A., J. Drago and J. F. Bertram (2001). "Nephron endowment in glial cell line-derived neurotrophic factor (GDNF) heterozygous mice." Kidney Int **60**(1): 31-36.

Cullen-McEwen, L. A., M. M. Kett, J. Dowling, W. P. Anderson and J. F. Bertram (2003). "Nephron number, renal function, and arterial pressure in aged GDNF heterozygous mice." Hypertension **41**(2): 335-340.

Daly, A. C., R. A. Randall and C. S. Hill (2008). "Transforming growth factor beta-induced Smad1/5 phosphorylation in epithelial cells is mediated by novel receptor complexes and is essential for anchorage-independent growth." Mol Cell Biol **28**(22): 6889-6902.

Davies, J. A., M. Ladomery, P. Hohenstein, L. Michael, A. Shafe, L. Spraggon and N. Hastie (2004). "Development of an siRNA-based method for repressing specific genes in renal organ culture and its use to show that the Wt1 tumour suppressor is required for nephron differentiation." Hum Mol Genet **13**(2): 235-246.

Dickinson, H., K. Moritz, E. M. Wintour, D. W. Walker and M. M. Kett (2007). "A comparative study of renal function in the desert-adapted spiny mouse and the laboratory-adapted C57BL/6 mouse: response to dietary salt load." Am J Physiol Renal Physiol **293**(4): F1093-1098.

Dickinson, H., D. W. Walker, E. M. Wintour and K. Moritz (2007). "Maternal dexamethasone treatment at midgestation reduces nephron number and alters renal gene expression in the fetal spiny mouse." Am J Physiol Regul Integr Comp Physiol **292**(1): R453-461.

Dickson, M. C., J. S. Martin, F. M. Cousins, A. B. Kulkarni, S. Karlsson and R. J. Akhurst (1995). "Defective haematopoiesis and vasculogenesis in transforming growth factor-beta 1 knock out mice." Development **121**(6): 1845-1854.

Discenza, M. T., S. He, T. H. Lee, L. L. Chu, B. Bolon, P. Goodyer, M. Eccles and J. Pelletier (2003). "WT1 is a modifier of the Pax2 mutant phenotype: cooperation and interaction between WT1 and Pax2." Oncogene **22**(50): 8145-8155.

Doublier, S., K. Amri, D. Seurin, E. Moreau, C. Merlet-Benichou, G. E. Striker and T. Gilbert (2001). "Overexpression of human insulin-like growth factor binding protein-1 in the mouse leads to nephron deficit." Pediatr Res **49**(5): 660-666.

Dressler, G. R., U. Deutsch, K. Chowdhury, H. O. Nornes and P. Gruss (1990). "Pax2, a new murine paired-box-containing gene and its expression in the developing excretory system." Development **109**(4): 787-795.

Dressler, G. R. and E. C. Douglass (1992). "Pax-2 is a DNA-binding protein expressed in embryonic kidney and Wilms tumor." Proc Natl Acad Sci U S A **89**(4): 1179-1183.

Dressler, G. R., J. E. Wilkinson, U. W. Rothenpieler, L. T. Patterson, L. Williams-Simons and H. Westphal (1993). "Deregulation of Pax-2 expression in transgenic mice generates severe kidney abnormalities." Nature **362**(6415): 65-67.

Dudley, A. T., K. M. Lyons and E. J. Robertson (1995). "A requirement for bone morphogenetic protein-7 during development of the mammalian kidney and eye." Genes Dev **9**(22): 2795-2807.

Dunker, N. and K. Krieglstein (2000). "Targeted mutations of transforming growth factor-beta genes reveal important roles in mouse development and adult homeostasis." Eur J Biochem **267**(24): 6982-6988.

Dunn, S. R., Z. Qi, E. P. Bottinger, M. D. Breyer and K. Sharma (2004). "Utility of endogenous creatinine clearance as a measure of renal function in mice." Kidney Int **65**(5): 1959-1967.

Durbec, P., C. V. Marcos-Gutierrez, C. Kilkenny, M. Grigoriou, K. Wartiowaara, P. Suvanto, D. Smith, B. Ponder, F. Costantini, M. Saarma and et al. (1996). "GDNF signalling through the Ret receptor tyrosine kinase." Nature **381**(6585): 789-793.

Dziarmaga, A., P. Clark, C. Stayner, J. P. Julien, E. Torban, P. Goodyer and M. Eccles (2003). "Ureteric bud apoptosis and renal hypoplasia in transgenic PAX2-Bax fetal mice mimics the renal-coloboma syndrome." J Am Soc Nephrol **14**(11): 2767-2774.

Eccles, M. R. (1998). "The role of PAX2 in normal and abnormal development of the urinary tract." Pediatr Nephrol **12**(9): 712-720.

Eickelberg, O., M. Centrella, M. Reiss, M. Kashgarian and R. G. Wells (2002). "Betaglycan inhibits TGF-beta signaling by preventing type I-type II receptor complex formation. Glycosaminoglycan modifications alter betaglycan function." J Biol Chem **277**(1): 823-829.

Eisner, C., R. Faulhaber-Walter, Y. Wang, A. Leelahavanichkul, P. S. Yuen, D. Mizel, R. A. Star, J. P. Briggs, M. Levine and J. Schnermann (2010). "Major contribution of tubular secretion to creatinine clearance in mice." Kidney Int **77**(6): 519-526.

Elvers, M., J. Pfeiffer, C. Kaltschmidt and B. Kaltschmidt (2005). "TGF-beta2 neutralization inhibits proliferation and activates apoptosis of cerebellar granule cell precurors in the developing cerebellum." Mech Dev **122**(4): 587-602.

Esparza-Lopez, J., J. L. Montiel, M. M. Vilchis-Landeros, T. Okadome, K. Miyazono and F. Lopez-Casillas (2001). "Ligand binding and functional properties of betaglycan, a co-receptor of the transforming growth factor-beta superfamily. Specialized binding regions for transforming growth factor-beta and inhibin A." J Biol Chem **276**(18): 14588-14596.

Esquela, A. F. and S. J. Lee (2003). "Regulation of metanephric kidney development by growth/differentiation factor 11." Dev Biol **257**(2): 356-370.

Ferrari, G., B. D. Cook, V. Terushkin, G. Pintucci and P. Mignatti (2009). "Transforming growth factor-beta 1 (TGF-beta1) induces angiogenesis through vascular endothelial growth factor (VEGF)-mediated apoptosis." J Cell Physiol **219**(2): 449-458.

Finger, E. C., N. Y. Lee, H. J. You and G. C. Blobe (2008). "Endocytosis of the type III transforming growth factor-beta (TGF-beta) receptor through the clathrin-independent/lipid raft pathway regulates TGF-beta signaling and receptor down-regulation." J Biol Chem **283**(50): 34808-34818.

Fried, L. F., R. Katz, M. Cushman, M. Sarnak, M. G. Shlipak, L. Kuller and A. B. Newman (2009). "Change in cardiovascular risk factors with progression of kidney disease." Am J Nephrol **29**(4): 334-341.

Gagliardini, E. and A. Benigni (2006). "Role of anti-TGF-beta antibodies in the treatment of renal injury." Cytokine Growth Factor Rev **17**(1-2): 89-96.

Gagliardini, E. and A. Benigni (2007). "Therapeutic potential of TGF-beta inhibition in chronic renal failure." Expert Opin Biol Ther **7**(3): 293-304.

Georgas, K., B. Rumballe, M. T. Valerius, H. S. Chiu, R. D. Thiagarajan, E. Lesieur, B. J. Aronow, E. W. Brunskill, A. N. Combes, D. Tang, D. Taylor, S. M. Grimmond, S. S. Potter, A. P. McMahon and M. H. Little (2009). "Analysis of early nephron patterning reveals a role for distal RV proliferation in fusion to the ureteric tip via a cap mesenchyme-derived connecting segment." Dev Biol.

Gewin, L., N. Bulus, G. Mernaugh, G. Moeckel, R. C. Harris, H. L. Moses, A. Pozzi and R. Zent (2010). "TGF-beta receptor deletion in the renal collecting system exacerbates fibrosis." J Am Soc Nephrol **21**(8): 1334-1343.

Gilbert, J. S., A. L. Lang, A. R. Grant and M. J. Nijland (2005). "Maternal nutrient restriction in sheep: hypertension and decreased nephron number in offspring at 9 months of age." J Physiol **565**(Pt 1): 137-147.

Godin, R. E., E. J. Robertson and A. T. Dudley (1999). "Role of BMP family members during kidney development." Int J Dev Biol **43**(5): 405-411.

Goodyer, P., A. Kurpad, S. Rekha, S. Muthayya, P. Dwarkanath, A. Iyengar, B. Philip, A. Mhaskar, A. Benjamin, S. Maharaj, D. Laforte, C. Raju and K. Phadke (2007). "Effects of maternal vitamin A status on kidney development: a pilot study." Pediatr Nephrol **22**(2): 209-214.

Goumans, M. J., G. Valdimarsdottir, S. Itoh, F. Lebrin, J. Larsson, C. Mummery, S. Karlsson and P. ten Dijke (2003). "Activin receptor-like kinase (ALK)1 is an antagonistic mediator of lateral TGFbeta/ALK5 signaling." Mol Cell **12**(4): 817-828.

Gray, S. P., K. M. Denton, L. Cullen-McEwen, J. F. Bertram and K. M. Moritz (2010). "Prenatal Exposure to Alcohol Reduces Nephron Number and Raises Blood Pressure in Progeny." J Am Soc Nephrol.

Gray, S. P., K. Kenna, J. F. Bertram, W. E. Hoy, E. B. Yan, A. D. Bocking, J. F. Brien, D. W. Walker, R. Harding and K. M. Moritz (2008). "Repeated ethanol exposure during late gestation decreases nephron endowment in fetal sheep." Am J Physiol Regul Integr Comp Physiol **295**(2): R568-574.

Grieshammer, U., C. Cebrian, R. Ilagan, E. Meyers, D. Herzlinger and G. R. Martin (2005). "FGF8 is required for cell survival at distinct stages of nephrogenesis and for regulation of gene expression in nascent nephrons." Development **132**(17): 3847-3857.

Grieshammer, U., M. Le, A. S. Plump, F. Wang, M. Tessier-Lavigne and G. R. Martin (2004). "SLIT2-mediated ROBO2 signaling restricts kidney induction to a single site." Dev Cell **6**(5): 709-717.

Groppe, J., C. S. Hinck, P. Samavarchi-Tehrani, C. Zubieta, J. P. Schuermann, A. B. Taylor, P. M. Schwarz, J. L. Wrana and A. P. Hinck (2008). "Cooperative assembly of TGF-beta superfamily signaling complexes is mediated by two disparate mechanisms and distinct modes of receptor binding." Mol Cell **29**(2): 157-168.

Gubhaju, L., M. R. Sutherland, B. A. Yoder, A. Zulli, J. F. Bertram and M. J. Black (2009). "Is nephrogenesis affected by preterm birth? Studies in a non-human primate model." Am J Physiol Renal Physiol **297**(6): F1668-1677.

Gundersen, H. J. and E. B. Jensen (1987). "The efficiency of systematic sampling in stereology and its prediction." J Microsc **147**(Pt 3): 229-263.

Guo, M., S. D. Ricardo, J. A. Deane, M. Shi, L. Cullen-McEwen and J. F. Bertram (2005). "A stereological study of the renal glomerular vasculature in the db/db mouse model of diabetic nephropathy." J Anat **207**(6): 813-821.

Guyton, A. (1991). Textbook of Medical Physiology. Philadelphia, W.B Saunders.

Guyton, A. C. (1990). "Long-term arterial pressure control: an analysis from animal experiments and computer and graphic models." Am J Physiol **259**(5 Pt 2): R865-877.

Guyton, A. C., T. G. Coleman, A. W. Cowley, Jr., J. F. Liard, R. A. Norman, Jr. and R. D. Manning, Jr. (1972). "Systems analysis of arterial pressure regulation and hypertension." Ann Biomed Eng **1**(2): 254-281.

Guyton, A. C. H., J. E (2000). Textbook of Medical Physiology. Philadelphia, W.B Saunders Company.

Harrison, M. and S. C. Langley-Evans (2009). "Intergenerational programming of impaired nephrogenesis and hypertension in rats following maternal protein restriction during pregnancy." Br J Nutr **101**(7): 1020-1030.

Hartwig, S., M. C. Hu, C. Cella, T. Piscione, J. Filmus and N. D. Rosenblum (2005). "Glypican-3 modulates inhibitory Bmp2-Smad signaling to control renal development in vivo." Mech Dev **122**(7-8): 928-938.

Hayman, J. M. J., J. W. J. Martin and M. Miller (1939). "Renal function and the number of glomeruli in the kidney." Archives of Internal Medicine **64**: 69 - 83.

Hellmich, H. L., L. Kos, E. S. Cho, K. A. Mahon and A. Zimmer (1996). "Embryonic expression of glial cell-line derived neurotrophic factor (GDNF) suggests multiple developmental roles in neural differentiation and epithelial-mesenchymal interactions." Mech Dev **54**(1): 95-105.

Hill, C., A. Flyvbjerg, H. Gronbaek, J. Petrik, D. J. Hill, C. R. Thomas, M. C. Sheppard and A. Logan (2000). "The renal expression of transforming growth factor-beta isoforms and their receptors in acute and chronic experimental diabetes in rats." Endocrinology **141**(3): 1196-1208.

Hill, C., A. Flyvbjerg, R. Rasch, M. Bak and A. Logan (2001). "Transforming growth factor-beta2 antibody attenuates fibrosis in the experimental diabetic rat kidney." J Endocrinol **170**(3): 647-651.

Holifield, J. S., A. M. Arlen, R. B. Runyan and R. J. Tomanek (2004). "TGF-beta1, -beta2 and -beta3 cooperate to facilitate tubulogenesis in the explanted quail heart." J Vasc Res **41**(6): 491-498.

Hoppe, C. C., R. G. Evans, J. F. Bertram and K. M. Moritz (2007). "Effects of dietary protein restriction on nephron number in the mouse." Am J Physiol Regul Integr Comp Physiol **292**(5): R1768-1774.

Hoppe, C. C., R. G. Evans, K. M. Moritz, L. A. Cullen-McEwen, S. M. Fitzgerald, J. Dowling and J. F. Bertram (2007). "Combined prenatal and postnatal protein restriction influences adult kidney structure, function, and arterial pressure." Am J Physiol Regul Integr Comp Physiol **292**(1): R462-469.

Hoppe, C. C., K. M. Moritz, S. M. Fitzgerald, J. F. Bertram and R. G. Evans (2009). "Transient hypertension and sustained tachycardia in mice housed individually in metabolism cages." Physiol Res **58**(1): 69-75.

Hoy, W. E., J. F. Bertram, R. D. Denton, M. Zimanyi, T. Samuel and M. D. Hughson (2008). "Nephron number, glomerular volume, renal disease and hypertension." Curr Opin Nephrol Hypertens **17**(3): 258-265.

Hoy, W. E., R. N. Douglas-Denton, M. D. Hughson, A. Cass, K. Johnson and J. F. Bertram (2003). "A stereological study of glomerular number and volume: preliminary findings in a multiracial study of kidneys at autopsy." Kidney Int Suppl(83): S31-37.

Hoy, W. E., M. D. Hughson, G. R. Singh, R. Douglas-Denton and J. F. Bertram (2006). "Reduced nephron number and glomerulomegaly in Australian Aborigines: a group at high risk for renal disease and hypertension." Kidney Int **70**(1): 104-110.

Hu, W., Z. Chen, Z. Ye, D. Xia, Z. Xia, J. Ma, M. Zhu and G. Chen (2010). "Knockdown of Cyclophilin D Gene by RNAi Protects Rat from Ischemia/ Reperfusion-Induced Renal Injury." Kidney Blood Press Res **33**(3): 193-199.

Hughson, M., A. B. Farris, 3rd, R. Douglas-Denton, W. E. Hoy and J. F. Bertram (2003). "Glomerular number and size in autopsy kidneys: the relationship to birth weight." Kidney Int **63**(6): 2113-2122.

Hughson, M. D., R. Douglas-Denton, J. F. Bertram and W. E. Hoy (2006). "Hypertension, glomerular number, and birth weight in African Americans and white subjects in the southeastern United States." Kidney Int **69**(4): 671-678.

Iglesias, D. M., P. A. Hueber, L. Chu, R. Campbell, A. M. Patenaude, A. J. Dziarmaga, J. Quinlan, O. Mohamed, D. Dufort and P. R. Goodyer (2007). "Canonical WNT signaling during kidney development." Am J Physiol Renal Physiol **293**(2): F494-500.

Jamison, R. L. (1973). "Intrarenal heterogeneity. The case for two functionally dissimilar populations of nephrons in the mammalian kidney." Am J Med **54**(3): 281-289.

Juarez, P., M. M. Vilchis-Landeros, J. Ponce-Coria, V. Mendoza, R. Hernandez-Pando, N. A. Bobadilla and F. Lopez-Casillas (2007). "Soluble betaglycan reduces renal damage progression in db/db mice." Am J Physiol Renal Physiol **292**(1): F321-329.

Kaartinen, V., J. W. Voncken, C. Shuler, D. Warburton, D. Bu, N. Heisterkamp and J. Groffen (1995). "Abnormal lung development and cleft palate in mice lacking TGF-beta 3 indicates defects of epithelial-mesenchymal interaction." Nat Genet **11**(4): 415-421.

Karavanova, I. D., L. F. Dove, J. H. Resau and A. O. Perantoni (1996). "Conditioned medium from a rat ureteric bud cell line in combination with bFGF induces complete differentiation of isolated metanephric mesenchyme." Development **122**(12): 4159-4167.

Kearney, P. M., M. Whelton, K. Reynolds, P. Muntner, P. K. Whelton and J. He (2005). "Global burden of hypertension: analysis of worldwide data." Lancet **365**(9455): 217-223.

Keller, G., G. Zimmer, G. Mall, E. Ritz and K. Amann (2003). "Nephron number in patients with primary hypertension." N Engl J Med **348**(2): 101-108.

Kim, H. S., M. S. Kim, A. L. Hancock, J. C. Harper, J. Y. Park, G. Poy, A. O. Perantoni, M. Cam, K. Malik and S. B. Lee (2007). "Identification of novel Wilms' tumor suppressor gene target genes implicated in kidney development." J Biol Chem **282**(22): 16278-16287.

Kim, S. J., P. Angel, R. Lafyatis, K. Hattori, K. Y. Kim, M. B. Sporn, M. Karin and A. B. Roberts (1990). "Autoinduction of transforming growth factor beta 1 is mediated by the AP-1 complex." Mol Cell Biol **10**(4): 1492-1497.

Kim, S. M., C. Eisner, R. Faulhaber-Walter, D. Mizel, S. M. Wall, J. P. Briggs and J. Schnermann (2008). "Salt sensitivity of blood pressure in NKCC1-deficient mice." Am J Physiol Renal Physiol **295**(4): F1230-1238.

Kirkbride, K. C., T. A. Townsend, M. W. Bruinsma, J. V. Barnett and G. C. Blobe (2008). "Bone morphogenetic proteins signal through the transforming growth factor-beta type III receptor." J Biol Chem **283**(12): 7628-7637.

Kispert, A., S. Vainio and A. P. McMahon (1998). "Wnt-4 is a mesenchymal signal for epithelial transformation of metanephric mesenchyme in the developing kidney." Development **125**(21): 4225-4234.

Kispert, A., S. Vainio, L. Shen, D. H. Rowitch and A. P. McMahon (1996). "Proteoglycans are required for maintenance of Wnt-11 expression in the ureter tips." Development **122**(11): 3627-3637.

Kobayashi, A., M. T. Valerius, J. W. Mugford, T. J. Carroll, M. Self, G. Oliver and A. P. McMahon (2008). "Six2 defines and regulates a multipotent self-renewing nephron progenitor population throughout mammalian kidney development." Cell Stem Cell **3**(2): 169-181.

Kochhar, A., D. J. Orten, J. L. Sorensen, S. M. Fischer, C. W. Cremers, W. J. Kimberling and R. J. Smith (2008). "SIX1 mutation screening in 247 branchio-oto-renal syndrome families: a recurrent missense mutation associated with BOR." Hum Mutat **29**(4): 565.

Kopp, J. B., V. M. Factor, M. Mozes, P. Nagy, N. Sanderson, E. P. Bottinger, P. E. Klotman and S. S. Thorgeirsson (1996). "Transgenic mice with increased plasma levels of TGF-beta 1 develop progressive renal disease." Lab Invest **74**(6): 991-1003.

Kreidberg, J. A., H. Sariola, J. M. Loring, M. Maeda, J. Pelletier, D. Housman and R. Jaenisch (1993). "WT-1 is required for early kidney development." Cell **74**(4): 679-691.

Kumaravelu, P., L. Hook, A. M. Morrison, J. Ure, S. Zhao, S. Zuyev, J. Ansell and A. Medvinsky (2002). "Quantitative developmental anatomy of definitive haematopoietic stem cells/long-term repopulating units (HSC/RUs): role of the aorta-gonad-mesonephros (AGM) region and the yolk sac in colonisation of the mouse embryonic liver." Development **129**(21): 4891-4899.

Kurtz, T. W., K. A. Griffin, A. K. Bidani, R. L. Davisson and J. E. Hall (2005). "Recommendations for blood pressure measurement in humans and experimental animals. Part 2: Blood pressure measurement in experimental animals: a statement for professionals from the subcommittee of professional and public education of the American Heart Association council on high blood pressure research." Hypertension **45**(2): 299-310.

Kuure, S., R. Vuolteenaho and S. Vainio (2000). "Kidney morphogenesis: cellular and molecular regulation." Mech Dev **92**(1): 31-45.

Lechner, M. S. and G. R. Dressler (1997). "The molecular basis of embryonic kidney development." Mech Dev **62**(2): 105-120.

Lee, S. B., K. Kanasaki and R. Kalluri (2009). "Circulating TGF-beta1 as a reliable biomarker for chronic kidney disease progression in the African-American population." Kidney Int **76**(1): 10-12.

Lelievre-Pegorier, M., J. Vilar, M. L. Ferrier, E. Moreau, N. Freund, T. Gilbert and C. Merlet-Benichou (1998). "Mild vitamin A deficiency leads to inborn nephron deficit in the rat." Kidney Int **54**(5): 1455-1462.

Lescher, B., B. Haenig and A. Kispert (1998). "sFRP-2 is a target of the Wnt-4 signaling pathway in the developing metanephric kidney." Dev Dyn **213**(4): 440-451.

Letterio, J. J., A. G. Geiser, A. B. Kulkarni, N. S. Roche, M. B. Sporn and A. B. Roberts (1994). "Maternal rescue of transforming growth factor-beta 1 null mice." Science **264**(5167): 1936-1938.

Lewis, K. A., P. C. Gray, A. L. Blount, L. A. MacConell, E. Wiater, L. M. Bilezikjian and W. Vale (2000). "Betaglycan binds inhibin and can mediate functional antagonism of activin signalling." Nature **404**(6776): 411-414.

Liu, A., A. Dardik and B. J. Ballermann (1999). "Neutralizing TGF-beta1 antibody infusion in neonatal rat delays in vivo glomerular capillary formation 1." Kidney Int **56**(4): 1334-1348.

Liu, I. M., S. H. Schilling, K. A. Knouse, L. Choy, R. Derynck and X. F. Wang (2009). "TGFbeta-stimulated Smad1/5 phosphorylation requires the ALK5 L45 loop and mediates the pro-migratory TGFbeta switch." Embo J **28**(2): 88-98.

Lopez-Casillas, F., S. Cheifetz, J. Doody, J. L. Andres, W. S. Lane and J. Massague (1991). "Structure and expression of the membrane proteoglycan betaglycan, a component of the TGF-beta receptor system." Cell **67**(4): 785-795.

Lopez-Casillas, F., H. M. Payne, J. L. Andres and J. Massague (1994). "Betaglycan can act as a dual modulator of TGF-beta access to signaling receptors: mapping of ligand binding and GAG attachment sites." J Cell Biol **124**(4): 557-568.

Lopez-Casillas, F., J. L. Wrana and J. Massague (1993). "Betaglycan presents ligand to the TGF beta signaling receptor." Cell **73**(7): 1435-1444.

Loria, A., V. Reverte, F. Salazar, F. Saez, M. T. Llinas and F. J. Salazar (2007). "Sex and age differences of renal function in rats with reduced ANG II activity during the nephrogenic period." Am J Physiol Renal Physiol **293**(2): F506-510.

Luyckx, V. A. and B. M. Brenner (2010). "The clinical importance of nephron mass." J Am Soc Nephrol **21**(6): 898-910.

MacAulay, J., K. Thompson, B. A. Kiberd, D. C. Barnes and K. M. Peltekian (2006). "Serum creatinine in patients with advanced liver disease is of limited value for identification of moderate renal dysfunction: are the equations for estimating renal function better?" Can J Gastroenterol **20**(8): 521-526.

MacKay, K., P. Kondaiah, D. Danielpour, H. A. Austin, 3rd and P. D. Brown (1990). "Expression of transforming growth factor-beta 1 and beta 2 in rat glomeruli." Kidney Int **38**(6): 1095-1100.

Maeshima, A., M. Miya, K. Mishima, S. Yamashita, I. Kojima and Y. Nojima (2008). "Activin A: autocrine regulator of kidney development and repair." Endocr J **55**(1): 1-9.

Maeshima, A., S. Shiozaki, T. Tajima, Y. Nakazato, T. Naruse and I. Kojima (2000). "Number of glomeruli is increased in the kidney of transgenic mice expressing the truncated type II activin receptor." Biochem Biophys Res Commun **268**(2): 445-449.

Maeshima, A., D. A. Vaughn, Y. Choi and S. K. Nigam (2006). "Activin A is an endogenous inhibitor of ureteric bud outgrowth from the Wolffian duct." Dev Biol **295**(2): 473-485.

Majumdar, A., S. Vainio, A. Kispert, J. McMahon and A. P. McMahon (2003). "Wnt11 and Ret/Gdnf pathways cooperate in regulating ureteric branching during metanephric kidney development." Development **130**(14): 3175-3185.

Maka, N., J. Makrakis, H. C. Parkington, M. Tare, R. Morley and M. J. Black (2008). "Vitamin D deficiency during pregnancy and lactation stimulates nephrogenesis in rat offspring." Pediatr Nephrol **23**(1): 55-61.

Makrakis, J., M. A. Zimanyi and M. J. Black (2007). "Retinoic acid enhances nephron endowment in rats exposed to maternal protein restriction." Pediatr Nephrol **22**(11): 1861-1867.

Mansano, R., M. Desai, A. Garg, G. Y. Choi and M. G. Ross (2007). "Enhanced nephrogenesis in offspring of water-restricted rat dams." Am J Obstet Gynecol **196**(5): 480 e481-486.

Martins, J. P., J. C. Monteiro and A. D. Paixao (2003). "Renal function in adult rats subjected to prenatal dexamethasone." Clin Exp Pharmacol Physiol **30**(1-2): 32-37.

Martus, W., D. Kim, J. L. Garvin and W. H. Beierwaltes (2005). "Commercial rodent diets contain more sodium than rats need." Am J Physiol Renal Physiol **288**(2): F428-431.

Massague, J., L. Attisano and J. L. Wrana (1994). "The TGF-beta family and its composite receptors." Trends Cell Biol **4**(5): 172-178.

Massague, J., J. Seoane and D. Wotton (2005). "Smad transcription factors." Genes Dev **19**(23): 2783-2810.

Matzuk, M. M., M. J. Finegold, J. G. Su, A. J. Hsueh and A. Bradley (1992). "Alpha-inhibin is a tumour-suppressor gene with gonadal specificity in mice." Nature **360**(6402): 313-319.

McLoone, V. I., J. V. Ringwood and B. N. Van Vliet (2009). "A multi-component model of the dynamics of salt-induced hypertension in Dahl-S rats." BMC Physiol **9**: 20.

McNamara, B. J., B. Diouf, R. N. Douglas-Denton, M. D. Hughson, W. E. Hoy and J. F. Bertram (2010). "A comparison of nephron number, glomerular volume and kidney weight in Senegalese Africans and African Americans." Nephrol Dial Transplant **25**(5): 1514-1520.

McNamara, B. J., B. Diouf, M. D. Hughson, R. N. Douglas-Denton, W. E. Hoy and J. F. Bertram (2008). "Renal pathology, glomerular number and volume in a West African urban community." Nephrol Dial Transplant **23**(8): 2576-2585.

Mead, A. L., T. T. Wong, M. F. Cordeiro, I. K. Anderson and P. T. Khaw (2003). "Evaluation of anti-TGF-beta2 antibody as a new postoperative anti-scarring agent in glaucoma surgery." Invest Ophthalmol Vis Sci **44**(8): 3394-3401.

Mendelsohn, C., D. Lohnes, D. Decimo, T. Lufkin, M. LeMeur, P. Chambon and M. Mark (1994). "Function of the retinoic acid receptors (RARs) during development (II). Multiple abnormalities at various stages of organogenesis in RAR double mutants." Development **120**(10): 2749-2771.

Merlet-Benichou, C., T. Gilbert, J. Vilar, E. Moreau, N. Freund and M. Lelievre-Pegorier (1999). "Nephron number: variability is the rule. Causes and consequences." Lab Invest **79**(5): 515-527.

Messerli, F. H., B. Williams and E. Ritz (2007). "Essential hypertension." Lancet **370**(9587): 591-603.

Meyer, T. N., C. Schwesinger, K. T. Bush, R. O. Stuart, D. W. Rose, M. M. Shah, D. A. Vaughn, D. L. Steer and S. K. Nigam (2004). "Spatiotemporal regulation of morphogenetic molecules during in vitro branching of the isolated ureteric bud: toward a model of branching through budding in the developing kidney." Dev Biol **275**(1): 44-67.

Michael, L. and J. A. Davies (2004). "Pattern and regulation of cell proliferation during murine ureteric bud development." J Anat **204**(4): 241-255.

Michos, O. (2009). "Kidney development: from ureteric bud formation to branching morphogenesis." Curr Opin Genet Dev **19**(5): 484-490.

Michos, O., A. Goncalves, J. Lopez-Rios, E. Tiecke, F. Naillat, K. Beier, A. Galli, S. Vainio and R. Zeller (2007). "Reduction of BMP4 activity by gremlin 1 enables ureteric bud outgrowth and GDNF/WNT11 feedback signalling during kidney branching morphogenesis." Development **134**(13): 2397-2405.

Miller, B. F. and A. W. Winkler (1938). "The Renal Excretion of Endogenous Creatinine in Man. Comparison with Exogenous Creatinine and Inulin." J Clin Invest **17**(1): 31-40.

Mills, P. A., D. A. Huetteman, B. P. Brockway, L. M. Zwiers, A. J. Gelsema, R. S. Schwartz and K. Kramer (2000). "A new method for measurement of blood pressure, heart rate, and activity in the mouse by radiotelemetry." J Appl Physiol **88**(5): 1537-1544.

Mimura, I., M. Nangaku, H. Nishi, R. Inagi, T. Tanaka and T. Fujita (2010). "Cytoglobin, a novel globin, plays an anti-fibrotic role in the kidney." Am J Physiol Renal Physiol.

Miyazaki, Y., K. Oshima, A. Fogo, B. L. Hogan and I. Ichikawa (2000). "Bone morphogenetic protein 4 regulates the budding site and elongation of the mouse ureter." J Clin Invest **105**(7): 863-873.

Miyazaki, Y., K. Oshima, A. Fogo and I. Ichikawa (2003). "Evidence that bone morphogenetic protein 4 has multiple biological functions during kidney and urinary tract development." Kidney Int **63**(3): 835-844.

Moore, M. W., R. D. Klein, I. Farinas, H. Sauer, M. Armanini, H. Phillips, L. F. Reichardt, A. M. Ryan, K. Carver-Moore and A. Rosenthal (1996). "Renal and neuronal abnormalities in mice lacking GDNF." Nature **382**(6586): 76-79.

Moreau, E., J. Vilar, M. Lelievre-Pegorier, C. Merlet-Benichou and T. Gilbert (1998). "Regulation of c-ret expression by retinoic acid in rat metanephros: implication in nephron mass control." Am J Physiol **275**(6 Pt 2): F938-945.

Moritz, K. M., E. M. Wintour, M. J. Black, J. F. Bertram and G. Caruana (2008). "Factors influencing mammalian kidney development: implications for health in adult life." Adv Anat Embryol Cell Biol **196**: 1-78.

Mozes, M. M., E. P. Bottinger, T. A. Jacot and J. B. Kopp (1999). "Renal expression of fibrotic matrix proteins and of transforming growth factor-beta (TGF-beta) isoforms in TGF-beta transgenic mice." J Am Soc Nephrol **10**(2): 271-280.

Mugford, J. W., P. Sipila, J. A. McMahon and A. P. McMahon (2008). "Osr1 expression demarcates a multi-potent population of intermediate mesoderm that undergoes progressive restriction to an Osr1-dependent nephron progenitor compartment within the mammalian kidney." Dev Biol **324**(1): 88-98.

Mugford, J. W., J. Yu, A. Kobayashi and A. P. McMahon (2009). "High-resolution gene expression analysis of the developing mouse kidney defines novel cellular compartments within the nephron progenitor population." Dev Biol.

Narlis, M., D. Grote, Y. Gaitan, S. K. Boualia and M. Bouchard (2007). "Pax2 and pax8 regulate branching morphogenesis and nephron differentiation in the developing kidney." J Am Soc Nephrol **18**(4): 1121-1129.

Nenov, V. D., M. W. Taal, O. V. Sakharova and B. M. Brenner (2000). "Multi-hit nature of chronic renal disease." Curr Opin Nephrol Hypertens **9**(2): 85-97.

Nyengaard, J. R. and T. F. Bendtsen (1992). "Glomerular number and size in relation to age, kidney weight, and body surface in normal man." Anat Rec **232**(2): 194-201.

Ohto, H., S. Kamada, K. Tago, S. I. Tominaga, H. Ozaki, S. Sato and K. Kawakami (1999). "Cooperation of six and eya in activation of their target genes through nuclear translocation of Eya." Mol Cell Biol **19**(10): 6815-6824.

Ortiz, L. A., A. Quan, A. Weinberg and M. Baum (2001). "Effect of prenatal dexamethasone on rat renal development." Kidney Int **59**(5): 1663-1669.

Oxburgh, L., G. C. Chu, S. K. Michael and E. J. Robertson (2004). "TGFbeta superfamily signals are required for morphogenesis of the kidney mesenchyme progenitor population." Development **131**(18): 4593-4605.

Pavenstadt, H., W. Kriz and M. Kretzler (2003). "Cell biology of the glomerular podocyte." Physiol Rev **83**(1): 253-307.

Pelton, R. W., B. Saxena, M. Jones, H. L. Moses and L. I. Gold (1991). "Immunohistochemical localization of TGF beta 1, TGF beta 2, and TGF beta 3 in the mouse embryo: expression patterns suggest multiple roles during embryonic development." J Cell Biol **115**(4): 1091-1105.

Pichel, J. G., L. Shen, H. Z. Sheng, A. C. Granholm, J. Drago, A. Grinberg, E. J. Lee, S. P. Huang, M. Saarma, B. J. Hoffer, H. Sariola and H. Westphal (1996). "Defects in enteric innervation and kidney development in mice lacking GDNF." Nature **382**(6586): 73-76.

Pietri, L., M. Bloch-Faure, M. F. Belair, L. P. Sanford, T. Doetschman, J. Menard, P. Bruneval and P. Meneton (2002). "Altered renin synthesis and secretion in the kidneys of heterozygous mice with a null mutation in the TGF-beta(2) gene." Exp Nephrol **10**(5-6): 374-382.

Plisov, S. Y., K. Yoshino, L. F. Dove, K. G. Higinbotham, J. S. Rubin and A. O. Perantoni (2001). "TGF beta 2, LIF and FGF2 cooperate to induce nephrogenesis." Development **128**(7): 1045-1057.

Puelles, V. G., W. E. Hoy, M. D. Hughson, B. Diouf, R. N. Douglas-Denton and J. F. Bertram (2010). "Glomerular number and size variability and risk for kidney disease." Current Opinion in Nephrology and Hypertension **19**: 1062 - 4821.

Quinlan, J., M. Lemire, T. Hudson, H. Qu, A. Benjamin, A. Roy, E. Pascuet, M. Goodyer, C. Raju, Z. Zhang, F. Houghton and P. Goodyer (2007). "A common variant of the PAX2 gene is associated with reduced newborn kidney size." J Am Soc Nephrol **18**(6): 1915-1921.

Raatikainen-Ahokas, A., M. Hytonen, A. Tenhunen, K. Sainio and H. Sariola (2000). "BMP-4 affects the differentiation of metanephric mesenchyme and reveals an early anterior-posterior axis of the embryonic kidney." Dev Dyn **217**(2): 146-158.

Reeves, P. G., F. H. Nielsen and G. C. Fahey, Jr. (1993). "AIN-93 purified diets for laboratory rodents: final report of the American Institute of Nutrition ad hoc writing committee on the reformulation of the AIN-76A rodent diet." J Nutr **123**(11): 1939-1951.

Reeves, P. G., K. L. Rossow and J. Lindlauf (1993). "Development and testing of the AIN-93 purified diets for rodents: results on growth, kidney calcification and bone mineralization in rats and mice." J Nutr **123**(11): 1923-1931.

Reidy, K. J. and N. D. Rosenblum (2009). "Cell and molecular biology of kidney development." Semin Nephrol **29**(4): 321-337.

Ritvos, O., T. Tuuri, M. Eramaa, K. Sainio, K. Hilden, L. Saxen and S. F. Gilbert (1995). "Activin disrupts epithelial branching morphogenesis in developing glandular organs of the mouse." Mech Dev **50**(2-3): 229-245.

Ross, S., E. Cheung, T. G. Petrakis, M. Howell, W. L. Kraus and C. S. Hill (2006). "Smads orchestrate specific histone modifications and chromatin remodeling to activate transcription." Embo J **25**(19): 4490-4502.

Ruf, R. G., P. X. Xu, D. Silvius, E. A. Otto, F. Beekmann, U. T. Muerb, S. Kumar, T. J. Neuhaus, M. J. Kemper, R. M. Raymond, Jr., P. D. Brophy, J. Berkman, M. Gattas, V. Hyland, E. M. Ruf, C. Schwartz, E. H. Chang, R. J. Smith, C. A. Stratakis, D. Weil, C. Petit and F. Hildebrandt (2004). "SIX1 mutations cause branchio-oto-renal syndrome by disruption of EYA1-SIX1-DNA complexes." Proc Natl Acad Sci U S A **101**(21): 8090-8095.

Ruta, L. A. (2009). Cardiovascular and Renal Outcomes for Mice Born with Moderate or Marked Nephron Deficits. Department of Physiology. Melbourne, Monash Universtiy. **PhD:** 196.

Ruta, L. A., H. Dickinson, M. C. Thomas, K. M. Denton, W. P. Anderson and M. M. Kett (2010). "High-salt diet reveals the hypertensive and renal effects of reduced nephron endowment." Am J Physiol Renal Physiol **298**(6): F1384-1392.

Saez, F., M. T. Castells, A. Zuasti, F. Salazar, V. Reverte, A. Loria and F. J. Salazar (2007). "Sex differences in the renal changes elicited by angiotensin II blockade during the nephrogenic period." Hypertension **49**(6): 1429-1435.

Sainio, K., P. Suvanto, J. Davies, J. Wartiovaara, K. Wartiovaara, M. Saarma, U. Arumae, X. Meng, M. Lindahl, V. Pachnis and H. Sariola (1997). "Glial-cell-line-derived neurotrophic factor is required for bud initiation from ureteric epithelium." Development **124**(20): 4077-4087.

Sajithlal, G., D. Zou, D. Silvius and P. X. Xu (2005). "Eya 1 acts as a critical regulator for specifying the metanephric mesenchyme." Dev Biol **284**(2): 323-336.

Sakurai, H., E. J. Barros, T. Tsukamoto, J. Barasch and S. K. Nigam (1997). "An in vitro tubulogenesis system using cell lines derived from the embryonic kidney shows dependence on multiple soluble growth factors." Proc Natl Acad Sci U S A **94**(12): 6279-6284.

Sakurai, H. and S. K. Nigam (1997). "Transforming growth factor-beta selectively inhibits branching morphogenesis but not tubulogenesis." Am J Physiol **272**(1 Pt 2): F139-146.

Sanchez, M. P., I. Silos-Santiago, J. Frisen, B. He, S. A. Lira and M. Barbacid (1996). "Renal agenesis and the absence of enteric neurons in mice lacking GDNF." Nature **382**(6586): 70-73.

Sandberg, M. B., A. B. Maunsbach and A. A. McDonough (2006). "Redistribution of distal tubule Na+-Cl- cotransporter (NCC) in response to a high-salt diet." Am J Physiol Renal Physiol **291**(2): F503-508.

Sanders, P. W. (2009). "Vascular consequences of dietary salt intake." Am J Physiol Renal Physiol **297**(2): F237-243.

Sanford, L. P., I. Ormsby, A. C. Gittenberger-de Groot, H. Sariola, R. Friedman, G. P. Boivin, E. L. Cardell and T. Doetschman (1997). "TGFbeta2 knockout mice have multiple developmental defects that are non-overlapping with other TGFbeta knockout phenotypes." Development **124**(13): 2659-2670.

Sanyanusin, P., L. A. Schimmenti, L. A. McNoe, T. A. Ward, M. E. Pierpont, M. J. Sullivan, W. B. Dobyns and M. R. Eccles (1995). "Mutation of the PAX2 gene in a family with optic nerve colobomas, renal anomalies and vesicoureteral reflux." Nat Genet **9**(4): 358-364.

Sariola, H. (2002). "Nephron induction revisited: from caps to condensates." Curr Opin Nephrol Hypertens **11**(1): 17-21.

Sarnak, M. J., A. S. Levey, A. C. Schoolwerth, J. Coresh, B. Culleton, L. L. Hamm, P. A. McCullough, B. L. Kasiske, E. Kelepouris, M. J. Klag, P. Parfrey, M. Pfeffer, L. Raij, D. J. Spinosa and P. W. Wilson (2003). "Kidney disease as a risk factor for development of cardiovascular disease: a statement from the American Heart Association Councils on Kidney in Cardiovascular Disease, High Blood Pressure Research, Clinical Cardiology, and Epidemiology and Prevention." Hypertension **42**(5): 1050-1065.

Sarraj, M. A., H. K. Chua, A. Umbers, K. L. Loveland, J. K. Findlay and K. L. Stenvers (2007). "Differential expression of TGFBR3 (betaglycan) in mouse ovary and testis during gonadogenesis." Growth Factors **25**(5): 334-345.

Sarraj, M. A., R. M. Escalona, A. Umbers, H. K. Chua, C. Small, M. Griswold, K. Loveland, J. K. Findlay and K. L. Stenvers "Fetal testis dysgenesis and compromised Leydig cell function in Tgfbr3 (beta glycan) knockout mice." Biol Reprod **82**(1): 153-162.

Sarraj, M. A., R. M. Escalona, A. Umbers, H. K. Chua, C. Small, M. Griswold, K. Loveland, J. K. Findlay and K. L. Stenvers (2010). "Fetal testis dysgenesis and compromised Leydig cell function in Tgfbr3 (beta glycan) knockout mice." Biol Reprod **82**(1): 153-162.

Saulnier, D. M., H. Ghanbari and A. W. Brandli (2002). "Essential function of Wnt-4 for tubulogenesis in the Xenopus pronephric kidney." Dev Biol **248**(1): 13-28.

Saxen, L. and H. Sariola (1987). "Early organogenesis of the kidney." Pediatr Nephrol **1**(3): 385-392.

Schmierer, B. and C. S. Hill (2007). "TGFbeta-SMAD signal transduction: molecular specificity and functional flexibility." Nat Rev Mol Cell Biol **8**(12): 970-982.

Schuchardt, A., V. D'Agati, V. Pachnis and F. Costantini (1996). "Renal agenesis and hypodysplasia in ret-k- mutant mice result from defects in ureteric bud development." Development **122**(6): 1919-1929.

Self, M., O. V. Lagutin, B. Bowling, J. Hendrix, Y. Cai, G. R. Dressler and G. Oliver (2006). "Six2 is required for suppression of nephrogenesis and progenitor renewal in the developing kidney." Embo J **25**(21): 5214-5228.

Seymour, P. A., K. K. Freude, C. L. Dubois, H. P. Shih, N. A. Patel and M. Sander (2008). "A dosage-dependent requirement for Sox9 in pancreatic endocrine cell formation." Dev Biol **323**(1): 19-30.

Shah, M. M., R. V. Sampogna, H. Sakurai, K. T. Bush and S. K. Nigam (2004). "Branching morphogenesis and kidney disease." Development **131**(7): 1449-1462.

Shah, M. M., J. B. Tee, T. N. Meyer, C. Meyer-Schwesinger, Y. Choi, D. E. Sweeney, T. F. Gallegos, K. Johkura, E. Rosines, V. Kouznetsova, D. W. Rose, K. T. Bush, H. Sakurai and S. K. Nigam (2009). "The Instructive Role of Metanephric Mesenchyme on Ureteric Bud Patterning, Sculpting and Maturation." Am J Physiol Renal Physiol.

Shakya, R., T. Watanabe and F. Costantini (2005). "The role of GDNF/Ret signaling in ureteric bud cell fate and branching morphogenesis." Dev Cell **8**(1): 65-74.

Sharma, K., Y. Jin, J. Guo and F. N. Ziyadeh (1996). "Neutralization of TGF-beta by anti-TGF-beta antibody attenuates kidney hypertrophy and the enhanced extracellular matrix gene expression in STZ-induced diabetic mice." Diabetes **45**(4): 522-530.

Shi, Y. and J. Massague (2003). "Mechanisms of TGF-beta signaling from cell membrane to the nucleus." Cell **113**(6): 685-700.

Shindo, T., H. Kurihara, K. Maemura, Y. Kurihara, O. Ueda, H. Suzuki, T. Kuwaki, K. H. Ju, Y. Wang, A. Ebihara, H. Nishimatsu, N. Moriyama, M. Fukuda, Y. Akimoto, H. Hirano, H. Morita, M. Kumada, Y. Yazaki, R. Nagai and K. Kimura (2002). "Renal damage and salt-dependent hypertension in aged transgenic mice overexpressing endothelin-1." J Mol Med **80**(2): 105-116.

Short, K. M., M. J. Hodson and I. M. Smyth (2010). "Tomographic quantification of branching morphogenesis and renal development." Kidney Int **77**(12): 1132-1139.

Siehl, J. M., E. Thiel, K. Heufelder, E. Snarski, S. Schwartz, V. Mailander and U. Keilholz (2003). "Possible regulation of Wilms' tumour gene 1 (WT1) expression by the paired box genes PAX2 and PAX8 and by the haematopoietic transcription factor GATA-1 in human acute myeloid leukaemias." Br J Haematol **123**(2): 235-242.

Sims-Lucas, S. (2007). Investigating the role of transforming growth factor-β2 in mouse metanephric development. PhD thesis, Monash University, p. 260.

Sims-Lucas, S., G. Caruana, J. Dowling, M. M. Kett and J. F. Bertram (2008). "Augmented and accelerated nephrogenesis in TGF-beta2 heterozygous mutant mice." Pediatr Res **63**(6): 607-612.

Sims-Lucas, S., L. Cullen-McEwen, V. P. Eswarakumar, D. Hains, K. Kish, B. Becknell, J. Zhang, J. F. Bertram, F. Wang and C. M. Bates (2009). "Deletion of Frs2alpha from the ureteric epithelium causes renal hypoplasia." Am J Physiol Renal Physiol **297**(5): F1208-1219.

Sims-Lucas, S., R. J. Young, G. Martinez, D. Taylor, S. M. Grimmond, R. Teasdale, M. H. Little, J. F. Bertram and G. Caruana (2010). "Redirection of renal mesenchyme to stromal and chondrocytic fates in the presence of TGF-beta2." Differentiation **79**(4-5): 272-284.

Singh, R. R., L. A. Cullen-McEwen, M. M. Kett, W. M. Boon, J. Dowling, J. F. Bertram and K. M. Moritz (2007). "Prenatal corticosterone exposure results in altered AT1/AT2, nephron deficit and hypertension in the rat offspring." J Physiol **579**(Pt 2): 503-513.

Singh, R. R., K. M. Moritz, J. F. Bertram and L. A. Cullen-McEwen (2007). "Effects of dexamethasone exposure on rat metanephric development: in vitro and in vivo studies." Am J Physiol Renal Physiol **293**(2): F548-554.

Skinner, M. A., S. D. Safford, J. G. Reeves, M. E. Jackson and A. J. Freemerman (2008). "Renal aplasia in humans is associated with RET mutations." Am J Hum Genet **82**(2): 344-351.

Smith, C. and S. Mackay (1991). "Morphological development and fate of the mouse mesonephros." J Anat **174**: 171-184.

Solhaug, M. J., P. M. Bolger and P. A. Jose (2004). "The developing kidney and environmental toxins." Pediatrics **113**(4 Suppl): 1084-1091.

Stark, K., S. Vainio, G. Vassileva and A. P. McMahon (1994). "Epithelial transformation of metanephric mesenchyme in the developing kidney regulated by Wnt-4." Nature **372**(6507): 679-683.

Stenvers, K. L., M. L. Tursky, K. W. Harder, N. Kountouri, S. Amatayakul-Chantler, D. Grail, C. Small, R. A. Weinberg, A. M. Sizeland and H. J. Zhu (2003). "Heart and liver defects and reduced transforming growth factor beta2 sensitivity in transforming growth factor beta type III receptor-deficient embryos." Mol Cell Biol **23**(12): 4371-4385.

Sutherland, M. R., L. Gubhaju, B. A. Yoder, M. T. Stahlman and M. J. Black (2009). "The effects of postnatal retinoic acid administration on nephron endowment in the preterm baboon kidney." Pediatr Res **65**(4): 397-402.

Tabatabaeifar, M., K. P. Schlingmann, M. Litwin, S. Emre, A. Bakkaloglu, O. Mehls, C. Antignac, F. Schaefer and S. Weber (2009). "Functional analysis of BMP4 mutations identified in pediatric CAKUT patients." Pediatr Nephrol **24**(12): 2361-2368.

Tang, B., E. P. Bottinger, S. B. Jakowlew, K. M. Bagnall, J. Mariano, M. R. Anver, J. J. Letterio and L. M. Wakefield (1998). "Transforming growth factor-beta1 is a new form of tumor suppressor with true haploid insufficiency." Nat Med **4**(7): 802-807.

Tomac, A. C., A. Grinberg, S. P. Huang, C. Nosrat, Y. Wang, C. Borlongan, S. Z. Lin, Y. H. Chiang, L. Olson, H. Westphal and B. J. Hoffer (2000). "Glial cell line-derived neurotrophic factor receptor alpha1 availability regulates glial cell line-

derived neurotrophic factor signaling: evidence from mice carrying one or two mutated alleles." Neuroscience **95**(4): 1011-1023.

Tomoda, T., T. Shirasawa, Y. I. Yahagi, K. Ishii, H. Takagi, Y. Furiya, K. I. Arai, H. Mori and M. A. Muramatsu (1996). "Transforming growth factor-beta is a survival factor for neonate cortical neurons: coincident expression of type I receptors in developing cerebral cortices." Dev Biol **179**(1): 79-90.

Torban, E., A. Dziarmaga, D. Iglesias, L. L. Chu, T. Vassilieva, M. Little, M. Eccles, M. Discenza, J. Pelletier and P. Goodyer (2006). "PAX2 activates WNT4 expression during mammalian kidney development." J Biol Chem **281**(18): 12705-12712.

Torres, M., E. Gomez-Pardo, G. R. Dressler and P. Gruss (1995). "Pax-2 controls multiple steps of urogenital development." Development **121**(12): 4057-4065.

Towers, P. R., A. S. Woolf and P. Hardman (1998). "Glial cell line-derived neurotrophic factor stimulates ureteric bud outgrowth and enhances survival of ureteric bud cells in vitro." Exp Nephrol **6**(4): 337-351.

Tsang, M. L., L. Zhou, B. L. Zheng, J. Wenker, G. Fransen, J. Humphrey, J. M. Smith, M. O'Connor-McCourt, R. Lucas and J. A. Weatherbee (1995). "Characterization of recombinant soluble human transforming growth factor-beta receptor type II (rhTGF-beta sRII)." Cytokine **7**(5): 389-397.

Tufro, A., J. Teichman, C. Woda and G. Villegas (2008). "Semaphorin3a inhibits ureteric bud branching morphogenesis." Mech Dev **125**(5-6): 558-568.

Valerius, M. T. and A. P. McMahon (2008). "Transcriptional profiling of Wnt4 mutant mouse kidneys identifies genes expressed during nephron formation." Gene Expr Patterns **8**(5): 297-306.

Van Vliet, B. N., J. McGuire, L. Chafe, A. Leonard, A. Joshi and J. P. Montani (2006). "Phenotyping the level of blood pressure by telemetry in mice." Clin Exp Pharmacol Physiol **33**(11): 1007-1015.

Vander, A. (1995). Renal Physiology. United States of America, McGraw-Hill.

Vehaskari, V. M. (2010). "Prenatal programming of kidney disease." Curr Opin Pediatr **22**(2): 176-182.

Vervoort, V. S., R. J. Smith, J. O'Brien, R. Schroer, A. Abbott, R. E. Stevenson and C. E. Schwartz (2002). "Genomic rearrangements of EYA1 account for a large fraction of families with BOR syndrome." Eur J Hum Genet **10**(11): 757-766.

Vilar, J., T. Gilbert, E. Moreau and C. Merlet-Benichou (1996). "Metanephros organogenesis is highly stimulated by vitamin A derivatives in organ culture." Kidney Int **49**(5): 1478-1487.

Vilchis-Landeros, M. M., J. L. Montiel, V. Mendoza, G. Mendoza-Hernandez and F. Lopez-Casillas (2001). "Recombinant soluble betaglycan is a potent and

isoform-selective transforming growth factor-beta neutralizing agent." Biochem J **355**(Pt 1): 215-222.

Villar-Martini, V. C., J. J. Carvalho, M. F. Neves, M. B. Aguila and C. A. Mandarim-de-Lacerda (2009). "Hypertension and kidney alterations in rat offspring from low protein pregnancies." J Hypertens **27 Suppl 6**: S47-51.

Vize, P. D., D. W. Seufert, T. J. Carroll and J. B. Wallingford (1997). "Model systems for the study of kidney development: use of the pronephros in the analysis of organ induction and patterning." Dev Biol **188**(2): 189-204.

Wada, W., J. J. Medina, H. Kuwano and I. Kojima (2005). "Comparison of the function of the beta(C) and beta(E) subunits of activin in AML12 hepatocytes." Endocr J **52**(2): 169-175.

Wang, X. F., H. Y. Lin, E. Ng-Eaton, J. Downward, H. F. Lodish and R. A. Weinberg (1991). "Expression cloning and characterization of the TGF-beta type III receptor." Cell **67**(4): 797-805.

Weber, S., V. Moriniere, T. Knuppel, M. Charbit, J. Dusek, G. M. Ghiggeri, A. Jankauskiene, S. Mir, G. Montini, A. Peco-Antic, E. Wuhl, A. M. Zurowska, O. Mehls, C. Antignac, F. Schaefer and R. Salomon (2006). "Prevalence of mutations in renal developmental genes in children with renal hypodysplasia: results of the ESCAPE study." J Am Soc Nephrol **17**(10): 2864-2870.

Weber, S., J. C. Taylor, P. Winyard, K. F. Baker, J. Sullivan-Brown, R. Schild, T. Knuppel, A. M. Zurowska, A. Caldas-Alfonso, M. Litwin, S. Emre, G. M. Ghiggeri, A. Bakkaloglu, O. Mehls, C. Antignac, E. Network, F. Schaefer and R. D. Burdine (2008). "SIX2 and BMP4 mutations associate with anomalous kidney development." J Am Soc Nephrol **19**(5): 891-903.

Welham, S. J., A. Wade and A. S. Woolf (2002). "Protein restriction in pregnancy is associated with increased apoptosis of mesenchymal cells at the start of rat metanephrogenesis." Kidney Int **61**(4): 1231-1242.

Weller, A., L. Sorokin, E. M. Illgen and P. Ekblom (1991). "Development and growth of mouse embryonic kidney in organ culture and modulation of development by soluble growth factor." Dev Biol **144**(2): 248-261.

Wiater, E., C. A. Harrison, K. A. Lewis, P. C. Gray and W. W. Vale (2006). "Identification of distinct inhibin and transforming growth factor beta-binding sites on betaglycan: functional separation of betaglycan co-receptor actions." J Biol Chem **281**(25): 17011-17022.

Wiater, E., K. A. Lewis, C. Donaldson, J. Vaughan, L. Bilezikjian and W. Vale (2009). "Endogenous betaglycan is essential for high-potency inhibin antagonism in gonadotropes." Mol Endocrinol **23**(7): 1033-1042.

Wiater, E. and W. Vale (2003). "Inhibin is an antagonist of bone morphogenetic protein signaling." J Biol Chem **278**(10): 7934-7941.

Wilson, H. M., A. W. Minto, P. A. Brown, L. P. Erwig and A. J. Rees (2000). "Transforming growth factor-beta isoforms and glomerular injury in nephrotoxic nephritis." Kidney Int **57**(6): 2434-2444.

Wilson, J. G., C. B. Roth and J. Warkany (1953). "An analysis of the syndrome of malformations induced by maternal vitamin A deficiency. Effects of restoration of vitamin A at various times during gestation." Am J Anat **92**(2): 189-217.

Wintour, E. M., K. Johnson, I. Koukoulas, K. Moritz, M. Tersteeg and M. Dodic (2003). "Programming the cardiovascular system, kidney and the brain--a review." Placenta **24 Suppl A**: S65-71.

Wintour, E. M., K. M. Moritz, K. Johnson, S. Ricardo, C. S. Samuel and M. Dodic (2003). "Reduced nephron number in adult sheep, hypertensive as a result of prenatal glucocorticoid treatment." J Physiol **549**(Pt 3): 929-935.

Wlodek, M. E., K. Westcott, A. L. Siebel, J. A. Owens and K. M. Moritz (2008). "Growth restriction before or after birth reduces nephron number and increases blood pressure in male rats." Kidney Int **74**(2): 187-195.

Woods, L. L. (1999). "Neonatal uninephrectomy causes hypertension in adult rats." Am J Physiol **276**(4 Pt 2): R974-978.

Woods, L. L., D. A. Weeks and R. Rasch (2004). "Programming of adult blood pressure by maternal protein restriction: role of nephrogenesis." Kidney Int **65**(4): 1339-1348.

Wright, T. E., D. P. Hill, F. Ko, P. M. Soler, P. D. Smith, M. Franz, E. H. Nichols and M. C. Robson (2000). "The effect of TGF-beta2 in various vehicles on incisional wound healing." Int J Surg Investig **2**(2): 133-143.

Wu, D. T., M. Bitzer, W. Ju, P. Mundel and E. P. Bottinger (2005). "TGF-beta concentration specifies differential signaling profiles of growth arrest/differentiation and apoptosis in podocytes." J Am Soc Nephrol **16**(11): 3211-3221.

Xiao, Y. Q., K. Liu, J. F. Shen, G. T. Xu and W. Ye (2009). "SB-431542 inhibition of scar formation after filtration surgery and its potential mechanism." Invest Ophthalmol Vis Sci **50**(4): 1698-1706.

Xu, P. X., J. Adams, H. Peters, M. C. Brown, S. Heaney and R. Maas (1999). "Eya1-deficient mice lack ears and kidneys and show abnormal apoptosis of organ primordia." Nat Genet **23**(1): 113-117.

Xu, P. X., W. Zheng, L. Huang, P. Maire, C. Laclef and D. Silvius (2003). "Six1 is required for the early organogenesis of mammalian kidney." Development **130**(14): 3085-3094.

Yamashita, H., P. ten Dijke, D. Huylebroeck, T. K. Sampath, M. Andries, J. C. Smith, C. H. Heldin and K. Miyazono (1995). "Osteogenic protein-1 binds to activin type II receptors and induces certain activin-like effects." J Cell Biol **130**(1): 217-226.

Yang, E. Y. and H. L. Moses (1990). "Transforming growth factor beta 1-induced changes in cell migration, proliferation, and angiogenesis in the chicken chorioallantoic membrane." J Cell Biol **111**(2): 731-741.

Yeo, C. and M. Whitman (2001). "Nodal signals to Smads through Cripto-dependent and Cripto-independent mechanisms." Mol Cell **7**(5): 949-957.

Ying, W. Z., K. Aaron and P. W. Sanders (2008). "Mechanism of dietary salt-mediated increase in intravascular production of TGF-beta1." Am J Physiol Renal Physiol **295**(2): F406-414.

Ying, W. Z. and P. W. Sanders (1998). "Dietary salt modulates renal production of transforming growth factor-beta in rats." Am J Physiol **274**(4 Pt 2): F635-641.

Yoshino, K., J. S. Rubin, K. G. Higinbotham, A. Uren, V. Anest, S. Y. Plisov and A. O. Perantoni (2001). "Secreted Frizzled-related proteins can regulate metanephric development." Mech Dev **102**(1-2): 45-55.

Yu, H. C., L. M. Burrell, M. J. Black, L. L. Wu, R. J. Dilley, M. E. Cooper and C. I. Johnston (1998). "Salt induces myocardial and renal fibrosis in normotensive and hypertensive rats." Circulation **98**(23): 2621-2628.

Zhang, Z., J. Quinlan, D. Grote, M. Lemire, T. Hudson, A. Benjamin, A. Roy, E. Pascuet, M. Goodyer, C. Raju, F. Houghton, M. Bouchard and P. Goodyer (2009). "Common variants of the glial cell-derived neurotrophic factor gene do not influence kidney size of the healthy newborn." Pediatr Nephrol **24**(6): 1151-1157.

Zhang, Z., J. Quinlan, W. Hoy, M. D. Hughson, M. Lemire, T. Hudson, P. A. Hueber, A. Benjamin, A. Roy, E. Pascuet, M. Goodyer, C. Raju, F. Houghton, J. Bertram and P. Goodyer (2008). "A common RET variant is associated with reduced newborn kidney size and function." J Am Soc Nephrol **19**(10): 2027-2034.

Zhao, J., J. D. Tefft, M. Lee, S. Smith and D. Warburton (1998). "Abrogation of betaglycan attenuates TGF-beta-mediated inhibition of embryonic murine lung branching morphogenesis in culture." Mech Dev **75**(1-2): 67-79.

Zimanyi, M. A., J. F. Bertram and M. J. Black (2004). "Does a nephron deficit in rats predispose to salt-sensitive hypertension?" Kidney Blood Press Res **27**(4): 239-247.

Zimanyi, M. A., K. M. Denton, J. M. Forbes, V. Thallas-Bonke, M. C. Thomas, F. Poon and M. J. Black (2006). "A developmental nephron deficit in rats is associated with increased susceptibility to a secondary renal injury due to advanced glycation end-products." Diabetologia **49**(4): 801-810.

Zimanyi, M. A., W. E. Hoy, R. N. Douglas-Denton, M. D. Hughson, L. M. Holden and J. F. Bertram (2009). "Nephron number and individual glomerular volumes in male Caucasian and African American subjects." Nephrol Dial Transplant.